Role of excitotoxicity in the degeneration of motor neurones in ALS

Thesis

UNRESTRICTED.

Role of excitotoxicity in the degeneration of motor neurones in ALS

Massimo Tortarolo

Thesis submitted for the degree of Doctor of Philosophy

The Open University of London

Laboratory of Molecular Neurobiology

Department of Neuroscience

Mario Negri Institute for Pharmacological Research

Milano

Submitted: September 30th, 2004

Submission date: 27 September 2004
Final date: 3 May 2005

Abstract

Amyotrophic lateral sclerosis (ALS) is a fatal neurological disorder involving selective degeneration of motor neurones. In a proportion of patients, ALS is caused by mutations in copper/zinc superoxide dismutase (SOD1), and mice expressing these mutants develop a syndrome that resembles human ALS. Using $SOD1^{G93A}$ transgenic mice, the role of glutamate-mediated toxicity and related intracellular pathways in motor neurone death has been investigated. GluR2 AMPA receptor subunits were decreased in spinal motor neurones of $SOD1^{G93A}$ mice before symptom onset. Since GluR2-lacking receptors are highly permeable to Ca^{2+}, a known trigger of excitotoxic neuronal death, this phenomenon may have a pathogenic role. In support of this, treatment with an AMPA antagonist, ZK-187638, ameliorated motor symptoms and prolonged the survival of $SOD1^{G93A}$ mice. GluR2-lacking receptors are also permeable to zinc, which can be highly toxic. *In situ* hybridisation showed low expression of the zinc extruder ZnT-1 on motor neurones, which may contribute to their vulnerability to excitotoxicity. Expression of glutamate transporters on astrocytes may also contribute to excitotoxic motor neurone death. In transgenic mice and in astrocytes transfected with $SOD1^{G93A}$, immunocytochemistry, Western blotting, *in situ* hybridisation and RT-PCR revealed down-regulation of GLT-1 protein, but not mRNA in astrocytes. However, the time-course in mice suggests that GLT-1 downregulation is not a primary pathological event. Activation of p38MAPK, a kinase putatively involved in glutamate mediated neurotoxicity, was observed in motor neurones at the onset of the disease, but

SB 239063, a p38MAPK inhibitor, did not ameliorate motor dysfunction or survival of $SOD1^{G93A}$ mice.

Altogether the results suggest that AMPA receptor mediated excitotoxicity is a primary cause of motor neurone degeneration in ALS. These observations may contribute to the development of new therapeutic strategies for this devastating disease.

Table of contents

List of figures

List of tables

List of abbreviations

ALS	Amyotrophic Lateral Sclerosis
AMPA	α-amino-3-hydroxy-5-methyl-4-isoxazole propionic acid
ANOVA	Analysis of variance
ATP	Adenosine Triphosphate
ATZ	3-amino-1,2,4-triazole
BDNF	Brain Derived Neurotrophic Factor
BOAA	β-*N*-oxalylamino- L-alanine
CDK5	Cyclin-Dependent Kinase 5
ChAT	Choline Acetyl Transferase
cDNA	Complimentary DNA
CNS	Central Nervous System
CSF	Cerebrospinal fluid
DAB	3'-3-diaminobenzidine tetrahydrocholride
DCDHF-DA	2',7'-dichlorodihydrofluorescin diacetate
DIV	Days *in vitro*
DHK	Dihydrokainate
DNA	Deoxyribonucleic Acid
DNase	Deoxyribonuclease
dNTP	Deoxynucleotide triphosphates
DMPO	5,5'-dimethyl-1-pyrrolline N-oxide
DTT	Dithiothreitol
EAAT	Excitatory Amino Acid Transporter

ECL	Enhanced chemiluminescence
EDTA	Ethylenediamine-N,N,N',N'-tetraacetic acid
EGTA	Ethylen glycol-bis(β-aminoethyl ether)-N,N,N',N'-tetraacetic acid
EMG	Electromyography
FALS	Familial ALS
FBS	Foetal Bovine Serum
f-MLP	N-Formylmethionine-Leucyl-Phenyl-alanine
GABA	γ-amino butyric acid
GFAP	Glial Fibrillary Acidic Protein
GEF	Guanine Exchange Factors
HEPES	4-(2-Hydroxyethyl)piperazine-1-ethanesulfonic acid
HRP	Horseradish peroxidase
hSOD1	Human SOD1
IGF	Insulin growth factror
IgG	Immunoglobulin G
iNOS	Inducible nitric oxide synthase
Ip	Intraperitoneal
KDa	Kilodaltons
Kb	Kilobases
LMN	Lower motor neurones
Loa	Legs-at-odd-angles
MAPK	Mitogen Activated Protein Kinase
MDCK	Madin-Darby Canine Kidney

MND	Motor Neurone Disease
mRNA	Messenger RNA
mSOD1	Murine SOD1
MTT	3-(4,5-dimethylthiazol-2-yl)-2,5-diphenyl tetrazolium bromide
NAIP	Neuronal apoptosis inhibitory protein
NBQX	6-nitro-7-sulfamobenzoquinoxaline-2,3-dione
NF-H	High molecular weight neurofilament
NF-L	Low molecular weight neurofilament
NGS	Normal goat serum
NMDA	The *N*-methyl-D-aspartate
NO	Nitric Oxide
PBS	Phosphate Buffered Saline
PBP	Progressive Bulbar Palsy
PCR	Polymerase chain reaction
PDC	L-*trans*-2,4-Pyrrolidine Dicarboxylate
PKA	Protein Kinase A
PKC	Protein Kinase C
PLS	Primary Lateral Sclerosis
PMA	Progressive Muscular Atrophy
PMN	Progressive Motor Neuronopathy
RNA	Ribonucleic Acid
RNase A	Ribonuclease A
ROS	Reactive Oxygen Species
RT-PCR	Reverse-transcriptase polymerase chain reaction

SDS	Sodium Dodecyl Sulfate
S.E.M	Standard error of the Mean
SOD1	Superoxide dismutase 1
$SOD1^{G93A}$	Superoxide dismutase 1 with G93A mutation
$SOD1^{WT}$	Superoxide dismutase 1 wild type
SOS	L-Serine-O-Sulphate
SSC	Saline-sodium citrate buffer
TBS	Tris buffered saline
TBST	TBS + 0,1% Tween-20
Tris	Tris(hydroxymethyl)methylamine
Trolox	6-hydroxy-2,5,7,8-tetramethylchroman-2-carboxylic acid
UMN	Upper motor neurones
UTP	Uridine triphosphate
VEGF	Vascular endothelial growth factor

Acknowledgements

I would like to express my deep gratitude to Dr Caterina Bendotti for the great academic and personal support given me in all these years spent in her laboratory.

A special thank go to Dr Marcus Rattray, Dr Rob Williams and their staff of the Biochemical Neuropharmacology Group at King's College, London, for giving me the opportunity to spend an extraordinary year in their laboratories to carry out the study on cultured astrocytes. I would particularly like to thank Dr Rattray for his help and advice during all the period of my Ph.D.

My sincere thanks also go to all the members of the Molecular Neurobiology Laboratory at Mario Negri Institute, Milan, both past and present, for their contribution to my work and for being friends. I would particularly like to thank Dr Pietro Veglianese, Dr Novella Calvaresi and Giugliano Grignaschi for providing some of the results reported in this thesis.

Finally, I thank Mario Negri Institute for Pharmacological Research, Milan, for giving me the opportunity to undertake my Ph.D.

I dedicate this Ph.D. thesis to Maria Teresa, Gino and Simonetta.

List of publications related to this thesis

***Tortarolo M**, Crossthwaite AJ, Conforti L, Spencer JP, Williams RJ, Bendotti C, Rattray M.* Expression of SOD1 G93A or wild-type SOD1 in primary cultures of astrocytes down-regulates the glutamate transporter GLT-1: lack of involvement of oxidative stress.

J Neurochem. 2004 Jan;88(2):481-93.

***Tortarolo M**, Veglianese P, Calvaresi N, Botturi A, Rossi C, Giorgini A, Migheli A, Bendotti C.* Persistent activation of p38 mitogen-activated protein kinase in a mouse model of familial amyotrophic lateral sclerosis correlates with disease progression.

Mol Cell Neurosci. 2003 Jun;23(2):180-92.

*Bendotti C, **Tortarolo M**, Suchak SK, Calvaresi N, Carvelli L, Bastone A, Rizzi M, Rattray M, Mennini T.* Transgenic SOD1 G93A mice develop reduced GLT-1 in spinal cord without alterations in cerebrospinal fluid glutamate levels.

J Neurochem. 2001 Nov;79(4):737-46.

In the spring of 1938, when Lou Gehrig, the star baseball player of the New York Yankees, was still only 34 and at the top of his career, his level of play fell off sharply. No one yet knew the terrible truth, but Gehrig's physical decline became more evident in the off-season, and in spring training the next year it became glaringly obvious. Gehrig moved like an old man: stiffly, slowly. He stumbled, his reflexes were slow, there was little speed or power in his swing. On June 1939, doctors at the Mayo Clinic in Rochester, Minnesota, diagnosed Lou Gehrig with a very rare form of degenerative disease: amyotrophic lateral sclerosis. There was no chance: he would ever play baseball again. Not only was his career over, but his life would soon be as well. On June 2, 1941 Lou Gehrig died at the age of 37.

CHAPTER 1

OVERALL INTRODUCTION

Progressive muscular weakness affecting the motor system was a clinical condition well known to the physicians of 19th century and for years it was considered as a muscular disorder. In 1869 the famous French neurobiologist and physician Jean-Martin Charcot, studying the pathological features of this syndrome, described the characteristic alterations of the corticospinal tract and the loss of motor neurones in the bulbar nuclei and proposed the term *amyotrophic lateral sclerosis*. The term *motor neurone diseases* was introduced in the sixties to indicate a group of similar diseases of the motor system, that differed in terms of involvement of upper and lower motor neurones and of the topography of muscular weakness: amyotrophic lateral sclerosis (ALS), progressive bulbar palsy (PBP), progressive muscular atrophy (PMA), primary lateral sclerosis (PLS) and other minor syndromes. However, the term *motor neurone disease* (MND) is commonly used in the United Kingdom to indicate the ALS syndrome. In the United States, ALS is often known as *Lou Gehrig's disease* after of the great baseball player who developed the disease in the 1930s. Amyotrophic lateral sclerosis remains the most important of the motor neurone disorders, representing 85-90% of cases of this kind of pathologies

1.1 The motor system

Since motor neurone disease is manifested as a clinical condition affecting motor neurones, I shall review the principles of motor system in man.

Muscle contraction is the final event of the fine and highly elaborate motor control system. The motor pathways are pathways that originate in the motor cortex or in the brainstem and descend down the spinal cord to control the *α-motor neurones*. These large neurones in the ventral horns of the spinal cord send their axons out via the spinal roots and directly cause muscle contraction (Figure 1.1). The motor pathways can control posture, reflexes and muscle tone, as well as the conscious voluntary movements.

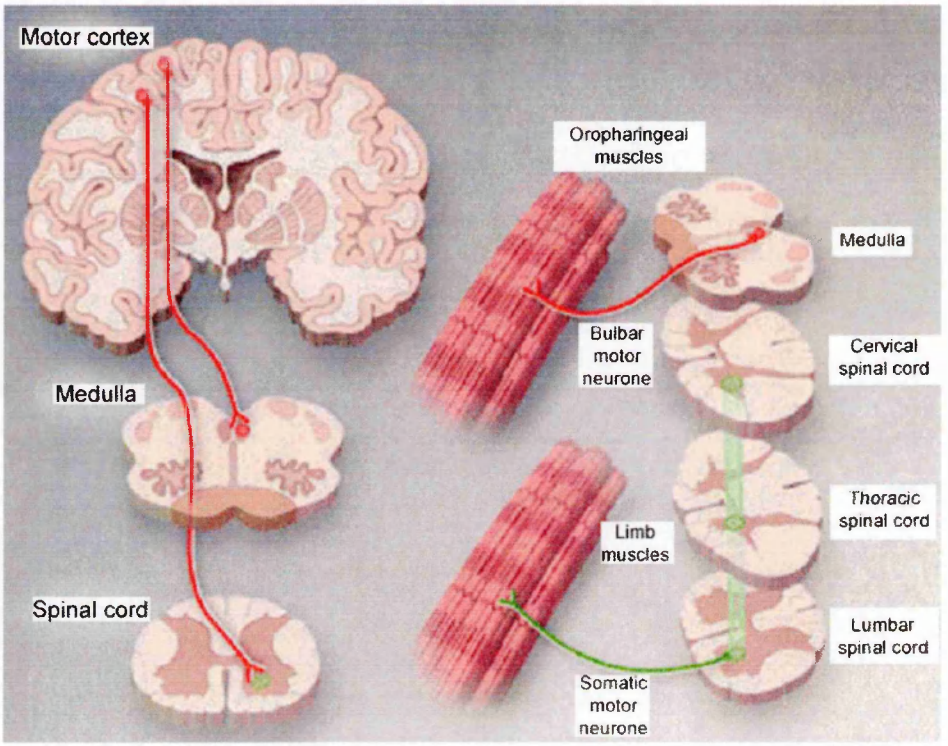

Figure 1.1: The motor system

Adapted from Rowland LP and Shneider NA, N Engl J Med., 2001

The *primary motor cortex* (also called Brodmann's area 4) is located in the precentral gyrus of the frontal lobe and receives information from a number of surrounding areas. Firing of *upper motor neurones* (UMNs) controls the *lower motor neurones* (LMNs) of the spinal cord and brainstem. The cortical areas that project to the primary motor cortex are called somatosensory cortex, prefrontal cortex and premotor areas (Brodmann's area 6), which are subdivided into the supplementary motor area (also called secondary motor cortex) and the premotor cortex. The somatosensory cortex is located in the post-central gyrus of the parietal lobe and provides information from the senses of touch and proprioception. This proprioceptive information is necessary for the proper guidance of movement. The remaining cortical areas that project to the primary motor cortex are located in the frontal lobe. Each of these regions is involved in the preparation of movement. The supplementary motor area and the premotor cortex are most active during the planning of movement, even when the movement is not executed, and are reciprocally connected to the primary motor cortex and each other. Input to the premotor cortex is primarily visual, whereas input to the supplementary motor cortex is primarily somatosensory. Each of these cortical regions is located just anterior to the primary motor cortex, with the supplementary motor cortex wrapping around into the longitudinal fissure separating the two hemispheres. Neuronal activity within the prefrontal cortex is associated, in particular, with sensory signals just preceding a movement. The prefrontal cortex receives projections from the posterior parietal cortex and projects to the secondary motor cortex and to the primary motor cortex. The prefrontal cortex may provide a mental

representation of a stimulus to be the target of a movement and in addition may make the choice to initiate a voluntary response to that stimulus. Based on the diversity of information reaching the primary motor cortex, this region controls the complex and coordinated movement of several muscles.

The primary motor cortex has a distinct group of motor neurone in layer 5 known as the *giant pyramidal cell* or *Betz cells*. However, this group of cell represents only a small portion of all the primary motor neurones in this layer. A single motor neurone in the primary motor cortex activates the contraction of a small group of skeletal muscles and control the force of contraction by varying its firing rate. Particular regions of the primary motor cortex control a particular region of the body and each region is additionally activated by adjacent regions of the cortex.

Axons from motor neurones in the primary motor cortex project downward through the brainstem to the ventral horn of the spinal cord where the activation of appropriate lower motor neurones occurs. Axons of the upper motor neurones are conveyed in the *corticospinal tract* of the pyramidal system. They descend to their destination within the lateral white matter of the spinal cord where they branch off to synapse primarily with interneurones, which play a crucial role in the final output, located within the ventral horn of the spinal segments where the lower motor neurones for the appropriate muscles are located. The corticospinal tract is divided into the lateral tract, which controls contraction of muscles in the extremities, and in the anterior tract, which controls axial and postural muscle contraction.

Lower motor neurones are located in the anterior grey matter of the ventral spinal cord and in the motor nuclei of the brainstem. Their axons directly innervate the muscle fibers.

Large lower motor neurones, called α-motor neurones, are the principal lower motor neurones innervating the muscle fibers. Medium size motor neurones, known as β-motor neurones, innervate both muscle fibers and intrafusal fibers. γ-motor neurones are small neurones innervating the intrafusal fibers only. α-motor neurones are the largest neurone types of the nervous system. They have long axons (up to 1 metre in same cases) and an extensive dendrite ramification, with dendrites that can reach 1 millimeter in length and extend well into the white matter, receiving thousands of synaptic contacts. One α-motor neurone innervates a single group of muscle fibers, generating a motor unit. Upon firing of the α-motor neuron, acetylcholine is released and binds to nicotinic acetylcholine receptors on the surface of muscle fibers, resulting in a rapid increase in intracellular calcium ion concentration, initiating the contraction. All of the muscle fibres in a motor unit contract at the same time and to their maximum. Each muscle is made up of many motor units and these motor units vary in their number of fibres (10 to 2000). The intensity of a muscle contraction therefore is determined by the number and size of the motor units activated.

1.2 Diagnosis of amyotrophic lateral sclerosis

Amyotrophic lateral sclerosis is one of the most devastating human disorders. It is an incurable fatal neuromuscular disease resulting from the selective degeneration of upper motor neurones in the motor cortex and lower motor neurones in the brainstem and spinal cord.

Diagnosis of ALS is often critical. In fact, many different clinical conditions may resemble ALS. To date, no one test or specific diagnostic marker can provide a definitive diagnosis of ALS, although the presence of upper and lower motor neurone signs in a single limb is strongly suggestive (Table 1.1). Thus, the diagnosis of ALS is primarily based on the symptoms and signs that the physician observes in the patient and on a series of tests to rule out other diseases. Criteria for clinical and pathological diagnosis have been defined during the ALS meeting held in El Escorial, Spain in 1994 and updated at Airlie House, Virginia four years later. However, these criteria unfortunately do not allow a presymptomatic diagnosis, which could be very useful in the future for effective therapeutic treatments.

Requirements for the diagnosis of ALS according to Airlie House guideline. The diagnosis of Amyotrophic Lateral Sclerosis requires:

A - the presence of:

1) evidence of lower motor neurone (LMN) degeneration by clinical, electrophysiological or neuropathologic examination,

2) evidence of upper motor neurone (UMN) degeneration by clinical examination, and

3) progressive spread of symptoms or signs within a region or to other regions, as determined by history or examination,

together with

B - the absence of:

1) electrophysiological and pathological evidence of other disease processes that might explain the signs of LMN and/or UMN degeneration, and

2) neuroimaging evidence of other disease processes that might explain the observed clinical and electrophysiological signs.

A careful history, physical and neurological examination must search for clinical evidence of UMN and LMN signs in four regions (brainstem, cervical, thoracic or lumbosacral spinal cord) of the central nervous system (CNS). Ancillary tests should be reasonably applied, as clinically indicated, to exclude other disease processes. These should include electrodiagnostic, neurophysiological, neuroimaging and clinical laboratory studies. The clinical diagnosis of ALS, without pathological confirmation, may be categorized into various levels of certainty by clinical assessment alone depending on the presence of UMN and LMN signs together in the same topographical anatomic

region in either the brainstem (bulbar cranial motor neurones) cervical, thoracic, or lumbosacral spinal cord (anterior horn motor neurones).

The terms Clinical Definite ALS and Clinically Probable ALS are used to describe these categories of clinical diagnostic certainty on clinical criteria alone:

Clinically Definite ALS

It is defined on clinical evidence alone by the presence of UMN, as well as LMN signs, in three regions.

Clinically Probable ALS

It is defined on clinical evidence alone by UMN and LMN signs in at least two regions with some UMN signs necessarily rostral to (above) the LMN signs.

Clinically Probable - Laboratory-supported ALS

It is defined when clinical signs of UMN and LMN dysfunction are in only one region, or when UMN signs alone are present in one region, and LMN signs defined by EMG criteria are present in at least two limbs, with proper application of neuroimaging and clinical laboratory protocols to exclude other causes.

Clinically Possible ALS

It is defined when clinical signs of UMN and LMN dysfunction are found together in only one region or UMN signs are found alone in two or more regions; or LMN signs are found rostral to UMN signs and the diagnosis of

Clinically Probable - Laboratory-supported ALS cannot be proven by evidence on clinical grounds. Other diagnoses must have been excluded to accept a diagnosis of Clinically Possible ALS.

Clinically Suspected ALS

It is a pure LMN syndrome, wherein the diagnosis of ALS could not be regarded as sufficiently certain to include the patient in a research study. Hence, this category is deleted from the revised El Escorial Criteria for the Diagnosis of ALS.

	Lower motor neurones	***Upper motor neurones***
Symptoms	Fatigue Weakness Cramps Twitching of muscles Incoordination	Weakness Incoordination Stiffness Slowing of distal movement
Signs	Weakness Fasciculations Suppression of reflexes Hypotonia Atrophy	Spasticity Brisk reflexes Babinski and Hoffman signs Weakness Pseudobulbar effect

Table 1.1: Lower and upper motor neurone dysfunctions

1.3 Clinical phenotype of amyotrophic lateral sclerosis

Amyotrophic lateral sclerosis is an unremitting, progressive, consistently fatal neurodegenerative disease. Upper and lower motor neurones, which control the movement of voluntary muscles, deteriorate and eventually die. When the motor neurones die, the brain can no longer initiate and control muscle movement. Because muscles no longer receive the input they need in order to function, they gradually weaken and deteriorate, producing deep atrophy of muscles.

In the beginning, ALS often displays asymmetrical symptoms and signs and may be quite focal, for example affecting the upper limbs with relative sparing of the lower limbs. The different extent and localization of involvement of motor system determines various early clinical features in different patients but ultimately, as the disorder progresses, the clinical expression of ALS is quite uniform, with extreme muscular wasting, spasticity and paralysis.

The clinical manifestation depends and varies on the basis of the combination of the UMN and LMN involvement. The different features are determined not only by the degeneration pattern but also by the stage of the disease and the body region involved.

Lower motor neurone involvement determines weakness and fatigue, associated to progressive muscular atrophy, *fasciculation* (muscular twitching and shaking of contiguous groups of muscle fibers) and *fibrillation* (muscular twitching and shaking involving individual muscle fibers acting without coordination), reduced muscle tone and absence of tendon reflex. Upper motor

neurone involvement causes weakness, incoordination, stiffness and slowing of movement, with *spasticity* (persistent contraction of muscle), increased tendon reflexes and *clonus* (alternating contractions and relaxations). An abnormal reflex commonly called *Babinski's sign* (the large toe extends upward as the sole of the foot is stimulated in a certain way) also indicates upper motor neurone damage.

The commonest initial manifestation of ALS is asymmetric distal weakness and muscular atrophy, which determine difficulty in performing and coordinating fine movements such as buttoning clothes and picking up objects. Occasionally, the involvement of proximal limb muscles at the early stage of ALS may cause difficulty in walking, climbing stairs and carrying out heavy work. A consistent and appreciable loss of strength requires the loss of about 50% of motor neurones. Before this point, compensatory reinnervation from nearby motor neurones permits a good maintenance of function, although with enlargement of motor units. At this stage, the loss of motor neurones is noticeable only through electromyography. Patients often report fasciculation, cramps and spasms.

Signs of bulbar involvement often develop during the course of the pathology but may also represent an initial feature in some cases. Bulbar motor neurone degeneration leads to difficulty in swallowing (*dysphagia*) and speaking or forming words (*dysarthria*), associated to fasciculation of the tongue. Bulbar signs are often closely related to respiratory deficit, due to the involvement of diaphragmatic muscular weakness. This leads to a poor prognosis and to a shorter life expectancy. However, limbs onset is found in 75-80% of cases and bulbar onset is evidenced in only 20-25%.

With the progression of the illness, the disease spreads to contiguous body segments. The upper motor neurone signs, which must be present in all defined case of ALS, are often quite difficult to recognize because of predominant muscle wasting determined by LMN involvement. The progressive loss of motor function results in increasing disability and paralysis, ultimately leading to a bed-bound state. Because the disease leaves cognitive abilities relatively unimpaired, patients are aware of their progressive loss of function. The usual course of ALS leads to death, occurring because of respiratory failure. In 50% of cases death occurs within 3 years from diagnosis.

"ALS is like a lit candle: it melts your nerves and leaves your body a pile of wax. Often it begins with the legs and works its way up. You lose control of your thigh muscles, so that you cannot support yourself standing. You lose control of your trunk muscles, so that you cannot sit up straight. By the end, if you are still alive, you are breathing through a tube in a hole in your throat, while your soul, perfectly awake, is imprisoned inside a limp husk, perhaps able to blink, or cluck a tongue, like something from a science fiction movie, the man frozen inside his own flesh. This takes no more than five years from the day you contract the disease."

Extract from "Tuesdays With Morrie" by Mitch Albom

1.4 Neuropathology of amyotrophic lateral sclerosis

In the last years, ultrastructural and immunohistochemical studies performed on post mortem tissues have helped to better describe the neuropathology of ALS, defining its histopathological features and giving important clues about the pathogenesis of this devastating disease. Apart from some cases of accidental death of ALS patients at early stage of the disease, the bulk of post mortem examinations are conducted on tissues representing the final stage of the pathology. As a result, the alterations observed reflect a very advanced state of neuronal degeneration and give little information about the triggering events causing the cell death. It is also true that patients have different degrees of neuronal degeneration in different areas of their central nervous system. For example, many patients with aggressive form of bulbar onset ALS at time of death often have relatively spared motor neurones in the spinal cord. However, the analysis of these groups of motor neurones has not yet given any clear indication on the events that occur early in the pathology.

The degree of degeneration observable at autopsy in the motor cortex of ALS patients is quite variable and may not be always evident, even in the presence of clear upper motor neurone signs. In the most severely affected cases, there is an obvious loss of giant Betz cells in cortical layer 5 associated with an extensive astrogliosis. However, there are not good markers to distinguish upper motor neurones and other pyramidal cell types in the cortex. Thus, the identification of the Betz cell is often based on morphological and size criteria. Large pyramidal neurones are diminished in number in the motor cortex

and in the surrounding regions somatosensory cortex, prefrontal cortex and premotor areas. Neurone cell bodies are atrophied (Kiernan and Hudson, 1991), with shorter fragmented dendrites (Hammer et al., 1979). Intracellular alterations are rarely identified in the spared Betz cells in classical ALS. Occasionally ubiquitinated neurofilament inclusions are reported. More evident lesions are observable in familial ALS (FALS) cases associated with SOD1 mutant.

Axonal degeneration of the descending corticospinal tracts results in clear demyelination of the tract. Thus, the spinal cord of ALS cases shows a typical bright pallor. An extensive gliosis is present, causing the typical sclerosis of lateral side of the spinal cord.

Loss of large motor neurones in the lower brain stem and spinal cord (lower motor neurones) is clearly observed at autopsy. As in the upper motor neurones of motor cortex, shrinkage and atrophy of cell body precede neuronal death (Kiernan and Hudson, 1991). This phenomenon is associated with alterations of axon and dendrite structure, which become thinner (Nakano and Hirano, 1987). Remaining motor neurones present several abnormalities: diffuse accumulation of phosphorylated neurofilaments is observed in the perikarya of motor neurones, especially in sporadic ALS (Hirano et al., 1984a), whereas focal accumulation is more common in familial cases (Hirano et al., 1984b; Mizusawa et al., 1989). Since phosphorylated neurofilaments are normally present only in the distal axons, this unusual distribution may indicate an altered slow axonal transport of neurofilaments in affected motor neurones. Phosphorylated neurofilaments are also packed in axonal swellings called

spheroids, together with peripherin and kinesin (Corbo and Hays, 1992; Toyoshima et al., 1998). Small spheroids, termed *globules*, are also observed in age matched controls and in normal aging nervous system but they are fewer in number and smaller than those observed in sporadic ALS patients (Hirano et al., 1984a). These features have not been described in familial ALS.

Cell bodies and proximal axons of spinal motor neurones show several types of inclusions with different shapes. Many of them are immunoreactive to *ubiquitin* (Leigh et al., 1988). This 76 amino acid polypeptide is involved in the non lysosomal ATP-dependent degradation of abnormal cytoplasmic proteins (*ubiquitin-proteasome* pathway) and in other cellular functions. The presence of ubiquitinated inclusions in the lower motor neurones is specific to ALS pathology, although characteristic inclusions in other neurodegenerative disorders (neurofibrillary tangles, Pick bodies) often are also ubiquitin immunopositive (Schiffer et al., 1991). The ubiquitinated inclusions found in ALS have been classified in two types: *skein-like* and *Lewy body-like* inclusions. Skein-like inclusions are a specific hallmark of ALS whereas Lewy body-like inclusions are not specific for ALS. Both the inclusions probably represent two different morphological stages of protein aggregations, from diffuse filamentous forms to dense and compact inclusions. Both skein-like and Lewy body-like inclusions contain tubules and filaments with diameters ranging from 15 to 25 nm as determined by electron microscopy (Murayama et al., 1989; Mizusawa et al., 1991; Schiffer et al., 1991). In skein-like arrays, ubiquitin labelling is concentrated on abnormally formed 15-20 nm filaments and neurofilament immunostaining localized on 10 nm filaments adjacent or in continuity with the

abnormal filaments (Migheli et al., 1994). Besides phosphorylated neurofilaments and ubiquitin inclusions, Lewy body-like inclusions also contain CDK5 kinase (Nakamura et al., 1997). More recently, dorfin, a RING finger-type E3 ubiquitin ligase, has also been localized in the inclusion bodies found in the motor neurones and neuronal processes of familial and sporadic ALS (Hishikawa et al., 2003).

Another type of intracellular inclusion is named *hyalin conglomerate inclusions*. They consist in large aggregates of phosphorylated and non phosphorylated neurofilaments associated with other cytoplasmic proteins and ubiquitin (Schochet et al., 1969; Leigh et al., 1989; Sasaki and Maruyama, 1991). Identified in sporadic and familial ALS, they however seem to be less specific for ALS pathology since they have been found in other neurological disorders (Sobue et al., 1990).

Bunina bodies are eosinophilic granules originally observed in familial ALS that are also found in sporadic and Guamaniam ALS. They can be considered ALS specific and they are clearly distinguishable from the other inclusion bodies. Surrounded by endoplasmic reticulum fragments and other debries, it has been hypothesized that they can originate from lysosomes (Sasaki and Maruyama, 1993).

1.5 Genetics of amyotrophic lateral sclerosis

In 90-95% of ALS cases, there is no apparent genetic linkage (sporadic ALS) but in the remaining 5-10% the disease is inherited mostly in a dominant

manner, with rare cases of recessive inheritance. The genetic form is named familial ALS or FALS. The clinical phenotype of sporadic and FALS is indistinguishable, although FALS patients do present some different features in the pathology, which are described in more detail in section 1.6.

In 1993, Rosen and colleagues reported that mutations in the gene coding for soluble, cytoplasmic enzyme *Cu,Zn superoxide dismutase* (SOD1) (locus on chromosome 21q22.11) were associated with a subset (about 15%) of familial ALS patients (Rosen et al., 1993). This landmark discovery represented an important step forward in the ALS research, permitting the creation of new experimental models to study the ALS pathology. SOD1 is an abundant protein, representing up to 2% of the soluble proteins of the brain. SOD1 is a 153 amino acid, cytoplasmic homodimer that convert superoxide, which is produced primarily as a by-product of oxidative phosphorylation in mitochondria, to water and hydrogen peroxide (Figure 1.2). Catalysis by SOD1 is mediated in two asymmetric steps by an essential copper atom, which is alternately reduced and oxidized by superoxide. The zinc atom has a structural function.

To date, more than one hundred different mutations have been identified in SOD1 gene in familial cases. The different mutations are almost entirely located on the five exons and scattered throughout the primary structure of the protein. The bulk of them determine an amino acid substitution (missense mutations). The remaining are nonsense, insertion and deletion mutations but none completely eliminate protein synthesis.

Almost all the SOD1 mutations known are inherited as a dominant trait, with the only exception of $SOD1^{D90A}$ (Andersen et al., 1995). However, it is not

clear yet how such a wide range of diverse mutations in SOD1, which is ubiquitously expressed in all the cells, can cause the selective motor neurone degeneration with no obvious clinical differences between the different mutant forms.

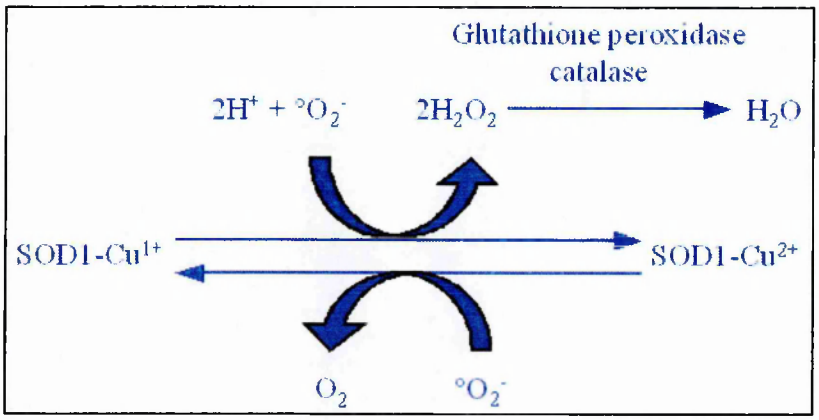

Figure 1.2: SOD1 chemistry

Normal superoxide dismutase 1 (SOD1) chemistry: SOD1-mediated dismutation of superoxide in two asymmetric steps.

It was initially proposed that the toxicity of mutated SOD1 is associated with the loss of superoxide dismutase activity. However, most mutated SOD1 forms appear to fully retain their enzymatic property. The creation of transgenic mice expressing SOD1 with some of the mutations found in the human patients, which develop a motor syndrome similar to human ALS, show that catalytic activity is unchanged or elevated (Gurney et al., 1994; Ripps et al., 1995a; Wong et al., 1995; Bruijn et al., 1997b). Furthermore, SOD1 knockout mice do not develop spontaneous motor neurone disease (Reaume et al., 1996). The

conclusion is that SOD1 mutants acquire one or more toxic properties, irrespective of the amount of superoxide dismutase activity that each of them retains.

Loci for several other genetic motor neurone disorders have been identified (Table 1.2). These include one example of a syndrome with dominant inheritance and apparently complete *penetrance* (probability of a genetic trait being expressed in the phenotype), with very juvenile onset (in the late teens) and a very slow progression of distal limb atrophy and motor neurone loss that does not reduce lifespan (ALS4). The locus has been mapped to chromosome 9q34, (Chance et al., 1998) and missense mutations (T3I, L389S, and R2136H) have been detected in the *senataxin* gene. This gene encodes a protein that has unknown function. It contains a DNA/RNA helicase domain with strong homology to human RENT1 and IGHMBP2, two genes encoding proteins known to have roles in RNA processing (Chen et al., 2004).

Two other ALS-like disorders associated with mutations, with recessive inheritance and juvenile onset, have been clearly described. Found in seven Tunisian families, one of them is characterized by initial atrophy and weakness of hands and feet, with later involvement of upper motor neurones, associated with spasticity of limbs, and long survival. The mutation locus has been localized at 15q15.22, but the affected gene has not yet been identified (Hentati et al., 1998). The second one is associated to a gene called ALS2 or *alsin*, originally mapped to chromosome 2q33, which has been found to encode a 184 KDa protein derived from 34 exons that span 80 Kb (Yang et al., 2001). To date, two deletion mutations have been discovered on this gene. The disease

related to ALS2 is distinguished by the predominance of spasticity of facial and limbs muscles. Sequence inspection of the gene reveals that the 650 amino acids of the amino-terminal of ALS2 contain all of the sequence motifs that are characteristic of guanine exchange factors (GEFs). These proteins are involved into recycle of a specific small G protein from its GDP-bound state to its GTP-state. There is no information so far about which G protein is the partner for this putative GEF. The carboxy-terminal half of ALS2 contains two further domains, which are similar to those of the Rho G-protein family that modulates dynamic actin assembly. Like SOD1, ALS2 is probably widely expressed.

Recently, a genome screening study of ALS families lacking SOD1 mutations allowed to identify a new putative locus on chromosome 16q12.1-q12.2. The region associated with disease was further refined in the major family that contributed to this result and was localized to D16S409-D16S3032, a 14.74-cM genetic interval that corresponds to a physical distance of 6.6 Mb (Abalkhail et al., 2003).

A set of small in-frame deletions or insertions in the repetitive tail domain of the large neurofilament subunit NF-H has been identified in about 1% of 1,300 sporadic ALS patients examined (Al-Chalabi et al., 1999). Search in this one domain alone has therefore found mutations in the overall patient population. They result about half as frequent as SOD1 mutations. Although the known neurofilament sequence variants are thought not to be capable by themselves of producing disease with high penetrance, it is likely that variants in neurofilaments are at least important risk factors for apparently sporadic disease.

A number of other genetic alterations have been identified, which may confer a higher predisposition to development of ALS syndrome. They include mitochondrial DNA microdeletions encoding for cytochrome-C oxidase (Borthwick et al., 1999), RNA processing errors in the glutamate transporter EAAT2 (Lin et al., 1998), an abnormal copy number of the survival motor neurone (SMN) gene (Corcia et al., 2002) and gene deletions of the chromosome 5q13-linked neuronal apoptosis inhibitory protein (NAIP) gene (Jackson et al., 1996). An increased frequency of the cytochrome P450 debrisoquine hydroxylase CYP2D6(B) allele, encoding a cytochrome P450 monooxygenase involved in drug metabolism and associated with a "poor metabolizer" phenotype, has been also described (Siddons et al., 1996).

Category	*Inheritance features*	*Chromosomal location*	*Gene identified*
ALS1	AD	21q22	SOD1
ALS2	AR	2q33-35	Alsin
ALS3	AD	Unknown	
ALS4	AD	9q34	senataxin
ALS5	AR	15q15.22	
ALS6	AD	18q21	
ALS/FT	AD	9q21-22	

AD: autosomal dominant; AR: autosomal recessive

Table 1.2: Familial ALS, known inheritance patterns

1.6 Epidemiology of amyotrophic lateral sclerosis

ALS is considered as a rare disease. However, its personal and socioeconomic impact is grater than its annual *incidence* (number of new identified patients per year). It has been calculated that considering a generation time of 20 years, one in 200 people have a family member affected by ALS. The epidemiology studies generally consider three distinct forms of the disease with different epidemiologic and pathologic characteristics: the two forms discussed above, sporadic ALS and familial ALS but also Western Pacific ALS, a form of the disease found particularly in this geographic area.

Sporadic ALS occurs in about 1-3 people per 100,000 population per year with a *prevalence* (number of surviving patients at any given time) of about 5-7 per 100,000. Typically, it strikes adults between the ages of 55 and 75. It is predominantly men who are affected, with a male to female ratio of 1.4 to 2.5. However, bulbar onset has been reported to be more frequent in female, probably due to the effect of sexual hormones on bulbar motor neurones expressing androgen receptors (Matsuura et al., 1993). People of all races and ethnic backgrounds are affected by it. The average survival for sporadic ALS patients is approximately 3 years after the onset of the disease.

Although familial ALS is almost indistinguishable from the sporadic form in terms of clinical phenotype, some differences distinguish FALS from an epidemiological point of view. FALS represent worldwide 5% to 10% of all ALS cases. Inheritance is predominantly autosomal dominant with some recessive exceptions. The average onset of FALS cases is approximately 47 years, a

decade earlier than the sporadic type. FALS occurs equally in males and females. In FALS, symptoms more frequently begin in the lower extremities compared to sporadic ALS. Once diagnosed, the familial form leads to death in 1 or 2 years, although some individuals survive 5 years. Very aggressive cases with a survival of less than 1 year have been also reported.

The incidence of ALS disease in Western pacific islands such as Guam, Rota and Micronesia, in the Kii Peninsula of Japan and in west New Guinea is approximately 100-150 fold higher than the other world regions. Although the clinical features of the Western Pacific ALS are similar to the others, this form is considered a distinct disease because it is often associated to Parkinsonism dementia, with pathological alteration resembling Alzheimer's disease (neurofibrillary tangles). This disease is not considered further in this thesis.

1.7 Experimental models of amyotrophic lateral sclerosis

Hystopathological studies performed on post mortem tissue obtained from ALS patients at autopsy may give important information about the status of motor neurones and other cells involved in the pathology at the final stage of the disease. However, they provide a poor contribution to the comprehension of the pathogenic mechanisms. Thus, the study of experimental models of ALS is necessary to investigate the triggering events occurring earlier in the pathology.

Mice carrying naturally occurring autosomal recessive mutations on unidentified genes provide animal models with motor system impairment. *PMN mice* show a progressive motor neuronopathy characterised by paralysis of the

limbs, neurogenic atrophy of muscles, axonal degeneration but with relative sparing of motor neurone cell body (Schmalbruch et al., 1991). The PMN locus has been identified on chromosome 13 but the gene involved is not known (Brunialti et al., 1995).

The *wobbler mice* represent another model of motor neurone disease (Mitsumoto and Bradley, 1982). They show a progressive forelimb weakness associated with proximal axonal degeneration and vacuolar changes within the anterior horn cells of the spinal cord with a little involvement of the brain. In this case, the gene responsible for this syndrome has been mapped on chromosome 11 but it has not been identified yet (Kaupmann et al., 1992).

Mice showing neuromuscular degeneration, with autosomal recessive mutation localized on the gene coding for the ATPase/DNA helicase have been described (Cook et al., 1995; Cox et al., 1998). Called *nmd mice*, they present rapidly progressive hindlimb weakness and motor neurone cell body degeneration.

Another spontaneous animal model of motor dysfunction is represented by *mnd mice*, considered in the past a model of ALS. These mice develop a late onset motor neurone degeneration characterized by progressive deterioration of motor function more severe in the lumbosacral than in the other regions, as well as variable pathology in the lower cranial nerves (Messer et al., 1987). However, the number of choline acetyltransferase (ChAT) immunopositive lumbar motor neurones are not different from normal mice (Mennini et al., 2002). The mnd mice carry a spontaneous homozygous mutation in the coding region of the gene *Cln8* belonging to the family of neuronal ceroid lipofuscinose-

related genes (CLNs) (Ranta et al., 1999). Thus, the presence of abnormal autofluorescent cytoplasmic inclusions rich in lipofuscin found in neurones but also in many other somatic organs, makes these animals a useful model for human neuronal ceroid lipofuscinosis rather than for ALS (Bronson et al., 1993).

Recently, Ahmad-Annuar and colleagues have described another mutant mouse model of motor neurone disease, the legs-at-odd-angles (*Loa*) mutant. In these mice mutations in the cytoplasmic dynein heavy chain gene (Dnchc1) cause motor neurone degeneration. Mice exhibiting the Loa phenotype suffer progressive loss of locomotor function and homozygous animals have neuronal inclusion bodies that are positive for SOD1, CDK5, neurofilament and ubiquitin proteins (Ahmad-Annuar et al., 2003). As this phenotype reproduces some aspects of human motor neurone degeneration disorders, it is possible that dynein may be a causative gene or susceptibility factor in human motor neurone disease. However, to date, no association between familial motor neurone disease and the genotypes presented by Loa mice has been found.

All these mice strains offer several advantages in the study of early phenomena occurring in a motor neurone disorder, involving a progressive and naturally occurring impairment of motor system. However, many features are quite dissimilar from human ALS pathology. Moreover, it is possible that the genetic alterations affecting these mice (if known) and the associated biochemical defects (if known) do not contribute to the human disease. Thus these models are not particularly reliable for testing therapeutic intervention or uncovering disease mechanisms, althought the study of the pathology occurring

in these mouse models may contribute to the discovery of still unknown risk factors for human ALS.

In 1993, Rosen *et al.* reported that missense mutations in the gene encoding Cu/Zn superoxide dismutase (SOD1) were associated with a fifth of familial cases of ALS (Rosen et al., 1993). This landmark discovery radically revolutionised the experimental approach for the study of ALS. In fact, for the first time it was possible to generate an animal model closely resembling the human disorder, using transgenic technology. This technique was used to insert in mouse genome the SOD1 gene carrying some of the mutation found in the FALS patients. Investigators have generated different lines of these transgenic mice overexpressing human SOD1 (hSOD1) with G93A, G37R and G85R mutation (substitution) (Gurney et al., 1994; Wong et al., 1995; Bruijn et al., 1997b) or mouse SOD1 (mSOD1) with G86R mutation (substitution) (Ripps et al., 1995b). Rats expressing $hSOD1^{G93A}$ have been also generated (Howland et al., 2002). All these animals develop a motor syndrome characterized by the selective motor neurone death. They show normal motor functions in the early phase of their life but then develop a progressive weakness, especially starting in the hind limbs, which eventually results in paralysis and death. The age of onset, the duration and several pathological features of this motor dysfunction show some differences in the different transgenic animals strains. However, all these transgenic mice and rats provide an excellent and suitable *in vivo* model resembling human ALS.

Mice expressing $hSOD1^{G85R}$ develop a late onset but very aggressive (2 weeks from the first symptoms to the death) pathology, even with a low

expression of the transgene. Motor neurones and astrocytes present inclusions immunopositive for ubiquitin and SOD1 (Bruijn et al., 1997b).

Transgenic mice expressing low level of hSOD1^{G37R} mutant show a motor disease restricted to lower motor neurones, whereas higher copy number causes more severe abnormalities and affects a variety of other neuronal populations. The most obvious cellular abnormality is the presence in axons and dendrites of membrane-bounded vacuoles, which appear to be derived from degenerating mitochondria (Wong et al., 1995).

Transgenic mice that express mutant SOD1^{G93A} develop motor system disease prevalently affecting motor neurones. Ultrastructural and microscopical analysis reveals that the earliest pathological feature in these mice is vacuolization of large neurones of the anterior horns of the spinal cord (Bendotti et al., 2001a). It has been hypothesised that these vacuoles originate from dilation of rough endoplasmic reticulum and from degenerating mitochondria. At the end stage, motor neuronal depletion is evident and hyaline, filamentous inclusions immunopositive for ubiquitin and neurofilaments are present in some of the surviving neurones (Gurney et al., 1994; Migheli et al., 1999).

It is noteworthy that transgenic mice overexpressing the wild type form of human SOD1 (hSOD1^{wt}) do not develop any motor symptoms or altered phenotype. However, some neurodegenerative changes consisting of swelling and vacuolization of mitochondria, axonal degeneration of some long fiber tracts and a moderate loss of spinal motor neurones at two years of age, have been reported (Jaarsma et al., 2000). Thus, hSOD1^{wt} transgenic mice have demonstrated that mutations on SOD1 gene are necessary to induce an evident

motor disease. Therefore, transgenic technology have directly clarified that SOD1 mutants cause pathology because of gain of function and not because of the loss of SOD1 catalytic properties. Moreover, expression of mutant forms of SOD1 restricted to astrocytes or neurones is not sufficient to cause motoneurone degeneration in transgenic mice (Gong et al., 2000; Pramatarova et al., 2001; Lino et al., 2002). These reports suggest that simultaneous alterations in both neuronal and astroglial cells are necessary to induce the pathology in ALS mice.

More recently, the transgenic technology has also permitted the creation of transgenic rats expressing the G93A mutant of SOD1. Motor neurone disease in these animals depends on high levels of mutant SOD1 expression. Disease onset in $SOD1^{G93A}$ rats is quite early and disease progression is very rapid (11 days to reach the end stage). Pathological abnormalities include vacuoles initially in the lumbar spinal cord and subsequently in more cervical areas, with inclusion bodies that stained for SOD1, Hsp70, neurofilaments and ubiquitin. Vacuolization and gliosis are evident before clinical onset and before motor neurone death in the spinal cord and brainstem (Howland et al., 2002).

Despite the existence of reliable *in vivo* models of motor neurone degeneration associated with human ALS, *in vitro* approaches are also very useful since they offer an easier manipulation and study of a simpler system. For example, gene transfection or pharmacological study of biochemical pathways in isolated cell populations may be extremely useful in elucidating intracellular mechanisms underling the disease and the exact timing of biochemical events, in a way that is not always realisable *in vivo*. Neuronal and

glial primary cultures, motor neurone like-cell line and organotypic slices therefore provide important tools to obtain information, which combined with data from *in vivo* studies, will hopefully help to find new therapeutic strategies for treatment of ALS.

1.8 Pathogenetic hypotheses in amyotrophic lateral sclerosis

To date, the mechanism(s) underling the motor neurone death in ALS still remains unknown, even in FALS where single gene mutations have been identified. The crucial point, which much research is focused on, is to clarify why and how the disease selectively affects motor neurones. In addition, the degeneration of motor neurones occurs in a progressive way, starting from adulthood. This suggests the existence of one or more triggering phenomenon that apparently strikes the motor system in a particular life period. Studies performed on human ALS autopsy samples or on transgenic mice expressing ALS linked SOD1 mutations during the presymptomatic stage and the whole course of the disease, have suggested the involvement of various processes as triggering (primary) or secondary events in ALS pathology. Thus, most researchers consider ALS as a multifactorial disease where many different alterations contribute to death of motor neurones. They include oxidative damage, mitochondrial dysfunction, alteration of cytoskeletal structure, formation of aggregates and excitotoxicity.

1.8.1 Oxidative damage

The role of oxidative stress as primary or secondary event in the pathogenesis of ALS still remains controversial. Increase of oxidative damage markers such as protein carbonyl adducts, lipid peroxidation and DNA damage, have been reported in human patients affected by both sporadic and inherited forms of ALS (Beal et al., 1997; Ferrante et al., 1997b; Liu et al., 1999) and in a transgenic mouse model of the disease (Ferrante et al., 1997a; Andrus et al., 1998; Liu et al., 1998). However, in other studies, no significant differences in markers of oxidative damage associated with the expression of SOD1 mutants were found (Shaw et al., 1995a; Bruijn et al., 1997a). Evidence of increased oxidative insult has been provided more consistently in sporadic ALS patients (Shaw et al., 1995a; Ferrante et al., 1997b; Pedersen et al., 1998).

Since no changes in the development of the mutated SOD1 mediated disease have been found in transgenic mice following either removal or elevation of wild type SOD1 (Bruijn et al., 1998), this suggests no direct involvement of the activity of SOD1 in oxidative damage generation.

Concerning the familial forms of ALS and SOD1 mutant transgenic mice, it has been hypothesized that a possible source of oxidative insult may be represented by the gain of toxic function of mutated SOD1 (Cleveland and Rothstein, 2001). Yim and co-workers showed that mutations of SOD1 protein can decrease its K_m for hydrogen peroxide (Yim et al., 1996; Yim et al., 1997). The use of hydrogen peroxide as a substrate by the reduced SOD1-Cu^+ form might produce the extraordinarily reactive hydroxyl radical (OH^-) leading to a

cascade of peroxidation (Wiedau-Pazos et al., 1996). On the other hand, other evidence does not support this hypothesis. Singh and colleagues demonstrated that a significant fraction of 5,5'-dimethyl-1-pyrrolline N-oxide (DMPO)/·OH formed during the reaction of SOD1 and familial ALS SOD1 mutants with hydrogen peroxide (H_2O_2) is derived from the incorporation of oxygen from water due to oxidation of DMPO to DMPO/·OH, presumably via DMPO radical cation. However, no differences were detected between wild type and mutant form of SOD1, (Singh et al., 1998).

Beckman and collaborators proposed that an altered folding of the enzyme caused by the mutations, might determine a grater access of abnormal substrates such as peroxinitrite ($^{-}$ONOO) to the catalytic copper site. This could lead to aberrant tyrosine nitration and numerous toxic events (Beckman et al., 1993).

Another hypothesis suggests that mutations may reduce the zinc bound allowing a rapid reduction of mutant SOD1 to the Cu^{1+} form by abundant intracellular reductants. The reduced SOD1 mutant would then run the normal catalytic step backwards, converting oxygen to superoxide. The superoxide so produced would react with nitric oxide producing peroxynitrite, which would promote intracellular damage, including protein nitration (Estevez et al., 1999).

The time course of accumulation of oxidative damage relative to disease onset and progression in ALS patients is not known. Even if oxidative damage is secondary and does not initiate toxic events, it is probable that oxidative stress contributes significantly to the neuronal death in ALS. Treatment with the antioxidant vitamin E (alpha-tocopherol) slowed down the onset and

progression of paralysis in transgenic mice expressing SOD1 carrying G93A mutation (Gurney et al., 1996). However, a clinical trial carried out on ALS patients with the same drug did not ameliorate survival or motor function (Desnuelle et al., 2001).

1.8.2 Mitochondrial dysfunction

Swollen mitochondria were observed in the motor neurones of transgenic mouse lines carrying the G93A (Dal Canto and Gurney, 1995; Bendotti et al., 2001a) or G37R (Wong et al., 1995) mutations at the early stage of the disease. They were also seen in the distal part of motor axons of phrenic and sciatic nerves in $SOD1^{G93A}$ mice before the onset of the pathology (Bendotti et al., 2001a). Decreases of complexes I and IV of the mitochondrial respiratory enzymes were reported in the spinal cord and brainstem homogenates of the same transgenic mouse line before clinical symptoms (Browne et al., 1998). Accumulation of $SOD1^{G93A}$ in swollen mitochondria of transgenic mice has been showed (Higgins et al., 2002) and there is recent evidence that shows that mutant SOD1 is selectively recruited by spinal cord mitochondria (Liu et al., 2004). It has been reported that $SOD1^{G93A}$ induces alterations of mitochondrial functions in transgenic mice and in NSC-34 motor neuron-like cells (Liu et al., 2002; Mattiazzi et al., 2002). These data suggest that mitochondrial alteration may be an early pathogenetic event in ALS. Energetic metabolism failure or proapoptotic release of cytochrome-C may trigger intracellular cascades that lead to motor neurone death. These alterations may be the result of changes in

mitochondrial permeability, induced by increased Ca^{2+} influx through glutamatergic receptors, and/or by intracellular increase of free radicals induced by mutant SOD1.

1.8.3 Cytoskeletal alterations

The idea that cytoskeleton abnormalities may play a role in ALS pathology arises from early reports of neurofilament accumulations in the cell bodies and proximal axons of motor neurones of both sporadic and familial ALS (Hirano et al., 1984a; Hirano et al., 1984b). Subsequently, aberrant assembly of neurofilaments in motor neurones has been established as a hallmark of the disease. Data showing that transgenes that encode mutant neurofilament subunits cause the selective degeneration and death of motor neurones in mice, lead to the hypothesis that damage to neurofilaments is directly involved in the pathogenesis of ALS (Cote et al., 1993; Xu et al., 1993). However, it has not yet been clarified whether neurofilament disorganisation represents a secondary product of pathological processes or whether it directly contributes to motor neurone death.

Several recent studies on transgenic mice have demonstrate that neurofilament content and organization strongly influence motor neurone disease induced by mutant SOD1 (Couillard-Despres et al., 1998; Williamson et al., 1998; Couillard-Despres et al., 2000; Kong and Xu, 2000). Eliminating neurofilaments by deletion of the NF-L subunit increases the survival of SOD1 mutant mice. Enhancing the expression of the NF-L or NF-H subunits slows

SOD1 mutant-mediated disease. In these studies transgenic mice showed increased amounts of neurofilament subunits in motor neurone cell bodies and reduced axonal neurofilament content. The protective effects of increased NF-H content in perikarya may be due to the ability of neurofilaments to "buffer" against a cascade of aberrant and harmful events in the cell body (Couillard-Despres et al., 1998). Since one of the earliest cellular abnormalities in motor neurones of mutant SOD1 mice is the reduction of slow axonal transport, the cosequent accumulation of neurofilaments in perikarya might represent a reactive process to counterbalance the toxicity of the SOD1 mutants (Williamson and Cleveland, 1999).

Al-Chalabi and colleagues have identified a set of small in-frame deletions or insertions in the repetitive tail domain of the NF-H neurofilament subunit in about 1% of sporadic ALS patients (Al-Chalabi et al., 1999). Although the known neurofilament variants cannot provoke by themselves motor neurone disease, the evidence strongly indicates that variants in neurofilaments may represent at least important risk factors for sporadic disease.

1.8.4 Protein aggregation and proteasome failure

Another hypothesis formulated about the pathogenesis of ALS concerns the propensity of SOD1 mutants to aggregate into cytoplasmic inclusion bodies. Aggregates intensely immunoreactive to SOD1 were detected in motor neurones and astrocytes of mice expressing mutant SOD1 as well as in human ALS cases linked to SOD1 (Bruijn et al., 1998). Johnston et al. showed that the

aggregation of SOD1 into insoluble high molecular weight complexes is an early event occurring in $SOD1^{G93A}$ mice (Johnston et al., 2000). These aggregates develop before the onset of clinical symptoms. In $SOD1^{G85R}$ mice they represent the first pathological sign of disease, increasing in number during disease progression (Bruijn et al., 1997b). The SOD1 aggregates have been classified in two classes. The first is represented by aggregates detectable by conventional histological stains and are characterized by intense and localized SOD1 immunoreactivity throughout the inclusions or, less frequently, only at the periphery of them. The second type includes cell body deposits that are more diffusely distributed. Misfolded SOD1 aggregates cannot be dissociated, even with strong detergents and reducing agents. Their harmful effects could result from altered catalytic activity mediated by the misfolded aggregated mutants, the cosequestering of essential cellular proteins such as chaperones and/or overload of the ubiquitin proteaosome pathway, which degrades damaged proteins (Cleveland and Rothstein, 2001). Consistent with the latter hypothesis, the aggregates from transgenic mice and human ALS patients are markedly immunopositive for ubiquitin (Stieber et al., 2000; Watanabe et al., 2001; Bendotti et al., 2004; Kabashi et al., 2004). Since one of the roles of ubiquitin is to label and target misfolded and no more active proteins to the proteasome machinery, it has been hypothesized that proteasome activity could be inhibited by SOD1, leading to accumulation of aberrantly folded forms of SOD1 and other proteins (Cleveland and Rothstein, 2001). However, it is not yet clear whether these aggregates are central to disease pathogenesis, harmless by-products, or potentially beneficial through the sequestration of abnormal proteins.

1.8.5 Inflammation

Neuroinflammatory changes are found in several neurodegenerative disorders such as Alzheimer's and Parkinson's disease (McGeer and McGeer, 2003; McGeer and McGeer, 2004). An increasing body of evidence suggests the involvement of inflammatory processes also in ALS. Accumulation of reactive microglia and astrocytes have been documented in the spinal cord and motor cortex of ALS patients and animal models of the disease (Kawamata et al., 1992; Hall et al., 1998), representing an important cellular clue about the existence of neuroinflammation processes occurring in motor neurone diseases. Elevated levels of cyclooxygenase 2 (COX-2), a highly inducible enzyme related to inflammation, reported in the spinal cord of human patients and transgenic ALS mice confirm these findings (Almer et al., 2001; Yasojima et al., 2001). Upregulation of proinflammatory factors before the development of motor neurone impairment in the $SOD1^{G93A}$ transgenic mice as well as the increasing of immune activation as disease progresses suggests that immune-inflammatory mechanisms could also contribute to the triggering of the disease (Alexianu et al., 2001). In particular, TNFα mRNA is increased in the spinal cord of $SOD1^{G93A}$ mice at early stage of the pathology (Elliott, 2001). The level of TNFα has also been shown to be increased in the blood of human ALS cases (Poloni et al., 2000). In addition, interleukin-6 is also upregulated in the spinal cord of $SOD1^{G93A}$ mice (Hensley et al., 2003) as well as in the cerebrospinal fluid of ALS patients (Sekizawa et al., 1998). Several inflammatory cytokines

can regulate and be regulated by the mitogen activated protein kinase p38 (p38MAPK) (Adams et al., 2001; Barone et al., 2001a). Recently, this MAP kinase has been suggested to be implicated in ALS pathology. Motor neurones in culture have shown a specific sensitivity to death pathways involving the p38MAPK cascade (Raoul et al., 2002). Treatment with minocycline, a second-generation tetracycline that, among other effects, seems to inhibit the activation of p38MAPK, delays the onset of motor neurone degeneration and increases the life span of $SOD1^{G37R}$ mice, diminishing the p38MAPK activation in reactive microglia (Kriz et al., 2002). Since activation of p38MAPK has been related to excitotoxic events and expression of AMPA receptors (Giardina and Beart, 2002; Rivera-Cervantes et al., 2004), it is possible that inflammatory processes and glutamate metabolism alteration may be linked in ALS pathology. This hypothesis will be discussed in more detail in chapter 7.

1.8.6 Excitotoxicity

Glutamate-induced excitotoxicity is considered another major mechanism that may contribute to the aetiology of ALS. An over-stimulation of neuronal glutamate receptors can cause neurone death via increases in cytosolic free calcium and activation of death cascades such as those involving mytogen activated protein kinase pathways. This phenomenon may be exacerbated by regulation of glutamatergic receptor activity or subunit composition, which can render them more permeable to Ca^{2+} and Zn^{2+}. Glutamate transporters play an important role in preventing an aberrant activation of these receptors removing

glutamate from synaptic cleft. Thus, changes in the equilibrium of this system may result in harmful events to motor neurones in ALS.

Excitotoxicity and the valuation of its potential role in ALS pathology has been the target of the experiments performed in this thesis. Thus, in the next section, I will review this topic in more detail.

1.9 Glutamatergic neurotransmission in the motor system and evidence concerning the role of excitotoxicity in amyotrophic lateral sclerosis

1.9.1 Glutamate neurotransmission

Glutamate is the most abundant and important excitatory neurotransmitter of the mammalian central nervous system. One fifth of the total glutamate, which is predominantly involved in metabolic processes of the cells, is stored in synaptic nerve terminals to be used as chemical mediator of nerve impulses by the glutamatergic pathways in the CNS. These are represented by numerous local circuits in different nervous system areas such as cortex, hippocampus, cerebellum, spinal cord and many others. Glutamate is also the principal excitatory neurotransmitter utilized by corticopontine, corticothalamic, corticobulbar and corticospinal tracts. Glutamatergic inputs to motor neurones principally derive from the descending corticospinal pathways and from spinal cord excitatory interneurones (Heath and Shaw, 2002).

During the normal glutamatergic neurotransmission, glutamate is released from presynaptic terminals in a calcium-dependent manner in response to

depolarization of the membrane. Glutamate crosses the synaptic cleft to bind and activate postsynaptic receptors. Glutamate receptors are classified in two groups: ionotropic receptors, formed by ion channels and metabotropic receptors, linked to G-proteins.

The glutamatergic signal is rapidly termined by the action of glutamate transporters that are mainly located on surrounding astrocytes. Glutamate transporters remove glutamate from the synaptic cleft. Within the astrocytes, glutamate is converted in glutamine by glutamine synthetase or metabolized to α-ketoglutarate. Glutamine is then exported from astrocytes and taken up by nerve terminals by SAT1 and SAT2 transporters, where it is used as precursor of the neurotransmitter glutamate by the action of phosphate-activated glutaminase, completing the recycling process (Laake et al., 1995).

1.9.2 Excitotoxic process

Excitotoxicity, which was first described by Olney in the 1970s (Olney et al., 1975), involves the activation of glutamate receptors in the central nervous system. High concentrations of glutamate, or neurotoxins acting at the same receptors, cause cell death through excessive receptor activation. Increased amount of glutamate in the synaptic cleft can arise from impaired glutamate uptake or from augmented release of glutamate from the nerve terminals. Molecular properties and localization of the different glutamate receptor subtypes can also influence the glutamate-mediated neurone degeneration. Moreover, the activation of intracellular pathways downstream the receptor

overstimulation or the subsequent activation of other ion channels may contribute to the death process. The molecular mechanisms involved in glutamate-mediated neuronal death are however not yet completely elucidated but several pathways have been shown to contribute to the toxic effects such as activation of Ca^{2+}-dependent enzymatic pathways, increased generation of intracellular free radicals through the aberrant activation of arachidonic acid cascade, xanthine oxidase and nitric oxide synthase, and the competitive interference with cystine uptake which lead to glutathione depletion (Heath and Shaw, 2002).

It is well established that one of the key mechanisms underlying the neuronal injury during the excitotoxic event involves the disregulation of calcium homeostasis. Under normal conditions, calcium levels control numerous intracellular processes. For this reason, neurones have a complex homeostatic machinery for calcium including calcium binding proteins (e.g parvalbumin and calbindin), mechanisms for sequestration within cellular compartments (endoplasmic reticulum and mitochondria) and membrane transporters that maintain the calcium intracellular concentration below 0.1 μmol/l (Heath and Shaw, 2002; Arundine and Tymianski, 2003). During the excitotoxic process, a first entry of sodium and chloride ions as a result of depolarization, is followed by an influx of calcium into the neurone through the ion channel of NMDA and GluR2-lacking AMPA receptors and also through voltage gated calcium channels and sodium-calcium exchange proteins. NMDA receptors have long been considered to be important in the generation of excitotoxic damage but it is now clear that excitotoxicity can result from activation of AMPA receptors,

particularly during chronic exposure to glutamate. AMPA receptors that not include GluR2 subunits in their molecular structure result highly permeable to calcium. In fact, GluR2 has a functional dominance in controlling the calcium influx due to a positively charged arginine located in the pore channel of the receptor that prevent calcium from entering. As a result, it is probable that neurones that express calcium-permeable AMPA receptors (do not express GluR2) are more susceptible to glutamate toxicity.

Upon excessive glutamate stimulation, the calcium concentration inside the cell raises to a critical level, because of the massive Ca^{2+} influx through over-activated glutamate receptors and/or calcium release form intracellular compartments. This causes the generation of free radicals, the transcriptional activation of specific cell death cascades and the activation of a variety of calcium-dependent enzymes such as lipases, phospholipases, endonucleases, protein kinase C, nitric oxide synthase and many others, which in turn lead to cell degeneration and death (Arundine and Tymianski, 2003).

1.9.3 Excitotoxic hypothesis and ALS

Excitotoxic damage has been associated to a wide range of neurological disorders. Excessive activation of glutamate receptors is believed to contribute to neuronal death after several insults including ischemia, trauma and epileptic seizure. Excitotoxicity might be also involved in the aetiology of chronic neurodegenerative pathologies such as Alzheimer's disease, Huntington's chorea and AIDS encephalopathy. Some disorders affecting the motor system

have been linked to glutamate-mediate neuronal death, suggesting a possible role of altered glutamatergic neurotransmission also in motor neurone diseases. The ingestion of food contaminated with domoic acid, a tricarboxylic acid similar to the glutamate receptor agonist kainic acid, causes various neurological symptoms. Among these, pure motor or sensorimotor neuropathy has been reported (Teitelbaum et al., 1990). *Lathyrism*, a chronic disease that affects predominantly cortical upper motor neurones, occurs as a result of the ingestion of β-*N*-oxalylamino-L-alanine (BOAA), a glutamate analogue (Ludolph et al., 1987; Ludolph and Spencer, 1996).

The excitotoxic hypothesis proposed for ALS arises from several studies indicating a disgregulated glutamate metabolism in ALS cases. Levels of glutamate was found significantly elevated in the plasma (Plaitakis and Caroscio, 1987) and in the cerebrospinal fluid (CSF) (Rothstein et al., 1990) of ALS patients. However, other studies did not confirm these results (Perry et al., 1990; Camu et al., 1993; Shaw et al., 1995b). Interestingly, extracts from plasma and CSF of ALS patients resulted toxic to cultured neurones (Roisen et al., 1982; Couratier et al., 1993; Cid et al., 2003) and this toxicity was abolished by AMPA receptor antagonists (Couratier et al., 1993; Couratier et al., 1994). However, a similar study could not reproduce a similar effect on motor neurones in culture (Iwasaki et al., 1995). Glutamate content was found to be reduced in several brain regions and in the spinal cord of the ALS patients (Perry et al., 1987). Furthermore, riluzole, which is the only drug officially approved for the treatment of ALS, is proposed to reduce damage to motor neurones by inhibiting the release of glutamate (Doble, 1996).

Taken together, these observations suggest that glutamate system may be disturbed at least in a subset of ALS patients, because of an aberrant metabolism or a failure in glutamate uptake capability, leading to raised extracellular levels of glutamate and reduced levels within CNS tissue. Moreover the fact that AMPA receptor antagonists can block the neurotoxic effect of CSF and plasma on neurones and delay the disease progress in ALS mice (Canton et al., 2001; Van Damme et al., 2003), suggests a possible role played by of these receptors. The AMPA receptor and glutamate transporter involvement in ALS will be widely discussed in chapter 3 and chapter 6 respectively.

1.10 The therapy for amyotrophic lateral sclerosis

To date, no cure has been found yet for ALS. However, in early 1996 the Food and Drug Administration (FDA) approved the first and the only official drug treatment for the disease: riluzole (Miller et al., 1996). Riluzole is believed to reduce damage to motor neurones by inhibiting the release of glutamic acid, considered an important detrimental factor involved in ALS pathology. This effect may be partly due to inactivation of voltage-dependent sodium channels on glutamatergic nerve terminals, as well as activation of a G-protein-dependent signal transduction process. Riluzole also blocks some of the postsynaptic effects of glutamate by non competitive blockade of N-methyl-D-aspartate (NMDA) receptors (Doble, 1996). Clinical trials with ALS patients showed that riluzole prolongs survival by several months, particularly in those patients with

difficulty in swallowing. The drug also extends the time before a patient needs ventilation support, prolonging the period spent within a less severe stage of illness (Riviere et al., 1998). Riluzole does not reverse the damage already done to motor neurones but may reduce further neuronal loss, as suggested by a study that used proton density magnetic resonance spectroscopy (Kalra et al., 1998).

This first disease-specific therapy offers the hope that new medications or combinations of drugs may one day slow the progression of ALS. Thus, plenty of clinical trials have been organized and are still running to test on human patients drugs that have shown effects on neuronal survival in experimental models, in the attempt to slow the progressive deterioration of motor function in people affected by ALS.

It has been hypothesized that neurotrophic factors may have a positive impact on neuronal toxicity and slow the progression of the disease. In particular, IGF-1 is a neurotrophic factor essential for normal development of the nervous system and shows protection of motor neurones in animal models and cell culture systems. Some clinical trials using recombinant human IGF-1 have been carried out. However, only one of two clinical studies performed in North America showed improvement of mortality rate and functional decline (Lai et al., 1997), whereas an European protocol failed to find any benefit on ALS progression (Borasio et al., 1998). In another study, Brain Derived Neurotrophic Factor (BDNF) was administered as a subcutaneous preparation. Although the results showed that BDNF had no significant benefit in ALS, it was well tolerated and few side effects were observed. Thus, two further trials of BDNF

were performed. A second 12 month trial where higher doses of BDNF were administered under the skin was initiated in North America. At the same time a third intrathecal BDNF study was commenced in Europe and North America. In this trial BDNF was administered directly into the cerebrospinal fluid to allow the drug to reach higher concentrations in the central nervous system, overcoming the blood brain barrier. Both the sub-cutaneous and intrathecal BDNF studies were halted as no improvements in survival were found (Clinical Trial Summary, Motor Neurone Disease Association Web site).

It has been reported that creatine improves the function of mitochondria and that has a neuroprotective effect in laboratory animals and in ALS transgenic mice in particular (Klivenyi et al., 1999). Thus, several clinical studies testing the effect of treatment with creatine on ALS patients were recently carried out. Creatine has not demonstrated benefit for people with ALS (Shefner et al, 14th International Symposium on ALS/MND meeting Milan, Italy, 2003).

Enrolment for phase III trial to test the promising tetracycline antibiotic minocycline has been recently opened. Minocycline has been shown to protect neurones and reduce cell death prolonging survival in animal models of stroke, trauma, Huntington's disease, Parkinson's disease (Yrjanheikki et al., 1998; Yrjanheikki et al., 1999; Chen et al., 2000; Wu et al., 2002) and in two different transgenic models of ALS (Kriz et al., 2002; Zhu et al., 2002b). The mechanisms of action of this drug is not fully understood but evidence suggests that it can inhibit the activity of caspase-1, caspase-3, inducible form of nitric oxide synthetase (iNOS), microglia activation, p38 mitogen activated protein

kinase (p38MAPK) as well as the release of cytochrome-C by mitochondria (Tikka et al., 2001; Zhu et al., 2002b).

Several other drugs have been tested in numerous clinical trials but unfortunately no one showed so far significant improvements of motor function impairment and life expectation. Novel areas of therapy are under investigation in animal models, including the vascular endothelial growth factor (VEGF), whose lack induces motor neurone degeneration (Oosthuyse et al., 2001), leukemia inhibitory factor (LIF), whose administration prolongs survival in $SOD1^{G93A}$ transgenic mice (Azari et al., 2001) and the use of stem cells (Silani et al., 2002).

Nevertheless, despite the large number of clinical trials testing many different drugs and the massive effort produced to investigate the cellular mechanisms involved in the selective motor neurone degeneration, to date ALS still remains orphan of an effective therapy.

1.11 Overall aim of the thesis

The aim of this thesis is to carry out a study that may allow to understand further the mechanisms that trigger or contribute to the development of ALS pathology. In particular, I have investigated the excitotoxic hypothesis, focusing on the possibility of development of novel therapeutic strategies.

Specific aims of this thesis have been:

to investigate whether there are early changes in subunit composition of glutamatergic AMPA receptor in the motor neurones of $SOD1^{G93A}$ transgenic ALS mice, which might explain an increased susceptibility of these cells to glutamate excitotoxicity.

to evaluate the effect of chronic treatment with a new AMPA receptor antagonist on symptom development and survival in $SOD1^{G93A}$ transgenic ALS mice, to determine whether AMPA receptor activation contributes to disease progression.

to investigate whether zinc ions may be involved in excitotoxicity to motor neurones and whether motor neurones may be more vulnerable to zinc toxicity than other neurones because of a different expression of a specific zinc transporter.

to evaluate whether there are deficits in expression of glial glutamate transporters in $SOD1^{G93A}$ transgenic ALS mice and to determine whether $SOD1^{G93A}$ can regulate glutamate transporter expression and function in primary astrocyte cultures.

to investigate the activation of p38MAPK pathway in $SOD1^{G93A}$ transgenic ALS mice to clarify whether its activation may be involved in ALS pathology and in regulation of AMPA receptor activity in particular.

CHAPTER 2

METHODS

(General procedures)

2.1 Animals

Procedures involving animals and their care were conducted in according to the institutional guidelines that are in compliance with national (D.L. no. 116, G.U. suppl. 40, Feb. 18, 1992, Circolare No.8, G.U., 14 luglio 1994) and international laws and policies (EEC Council Directive 86/609, OJ L 358, 1 DEC.12, 1987; NIH Guide for the Care and use of Laboratory Animals, U.S. National Research Council, 1996). The animals were housed under standard conditions (22 ± 1°C, 60% relative humidity, 12 hour light/dark schedule), 3-4 per cage, with free access to food (Altromin, MT, Rieper) and water.

At the Mario Negri Institute we have developed a colony of transgenic mice originally obtained from Jackson Laboratories (B6SJL-TgNSOD-1-G93A-1Gur) expressing about 20 copies of mutant human SOD1 with a Gly 93 Ala substitution ($SOD1^{G93A}$) or wild type human SOD1 ($SOD1^{wt}$) on a C57BL/6 mice strain. Mice expressing $SOD1^{G93A}$ (Figure 2.1) develop the first signs of muscular dysfunction around two months of age, with an impairment of the evoked response tested electromiographically (EMG). Thereafter, tremors appear in the hind limb, associated with a progressive reduction in the extension reflex when the mice are raised by the tail. At four months of age, the mice show a progressive muscular weakness starting from the hind limb, revealed by the increasing difficulty to stay on a rotating bar and by a reduction in stride length on an inclined ramp. At this stage, more than 50% of motor neurones of the lumbar spinal cord are lost and one month later these mice die.

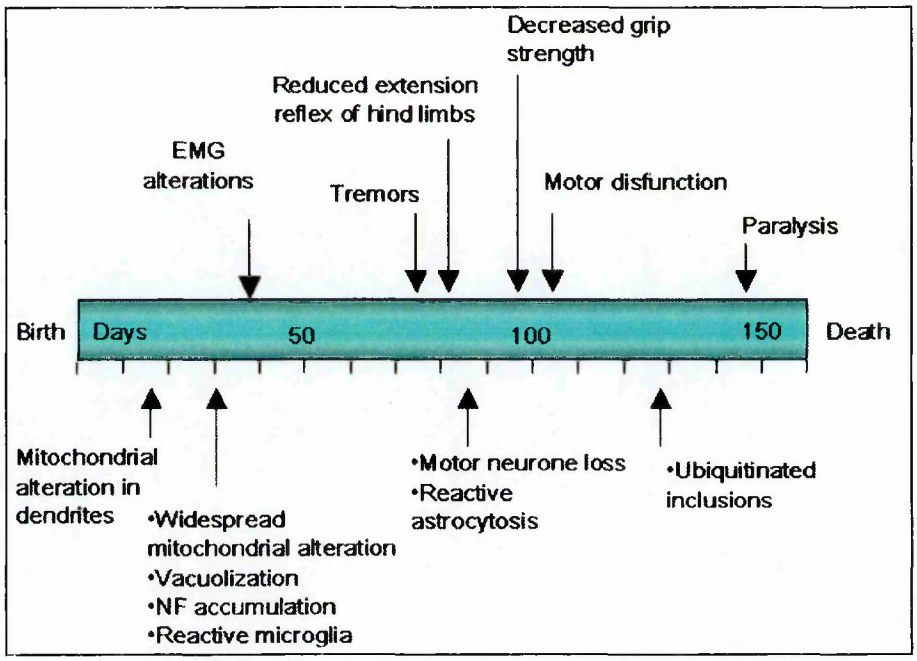

Figure 2.1: Graphic representation of the behavioural and neuropathological progression of the disease occurring in SOD1^{G93A} transgenic mice.

Mitochondrial vacuolisation and the swelling of motor neurones are among the earliest events and are accompanied by a decreased function of the mitochondria. Later, but still at the asymptomatic stage, the SOD1^{G93A} mice show signs of cytoskeletal disorganization in the motor neurones, with the accumulation of phosphorylated neurofilaments. The accumulation of detergent-insoluble proteins and ubiquitinated intracellular inclusions are particularly evident at advanced stages of the disease. Reactive gliosis, which involves hypertrophy and the activation of astrocytes and the proliferation and activation of microglia, is detectable with the degeneration of motor neurones and becomes prominent when the cell loss is remarkable. Hypertrophic astrocytes and reactive microglia are usually located around degenerating motor neurones.

For the present study female mice have been killed at 8, 14 and 19 weeks of age corresponding respectively to a presymptomatic, early symptomatic and advanced stage of the progression of the motor dysfunction. Age-matched non transgenic littermates or transgenic mice expressing wild type human SOD1 have been used as controls.

2.2 Primary astrocyte cultures

Primary cortical astrocyte cultures were prepared from 15-16 day old Swiss mouse embryos (NIH, Harlan, U.K.). Cortices were dissected away from brain and mechanically dissociated using a fire-polished glass Pasteur pipette in Phosphate Buffered Saline (PBS) Ca^{2+} and Mg^{2+} free, supplemented with glucose (33 mM). Cells were plated into 24-well or 6-well Nunc multiwell plates that had been previously coated overnight with 1.5 μg/ml poly-L-ornithine (Gibco-BRL Life Technologies, Gathiesburg, MD, USA) and then sequentially washed in water and PBS before coating with culture medium supplemented with 10% heat inactivated foetal bovine serum (FBS, Gibco-BRL Life Technologies) for 2 hours. Following removal of the final coating solution, cells were seeded (500,000/ml) in a medium composed of a mixture of Dulbecco's modified Eagle's medium and F-12 nutrient (1:1 vol/vol) (Gibco-BRL Life Technologies) supplemented with 33 mM glucose, 2 mM glutamine, 6.5 mM sodium bicarbonate, 5 mM HEPES buffer (pH 7.4), 100 μg/ml streptomycin, 60 μg/ml penicillin, 10% FBS (all from Gibco-BRL Life Technologies). Cells were cultured at 37°C in a humidified atmosphere of 95% air and 5% CO_2. Medium

was replaced after 6, 10 and 13 days in vitro (DIV) and cultures were also washed twice with PBS/glucose at 10 and 13 DIV to remove neuronal cells. Cells were used for transfection after 15-16 DIV when the astrocytes were confluent and neither neurones nor oligodendrocytes could be found in the cultures.

2.3 In situ hybridization

Mice were killed by decapitation and brain and spinal cord rapidly removeved. Tissue were immediately frozen in 2-methylbutane at -45°C and coserved at -80° until the experiments. Frozen lumbar spinal cords and brains of transgenic and non transgenic mice were cut on a cryostat at -20°C and sections (14 µm) mounted on poly-L-lysine coated microscope slides. Sections were then fixed in 4% para-formaldehyde for 15 minutes followed by two 10 minutes incubations in PBS, acetylated (0.1 M triethanolamine and 0.25% acetic anhydride in 0.9% NaCl), dehydrated through a graded series of ethanol, delipidated for 5 minutes in chloroform, air dried and stored frozen at -80°C. At the day of the experiment the slides were brought to room temperature and hybridized with ^{35}S-labelled RNA probes obtained by *in vitro* transcription (Bendotti et al., 1990). The reaction mixture for the *in vitro* transcription contained: 1 µg of DNA, 1X transcription buffer, 10 mM dithiothreitol (DTT), 15 U of human placental RNase inhibitor, 0.5 mM ATP, 0.5 mM GTP, 0.5 mM CTP, 10 µM UTP (all the reagent were purchased from Promega, Madison, WI, USA) and 2.5 µM ^{35}S-UTP (1,000 Ci/mmol; Amersham Biosciences, Little Chalfont,

Buckinghamshire, UK). After a 1 hour incubation at 37°C, the templates were digested with 1 U of DNase I - RNase free (Promega) for 15 minutes at 37 °C. The templates were hydrolysed in mild alkalin buffer (80 mM $NaHCO_3$ and 120 mM Na_2HCO_3) at 60°C to obtain fragments of 150-200 base pairs in lenght. The mixtures were neutralized and the ^{35}S-labelled riboprobes were purified by G-50 Sephadex Quick Spin Colomns (Roche, Basel, Switzerland). Probes were diluted to 1.5 X 10^4 cpm/µl with hybridization buffer containing 50% formamide, 2X sodium saline citrate buffer (SSC), 10 mM Tris/HCl pH 7.5, 1X Denhart's solution, dextran sulfate 10%, 0.2% SDS, 100 mM DTT, 500 µg/ml double-strand Salmon Sperm DNA (Roche). Sections were incubated overnight at 55°C in sealed humidified chambers using Parafilm coverslips. After hybridization, coverslips were removed and sections were incubated in 1X SSC for 10 minutes at room temperature. Sections were then washed for 30 minutes at 37°C in 20 µg/µl of RNase A in RNase buffer (0.5 M NaCl, 1 mM EDTA and 10 mM Tris/HCl, pH 8.0) followed by 30 minutes at 37°C in RNase buffer alone. Sections were then washed in 1X SSC for 30 minutes at room temperature, 0.5X SSC for 30 minutes at 65°C and 0.5X SSC for 10 minutes at room temperature before dehydrating through a graded series of ethanol. The slides were exposed to Beta-max film (Amersham Biosciences) for 7 days, dipped in photographic emulsion (Ilford K5 diluted 1:1 with 0.1% Tween 20) and exposed for 15 days at 4°C. Sections were then developed, counterstained with cresyl violet and examined by light and dark field microscope before the quantitative analysis of the grain density. The specificity of the *in situ* hybridisation for the different trasncripts was verified by the absence of the signal using sense

radiolabelled probes. Densitometric analysis of autoradiographic films was done using a computer-assisted image analysis system (AIS 3.0, Imaging Research Inc., St. Catherines, Ont. Canada). Grain density in single motor neurones was quantitatively evaluated using a computerized microscope image analyzer (IBAS 2, PC 386, Zeiss-Kontron, Munchen, Germany) according to the procedure by Masseroli and coworkers (Masseroli et al., 1993). Cresyl violet stained cells were used to define the circular frame outlining the cell and the grain density over a single cell was expressed as number of grains/μm^2 cell area. Motor neurones from at least two sections from each animal was determined and the mean values of these measures were used for statystical analysis by analysis of variance (ANOVA Two-Way) followed by Tukey's test. All the statistical analyses were done using the GraphPad Prism 2.0a for Power Macintosh (GraphPad Software Inc., San Diego, CA, USA), designed by Dr. Harvey J. Motulsky (1994-1995).

2.4 Immunohistochemistry

Mice were anaesthetised with Equithesin (1% phenobarbitol / 4% (vol / vol) chloral hydrate, 30 µl /10 g, ip.) and transcardially perfused with 20 ml saline followed by 50 ml of sodium phosphate buffered 4% paraformaldehyde solution. Spinal cords were removed, post fixed in fixative for two hours, transferred to 20% sucrose solution in PBS overnight, then in 30% sucrose solution until they sank. Finally spinal cords were frozen in 2-methylbutane at -45°C and conserved at -80° until the experiments. Fixed and frozen lumbar spinal cords of

transgenic and non transgenic mice were cut on a cryostat at -20°C to obtain coronal sections of 30 μm at the L2-L4 levels. Free-floating sections were first treated with H_2O_2 1% in PBS 0.01 M for 10 minutes. Then they were incubated in 10% normal goat serum (NGS), 0.1% Triton X-100 in PBS 0.01 M, for 1 hour and kept overnight at 4°C in the primary antibody solution. The following day, after three washing in PBS 0.01 M, sections were incubated with biotinylated secondary antibody (1:200, Vectastain kit, Vector Laboratories, Burlingame, CA, US) for 1 hour, washed and incubated in avidine-biotin-peroxidase solution (Vectastain kit, Vector Laboratories). Immunostaining was revealed by the reaction with 3'-3-diaminobenzidine tetrahydrocholride (10 mg/20 ml in TBS + 6 μl H_2O_2 30%). Subsequently, sections were washed, dried and mounted on poly-L-lysine coated slides, dehydrated through graded alcohols, fixed in xylene, verslipped using DPX mountant (BDH, Poole, UK) and analyzed using light microscope. Controls sections were incubated without the primary antibody or using the primary antisera preadsorbed with the respective antigen to test the signal specificity.

2.5 Western blot

Mice were killed by decapitation and the spinal cord and brain were rapidly removed, frozen in 2-methylbutane at -45°C and stored at -80°C until the experiment. Frozen spinal cords and brain of transgenic and non transgenic mice were sonicated in boiling lysis buffer (20 mM Tris/HCl, pH 7.5, 10% SDS) and centrifugated at 13000 rpm for 3 minutes at 4°C. Protein concentrations

from supernatant were determined using a BCA Protein Assay Reagent Kit (Pierce, Rockford,IL,USA). Samples were then boiled for 3 minutes in loading buffer (100 mM Tris/HCl, pH 7.5, 15% β-mercaptoethanol, 4% SDS; 15% glycerol, 5 mM EGTA, 5 mM EDTA, 0,2% bromophenol blue) and run on polyacrylamide-SDS gel and transferred to nitrocellulose membrane (Scheicher and Schuell, Keene, NH, USA) Membranes were incubated in blocking buffer made of TBST (20 mM Tris/HCl, 150 mM NaCl, 0,1% Tween-20) with 5% skimmed milk for 2 hours at room temperature, followed by incubation overnight at 4°C with primary antibody diluted in TBST with 5% bovineserum albumin. The blots were then washed three times in TBST and incubated with secondary antibody in TBST with 5% skimmed dry milk, for 1 hour at room temperature. Blots were then developed by the ECL technique (Amersham Biosciences) according to the manufacturer's instructions. Densitometric analysis of autoradiographic bands was done using a computer-assisted image analysis system (AIS 3.0, Imaging Research Inc.). Statistical analysis was performed using One-Way ANOVA followed by Bonferroni`s post-hoc test (GraphPad Prism 2.0a for Power Macintosh, GraphPad Software Inc.).

2.6 Material

Unless otherwise stated, the reagents used for the experiments were obtained from Sigma-Aldrich (Poole, U.K.).

CHAPTER 3

Study of the expression of glutamate AMPA receptor subunits in the spinal cord of $SOD1^{G93A}$ transgenic mice

3.1 Introduction

3.1.1 Glutamate receptors

The excitatory amino acid receptors can be classified as ionotropic receptors, where receptor activation is directly coupled to a membrane ion channel, and metabotropic receptors, where receptor activation is coupled to an intracellular biochemical cascade that indirectly leads to opening or closing of membrane ion channels.

3.1.1.1. Ionotropic receptors

The ionotropic glutamate receptors are multimeric structures formed by four or five subunits and are subdivided into three groups according to pharmacologic and structural similarities: *NMDA (*N-methyl-D-aspartate), *AMPA (*alpha-amino-3-hydroxy-5-methyl-4-isoxazolepropionic acid) and *Kainate* receptors. All ionotropic glutamate receptor subunits share a common basic structure. Like other ligand gated ion channels, such as the $GABA_A$ receptor, the ionotropic glutamate receptor subunits possess four hydrophobic regions (transmembrane domains) within the central portion of the sequence. However, in contrast to other receptor subunits, the second transmembrane domain forms a re-entrant loop that forms the pore region of the ion channel and that gives these receptors an extracellular N-terminus and intracellular C-terminus. The

extracellular N-terminus, together with a loop between transmembrane domains III and IV, forms the ligand binding domain (Standley and Baudry, 2000)

3.1.1.1.a NMDA receptors

The NMDA receptor has been extensively studied and it is known that these receptors have a high Ca^{2+} permeability. They are blocked by Mg^{2+} in a voltage-dependent manner, have a requirement for glycine as a coagonist, and modulatory sites for polyamines, reducing agents, Zn^{2+} and protons (Heath and Shaw, 2002). Molecular biological techniques have revealed that the NMDA receptor channel complex comprises two subunits: NR1 and NR2. There are eight splice variants of NR1 (Zukin and Bennett, 1995) and it is thought that NR1 is a component of all native NMDA receptors. Although NR1 subunits can be assembled into homomeric NR1 channels, there are four NR2 subunit types (NR2A-NR2D), which when coexpressed with NR1 are thought to form native NMDA receptor channel complexes. The different NR2 subunits confer different physiological and pharmacological properties to the receptors (Meguro et al., 1992): for example, NR1-NR2C channels are more sensitive to Mg^{2+} blockade and display the highest affinity sites for glycine binding compared to other heteromeric channels, whereas the NR1-NR2A channel differs from the others in its response to reducing agents. The NR1 subunit is ubiquitous throughout the CNS, whereas there are regional differences in distribution of NR2 subunits. NMDAR3 has been recently identified as third NMDA receptor subunit but little is known about its physiological role (Das et al., 1998).

3.1.1.1.b AMPA receptors

AMPA receptors mediate fast synaptic transmission in the CNS. These receptors were originally classified on the basis of their activation by the agonist quisqualate but not NMDA. The use of quisqualate as an agonist for these receptors has now been abandoned in favour of the more selective agonist α-amino-3-hydroxy-5-methyl-4-isoxazole propionic acid (AMPA) and these receptors are thus referred to either as non-NMDA ionotropic receptors or AMPA/kainate receptors. AMPA receptors are also potently activated by kainate. Molecular biological techniques have so far revealed the existence of four glutamate receptor subunits (GluR1-GluR4), products from separate genes, that are AMPA receptor subunits. Each of these subunits can form homomeric and heteromeric channel assemblies with other subunits. The AMPA receptors exist *in vivo* as pentameric architecture, generating a number of different arrangements, which can vary between neuronal subtypes and even individual neurones. AMPA receptor composition is not rigid but it can change being dynamically influenced by the environmental conditions (Luscher et al., 2000; Zhou et al., 2001; Lee et al., 2004).

The GluR2 subunit is particularly important in determining the calcium permeability of the assembled AMPA receptor. In fact, without GluR2, AMPA receptors have a non linear current voltage relationship and are relatively Ca^{2+} permeable. However, heteromeric AMPA receptors containing GluR2 have linear current voltage properties and low permeability to Ca^{2+}. GluR2 therefore

has a dominant effect to reduce Ca^{2+} permeability. In most CNS neurones AMPA/kainate responses show little Ca^{2+} permeability and this is in accordance with the widespread expression of GluR2 throughout the CNS. The calcium impermeability of the GluR2 subunit is due to post-transcriptional editing of its mRNA, which results in a change of a single amino acid in the second transmembrane region from glutamine (Q) to arginine (R) (Michaelis, 1998; Dingledine et al., 1999). This is the so called Q/R editing site. GluR2(Q) is calcium permeable (Figure 3.1 B) whilst GluR2(R) is not (Figure 3.1 A). Almost all the GluR2 protein expressed in the CNS is in the GluR2(R) form, generating calcium impermeable AMPA receptors. This, along with the interactions with other intracellular proteins, makes GluR2 perhaps the most important AMPA receptor subunit in the context of neurodegeneration.

Each of the AMPA receptor subunits can exist in two isoforms due to alternative splicing of a gene region encoding about 30 amino acids near the fourth transmembrane domain. These isoforms are known as *flip* and *flop* forms. The flip isoform of the protein is mainly represented in prenatal and early postnatal neurones. A postnatal developmental change determines the augmented expression of the flop forms of the AMPA receptor subunits. The flop isoform shows more rapid glutamate-induced desensitization than the flip isoform. Thus, it is probable that the flip/flop alternative splicing control desensitization and recovery of the AMPA receptors (Myers et al., 1998).

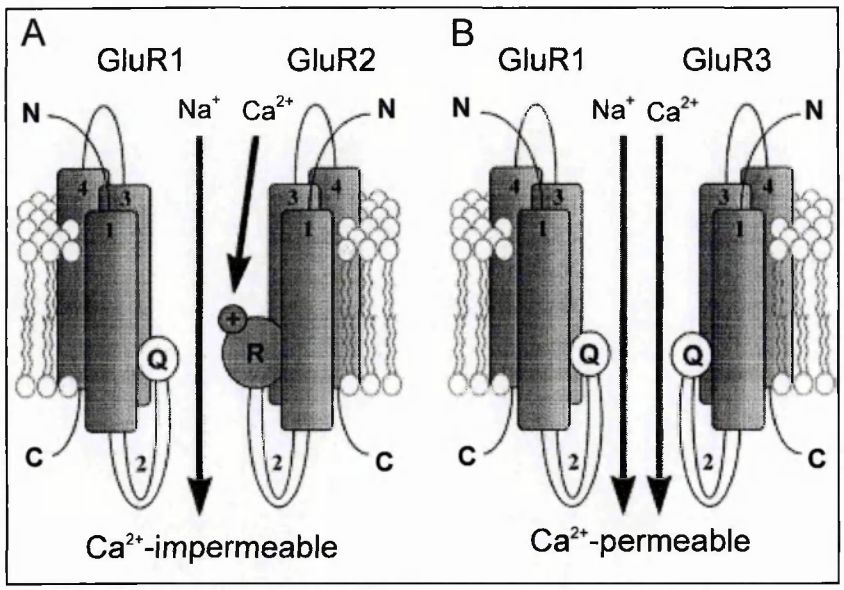

Figure 3.1: GluR2 subunit editing regulates AMPA receptor permeability to calcium

From Pellegrini-Giampietro E. et al, TINS, 1997

3.1.1.1.c Kainate receptors

Kainate receptors constitute a separate group from the NMDA and AMPA receptors, although they share many of the same structural characteristics. They are built from multimeric assemblies of GluR5-7 and KA-1/2 subunits. Like the other ionotropic glutamate receptors, they possess an extracellular N-terminus that represents the ligand binding domain and a re-entrant loop that forms the pore region of the channel. They also undergo both splice and RNA editing, giving rise to a large number of possible receptors with different

pharmacological and functional properties. The agonist kainate is not selective for kainate receptors, also acting as a non desensitizing agonist of AMPA receptors (Heath and Shaw, 2002).

3.1.1.2. Metabotropic receptors

To date, at least eight metabotropic glutamate receptors (mGluR1-8) are known (Michaelis, 1998). These are G-protein coupled receptors that have been subdivided into three groups. Group I comprises mGluR1 and mGluR5 and these receptors appear to be coupled to postsynaptic inositol phosphate metabolism. Group II includes mGluR2 and mGluR3, and Group III comprises mGluR4, mGluR6, mGluR7 and mGluR8. Groups II and III can couple to an inhibitory cAMP cascade in many expression systems, but may also couple to other transduction mechanisms under physiological conditions. The Group II and III receptors have been suggested to mediate presynaptic actions of glutamate in several brain areas, although this does not preclude the possibility that these receptors may also mediate postsynaptic effects in some locations. Similarly, there is evidence that Group I receptors may be found in presynaptic locations in some cases (Heath and Shaw, 2002).

3.1.2 Glutamate receptors and ALS

Glutamate can cause neuronal death through the activation of both NMDA and AMPA receptors by excitotoxic calcium-dependent mechanism. However,

NMDA stimulation seems to be more related to acute glutamatergic insults, whereas AMPA receptors are mainly involved in slow neuronal degeneration, phenomenon occurring in chronic diseases such as ALS (Weiss and Choi, 1991).

It is quite well established that motor neurones are more susceptible than other spinal neurones to toxicity mediated by AMPA receptors. In 1993, Rothstein and collaborators reported that the inhibition of glutamate transport and the consequent increase of synaptic glutamate concentration in organotypic spinal cord slices, produced slow degeneration of motor neurones and that motor neurone toxicity were selectively prevented by AMPA but not by NMDA glutamate receptor antagonists (Rothstein et al., 1993). Excitotoxic agonists selective for AMPA receptors applied directly onto the lumbar spinal cord, preferentially affect motor neurones (Ikonomidou et al., 1996). In spinal mixed cultures, brief exposure to AMPA/kainate agonists induces the selective loss of motor neurones in a calcium-dependent manner (Carriedo et al., 1995; Carriedo et al., 1996). These results has been confirmed by many other studies performed in different *in vitro* systems (Bar-Peled et al., 1999; Carriedo et al., 2000; Saroff et al., 2000; Van Den Bosch et al., 2000; Vandenberghe et al., 2000a).

It has been hypothesized that this selective vulnerability of motor neurone to AMPA activation, in respect to other spinal neurones, might result from differences in AMPA receptor subunit expression. For example, the presence of AMPA receptors lacking GluR2 or lacking edited GluR2 would confer an increased Ca^{2+} permeability, which in turn can lead to deleterious enhanced

levels of intracellular calcium and cell death as described in section 1.9.2. A large body of evidence reports the presence of calcium-permeable AMPA receptors on motor neurones. Carriedo and colleagues showed that cultured motor neurones, selectively killed by kainate in a Ca^{2+}-dependent manner, were capable of taking up cobalt after kainate stimulation, Co^{2+} labelling being a selective marker for neurones possessing Ca^{2+}-permeable AMPA receptors (Carriedo et al., 1995; Carriedo et al., 1996). These experiments were the first clue about the possibility that possession of these receptor channels may be one of the factors that predispose motor neurones to degeneration in diseases such as ALS, where glutamatergic neurotransmission may be altered in same way. Subsequently, many other works on rodent motor neurone cultures reinforced these findings (Launey et al., 1998; Terro et al., 1998; Bar-Peled et al., 1999; Greig et al., 2000; Van Den Bosch et al., 2000).

Support for such an hypothesis was strengthened by several reports showing that human motor neurones do not express or have very low expression of GluR2 mRNA (Williams et al., 1997; Heath et al., 2002; Kawahara et al., 2003) or GluR2 protein (Shaw et al., 1999). This suggests that lack or low expression of GluR2 subunit may be the cause of the existence of Ca^{2+}-permeble AMPA receptors on motor neurones, making them more prone to excitotoxicity. GluR2 expression has been widely examined also in animal models. Apart from one paper reporting the absence of GluR2 on motor neurones in dissociated rat spinal cord cultures (Bar-Peled et al., 1999), several studies have clearly demonstrated the abundant presence of this subunit in cultured motor neuronal cells of rodents (Greig et al., 2000; Van Den Bosch et

al., 2000; Vandenberghe et al., 2000b; Laslo et al., 2001). Moreover, GluR2 seems to be entirely edited at the Q/R site (Vandenberghe et al., 2000a). However, despite the high expression of edited GluR2, this subunit may be excluded from a subset of AMPA receptors, generating AMPA receptors permeable to calcium, as demonstrated by the Co^{2+} labelling (Carriedo et al., 1995; Carriedo et al., 1996; Launey et al., 1998; Terro et al., 1998; Bar-Peled et al., 1999; Greig et al., 2000; Van Den Bosch et al., 2000), by the action of Joro spider toxin, a selective blocker of Ca^{2+}-permeable AMPA receptors that prevents AMPA evocated current in motor neurones (Greig et al., 2000) and by motor neurone death occurring after kainate exposure (Van Den Bosch et al., 2000). Thus, it is plausible that GluR2-containing and GluR2-lacking AMPA receptors can coexist in single motor neurones.

Nevertheless, it has been reported that there are not significant differences between motor neurones and dorsal horn neurones in terms of GluR2 abundance and whole cell relative Ca^{2+} permeability (Vandenberghe et al., 2000a), in spite of a lower Co^{2+} uptake in the dorsal horn neurones (Albuquerque et al., 1999; Bar-Peled et al., 1999). This would mean that, in physiological conditions, the presence of calcium-permeable AMPA receptors might not be enough to explain selective vulnerability of motor neurones. However, AMPA receptor current density is threefold higher in motor neurones than in dorsal horn neurones, suggesting a higher density of functional AMPA receptors in motor neurone surface (Vandenberghe et al., 2000b).

Other factors may render motor neurones more responsive to AMPA-mediated increase of Ca^{2+} influx in comparison to other cell types. It has been

reported that immunoreactivity for Ca^{2+} buffering protein calretinin was negative in cultured rat motor neurones (Terro et al., 1998). Other two proteins involved in calcium sequestration, parvalbumin and calbindin, were not found in human spinal motor neurones (Ince et al., 1993). Moreover, motor neurone death induced by increased intracellular calcium upon AMPA receptor stimulation is attenuated by overexpression of parvalbumin in transgenic mice (Van Den Bosch et al., 2002b). Therefore, low cytosolic calcium buffering capacity may also contribute to render motor neurones particularly exposed to glutamatergic insults.

Another hypothesis proposed regards the mitochondrial susceptibility demonstrated by motor neurones. It has been shown that AMPA or kainate exposure selectively triggers mitochondria Ca^{2+} overloading in these cells with only a little effect on cortical GABAergic neurones, which also express calcium-permeable AMPA receptors (Carriedo et al., 2000). The accumulation of calcium in mitochondria causes mitochondrial membrane depolarization and consequent reactive oxygen species (ROS) generation. Mitochondria impairment has been well documented in animal models of ALS (Dal Canto and Gurney, 1995; Wong et al., 1995; Bendotti et al., 2001a; Higgins et al., 2002), suggesting that excitotoxic insults mediated by AMPA receptors might be harmful to motor neurones through damaging the mitochondrial system. Altered mitochondria have been observed in motor neurone dendrites of ALS mice a long time before the massive loss of motor neurones (Bendotti et al., 2001a). Interestingly, it has been shown that the majority of GluR2-lacking and

consequently Ca^{2+}-permeable AMPA receptors present on motor neurones are localized on dendrites (Launey et al., 1998; Vandenberghe et al., 2001).

All the above observations regarding composition, distribution and working properties of AMPA receptors are relative to normal motor neurones. They suggest that motor neurones are predisposed to be injured by excitotoxic damage because of the presence of a subset of calcium-permeable AMPA receptors and their peculiar cellular characteristics, which render them more sensitive to abnormal calcium influx.

It is also conceivable that molecular and functional features of AMPA channels may be altered in certain disease states, representing a triggering or enhancing event for the pathology. It has been described that GluR2 mRNA is downregulated in susceptible neurones of animal models after transient forebrain ischemia or kainite-induced epilepsy (Pellegrini-Giampietro et al., 1997). Traumatic spinal cord injury determines a persistent reduction of GluR2 protein and mRNA in motor neurones near the injury site (Grossman et al., 1999) and decrease of GluR3 and GluR4 expression in white matter astrocytes (Park et al., 2003). These data demonstrate the dynamic nature of AMPA receptor composition that could lead to the induction of calcium-permeable receptors as a component of the pathological process. This hypothesis has been also investigated in ALS. Several papers have reported the decreased transcription of GluR2 mRNA in ventral spinal cord of ALS cases, compared to normal control (Virgo et al., 1996; Takuma et al., 1999). In particular, significant downregulation of the flop form of GluR2 has been observed, suggesting the formation of slowly desensitizing AMPA receptors (Tomiyama et al., 2002).

However, Kawahara and coworkers have recently showed unchanged level of GluR2 mRNA in single motor neurones of ALS patient examined by quantitative RT-PCR (Kawahara et al., 2003), even if the editing efficiency was incomplete in 44% of cases (Kawahara et al., 2004). Therefore, the role of this subunit in ALS pathology remains controversial.

The study of *in vitro* or animal models of the disease has not clarified this issue. Expression of SOD1 mutants enhances AMPA-mediate toxicity in cultured motor neurones, associated with increased intracellular calcium levels and mitochondrial dysfunction (Roy et al., 1998; Kruman et al., 1999; Spalloni et al., 2004). However, GluR2-immunoreactivity did not appear to be altered in spinal cord of mice overexpressing G86R mutant murine SOD1 (Morrison et al., 1998). Recently, unchanged levels of AMPA receptor subunit mRNAs have been also reported in cultured motor neurones expressing SOD1 with G93A mutation, although elevated expression flip forms was found (Spalloni et al., 2004). In general, none of these studies have determined whether there are changes in AMPA receptors at presymptomatic stages of ALS.

Support for an involvement of AMPA receptors in ALS pathology comes from two studies showing that treatment with AMPA antagonist drugs ameliorates symptoms and survival of transgenic ALS mice (Canton et al., 2001; Van Damme et al., 2003).

3.2 Hypothesis and aim

The hypothesis tested in this part of the thesis is that the expression of G93A mutant of human SOD1 in transgenic mice may result in changes of AMPA receptor subunit expression in motor neurones, making them prone to be preferentially injured by glutamatergic insults.

Thus, the aim of this section is to evaluate protein and mRNA expression of AMPA receptor subunits in the lumbar spinal cord of $SOD1^{G93A}$ mice during the progression of disease, in order to clarify whether early alterations may be involved in pathology.

3.3 Methods

3.3.1 *In situ* hybridisation for glutamate AMPA receptor subunit mRNAs in $SOD1^{G93A}$ mice

In situ hybridisation was performed as described in section 2.4. Lumbar spinal cords (L2-L4 levels) of $SOD1^{G93A}$, $SOD1^{wt}$ and non transgenic mice used as control at 8, 14 and 19 weeks of age (4 to 6 mice each group), were used.

^{35}S-labelled RNA probes complementary to the flop variant of GluR1, GluR2, GluR3 and GluR4 mRNAs were prepared through *in vitro* transcription of cDNA fragments. GluR1, GluR2 and GluR3 (inserts were 2992, 3505 and 3083 base pairs in length respectively) were cloned between the EcoR1 site (5') and the Xho1 site (3') of the polylinker region of pBluescript SK (-) plasmid. Antisense transcripts were obtained using T7 RNA polymerase enzyme and

sense transcripts were obtained using T3 RNA polymerase enzyme. GluR4 insert was 2971 base pairs in length and was cloned between the EcoR1 site (5') and the BamH1 site (3') of the polylinker region of the same plasmid. Antisense transcript was obtained using T3 RNA polymerase enzyme and sense transcript was obtained using T7 RNA polymerase enzyme. The plasmids were kindly provided by Dr Pellegrini Giampietro, Departement of Preclinical and Clinical Pharmacology Mario Aiazzi Mancini, Universita' di Firenze, Firenze, Italy.

3.3.2 Immunohistochemical analysis of glutamate AMPA receptor subunits in SOD1^{G93A} mice

Immunohistochemical analysis was performed as described in section 2.5. Fixed and frozen lumbar spinal cords of SOD1^{G93A} mice at 8, 14 and 19 weeks of age, SOD1^{wt} mice and non transgenic mice at 8 weeks of age used as control (3-4 mice each group, 3 indipendent experiments performed with different animals) were used. The primary antibodies used were: monoclonal anti-GluR2 (1:200, Chemicon International, Harrow, UK) or monoclonal anti-GluR3 (1:100, Chemicon International) or monoclonal anti-GluR4 (1:500, Chemicon International), diluted in PBS 0.01M additioned with 4% NGS and 0.1% Triton X-100. Biotinylated anti-mouse secondary antibody was used.

3.3.3 Western blot analysis of glutamate AMPA receptor subunits in SOD1^{G93A} mice

Western blot analysis was performed as described in section 2.6. Frozen spinal cords of SOD1^{G93A} mice at 8 and 19 weeks of age and non transgenic mice at 8 weeks of age used as control (3 mice each group) were used. Eighty µg protein/lane of each sample were run on precast polyacrylamide-SDS gradient gel (4%-15%) (Bio-Rad laboratorie, Hercules, CA, USA). The primary antibodies used were: monoclonal mouse anti-GluR2 (1:500, Chemicon International) or monoclonal mouse anti-GluR3 (1:500, Chemicon International) or monoclonal mouse anti-actin (1:2000, Chemicon International). Anti-mouse IgG conjugated to horseradish peroxidase (1:2000, Sigma, Poole, UK) was used as secondary antibody. Blots were developed using ECL plus Western Blotting Detection System (Amersham Biosciences) according to the manufacturer's instructions

3.4 Results

3.4.1 Analysis of AMPA receptor subunit mRNAs in the spinal cord of SOD1^{G93A} mice

The mRNA expression of AMPA glutamate receptor subunits GluR1, GluR2, GluR3 and GluR4 (flop variants) was investigated in the lumbar spinal cord of ALS transgenic mice expressing G93A mutant of human SOD1 enzyme.

The lumbar tract of the cord was chosen because the hindlegs of these mice are affected erlier and more severely compared to the forelegs. In fact, only the 50% of the motor neurones are spared in this spinal cord area. The analysis was performed by *in situ* hybridisation technique.

3.4.1.1 Expression of AMPA receptor subunit mRNAs in the spinal cord of control mice

Apart from GluR1, the other three AMPA subunits GluR2, GluR3 and GluR4 show a quite high level of mRNA expression in the spinal cord grey matter of C57BL/6 mice, used as control in this study (Figure 3.2).

GluR1 mRNA presents a very faint signal distributed along the whole spinal cord sections (Figure 3.2 A), with very low expression in the motor neurones (Figure 3.2 a), as already reported in rats by Greig et al. (Greig et al., 2000).

On the contrary, GluR2 mRNA is highly expressed in the *substantia gelatinosa* and in the other laminae of the dorsal horn of the spinal cord, with a prominent signal found in Laminae I and II (Figure 3.2 B). Labelling is also present in many other cells of the grey matter, in particular in the motor neurones of the ventral horn (Figure 3.2 b).

Low levels of mRNA has been detected for GluR3 in the substantia gelatinosa (Figure 3.2 C), whereas a quite high signal for this subunit is

observed in the ventral horn motor neurones, even if it seems to be less intense in comparison to GluR2 (Figure 3.2 c).

GluR4 mRNA does not result expressed at significant levels in dorsal horn of the spinal cord but an elevated silver grain density is observable in the intermediate and ventral laminae (Figure 3.2 D). In the laminae IX, the accumulation of black grain on the motor neurones is particularly evident (Figure 3.2 d).

3.4.1.2 Expression of AMPA receptor subunit mRNAs in the spinal cord of $SOD1^{G93A}$ mice

A quantitative analysis of mRNA expression of AMPA receptor subunits was carried out in the ventral and dorsal horn of spinal cord and in particular in the motor neurones of $SOD1^{G93A}$ mice at different stages of the disease: presymptomatic (8 weeks of age), early symptomatic (14 weeks of age) and end stage (19 weeks of age). Given its almost undetectable expression revealed in the spinal cord of control mice, the GluR1 subunit mRNA was not considered in this analysis. Non transgenic mice and mice overexpressing wild type human SOD1 ($SOD1^{wt}$) were used as controls.

a) GluR2:

The widespread distribution of GluR2 mRNA observed in the whole grey matter of lumbar spinal cord of control mice does not change in $SOD1^{G93A}$ transgenic mice. Quantitative analysis of autoradiographic opical density of

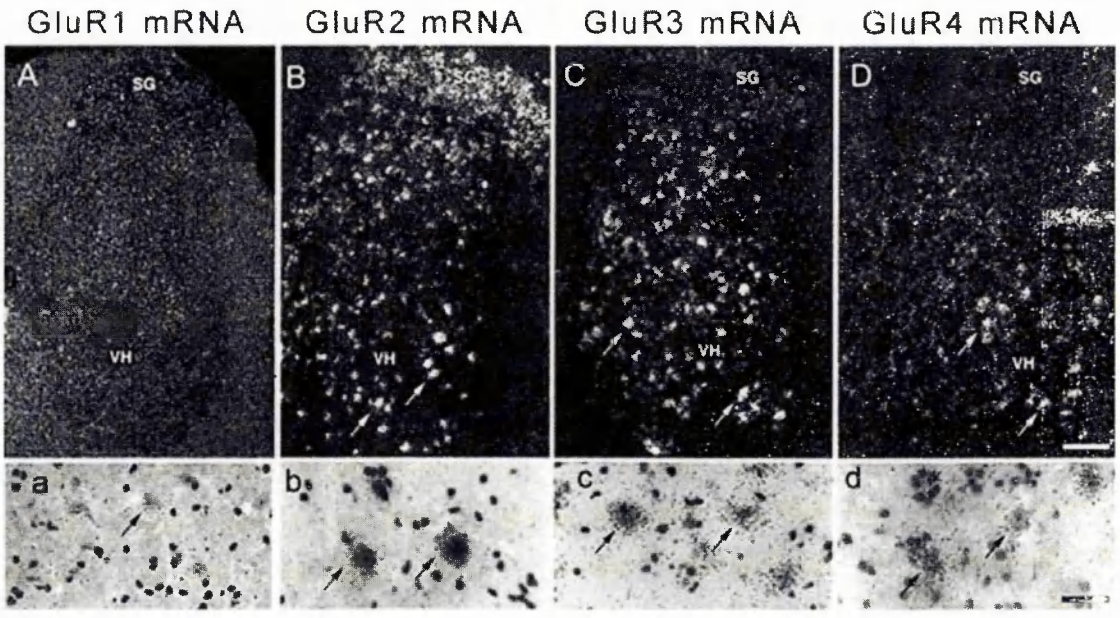

Figure 3.2: mRNAs distribution of AMPA receptor subunits in mouse spinal cord

Representative hemisections of lumbar spinal cord. GluR1 mRNA presents a very low expression in the whole spinal cord (A) with very low expression in the motor neurones (a). GluR2 mRNA is highly expressed in the dorsal horn (Laminae I and II) (B). Labelling is also present in many other cells of the grey matter, in particular in the motor neurones of the ventral horn (b). Low levels of GluR3 mRNA are observed in substantia gelatinosa (C) whereas a quite high signal is revealed in the ventral horn motor neurones (c). GluR4 mRNA is not expressed at significant levels in dorsal horn (D) but an elevated silver grain density is observable on the motor neurones in the laminae IX (d). Scale bar: (A-D)=100 μm; (a-d)=30 μm.

dorsal (laminae I, II, III and IV) (Figure 3.3) and ventral (laminae VII, VIII, and IX) (Figure 3.4) regions of the spinal cord performed with image analysis, revealed no significant variation in the expression GluR2 RNA messenger in $SOD1^{G93A}$ mice at all the disease stages examined, compared to age-matched controls. Since the nature of my study, I put my attention on variation of GluR2 mRNA expression in the motor neurones. Using a computerized microscope image analyzer, the IBAS 2, Kontron/Zeiss, according to the procedure by Masseroli and co-workers (Masseroli et al., 1993), I quantitatively evaluated the silver grain density in single motor neurones of presymptomatic, symptomatic and end stage $SOD1^{G93A}$ mice. Quantitative analysis of the grain density on these cells did not show significant variations in transgenic mice at all stages of the disease when compared with age-matched controls (Figure 3.5).

b) GluR3:

The general distribution of GluR3 mRNA in the whole spinal cord of $SOD1^{G93A}$ mice does not show appreciable differences when compared to control mice. Also in this case, quantitative analysis of autoradiographic opical density did not show statistical differences in the general expression pattern of GluR3 mRNA in dorsal (Figure 3.6) and ventral (Figure 3.7) horn of $SOD1^{G93A}$ mice compared to controls. However, quantitative analysis of autoradiographic grain density on motor neurones of transgenic mice revealed a trend to an increasing of mRNA at 8 weeks of age, which become significant at

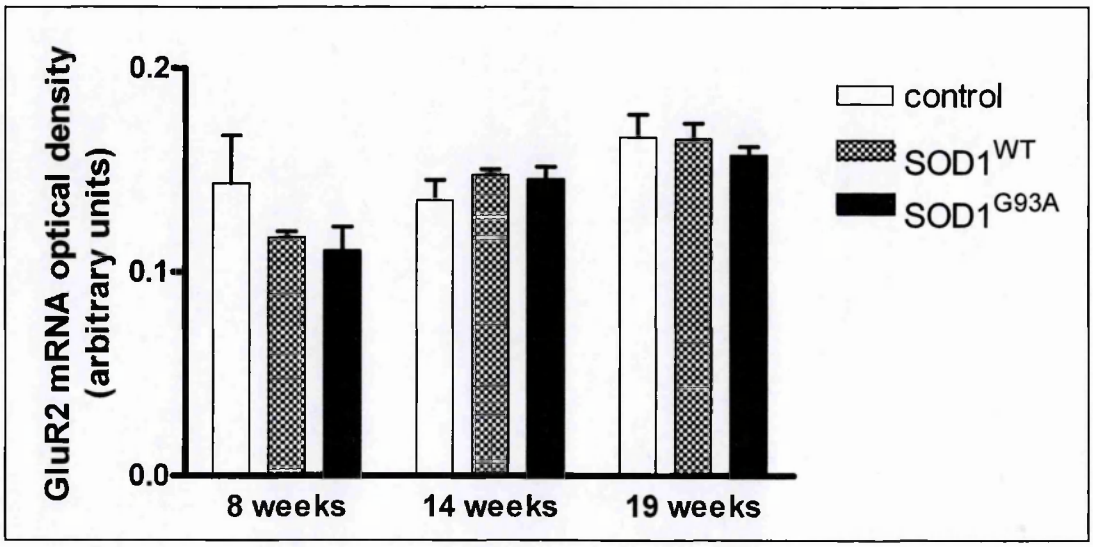

Figure 3.3: GluR2 mRNA expression in the dorsal horn of SOD1^{G93A} mouse spinal cord

Quantitative analysis of autoradiographic opical density revealed no significant variation in GluR2 mRNA expression in the spinal cord dorsal horn (laminae I, II, III and IV) of SOD1^{G93A} mice in respect to non transgenic mice (control) and SOD1^{wt} mice, at all the ages considered (two sections from each animal). Each column is the mean ± S.E.M. (n = 4 to 6), data analysed by Two-Way ANOVA followed by Tukey's test.

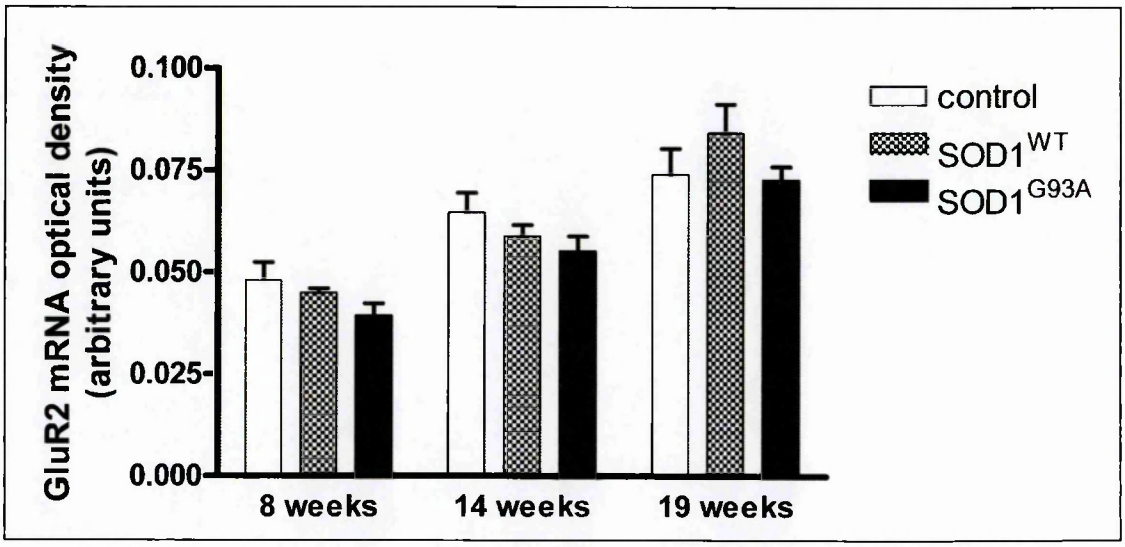

Figure 3.4: GluR2 mRNA expression in the ventral horn of $SOD1^{G93A}$ mouse spinal cord

Quantitative analysis of autoradiographic opical density revealed no significant variation in GluR2 mRNA expression in the spinal cord ventral horn (laminae VII, VIII, and IX) of $SOD1^{G93A}$ mice in respect to non transgenic mice (control) and $SOD1^{wt}$ mice, at all the ages considered (two sections from each animal). Each column is the mean ± S.E.M. (n = 4 to 6), data analysed by Two-Way ANOVA followed by Tukey's test.

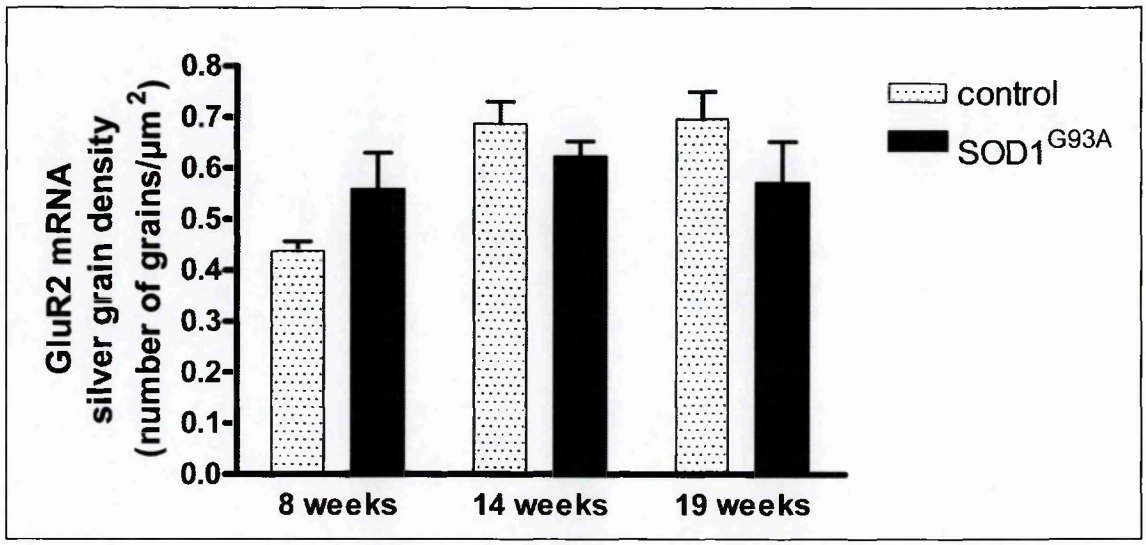

Figure 3.5: GluR2 mRNA expression in the ventral motor neurones of SOD1^{G93A} mouse spinal cord

Quantitative estimation of GluR2 mRNA expression in the motor neurones of SOD1^{G93A} mice was performed by evaluating the silver grain density in single motor neurones of presymptomatic (8 weeks of age), symptomatic (14 weeks of age) and end stage (19 weeks of age) mice (two sections from each animal). No significant variations was observed in transgenic mice at all stages of the disease when compared with age-matched controls (non transgenic mice). Each column is the mean ± S.E.M. (n = 4 to 6), data analysed by Two-Way ANOVA followed by Tukey's test.

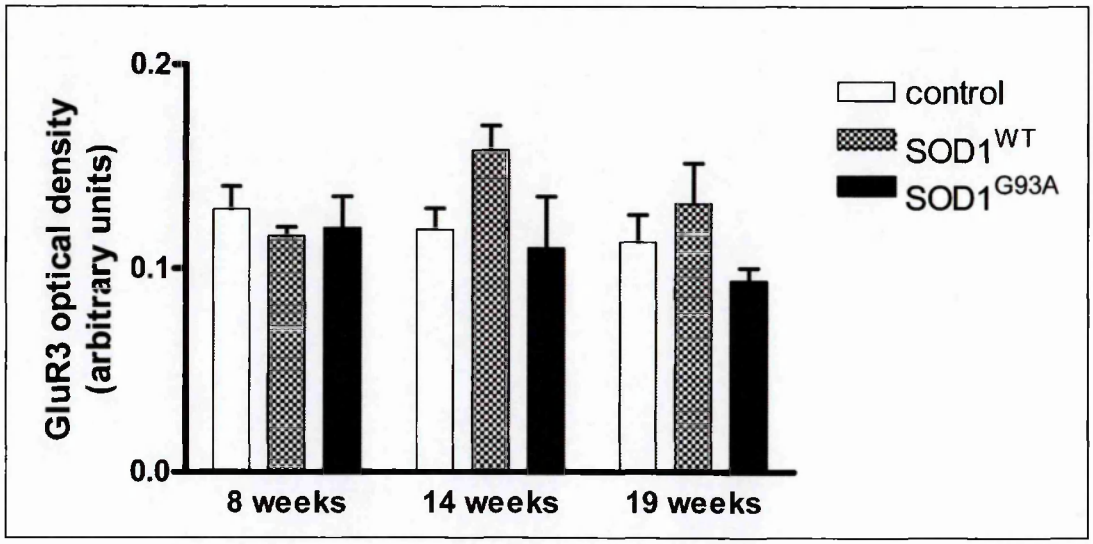

Figure 3.6: GluR3 mRNA expression in the dorsal horn of SOD1^{G93A} mouse spinal cord

Quantitative analysis of autoradiographic opical density revealed no significant variation in GluR3 mRNA expression in the spinal cord dorsal horn (laminae I, II, III and IV) of SOD1^{G93A} mice in respect to non transgenic mice (control) and SOD1^{wt} mice, at all the ages considered (two sections from each animal). Each column is the mean ± S.E.M. (n = 4 to 6), data analysed by Two-Way ANOVA followed by Tukey's test.

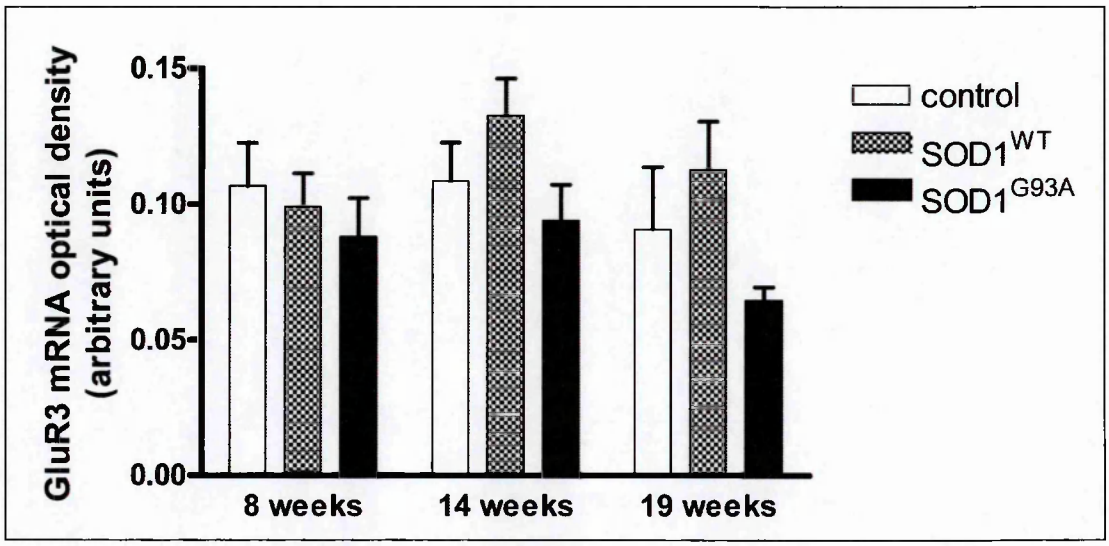

Figure 3.7: GluR3 mRNA expression in the ventral horn of SOD1^{G93A} mouse spinal cord

Quantitative analysis of autoradiographic opical density revealed no significant variation in GluR3 mRNA expression in the spinal cord ventral horn (laminae VII, VIII, and IX) of SOD1^{G93A} mice in respect to non transgenic mice (control) and SOD1^{wt} mice, at all the ages considered (two sections from each animal). Each column is the mean ± S.E.M. (n = 4 to 6), data analysed by Two-Way ANOVA followed by Tukey's test.

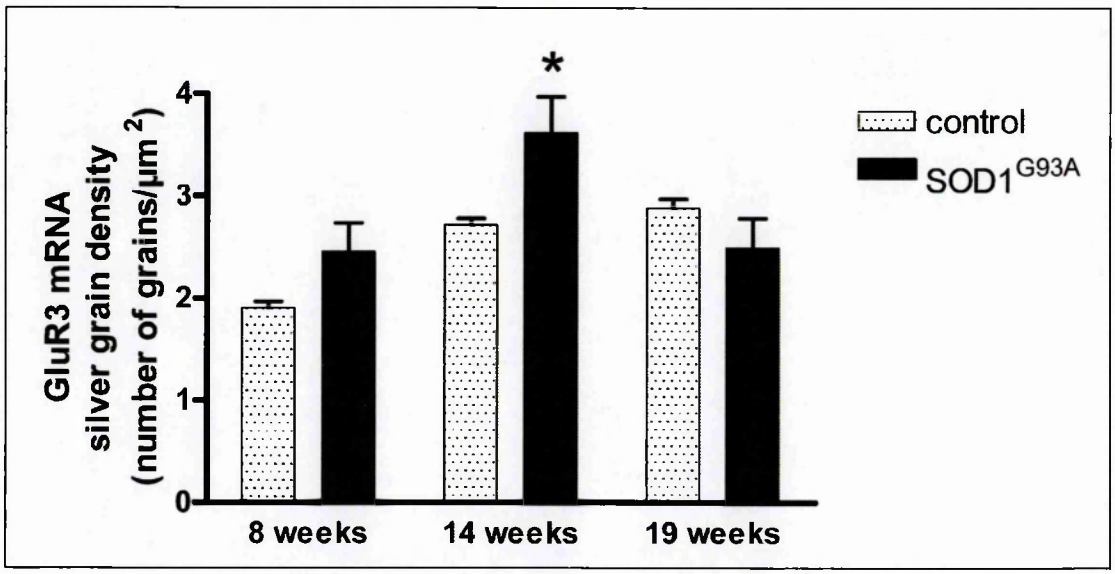

Figure 3.8: GluR3 mRNA expression in the ventral motor neurones of SOD1^{G93A} mouse spinal cord

*Quantitative estimation of GluR3 mRNA expression in the motor neurones of SOD1^{G93A} mice was performed by evaluating the silver grain density in single motor neurones of presymptomatic (8 weeks of age), symptomatic (14 weeks of age) and end stage (19 weeks of age) mice (two sections from each animal). Significant increased of GluR3 mRNA expression was revealed in transgenic mice at 14 weeks of age when compared with age-matched controls (non transgenic mice). Each column is the mean ± S.E.M. (n = 4 to 6), data analysed by Two-Way ANOVA followed by Tukey's test, * = $p < 0.05$.*

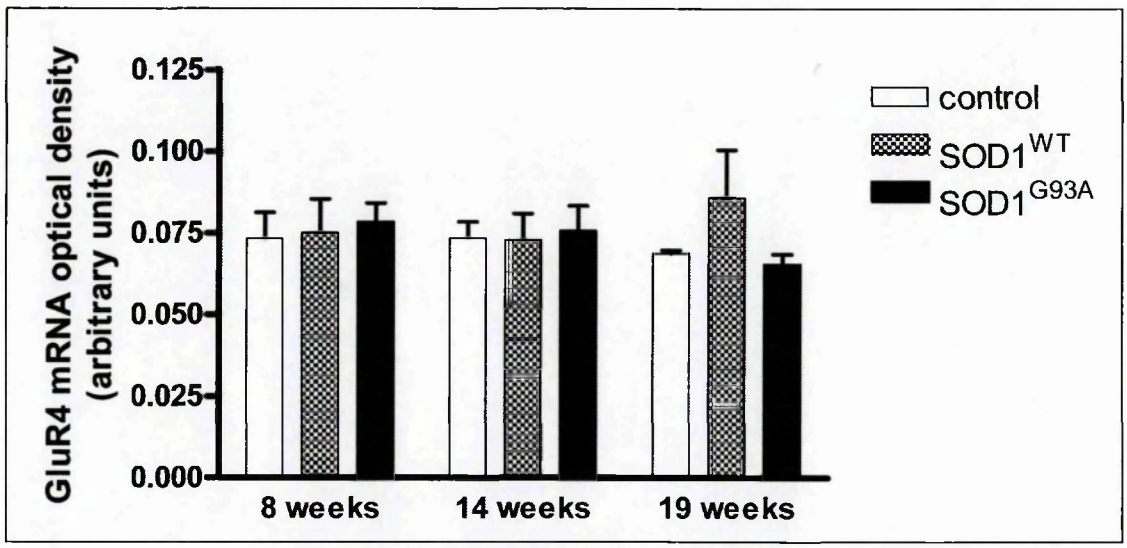

Figure 3.9: GluR4 mRNA expression in the dorsal horn of $SOD1^{G93A}$ mouse spinal cord

Quantitative analysis of autoradiographic opical density revealed no significant variation in GluR4 mRNA expression in the spinal cord dorsal horn (laminae I, II, III and IV) of $SOD1^{G93A}$ mice in respect to non transgenic mice (control) and $SOD1^{wt}$ mice, at all the ages considered (two sections from each animal). Each column is the mean ± S.E.M. (n = 4 to 6), data analysed by Two-Way ANOVA followed by Tukey's test.

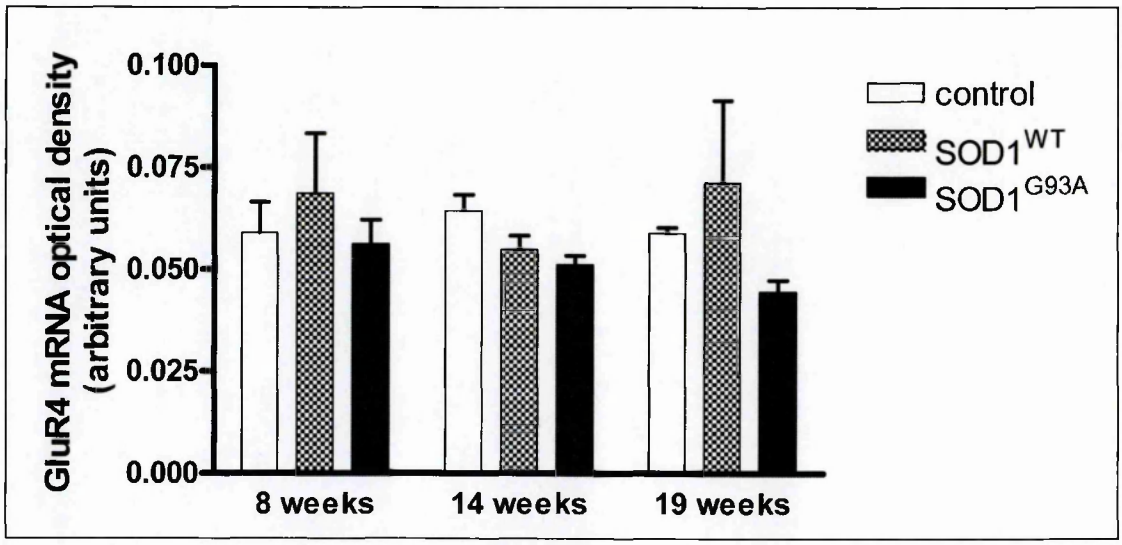

Figure 3.10: GluR4 mRNA expression in the ventral horn of SOD1^{G93A} mouse spinal cord

Quantitative analysis of autoradiographic opical density revealed no significant variation in GluR4 mRNA expression in the spinal cord ventral horn (laminae VII, VIII, and IX) of SOD1^{G93A} mice in respect to non transgenic mice (control) and SOD1^{wt} mice, at all the ages considered (two sections from each animal). Each column is the mean ± S.E.M. (n = 4 to 6), data analysed by Two-Way ANOVA followed by Tukey's test.

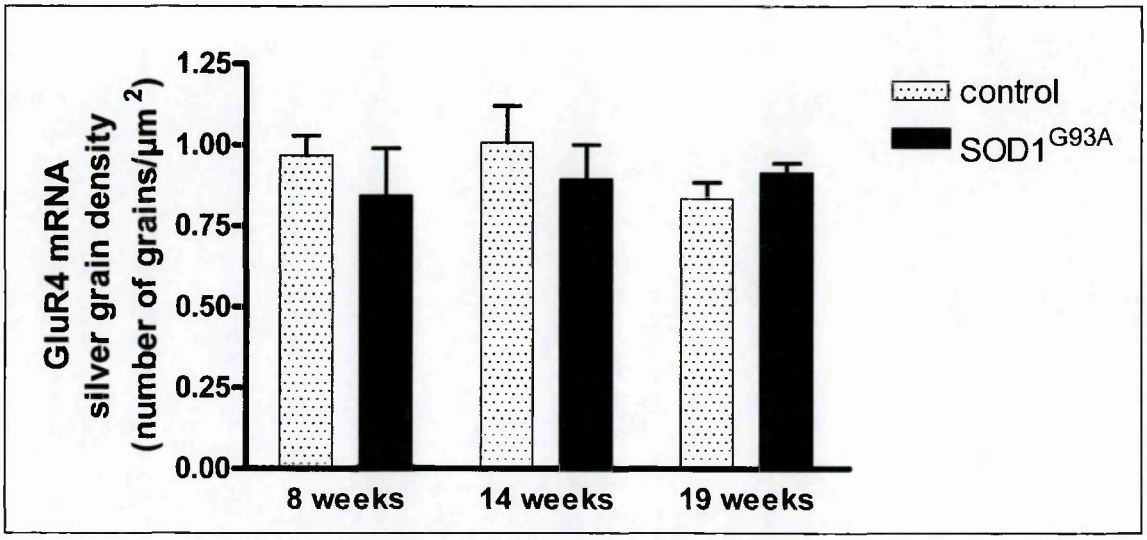

Figure 3.11: GluR4 mRNA expression in the ventral motor neurones of SOD1^{G93A} mouse spinal cord

Quantitative estimation of GluR4 mRNA expression in the motor neurones of SOD1^{G93A} mice was performed by evaluating the silver grain density in single motor neurones of presymptomatic (8 weeks of age), symptomatic (14 weeks of age) and end stage (19 weeks of age) mice (two sections from each animal). No significant variations was observed in transgenic mice at all stages cosidered when compared with age-matched non transgenic mice (controls). Each column is the mean ± S.E.M. (n =4 to 6), data analysed by Two-Way ANOVA followed by Tukey's test.

14 weeks of age, compared with age-matched control mice. In transgenic mice at 19 weeks of age, mRNA in surviving motor neurones is not different from respective control (Figure 3.8).

c) GluR4

Also in $SOD1^{G93A}$ mice, GluR4 mRNA is almost absent in the dorsal horn of lumbar spinal cord of control mice. No appreciable differences were found after autoradiographic optical density examination of dorsal (Figure 3.9) or ventral (Figure 3.10) horn. Similarly, quantitative analysis of grain density on motor neurones of $SOD1^{G93A}$ mice did not show significant alteration of mRNA level, at all stages of the disease (Figure 3.11).

3.4.2 Study of AMPA receptor subunit protein expression in the spinal cord of $SOD1^{G93A}$ mice

The protein expression and distribution of glutamate AMPA receptor subunits GluR2, GluR3 and GluR4 in the spinal cord of $SOD1^{G93A}$ transgenic mice was examined using immuhistochemistry and Western blot techniques. Since the almost absent expression of GluR1 mRNA in the lumbar motor neurones of control mice, experiments to determine the protein expression of this subunit were not performed.

3.4.2.1 *Expression and distribution of AMPA receptor subunit proteins in the spinal cord of SOD1^{G93A} mice examined by immunohistochemical analysis*

Immunolabelling for AMPA receptor subunits was performed in the lumbar spinal cord of SOD1^{G93A} mice at different stages of the disease and compared to non transgenic mice and mice overexpressing wild type human SOD1.

GluR2:

In control mice GluR2 immunoreactivity is localized throughout the whole grey matter. A dense staining is observed in the cells and neuropil of substantia gelatinosa and in motor neurones of ventral horn (Figure 3.12 A). In the motor neurones, immunostaining is distributed in the cytoplasm of the cell body and neurites, with an intense granular immunoreactivity in the perinuclear region (Figure 3.12 a).

In SOD1^{G93A} mice there are no substantial changes in GluR2 immunostaining observed in dorsal horn, whereas a decrease of signal is observed in the ventral region, at all stages of the disease, associated with a progressive loss of motor neurones (Figure 3.12 B, C and D). In particular, in the SOD1^{G93A} mice at 8 and 14 weeks of age, we could observe a decrease of GluR2 immunostaining and a more homogeneous distribution of labelling in the cytoplasm, associated with changes in the morphology of motor neurones and loss of neurites particularly at 14 week of age (Figure 3.12 b and c). These modifications were strongly marked in some animals, less evident in others and

were not seen in control mice or in mice overexpressing wild type form of human SOD1 (Figure 3.12 e)

GluR3:

Reflecting what is observed for the mRNA, GluR3 immunoreactivity is less intense than the one revealed for GluR2 in the dorsal laminae. The immunostaining in ventral horn is mainly localized in the motor neurones, as well as in other smaller neurones of this region (Figure 3.13 A). Within the motor neurones the immunostaining is homogenously distributed in the cytoplasma of the cell body and neurites (Figure 3.13 a).

In the $SOD1^{G93A}$ mice at 8 weeks of age there was a general increase of immunoreactivity in neurones of grey matter in ventral horn and intermediate area. An increased immunostaining is also revealed in the cytoplasm of several motor neurones in lamina IX (Figure 3.13)

GluR4

Immunoreactivity of GluR4 subunit protein is distributed in almost all the cells of grey matter of lumbar spinal cord of control mice (Figure 3.14 A). Unlike the immunohistochemistry reported for rat spinal cord (Tachibana et al., 1994), we observe a prominent staining of nuclei of the cells. In particular, the nuclei of motor neurones of ventral regions are very intensely and homogeneously labelled (Figure 3.14 a).

The GluR4 immunoreactivity was also prominent in the nuclei of motor neurones of $SOD1^{G93A}$ mice, with levels that do not apparently differ from controls (not shown).

3.4.2.2 Quantitative analysis of AMPA receptor subunit proteins in the total spinal cord of $SOD1^{G93A}$ mice examined by Western blot technique

The total amount of AMPA subunit proteins expressed in the spinal cord of $SOD1^{G93A}$ mice was tested by Western blotting. This was studied at presymptomatic (8 weeks of age) and final (19 weeks of age) stage of the disease. Since variation in distribution and expression observed in the immuhistochemical studies was detected only for GluR2 and GluR3, the Western blot analysis was performed for these two subunits only (Figure 3.15 A).

Quantitative determination of band optical density did not reveal any significant change in the total amount of these subunits. However, a trend to decrease (about -20%) is observable for GluR2 in $SOD1^{G93A}$ mice at presymptomatic phase (Figure 3.15 B). This was not revealed for GLUR3 (Figure 3.15 C). At 19 weeks of age, the band density for both GluR2 and GluR3 appears decreased (about 30%) in respect to controls, although the decrease does not reach statistical significance.

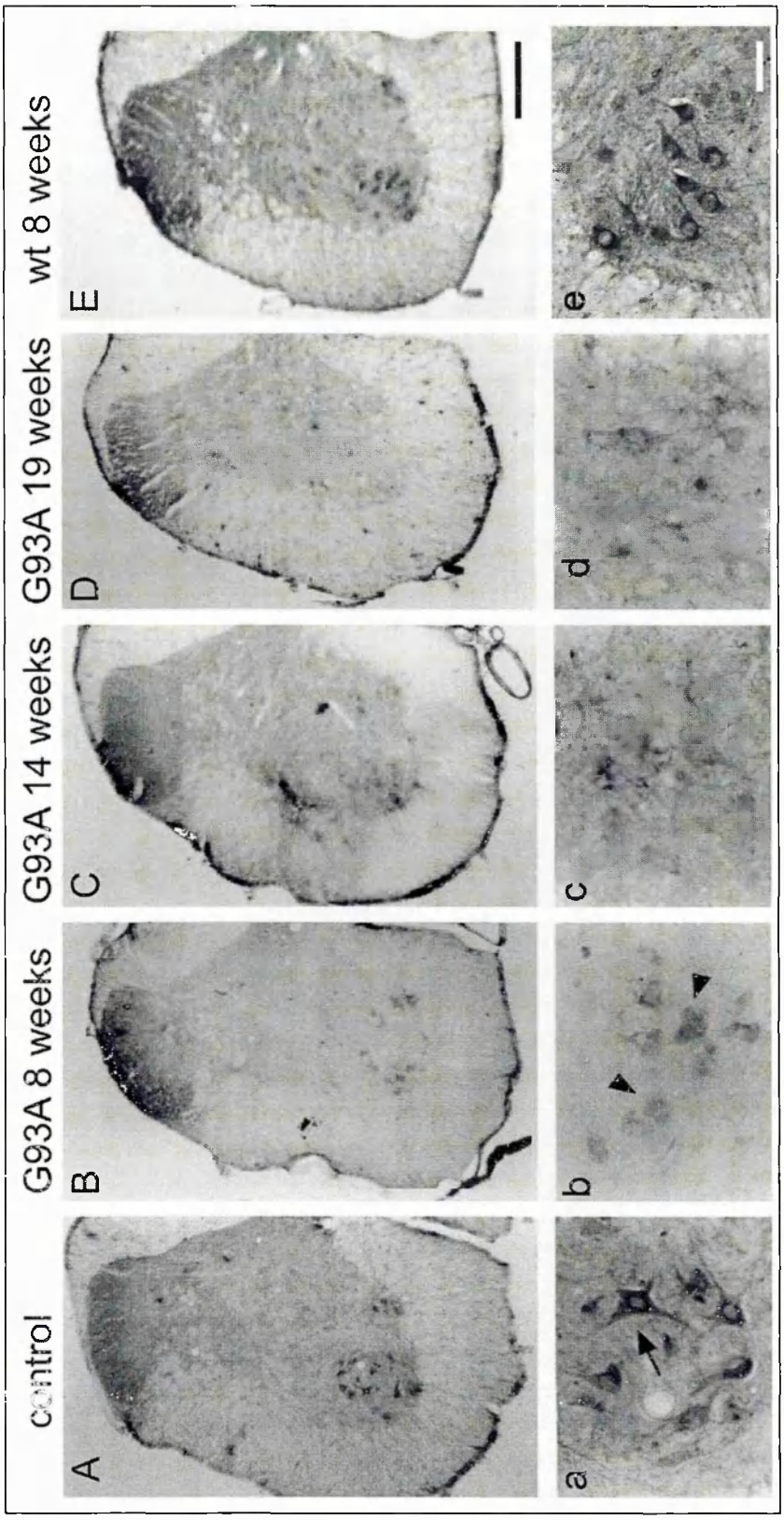
control
G93A 8 weeks
G93A 14 weeks
G93A 19 weeks
wt 8 weeks
A
B
C
D
E
a
b
c
d
e

Figure 3.12

Figure 3.12: GluR2 immunoreactivity in lumbar spinal cord of SOD1^{G93A} mice

In control (non transgenic) mice at 8 weeks of age, a widespread GluR2 immunoreactivity is localized throughout the whole grey matter with a marked staining in the dorsal laminae and in motor neurones of ventral horn (A). In the motor neurones, immunostaining is distributed in the cytoplasm of the cell body and neurites (a). No significant changes in GluR2 immunostaining are observed in the dorsal horn of SOD1^{G93A} mice (B,C,D). On the contrary, decreased labelling is revealed in the ventral region, at all stages of the disease, associated with a progressive loss of motor neurones. In particular, in the SOD1^{G93A} mice a 8 and 14 weeks of age, we could observe a decrease of GluR2 immunostaining associated with changes in the morphology of motor neurones with a loss of neurites (b,c,d). No evident changes in GluR2 immunoreactivity are observed in SOD1^{wt} mice (E-e). Scale bars: (A-E = 200 μm); (a-e= 50 μm).

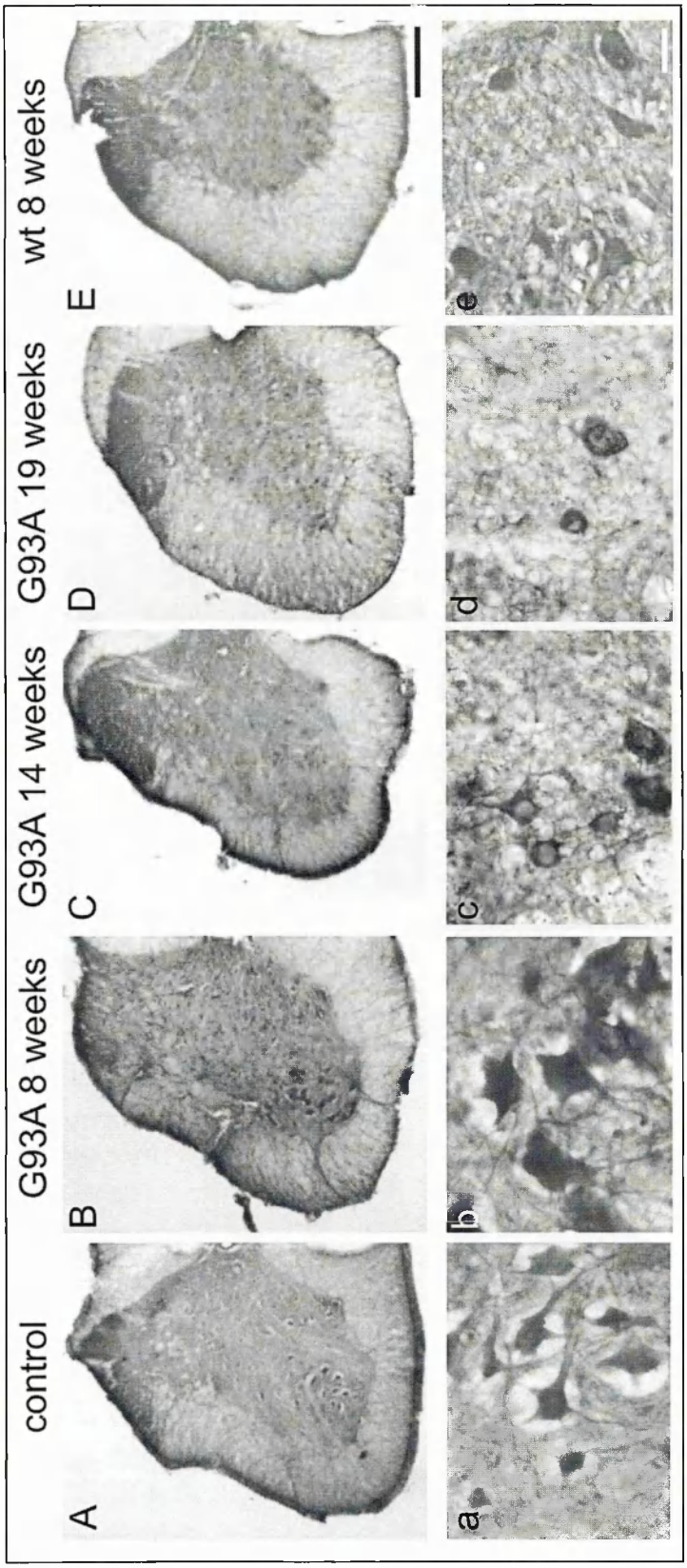
control
G93A 8 weeks
G93A 14 weeks
G93A 19 weeks
wt 8 weeks
A
B
C
D
E
a
b
c
d
e

Figure 3.13

Figure 3.13: GluR3 immunoreactivity in lumbar spinal cord of SOD1^{G93A} mice

The immunostaining in ventral horn of non transgenic mice at 8 weeks of age (control) is mainly localized in the motor neurones, as well as in other smaller neurones of this region (A). Within the motor neurones the immunostaining is homogenously distributed in the cytoplasma of the cell body and neurites (a). In the SOD1^{G93A} mice at 8 weeks of age there was a general increase of immunoreactivity in neurones of grey matter in ventral horn and intermediate area (B). An increased immunostaining is also revealed in the cytoplasm of several motor neurones in lamina IX (b). No evident changes in GluR3 immunoreactivity are observed in SOD1^{wt} mice (E,e). Scale bars: (A-E = 200 μm); (a-,e = 20 μm).

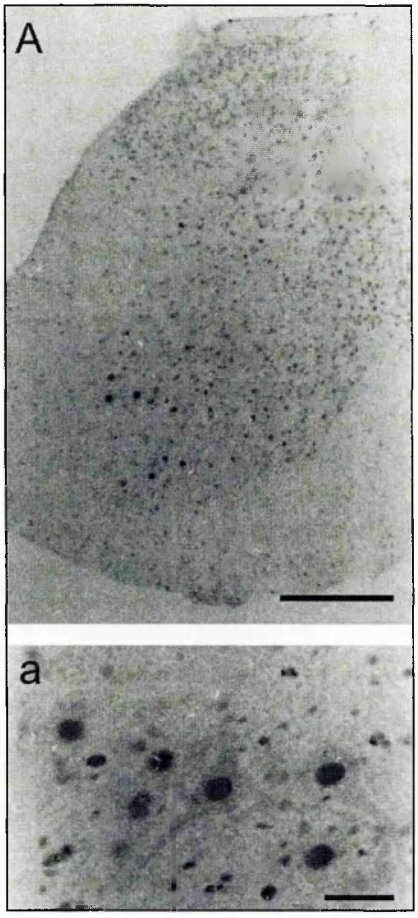

Figure 3.14: GluR4 immunoreactivity in lumbar spinal cord of SOD1^{G93A} mice

Immunoreactivity of GluR4 subunit protein is distributed in almost all the cells of grey matter of lumbar spinal cord of control mice (A). A prominent staining of nuclei of the cells is observed. In particular, the nuclei of motor neurones of ventral regions are very intensely and homogeneously labelled (a). The GluR4 immunoreactivity in SOD1^{G93A} mice does not apparently differ from non transgenic controls (not shown). Scale bars: (A = 200 μm); (a = 20 μm).

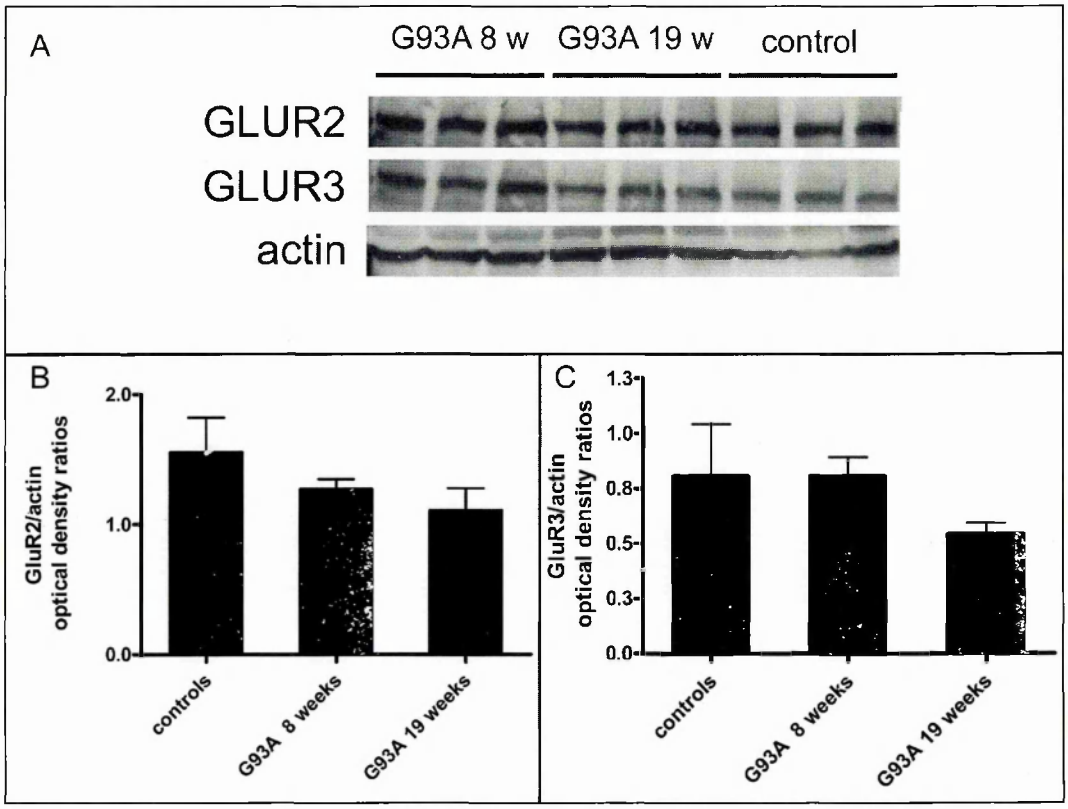

Figure 3.15: Western blot analysis of the expression of AMPA receptor subunits GluR2 and GluR3 in the spinal cord of SOD1^{G93A} mice

(A) No evident differences in GluR2 and GluR3 band intensity was oserved in SOD1^{G93A} mice at presymptomatic (8 weeks of age) and final stage of the disease (19 weeks of age), when compared to controls (non transgenic mice at 8 weeks of age). (B-C) Results show quantitative evaluation of GluR2 (B) and GluR3 (C) protein levels expressed as ratio between their band intensity and actin band intensity from the same blot. Each column shows the mean ± S.E.M. (n = 3). Data analysed by One-Way ANOVA followed by Bonferroni's multiple comparison test.

3.5 Discussion

In this part of the project, I investigated the expression of AMPA receptor subunits in the spinal cord of a murine model of ALS, the $SOD1^{G93A}$ transgenic mouse. In fact, alterations of AMPA receptor composition may result in aberrant glutamate firing of motor neurones and increased calcium entry to cause selective death of these cells. Therefore, this kind of evaluation may give further important clues about the possible role of excitotoxicity in ALS.

The main result coming out from this study regards the decreased expression of GluR2 subunit in the motor neurones of $SOD1^{G93A}$ mice at presymptomatic stage of the disease, compared to non transgenic and $SOD1^{wt}$ mice. This data represents the first evidence of altered glutamate receptor expression in this mouse model of ALS.

The decline of this subunit is only seen at the level of protein expression, without involving the mRNA production, as demonstrated by the *in situ* hybridisation study. In fact, quantitative evaluation of these experiments showed no significant changes in mRNA expression either in dorsal or ventral horn of the spinal cord, with no changes in motor neurones. On the contrary, the immunostaining for GluR2 appeared diminished in the cell bodies of many large motor neurones of transgenic mice at presymptomatic stage of the pathology. This phenomen was not observed in neurones of dorsal laminae. Although the immunohistochemical analysis does not provide a reliable quantitative evaluation of the results, the decrease of immunolabelling was observed in the motor neurones of a high percentage of the mice examined. Moreover, this data

was in part supported by immunoblotting that showed a trend to decrease of the band density for GluR2 at presymptomatic stage of the disease. However, quantitative analysis did not reveal significant changes, probably due to unchanged high levels of GluR2 in the dorsal horn.

Another interesting result emerging from this study is the apparent general increase of GluR3 protein expression observed by immunohistochemistry in the spinal cord, and in particular in motor neurones, of $SOD1^{G93A}$ mice at the same phase of the disease, even if the difference were less marked than the one observed for GluR2 subunit. In this case the quantitative estimation of mRNA in motor neurones showed a trend to increase at 8 weeks of age, which became significant at 14 weeks of age, confirming the general GluR3 tendency to increase.

The other subunits, GluR1 and GluR4 were not examined in as much detail since GluR1 mRNA was not found on motor neurones of control mice and GluR4 protein showed an unusual distribution.

It is known that the presence of the Q/R edited form of GluR2 in the molecular structure of AMPA receptors determines the calcium impermeability of their channel. As outlined in the introduction to this chapter, changes in GluR2 levels in the motor neurones can results in increased calcium permeability of AMPA receptors and might lead to or derive from pathological condition in ALS, determining or contributing to motor neurone degeneration.

Whether the expression of GluR2 in the motor neurones of ALS patients is altered or not still remains uncertain. Confirming our results obtained in $SOD1^{G93A}$ mice, Kawahara and collaborators have recently demonstrate

unchanged level of GluR2 mRNA in single motor neurones of human ALS (Kawahara et al., 2003). However, GluR2 transcripts in the motor neurones of 44% of ALS cases examined were incompletely edited (Kawahara et al., 2004). Spalloni and colleagues have recently reported unchanged levels of GluR2 subunit mRNA in cultured mouse motor neurones expressing $SOD1^{G93A}$ in respect to control (Spalloni et al., 2004), giving further confirmation of the lack of mRNA transcription involvement. In contrast to these negative findings, one study showed a decrease of GluR2 messanger RNA in total ventral grey matter of ALS patient spinal cord, evaluated by PCR technique (Takuma et al., 1999). Diminished mRNA levels for this AMPA subunit in whole human spinal cord homogenates was also described by Virgo and colleagues (Virgo et al., 1996). In all these reports, the protein level of GluR2 was not evaluated. Expression studies in human tissue are necessarily carried out on postmortem samples, which derive in most instances from end stage cases of the disease, when a large number of motor neurones are degenerated. Therefore, the reduction of GluR2 mRNA level observed in the whole spinal cord may reflect the massive loss of these cells. Thus, whether alteration of AMPA subunit expression can occur in early phase of human pathology is difficult to establish. Moreover, there are no studies about the protein expression of GluR2 in human patients. Transgenic mouse models of ALS such as the one used in this study provide therefore a good tool to clarify these aspects.

The results obtained in this study indicate that post transcriptional events can lead to decrease of GluR2 protein expression in the lumbar motor neurones of $SOD1^{G93A}$ mice in respect to normal animals, even without decrement of its

mRNA. It suggests that pathological condition induced by the expression of ALS-linked mutant form of SOD1 may affect the translation or the biological stability of GluR2 protein.

Since this effect was already observed in mice at 8 weeks of age, when the symptoms are not yet evident, it can be assumed that this phenomenon may be a causative event of the disease that could help to trigger the pathology in these mice. Supporting this hypothesis, it has been showed that calcium entry into the motor neurones through the Ca^{2+}-permeable AMPA receptors induces a selective damage to mitochondria into these cells (Carriedo et al., 2000). A very early pathological marker observed in $SOD1^{G93A}$ mice is the vacuolisation of mitochondria in motor neurones (Bendotti et al., 2001a). Therefore, altered glutamatergic stimulation due to GluR2 deficiency might be the cause of this precocious mitochondria failure, indicating the excitotoxicity as a possible early event in $SOD1^{G93A}$ mice pathology. Support for such a theory comes from studies carried out on mixed spinal cord cultures derived from the same transgenic mice. The authors showed an increased vulnerability of motor neurones expressing $SOD1^{G93A}$ mutant to AMPA mediated glutamate toxicity (Spalloni et al., 2004) associated with enhanced reactive oxygen speciesl production, sustained elevations of intracellular calcium levels, and mitochondrial dysfunction (Kruman et al., 1999). On the other hand, it has recently been shown that mitochondrial dysfunction induced by complex I and complex II inhibitors predisposes cultured motor neurones to excitotoxicity mediated by glutamate ionotropic receptor (Kanki et al., 2004). It suggests that glutamate receptor alteration could also be secondary to early mitochondrial

failure determined by other factors such as the accumulation of mutated SOD1 onto mitochondria surface of motor neurones (Liu et al., 2004).

GluR2 immunoreactivity has been investigated in another transgenic model of ALS, the $SOD1^{G86R}$ mice, which carry mutated murine gene as transgene. Unlike the present study, Morrison and colleagues did not find apparent changes in GluR2 immunostaining in spinal cord of these mice at both presymptomatic and symptomatic stage of the pathology (Morrison et al., 1998). However, the $SOD1^{G86R}$ mice develop an extremely aggressive disease and only few days pass between the onset of symptoms and total immobility and death (Ripps et al., 1995a). This rapid development of the pathology, so different from the disease progression occurring in ALS patients and in $SOD1^{G93A}$ mice used in our study, render this model quite dissimilar from the chronic course of the human illness. Consequently, the acute motor dysfunction displayed by these mice can be ascribed to different processes, which could not involve the glutamatergic system.

Reduction of GluR2 subunits has been also observed in other pathological conditions. It has been shown that GluR2 mRNA is downregulated in susceptible neurones of animal models after transient forebrain ischemia or kainate-induced epilepsy (Pellegrini-Giampietro et al., 1992; Pollard et al., 1993; Friedman et al., 1994; Pellegrini-Giampietro et al., 1994). Another study demonstrated that traumatic spinal cord injury determines a long-lasting decrease of GluR2 mRNA and protein in motor neurones near the injury site (Grossman et al., 1999). Contrary to what observed in our model, in these cases the authors reported the decrement of GluR2 messanger RNA but the

paradigms used are represented by acute condition of neurological injury, whereas the ALS-like pathology displayed by $SOD1^{G93A}$ mice is a chronic disease. Therefore, the mechanisms underlying the reduction of GluR2 expression can be different. On the other hand, these data confirm that AMPA receptor architecture can undergo dynamic modification when stressed by harmful circumstances.

The mechanisms underlying the decreased expression of GluR2 observed in our experiments and in particular how the expression of the mutant $SOD1^{G93A}$ can affect the GluR2 availability in the motor neurones remain to be elucidated.

It has been demonstrated that excessive glutamate stimulation of cultured hyppocampal neurones induces AMPA receptor internalization mediated by dynamin-dependent endocytotic process (Carroll et al., 1999; Lissin et al., 1999). Zhou and collaborators found that the glutamate-induced internalization of AMPA receptors is caused by calcium influx, which in turn determines depolymerization of actin filaments (Zhou et al., 2001). The role of actin filaments in AMPA receptor anchoring to postsynaptic membrane surface suggests that disorganization of cytoskeletal structure can directly be involved in decreased expression of GluR2 in ALS. Neurofilament accumulations in the cell bodies and proximal axons of motor neurones have been documented in both sporadic and familial ALS (Hirano et al., 1984a; Hirano et al., 1984b). Several studies carried out on transgenic mice have shown that neurofilament content and organization strongly influence motor neurone disease induced by mutant SOD1 (Couillard-Despres et al., 1998; Williamson et al., 1998; Couillard-

Despres et al., 2000; Kong and Xu, 2000). However, direct involvement of actin in ALS pathology has never been reported, although it cannot be excluded.

Another possible mechanism involved in GluR2 protein downregulation relates to the p38MAPK pathway. Recently, it has been reported that inhibition of p38MAPK cascade can reverse the decrease of GluR2 expression observed in cortical neurones of neonatal rats after treatment with glutamate (Rivera-Cervantes et al., 2004). Zhu and colleagues have reported that AMPA receptor subunits with short intracellular tails such as GluR2 are continuously added to and removed from synapses during normal neuronal activity. In particular, they showed that removal of GluR2 require activation of Rap, a member of the Ras superfamily of small GTPases, and the activation of p38MAPK pathway (Zhu et al., 2002a). Since over activation of p38MAPK has been hypothesized to be involved in ALS pathology (Kriz et al., 2002; Raoul et al., 2002; Van Den Bosch et al., 2002a; Bendotti et al., 2004), it is possible that decrease of GluR2 protein in motor neurones of ALS $SOD1^{G93A}$ mice can be due to early activation of this pathway with consequent internalisation and degradation. This aspect will be discussed more in detail in chapter 7.

Our results have shown an increased level of GluR3 mRNA in the spinal motor neurones of $SOD1^{G93A}$ mice, which resulted significant at symptomatic stage of the disease. Moreover, immunohistochemistry also showed an overexpression of GluR3 protein in motor neurones already at presymptomatic phase of the pathology. This was not confirmed, however, by Western blotting, probably due to underestimation of the result deriving from the use of protein extract of whole spinal cord. These data are in line with the results reported in

two recent studies. It has been shown that cultured spinal motor neurones derived from the same strand of transgenic ALS mice express higher levels of GluR3 mRNA in respect to controls, associated with unchanged levels of GluR2 mRNA (Spalloni et al., 2004). An Australian group claimed they found increased amount of GluR3 protein in the spinal cord of $SOD1^{G93A}$ mice analysed by proteomic approach, despite the fact that they did not show the results (Rembach et al., 2004). In the same work, Rembach and collaborators treated $SOD1^{G93A}$ mice with antisense peptide nucleic acid directed against GluR3, obtaining a significant extension of survival and improvement of symptoms. However, they could not show any downregulation of GluR3 protein in the spinal cord of transgenic mice.

Since GluR3 is a Ca^{2+}-permeable AMPA receptor subunit, it is assumable that decrease of GluR2 subunit level, associated with overexpression of GluR3 may result in increased number of AMPA receptors that permit the entrance of calcium during glutamatergic firing, contributing to motor neurone degeneration in $SOD1^{G93A}$ ALS mice. However, given the lack of GluR2 mRNA involvement and the significant elevation of GluR3 mRNA in motor neurones when the symptoms are already evident, a possible scenario is that the expression of $SOD1^{G93A}$ mutant first determines early post transcriptional modifications of GluR2 protein, leading to its excessive degradation; motor neurones, in the attempt of replacing GluR2, activate the transcription not of GluR2 but of another AMPA subunit, GluR3. This causes the assembling of a high number of calcium-permeable AMPA receptors, which lead in turn to excitotoxicity and motor neurone death. Although rather speculative, this hypothesis deserves

further investigation that allow to examine the simultaneous expression of the receptor subtypes in the same motor neurone.

Analysis of mRNA expression, carried out by *in situ* hybridisation, revealed low levels of GluR1 mRNA in the whole spinal cord and in particular in the motor neurones of control mice. This result is according with previous studies reporting low expression of this subunit in the motor neurones of rats (Furuyama et al., 1993; Grossman et al., 1999; Greig et al., 2000) but in contrast with other works showing relatively high levels of mRNA GluR1 in the same animals (Van Den Bosch et al., 1999) and in humans (Williams et al., 1997). However, there are not published studies regarding GluR1 mRNA expression in mouse motor neurones. Thus, this represents the first report showing low levels of this subunit in mice.

Messanger RNA of GluR4 subunit resulted moderately expressed in the motor neurone of control mice and no significant differences of expression were detected in $SOD1^{G93A}$ transgenic mice. Surprisingly, immunohistochemical analysis of GluR4 protein distribution revealed a prominent nuclear staining of the cells. In particular, the nuclei of motor neurones of ventral regions were intensely and homogeneously labelled. This is in contrast with previous study performed in rat spinal cord and showing a cytoplasmic localization of GluR4 protein (Tachibana et al., 1994). The nuclear distribution found in mice does not seem to be due to low specificity of the antibody utilized. In fact, experiments carried out with the same antibody on rat brains showed cytoplasmic labelling of neurones similar to that reported in the literature, demonstrating its specificity.

Thus, it is possible that this antibody recognise epitopes of nuclear proteins in C57 mice.

CHAPTER 4

Study of the effect of the treatment with a glutamate AMPA receptor antagonist on $SOD1^{G93A}$ transgenic mice

4.1 Introduction

An altered subunit composition of glutamate AMPA receptors on motor neurones may result in their aberrant activation, which in turn can lead to excitotoxic events and motor neurone death in ALS. Because of this hypothesis, several competitive AMPA antagonist drugs were tested in animal models of motor neurone disease. The selective AMPA antagonist NBQX showed protective effects on MND mice, significantly improving the motor function scores, and on $SOD1^{G93A}$ mice, prolonging their survival (Mennini et al., 1999; Van Damme et al., 2003). The same effect on $SOD1^{G93A}$ mice was obtained in a study with another AMPA antagonist RPR 119990, which also improved the grip muscle strength of these ALS mice (Canton et al., 2001). These promising results indicate that blockade of AMPA-mediated glutamatergic neurotransmission might represent a new therapeutic approach for the treatment of ALS. However, the use of competitive AMPA receptor antagonists in clinical therapy could cause problems because of the involvement of AMPA receptors in most physiological brain functions. Thus, the discovery of non-competitive allosteric modulators of AMPA receptors, acting on a region different from the glutamate binding site, gives rise to new therapeutic agents with pharmacological properties different from the common AMPA antagonists. The first allosteric modulators of AMPA receptors were the 2,3-benzodiazepines, including non competitive GYKI 52466 and its more potent

analogue GYKI 53655, which selectively inhibit AMPA receptors by interacting at a distinct site (Paternain et al., 1995; Bleakman et al., 1996).

The particular property of non competitive AMPA antagonists that is of potential clinical benefit, is that they are effective even in the presence of high levels of glutamate. Since it has been hypothesized that one of the factors contributing to excitotoxic firing on motor neurones might be the decreased expression and functioning of glial glutamate transporters (Rothstein et al., 1992; Rothstein et al., 1995; Trotti et al., 1999), which leads in turn to high levels of glutamate in the synaptic cleft, the treatment with such kinds of drugs might be extremely useful in ALS therapy.

A benzodiazepine derivative, ZK 187638 (2,3-dimethyl-6-phenyl 12H-[1,3]dioxolo[4,5-h]imidazol[1,2-c][2,3] benzodiazepine), has been characterized as a non competitive AMPA receptor antagonist (Csuzdi *et al.,* PCT Int.Appl. WO 97 28, 163; Chem. Abstr., 127, 205597n., 1997; Elger et al., unpublished results). Preliminary studies showed that, compared to other AMPA antagonists, this compound demonstrated a good bioavailability in the central nervous system after oral administration. This represents an advantage for treatment of chronic diseases.

4.2 Hypothesis and aim

The hypothesis investigated in this chapter is that, since motor neurones in ALS are prone to excitotoxicity mediated by AMPA receptors because of their

subunit composition, a non competitive AMPA antagonist will prevent motor neurone loss in $SOD1^{G93A}$ mice.

The aim of this study is to test the effect a new non competitive AMPA receptor antagonist, ZK 187638, on motor functions and survival of $SOD1^{G93A}$ mice.

4.3 Methods

4.3.1 Evaluation of ZK 187638 levels in plasma and CNS tissues

This part of the study was carried out in collaboration with the Drugs Metabolism Laboratory at Mario Negri Institute, Milano.

Blood samples from $SOD1^{G93A}$ and non transgenic mice were collected in heparinized tubes and centrifuged to separate the plasma, which was stored at -20°C until analysis. Brains from the same animals were removed immediately after exsanguination, blotted with paper to absorb excess surface blood and stored at -20°C. Plasma were precipitated with acetonitrile (1:2) and the supernatant was taken directly for LC/MS/MS quantification, using calibration curves in a matrix and a related compound as internal standard. Separation was on an XTerra MS C18 column (10 cm x 2.1 mm I.D., 3.5 µm particle size; pre-column 1 cm x 2.1 mm) at 25°C. The mobile phase was A: H_2O + 0.1% acetic acid, B: acetonitrile + 0.1 acetic acid, flow rate 0.3 ml/min, gradient 75% A to 5% A in 5 minutes. The retention time was 3.2 minutes for ZK 187638, 3.1 minutes for the I.S. Mass spectrometric detection was by TIS Pos MS.

CNS tissue was homogenized (20 ml/g) in KH_2PO_4 0.01 M, pH 7.4, and 0.5 ml containing approximately 25 mg of tissue was extracted as described for plasma. Separation was on a Discovery C18 Column (15 cm x 4.6 mm I.D., 5 µm particle size) (Supelco, Bellefonte, USA), protected by a Lichrospher RP-select B 5-µm pre-column (Merck, Darmstadt, Germany), at room temperature. The mobile phase was 0.01 M KH_2PO_4: CH_3OH: CH_3CN (39:58:3 v/v) adjusted to pH 5.0 with H_3PO_4, at a flow rate of 1 ml/min. The retention times were approximately 10.6 minutes for ZK 187638 and 14.6 minutes for the I.S.

4.3.2 Chronic treatment of SOD1^{G93A} mice with ZK 187638

Transgenic SOD1^{G93A} mice received ZK 187638 orally, suspended in 10% Tween 80 (10 ml/Kg), and every other day starting from 11 weeks of age. At this age mice showed neurological symptoms of the disease such as tremors and reduced extension reflex of hind limbs when raised by the tail and neuropathological features like massive vacuolisation of motor neurones, as described in section 2.1 (Bendotti and Carri, 2004). One group of SOD1^{G93A} animals (n=23) received repeated doses of the drug at 70 mg/Kg. Another group of SOD1^{G93A} mice (n=24) was treated with a first dose of 100 mg/Kg and then with 140 mg/Kg. A third group of transgenic mice (n=19) received only the vehicle by the same schedule. Nine animals for each group were selected before the beginning of the treatment for the survival study. The other mice were scarified at 19 weeks of age for the histological analysis. Data for the motor behavioural and neurological tests were collected form the whole groups

of animals. Three groups of non transgenic mice (n= 10) were also treated with the two doses of ZK 187638 and vehicle.

4.3.3 Motor behavioral and neurological tests performed during chronic treatment with ZK 187638

Quantitative assessment of the motor behavioral deficit was carried out by measuring the stride length and rotarod performance. Evaluation of survival was also performed. Body weight was recorded during treatment.

Stride length test:

To measure stride length, mice were trained to walking a 75 cm long ramp raised to a height of 13 cm at one end. A bright light was placed at the base of the ramp to provide an aversive stimulus. The mice's hind feet were painted with children's poster paints and the tracks left as they ran up the ramp were recorded on paper tape lining the floor of the ramp. Stride length was defined as the distance between successive right-to-right and left-to-left footprints.

Rotarod test:

$SOD1^{G93A}$ mice were trained to remain on the rod and habituated to the handling involved for at least a week before testing. On the day of testing, mice were transferred to the rotarod room at least 15 minutes before the test. Strategies to overcome deficits (gripping the rod and rotating with it, falling and jumping back, etc.) were noted but not considered for the test. Performance

was evaluated as the time (sec.) spent on the rotating rod (12 rpm) without falling off (RotaRod treadmill for mice, Ugo Basile, Comerio, VA, Italy). The test was stopped after 3 minutes. Mice that fell off before the third minute were tested three times, with at least 5 minutes between tests.

Survival:

$SOD1^{G93A}$ mice were killed if they were unable to roll over when they were laid down on their side. This time was used for calculating the survival curves.

Statistics:

For each experimental group the median, mean, standard deviation and standard error were calculated. Deviation from Gaussian distribution was tested by the Kolmogorov-Smirnov test. All the data passed the normality test. Body weight, stride length and rotarod performance of $SOD1^{G93A}$ mice were analysed by ANOVA for repeated measures (weeks) and the different groups (treatments), followed by post-hoc Dunnett's test to compare the effect of drug and vehicle at the individual weeks. The survival of $SOD1^{G93A}$ mice treated with the drug or vehicle was analysed by the log-rank test. All the statistical analyses were done using the GraphPad Prism 2.0a for Power Macintosh (GraphPad Software Inc.).

4.3.4 Immunohistochemical analysis of ChAT positive motor neurones in $SOD1^{G93A}$ mice treated with ZK 187638

Immuhistochemical analysis was performed as decribed in section 2.5. Fixed and frozen lumbar spinal cords of $SOD1^{G93A}$ mice treated with vehicle (n=5), 70 mg/kg (n=5) or 140 mg/kg (n=6) of ZK 187638 and respective non transgenic mice groups (n=5 each) were use. Section were incubated with primary antibody (anti ChAT, 1:250, Chemicon International) in TBS + 3% NGS for 2 hours at room temperature and then overnight at 4°C.

Biotinylated anti-mouse secondary antibody (1:200, Vectastain kit, Vector Laboratories) was used. Slides were examined by light microscopy and the number of ChAT immunopositive neurones was determined in the lumbar spinal cord every ten sections (segments L2-L4) according to a previously reported procedure (Mennini et al., 2002). Five serial sections for each animal were processed for ChAT immunostaining, the number of ChAT immunopositive motor neurones was calculated for each hemisection, and the means of these determinations were used as individual data for statistical analysis. Differences in the number of motor neurones from the lumbar spinal cord of $SOD1^{G93A}$ mice were analysed by ANOVA followed by Tukey's test (GraphPad Prism 2.0a for Power Macintosh, GraphPad Software Inc.).

4.3.5 In situ hybridisation for mRNA of glutamate AMPA receptor subunit GluR2 in $SOD1^{G93A}$ mice treated with ZK 187638

In situ hybridisation to detect the mRNA of AMPA receptor subunit GluR2 in spinal cord and brain of $SOD1^{G93A}$ mice at 19 weeks of age treated with

vehicle (n=5), 70 mg/Kg (n=5) or 140 mg/Kg (n=6) of ZK 187638 were performed as described in section 2.4 and 3.3.1.

4.4 Results

4.4.1 Pharmacokinetic and metabolic studies

Before starting the treatment of $SOD1^{G93A}$ mice, pharmacokinetic and metabolic studies were performed in order to evaluate the bioavailability of the drug. Data about the brain-plasma distribution of ZK187638 were obtained after acute administration of this compound in $SOD1^{G93A}$ mice. Single oral administration of 70 and 140 mg/Kg of ZK187638 produced plasma concentrations at 3 hours of 3.9 ± 0.4 µg/ml and 8.7 ± 0.6 µg/ml (mean ± S.E.M., n=7) respectively. A higher dose (210 mg/Kg) did not produce increased plasma concentration (9.7 ± 0.7 µg/ml, n=7). Similar results were achieved in brain tissue where the compound reached concentrations 2.6-3.9 times higher than those observed in plasma, showing that the drug effectively reaches the central nervous system.

To evaluate drug concentration in plasma and brain after chronic administration, $SOD1^{G93A}$ and non transgenic mice were treated every other day starting from 11 weeks of age and until the death of transgenic animals. Plasma concentrations of ZK 187638 in $SOD1^{G93A}$ mice and in non transgenic controls on the last day of the repeated oral dosing schedule were essentially dose related. Drug concentration of 2.6 ± 0.6 (n=8) and 4.3 ± 1.8 µg/ml (n=8) were

found in SOD1^{G93A} mice and drug concentration of 1.6 ± 0.9 (n=7) and 2.6 ± 2.9 µg/ml (n=8) were found in non transgenic littermates after 70 and 140 mg/Kg, respectively. Brain concentrations (6.7 ± 1.6 and 13.1 ± 9.8 in SOD1^{G93A} mice and 3.9 ± 0.9 and 7.5 ± 3.2 µg/g in non transgenic mice, after 70 and 140 mg/Kg respectively) were about three times higher than plasma concentrations and there was a linear relationship between plasma and brain concentrations in both transgenic and non transgenic mice. ZK187638 brain concentrations were also similarly correlated with spinal cord concentrations.

At least two putative metabolite peaks were observed in the plasma chromatograms of SOD1^{G93A} and controls. These peaks were never found in drug free samples, suggesting they represent metabolites of ZK187638.

4.4.2 Treatment of SOD1^{G93A} mice and evaluation of behavioural benefits

In order to mimic the therapeutical conditions used in the treatment of ALS patients, which receive the drugs after the diagnosis of the disease based on symptom and sign observation, chronic treatment of SOD1^{G93A} mice was started at first symptom indication represented by tremors and reduced adduction of the hind limbs when raised by the tail. This phase of the disease is displayed at 11 weeks of age. ZK 187638 was administrated orally, suspended in 10% Tween 80 (10 ml/Kg) and every other day. One group of SOD1^{G93A} animals (n=23) received repeated doses of the drug at 70 mg/Kg. Another

group of $SOD1^{G93A}$ mice (n=24) was treated with a first dose of 100 mg/Kg and then with 140 mg/Kg. A third group of transgenic mice (n=19) received only the vehicle by the same protocol.

The motor function deficit of the animals of all the groups was quantitatively evaluated measuring stride length and rotarod performance. Body weight was also recorded during all the treatments. ZK 187638 70 and 140 mg/Kg had no effect on the body weight, rotarod performance and gait of non transgenic mice (data not shown).

Impairment of motor functions, revealed by stride length and rotarod tests, in vehicle treated $SOD1^{G93A}$ transgenic mice started at about 15 weeks of age and became rapidly worse until the mice died in a range of age between 20 and 24 weeks. Oral administration of 70 and 140 mg/Kg of ZK 187638 slowed the reduction of stride length compared to vehicle treated mice. At 17 and 18 weeks of age the mean stride of mice treated with these doses was significantly longer than the vehicle group (Figure 4.1). ZK 187638 also significantly ameliorated the rotarod performance of $SOD1^{G93A}$ mice. The time spent on the rotarod by transgenic mice treated with 70 and 140 mg/Kg of ZK 187638 was significantly longer than in vehicle treated mice. The highest dose showed a significantly improved performance, which was better than untreated mice even at 18 weeks of age (Figure 4.2). The improvement in gait and rotarod performance in treated mice persisted after this time point. However, since many vehicle treated mice died at this time and the group sizes become heavily unbalanced, graphic representation and statistical analysis of these data are omitted.

Treatment with 70 and 140 mg/Kg of ZK 187638 also reduced the body weight loss of $SOD1^{G93A}$ (Figure 4.3). Moreover, administration of both the doses of the drug extended the mean survival of treated animals. The life expectancy resulted prolonged by 11 and 17 days for 70 and 140 mg/Kg dose respectively, when compared to vehicle treated mice. However, the effect was significant only for the group treated with 140 mg/Kg (Figure 4.4).

4.4.3 Analysis of motor neurone survival in $SOD1^{G93A}$ mice treated with ZK 187638

To investigate whether ZK 187638 influenced motor neurone death, a group of $SOD1^{G93A}$ mice treated with vehicle (n=5), 70 mg/Kg (n=5) or 140 mg/Kg (n=6) of ZK 187638 and respective non transgenic mice groups (n=5 each) were killed and perfused with fixative at 19 weeks of age. Sections from the lumbar spinal cord were examined by immunohistochemical technique (Figure 4.5). Quantitative analysis of choline acetyl transferase (ChAT) immunopositive motor neurones showed a significant reduction in the number of cells in $SOD1^{G93A}$ mice treated with vehicle (59 ± 7%), compared to non transgenic littermates. ZK 187638 140 mg/Kg, but not 70 mg/Kg, slightly but significantly reduced the magnitude of motor neurone loss (48 ± 8%) ($p < 0.05$, ANOVA with post-hoc Tukey's test). High magnification of the ChAT immunostained motor neurones from $SOD1^{G93A}$ mice treated with vehicle showed marked changes in their morphology (loss of neuritic processes,

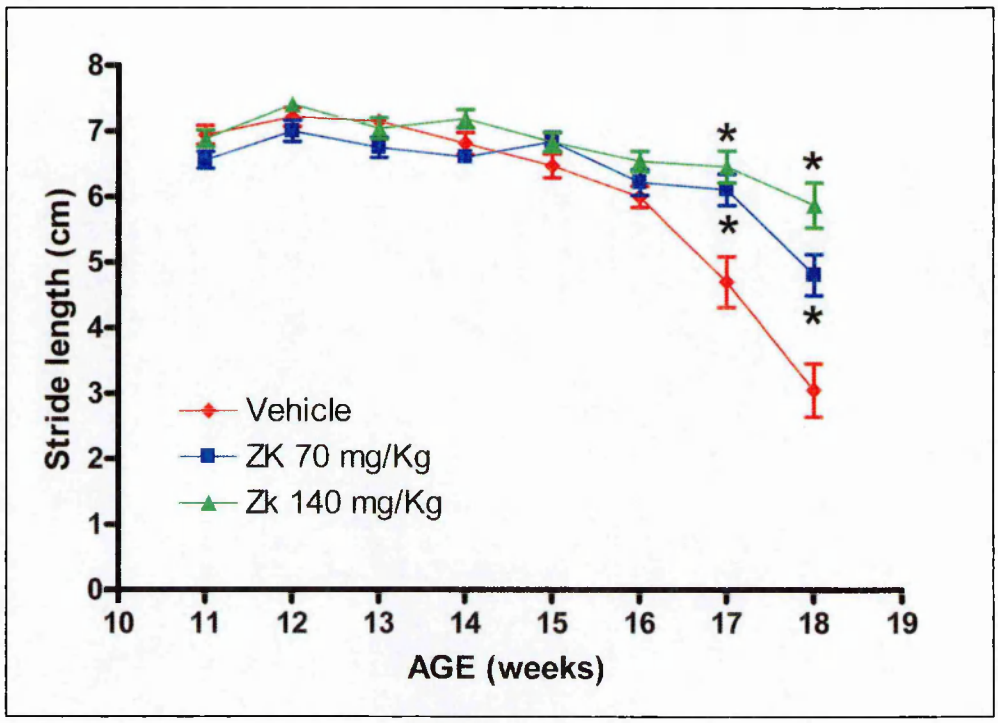

Figure 4.1: Effect of the treatment with ZK 187638 70 and 140 mg/Kg on the stride length of SOD1^{G93A} mice

*Oral administration of 70 and 140 mg/Kg of ZK 187638 significantly slowed the reduction of stride length occurring in SOD1^{G93A} mice when compared to vehicle treated transgenic mice. The curves were interrupted at 18 weeks of age since after this time point some died because of the disease, reducing the size of the groups. Data from vehicle (red diamonds, n=19), ZK 187638 70 mg/Kg (blue squares, n=23) and ZK 187638 140 mg/Kg (green triangles, n=24) mice are presented as mean ± S.E.M. Data were analyzed by ANOVA for repeated measures followed by post-hoc Dunnett's test between treatments. *= $p < 0.05$ compared to vehicle treated group.*

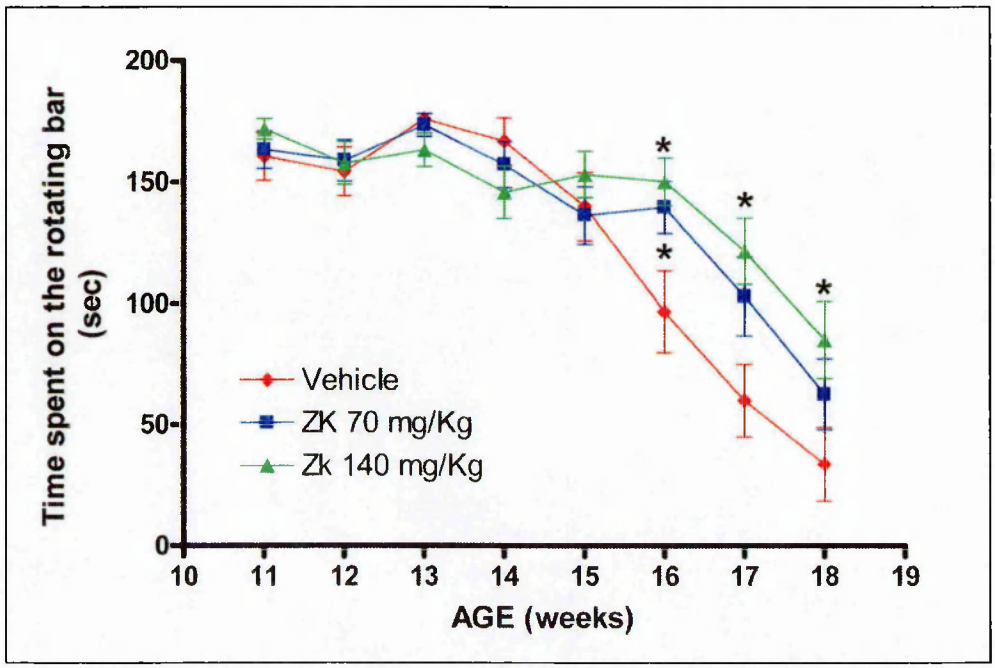

Figure 4.2: Effect of the treatment with ZK 187638 70 and 140 mg/Kg on the rotarod performance of SOD1^{G93A} mice

*Treatment with ZK 187638 70 and 140 mg/Kg significantly ameliorated the rotarod performance of SOD1^{G93A} mice. The highest dose showed a significant improving of performance that was better than untreated mice even at 18 weeks of age. The curves were interrupted at 18 weeks of age since some animals died of the disease after this age, rendering the animal groups unbalanced. Data from vehicle (red diamonds, n=19), ZK 187638 70 mg/Kg (blue squares, n=23) and ZK 187638 140 mg/Kg (green triangles, n=24) mice are presented as mean ± S.E.M. Data were analyzed by ANOVA for repeated measures followed by post-hoc Dunnett's test between treatments. * = $p < 0.05$ compared to vehicle group.*

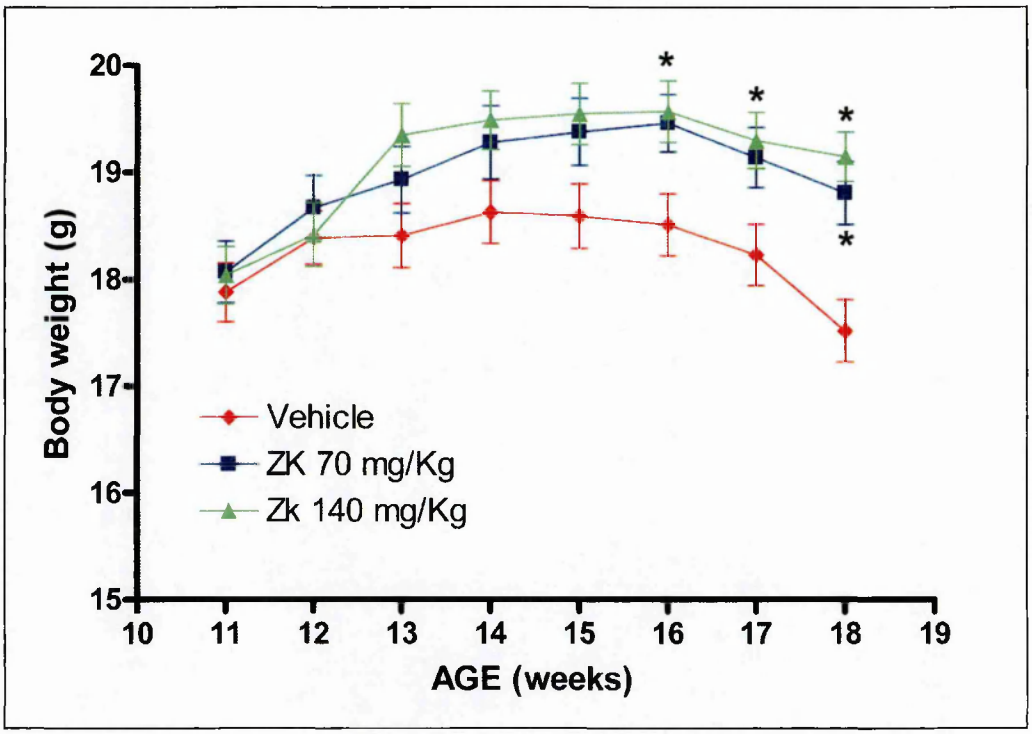

Figure 4.3: Effect of the treatment with ZK 187638 70 and 140 mg/Kg on body weithg of SOD1^{G93A} mice

Treatment with ZK 187638 70 and 140 mg/Kg reduced the body weight loss occurring in SOD1^{G93A} transgenic mice. The curves were interrupted at 18 weeks of age since some died because of the disease after this age, rendering the animal groups unbalanced. Data from vehicle (red diamonds, n=19), ZK 187638 70 mg/Kg (blue squares, n=23) and ZK 187638 140 mg/Kg (green triangles, n=24) mice are presented as mean ± S.E.M. Data were analyzed by ANOVA for repeated measures followed by post-hoc Dunnett's test between treatments.

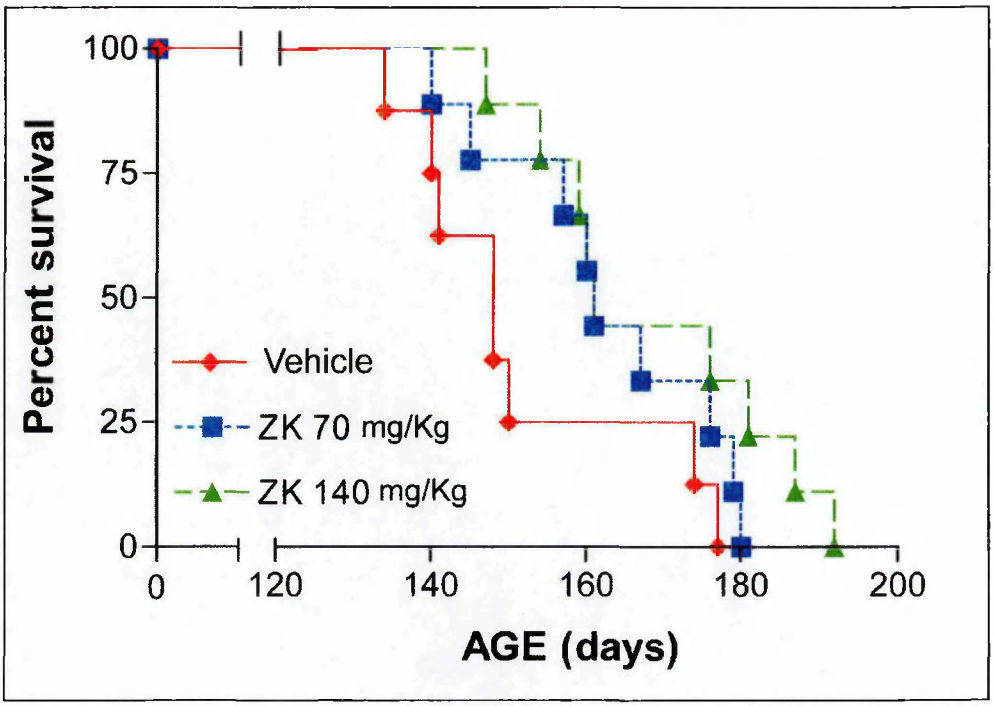

Figure 4.4: Effect of the treatment with ZK 187638 70 and 140 mg/Kg on survival of SOD1^{G93A} mice

Administration of both ZK 187638 70 and 140 mg/Kg ameliorated the life expectancy of SOD1^{G93A} mice, extending the mean survival of treated animals in respect to vehicle treated mice. The life expectancy resulted prolonged by 11 and 17 days for 70 and 140 mg/Kg dose respectively. However, the effect was significant only for the group treated with 140 mg/Kg. Data on survival were analysed by the log rank test (ZK 187638 70 mg/Kg p=0.15; ZK 187638 140 mg/Kg p=0.04, n=9 for each group).

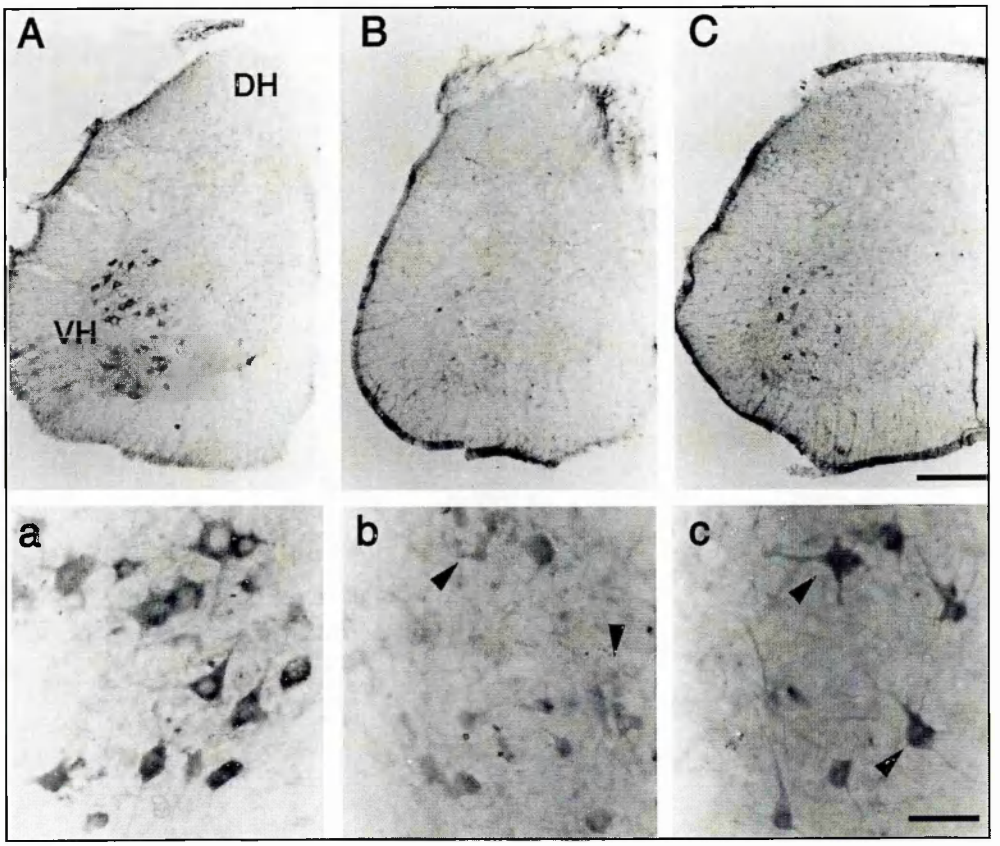

Figure 4.5

Figure 4.5: Effect of the treatment with ZK 187638 70 and 140 mg/Kg on ChAT positive motor neurone degeneration occurring in SOD1^{G93A} mice

A-C: Transverse semisections of lumbar (L2-L4) spinal cord showing ChAT immunopositive motor neurones in the ventral horn. Prominent loss of motor neurones is observed in SOD1^{G93A} mice at 19 weeks of age treated with vehicle (B) versus age matched non transgenic littermates (A). The effect is less marked in 19 week old SOD1^{G93A} mice treated with ZK 187638 140 mg/Kg (C). a-c: High-magnification of the ChAT immunopositive motor neurones in the lamina XI of the ventral horn of spinal cord. There is marked vacuolization of the cytoplasm and apparent swelling of the motor neurones in SOD1^{G93A} mice (arrowheads) receiving vehicle (b), while in those treated with ZK 187638 140 mg/Kg (c) the surviving motor neurones show a better morphology , with intense immunostaining in the perikarya and neurites similar to the non trangenic mice (a) . Scale bar = (A-C) 200 µm; (a-c) 50 µm

shrinkage or vacuolisation of the cell bodies). This effect was less prominent in the age matched mice treated with ZK 187638 140 mg/Kg.

4.4.4 mRNA expression of GluR2 AMPA receptor subunit in SOD1^{G93A} mice after treatment with ZK 187638

Since we found a decreased expression of GluR2 protein in the motor neurones of SOD1^{G93A} mice, we wished to investigate whether the treatment with ZK 187638, which has shown improvement of symptoms and survival of SOD1^{G93A} mice, has also determined changes in GluR2 expression. Unfortunately, we could not perform immunohistochemical analysis to determine GluR2 protein levels in the motor neurones, as perfused tissues of treated transgenic mice were not available. Thus, I just carried out the analysis of GluR2 mRNA by *in situ* hybridisation.

In order to determine whether the treatment with ZK 187638 can selectively change the GluR2 mRNA transcription in nervous system regions involved in the pathology, the study was performed on brain areas not affected by the neurodegeneration (hippocampus and prefrontal cortex) and in the spinal cord of SOD1^{G93A} and non transgenic mice at 19 weeks of age, treated with ZK 187638 (70 and 140 mg/Kg) or vehicle. Quantitative analysis of autoradiographic opical density of GluR2 mRNA radiolabelling in prefrontal cortex and CA1/CA2 area of hippocampus of SOD1^{G93A} mice treated with ZK 187638 (70 and 140 mg/Kg), revealed no significant changes in GluR2 mRNA expression when compared to untreated transgenic mice (Figure 4.6) or non

transgenic mice groups. The same analysis carried out on spinal cord showed unchanged level of GluR2 mRNA in dorsal regions (laminae I, II, III and IV) (Figure 4.7). However, examination of autoradiographic opical density of ventral horn (laminae VII, VIII, and IX) revealed significant increased expression GluR2 RNA messenger in $SOD1^{G93A}$ mice treated with ZK 187638 140 mg/Kg, compared to $SOD1^{G93A}$ mice treated with ZK 187638 70 mg/Kg or untreated transgenic animals (Figure 4.8). ZK 187638 70 mg/Kg did not show the same effect

4.5 Discussion

Preferential vulnerability of motor neurones to AMPA mediated glutamatergic stimulus has been well documented by numerous studies *in vitro*. Alteration of molecular structure of AMPA receptors occurring in certain pathological conditions might, therefore, exacerbate this sensitivity and produce excitotoxic damage to motor neurones. Early decrease of GluR2 protein levels in the motor neurones of $SOD1^{G93A}$ ALS mice, observed in this study (see chapter 3), could result in augmented number of calcium permeable AMPA receptors, which can cause motor neurone degeneration via glutamate-mediated damage to these cells. These current observations suggest that AMPA receptor activation is directly involved in ALS pathology. In this part of the project, we successfully tested the effect of two different doses of a new 2,3 benzodiazepine, ZK 187638, which displays non competitive AMPA antagonist properties, on the disease progression of $SOD1^{G93A}$ transgenic mice. The treatment determined

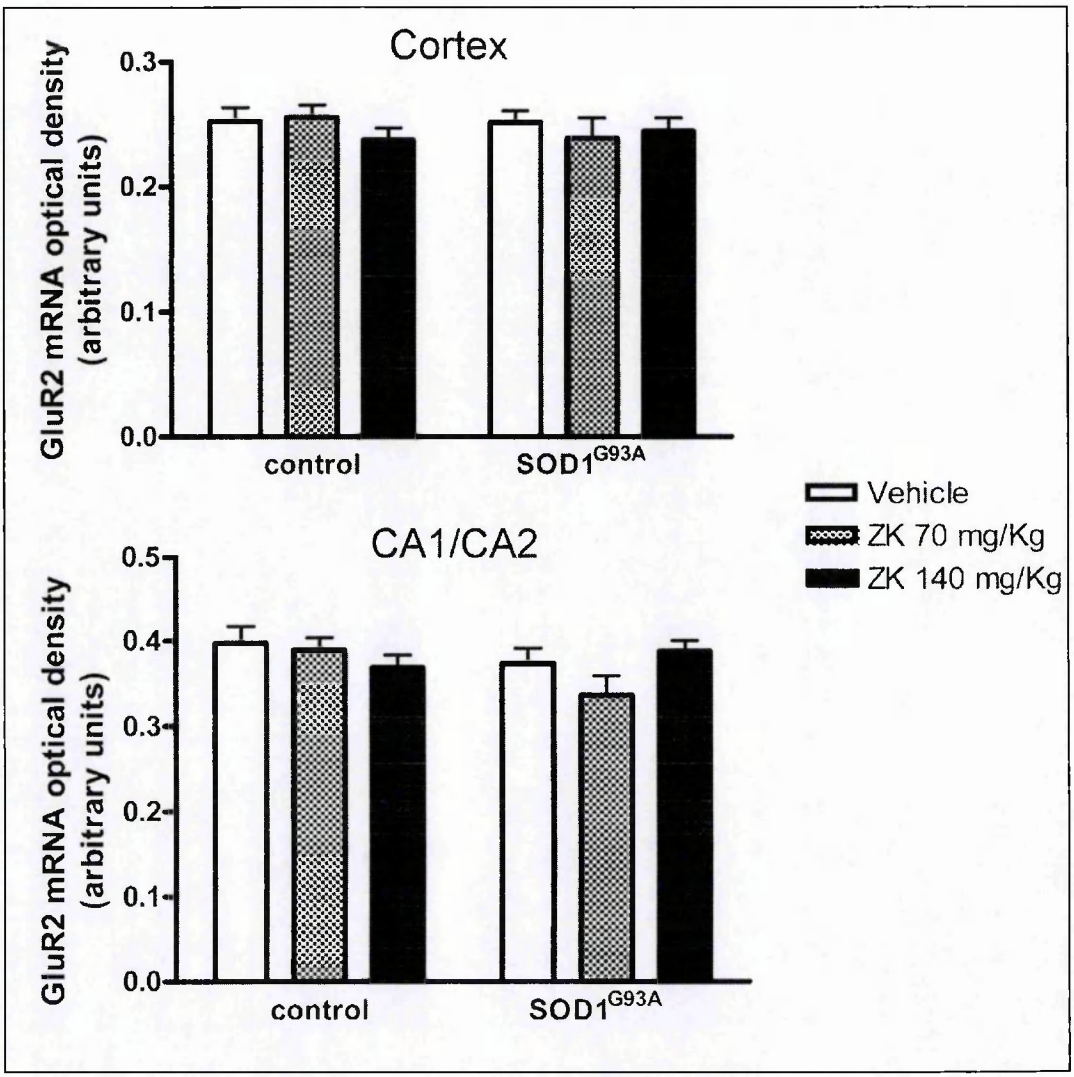

Figure 4.6: GluR2 mRNA expression in brain areas of SOD1^{G93A} mice treated with ZK 187638

Quantitative analysis of autoradiographic opical density revealed no significant variation in GluR2 mRNA expression in prefrontal cortex and CA1/CA2 region of hippocampus of SOD1^{G93A} mice treated with ZK 187638 70 and 140 mg/Kg in respect to non transgenic mice (control) and SOD1^{G93A} mice treated with vehicle (two sections from each animal). The mice used for the experiments were killed at 19 weeks of age. Each column is the mean ± S.E.M. (n =4 to 6); data analysed by Two-Way ANOVA followed by Tukey's test.

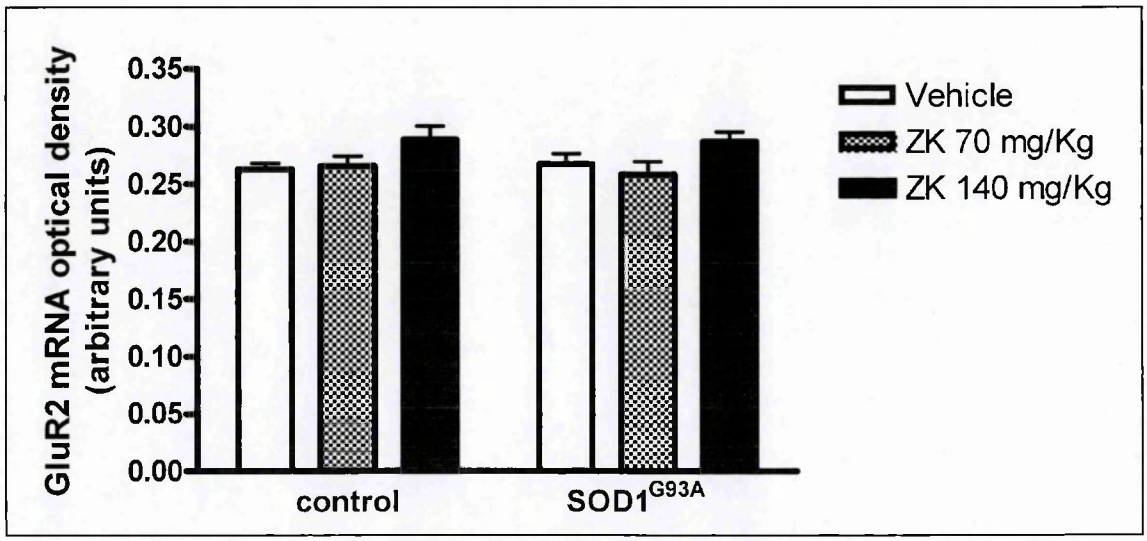

Figure 4.7: GluR2 mRNA expression in the dorsal horn of SOD1^{G93A} mouse spinal cord after treatment with ZK 187638

Quantitative analysis of autoradiographic opical density revealed no significant variation in GluR2 mRNA expression in the spinal cord dorsal horn (laminae I, II, III and IV) of SOD1^{G93A} treated with ZK 187638 70 and 140 mg/Kg in respect to non transgenic mice (control) and SOD1^{G93A} mice treated with vehicle (two sections from each animal). The mice used for the experiments were killed at 19 weeks of age. Each column is the mean ± S.E.M. (n =4 to 6); data analysed by Two-Way ANOVA followed by Tukey's test.

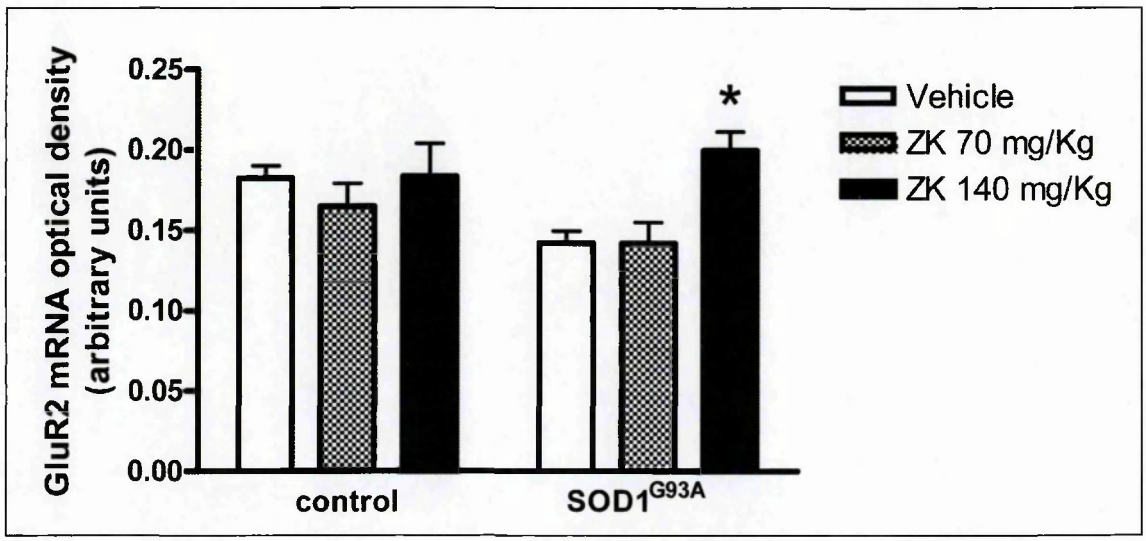

Figure 4.8: GluR2 mRNA expression in the ventral horn of SOD1^{G93A} mouse spinal cord after treatment with ZK 187638

*Quantitative analysis of autoradiographic opical density revealed a significant increase of GluR2 mRNA levels in the spinal cord ventral horn (laminae VII, VIII, and IX) of SOD1^{G93A} treated with ZK 187638 140 mg/Kg in respect to SOD1^{G93A} mice treated with vehicle or ZK 187638 70 mg/Kg (two sections from each animal). The mice used for the experiments were killed at 19 weeks of age. Each column is the mean ± S.E.M. (n =4 to 6); data analysed by Two-Way ANOVA followed by Tukey's test. *= $p < 0.05$*

the improvement of symptoms, revealed by stride length measurement and recording of performances on rotarod, and the significant prolongation of the life span of ALS mice. The effect of 140 mg/Kg of ZK 187638 on the survival of $SOD1^{G93A}$ mice (11.3% prolongation from birth) was comparable to that gained with other AMPA receptor antagonists used in two previous studies. Canton and collaborators showed that a new synthetised compound with AMPA antagonist characteristics, RPR 119990, was active in improving grip muscle strength and extending life duration of $SOD1^{G93A}$ mice (Canton et al., 2001). Similar effects on $SOD1^{G93A}$ mice were also obtained in another study using a potent and selective AMPA antagonist, NBQX (Van Damme et al., 2003). Moreover, NBQX treatment relieved motor symptoms also in a different mouse model of motor neurone disease, the MND mice (Mennini *et al.,* 1999).

Taken together, all these results provide functional demonstration of the role played by AMPA receptors in the development of the disesase in mouse model of ALS. All these AMPA antagonists ameliorate symptoms and prolong survival of ALS mice. In our study, the administration of the highest dose of ZK 187638 was also associated with a modest but significant reduction in the loss of ChAT immunoreactive motor neurones in the lumbar spinal cord, suggesting that the slowing of disease progression correlates with a neuroprotective effect. However, in none case, these drugs could completely stop the progression of the pathology. Similar effects are also obtained, in mice and ALS patients, by riluzole, a drug that inhibits the release of glutamate and represents the only pharmacological treatment currently approved for ALS. This suggests that

blocking the glutamatergic system and in particular AMPA receptor activation is not sufficient to arrest the death processes that lead to motor neurone degeneration. ALS is considered a multifactorial disease, which involves the harmful activation of several cellular death pathways triggered by unknown initial events. Thus, it is possible that structural alterations of AMPA receptors and their consequent abnormal activation can represent either the early triggering factor of the pathology or one of the elements that successively contributes, among the others, to the final event represented by motor neurone death. Therefore, the ineffectiveness of AMPA antagonists in completely reverting the disease progression may be due *a)* to the tardy beginning of the treatment, which starts when AMPA receptors overactivation has already compromised motor neurone health and/or *b)* to the activation of others death processes, which act independently and that cannot be stopped by AMPA antagonists. Despite the efficacy of the treatment with AMPA antagonists could be higher if administered very early, to date, in human therapy, the administration of drugs can only start when the manifestation of symptoms allow clear diagnosis. This is the consequence of the lacking of early diagnostic markers, which would permit to begin the treatment when motor neurones are not yet compromised. Thus, it is important to find compounds that can show good effects even if administered after the beginning of symptoms. Interestingly, unlike the treatment with other AMPA antagonists reported in previous works (Canton et al., 2001; Van Damme et al., 2003), the administration of ZK 187638 slowed the disease progression starting when $SOD1^{G93A}$ mice already showed evident motor dysfunction such as tremors and reduced adduction of the hind

limbs when raised by the tail, a condition more closely related to therapeutic intervention in symptomatic ALS patients. In spite of the lack of resolutive effects of this compound, improvement of symptomatology and survival represent a good result with a view to develop new therapeutic agents for the symptomatic treatment of patients with ALS. In regard to this aspect, ZK 187638 has shown encouraging properties compared to the drugs used in other successful studies.

Despite RPR 119990 (Canton et al., 2001) and NBQX (Mennini et al., 1999; Van Damme et al., 2003) were administered via subcutaneous and itraperitoneal injections, the bioavailability in nervous system of these compounds was very low. We showed that, unlike these drugs, ZK 187638 offers a good *in vivo* availability in the brain after oral administration and a rapid distribution across the blood brain barrier. Oral administration and good bioavailability in nervous system would represent an advantage considering a future use in clinical therapy of chronic neurodegenerative diseases. Moreover, three month treatment with ZK 187638 was well tolerated by control mice.

Unlike the other AMPA antagonists tested in ALS mouse models, ZK 187638 belongs to a compound class that acts as non competitive AMPA allosteric modulators on a region different from the glutamate binding site. These properties make ZK 187638 effective even in the presence of high levels of glutamate and minimize the side effects due to interaction with the numerous glutamatergic pathways of central nervous system. For the same reason, this kind of drug could replace molecules such riluzole, which acts aspecifically inhibiting glutamate release with general consequences. Therefore, all these

characteristics render ZK 187638 extremely promising in consideration of future development of new therapeutic agents for the cure of ALS.

In this section of the study, we also wished to test whether blocking AMPA receptor activity could modify the expression of AMPA subunit GluR2, which was found decreased in motor neurones of presymptomatic $SOD1^{G93A}$ mice (see chapter 3). Unfortunately, we could not investigate the expression and localization of the protein because of technical reasons, as we did not have any more perfused tissue samples to analyse. Thus, we performed *in situ* hybridisation to test whether treatment with AMPA antagonist drug can influence the GluR2 mRNA transcription. We did not find changes in mRNA levels in brain areas not involved in the pathology, such as prefrontal cortex and hippocampus, and in dorsal horn of spinal cord. However, 140 mg/ml of ZK 187638 caused significant increase of GluR2 mRNA in the ventral spinal cord of $SOD1^{G93A}$ mice. The mechanisms involved in this upregulation have not been clarified and need further investigation. It can be speculated that, besides the property as AMPA receptor allosteric modulator, high doses of ZK 187638 may also displays effects on transcription of AMPA receptor subunits and in particular of GluR2. Upregulation of this subunit could reinforce the AMPA antagonist action and contribute to neuroprotection by reducing the number of calcium-permeable glutamate receptors. This hypothesis is supported by the fact that the treatment with the highest dose of ZK 187638 (140 mg/ml) also caused significant extension of survival and reduced motor neurone loss. However, the regulatory effect of ZK 187638 on GluR2 protein level and effects in motor neurones require further work.

CHAPTER 5

Study of the involvement of zinc transporter ZnT-1 in ALS

5.1 Introduction

5.1.1 Zinc ions and ALS

An increasing body of evidence indicates that the neuronal toxicity mediated by Ca^{2+}-permeable AMPA receptors can be also ascribed to zinc influx through the ion channel. The divalent cation Zn^{2+} is abundant in mammalian brain. It is not uniformly distributed, with the highest concentration in the grey and white matter of certain forebrain regions such as cortex, hippocampus and amygdala (Frederickson, 1989). Apart from its function as cofactor for many enzymes and transcription factors, zinc seems to play an important role in excitatory neurotransmission. It is localized in synaptic vesicles at glutamatergic nerve terminals and it is released at high concentration during excitatory synaptic activity (Assaf and Chung, 1984). The physiological relevance of this phenomenon is not yet clearly understood. Electrophysiological studies performed on cultured neurones have shown that zinc can decrease NMDA receptor activation and enhance AMPA receptor responses (Smart et al., 1994), modulating glutamatergic activity. Abnormal zinc release form glutamatergic presynaptic terminals may be toxic to postsynaptic neurones in several neurological disorders such as ischemia, seizures and trauma (Frederickson et al., 1989; Koh et al., 1996; Suh et al., 2000). Accumulation of Zn^{2+} in neurones that are selectively damaged in these conditions strongly supports this hypothesis (Tsuda et al., 1997). Zinc can enter in the neurones through both NMDA and Ca^{2+}-permeable AMPA receptors and

through extrasynaptic voltage sensitive calcium channels (Figure 5.1). However, it has been shown that AMPA receptors have a much higher permeability to zinc than NMDA receptors in cultured neurones (Sensi et al., 1999b), suggesting the preferential involvement of these receptors in Zn^{2+}-mediated toxicity. The probable mechanism underling the harmful effect of zinc influx has been recently proposed. Sensi and colleagues reported that zinc entry through the calcium-permeable AMPA receptors produces reactive oxygen species (ROS) generation in cultured cortical neurones (Sensi et al., 1999b; Sensi et al., 1999a). This phenomenon is directly related to mitochondrial zinc overloading and mitochondrial membrane depolarization (Sensi et al., 2000). Zinc effects on mitochondria require much lower intracellular concentrations than calcium and seem to last longer and to be less reversible. Thus, it is possible that zinc influx can mediate AMPA receptor dependent glutamate-mediated injury to motor neurones in ALS pathology, where mitochondrial dysfunction has been well documented. In fact, it has been shown that motor neurone somata and dendrites in mice are in contact with nerve terminals containing large vesicles rich in zinc ions (Jo et al., 2000) and that some of these terminals are glutamatergic terminals (Wang et al., 2001). Zn^{2+} might also induce neuronal injury through extra-mitochondrial pathways such as activation of PKC, which can result in ROS generation.

Indirect evidence supporting zinc involvement in the motor neurone death occurring in ALS comes from several studies performed on transgenic mice expressing mutant SOD1. The expression of metallothioneins, a low molecular weight protein family involved in maintaining intracellular concentration of

metals such as zinc below toxic levels, is increased in spinal motor neurones and astrocytes of transgenic $SOD1^{G93A}$ mice (Gong and Elliott, 2000; Nagano et al., 2001). The same ALS mice, crossed with metallothionein knock out mice, displayed symptoms and died significantly earlier (Nagano et al., 2001). Another zinc binding protein, S100A6, has been found to be overexpressed in the same mice (Hoyaux et al., 2000). Moreover, it has been recently reported that chronic administration of zinc sulphate decreases survival of ALS mice (Groeneveld et al., 2003). However, whether zinc may play a toxic role in motor neurone death in ALS is not yet clearly understood.

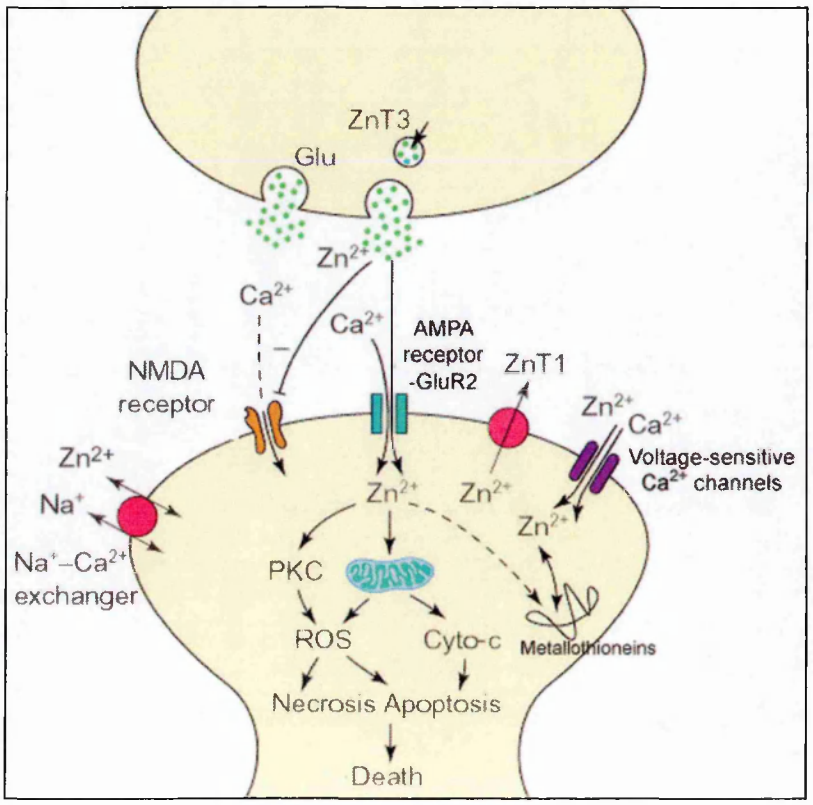

Figure 5.1: Role of Zn^{2+} in neurodegeneration

Adapted from Weiss J.H. et al, TiPS, 2000

5.1.2 Possible involvement of zinc transporter ZnT-1 in motor neurone degeneration in ALS

Hydrophilic zinc ions cannot cross biological membranes by passive diffusion. Beside zinc entry via receptors and channels as described above, there are several specific transporters that mediate zinc uptake and release (Figure 5.1). ZnT-1 renders cells resistant to high level of intracellular zinc (Palmiter and Findley, 1995). ZnT-2, ZnT-3 and ZnT-4 are thought to sequester zinc in intracellular compartments. In particular, ZnT-3 has been shown to be involved in zinc accumulation into synaptic vesicles in glutamatergic terminals (Palmiter et al., 1996; Huang and Gitschier, 1997; Wenzel et al., 1997).

Among these transporters, ZnT-1 seems to be most implicated in neuronal protection. Localized on cellular membranes, ZnT-1 is a protein of about 500 amino acids with six transmembrane regions. It has consensus site for N-glycosylation and phosphorylation by protein kinase C and tyrosine kinases (McMahon and Cousins, 1998a). Zinc transport process is sodium independent, does not require ATP and it has low affinity for other metals such as cadmium and copper (McMahon and Cousins, 1998a). *In vitro* and *in vivo* studies have shown that metal response element binding transcription factor (MTF-1) mediates the response to zinc of the ZnT-1 gene (Langmade et al., 2000). ZnT-1 is thought to be a zinc exporter. Thus, cells with low expression of this transporter are extremely sensitive to zinc influx (Palmiter and Findley, 1995).

The distribution of ZnT-1 in mouse brain has recently been elucidated, with the highest expression in cerebral cortex, cerebellum, hippocampus,

hypothalamus and olfactory bulb (Sekler et al., 2002). The fact that ZnT-1 is almost undetectable in mouse brain at birth and that its expression and synaptic zinc increase significantly after the first postnatal week, suggests that ZnT-1 may be important in protecting developing neurones against potential toxic zinc (Nitzan et al., 2002). However, to date, no data about the distribution and the possible protective function of ZnT-1 in the spinal cord and in particular in motor neurones have been reported. Thus, it is not known whether lack of zinc efflux mediated by this transporter may be involved in motor neurone death following potential harmful glutamatergic stimulus mediated by calcium and zinc permeable AMPA receptors.

5.2 Hypothesis and aim

Changes in the subunit composition and/or activity of AMPA glutamate receptors may alter their permeability to divalent ions and cause an accumulation of free zinc in the motor neurones of $SOD1^{G93A}$ mice. The selectivity of death processes occurring in motor neurones may possibly relate to a lower capability of these cells to extrude excess zinc and this might be reflected by low levels of zinc transporter expression. Thus, the aim of this thesis section is to investigate whether mouse motor neurones express zinc transporter ZnT-1 and whether its expression level is lower in transgenic $SOD1^{G93A}$ mice.

5.3 Methods

5.3.1 *In situ* hybridisation for zinc transporter ZnT-1 mRNA in SOD1^{G93A} mice

In situ hybridization was carried out as described in section 2.4. Frozen lumbar spinal cords and brains of SOD1^{G93A} and non transgenic mice used as control at 8, 14 and 19 weeks of age (3 to 4 mice each group), were analyzed. At the day of the experiment the slides were brought to room temperature and hybridized with ^{35}S-labelled RNA probes complementary to mRNA of ZnT-1 zinc transporter. Total RNA was extracted from mouse hippocampus using RNABee reagent (Biogenesis, Poole, UK) and reverse transcribed using M-MLV reverse transcriptase in the presence of 12.5 μg/ml oligo-dT, 1 mM dNTP, 5 mM $MgCl_2$ and RNasin in 1X RT buffer (all from Promega). PCR was performed using oligonucleotide primers that were designed based on the sequences reported by Langmade and collaborators (Langmade et al., 2000), to amplify a specific region of ZnT-1 cDNA of 496 bp. The primers used had the following sequence (5'-3'): TGA CAA TCT GGA AGC GGA AGA CAAC (forward) and GGA AGC GGG GTC CTC ACA TTT TATG (reverse). PCR was carried out in the presence of 1.5 mM $MgCl_2$, 50 μM dNTP, 0.1 μM sense and antisense primers, 1.25 U *Taq* DNA polymerase and 2.5 μl of RT product (cDNA), in 1X PCR buffer (all from Promega).

Then it was cloned into PCR2.1 plasmid (Invitrogen, Carlsbad, CA, USA). Riboprobe template was prepared by amplification of the plasmid (2 ng) in a

volume of 500 µl with the following primers (5'-3'): ACC GAG CAA TTA A CC CTC ACT AAA GGG CCG CCA GTG TGC TGG AAT TCG (forward) and CGT TGT AAA ACG ACG GCC (reverse), that flanked the insert, and incorporated a T3 and T7 site into the template.

Antisense and sense riboprobes were synthesized by *in vitro* transcription from 1 µg of linear DNA templates using, respectively, T3 or T7 RNA polymerase enzymes (Promega) in a reaction mixture containing 1X transcription buffer, DTT 10 µM, RNase inhibitor 30 U (Roche), non labelled NTP 0,5 mM and UTP 10 µM (Promega) and ^{35}S-UTP 50 mCi (Amersham Bioscences). Probes were degraded to 150 base fragments by alkaline hydrolysis. The specificity of the in situ hybridisation was verified by the absence of the signal using sense radiolabelled probes and by the previous treatment of the sections with RNase.

5.3.2 Immunohistochemical analysis of zinc transporter ZnT-1 in SOD1^{G93A} mice

Immunohistochemical analysis was performed as described in section 2.5. Frozen spinal cords of three non transgenic mice and four SOD1^{G93A} mice for each age considered were used. Sections were incubated with primary antibody obtained from New Zealand White Rabbits immunized with ZnT-1 peptide, kindly provided by Dr Cousins, Food Science and Human Nutrition Department and Center for Nutritional Sciences, University of Florida, USA and Dr Perozzi, University of Rome, Italy (McMahon and Cousins, 1998b). Total IgG fraction

prepared by affinity chromatography from the whole serum was used for the experiments. Incubation with primary antibody (1.6 μg/ml) was performed in 0.1% Triton X-100 and 1% normal goat serum overnight at 4 °C under constant shaking. After three washes, spinal cord sections were incubated in biotinylated anti-rabbit antibody (1:200, Vector Laboratories) in PBS containing 1% normal goat serum and 0.1% Triton X-100 for 60 minutes at room temperature. The secondary biotinylated antibody was revealed by TSA Kit amplification (Renaissance direct-NEL 705A, Dupont NEN, Bosto, MA, USA). Sections were incubated in TNB buffer (0.1M Tris/HCl, pH7.5, 0.15 M NaCl, 0.5% blocking reagent) for 90 minutes followed by incubation in streptavidin-HRP in TNB (1:50) for 30 minutes. After 3 washes with TNT buffer (0.1 M Tris/HCl, pH7.5, 0.15 M NaCl, 0.05% Tween 20) the streptavidin-HRP was revealed with Tyramide conjugated to Cy5 (red, 1:50 dilution) in amplification diluent for 10 minutes, then washed with TNT. Processed sections were mounted on slides and coverslipped with Fluorsave (Calbiochem, Notthingam, UK) and analysed by fluorescence microscope.

5.3.3 Western blot analysis of zinc transporter ZnT-1 in SOD1^{G93A} mice

Western blot analysis was carried out as described in section 2.6. Frozen brain of C57BL/6 mouse was used. Eighty μg protein/lane were run on precast polyacrylamide-SDS gradient gel (4%-15%) (Bio-Rad laboratorie, Hercules, CA, USA), and transferred to nitrocellulose membrane (Scheicher and Schuell). Antibody rose against ZnT-1 (see section 5.3.2), diluted (5 μg/ml) in TBST with

5% bovine serum albumin was used as primary antibody. The blots were then washed three times in TBST and incubated with secondary antibodies: anti-rabbit IgG conjugated to horseradish peroxidase (1:2000, Sigma) in TBST with 5% skimmed milk, for 1 hour at room temperature. Blots were developed by the ECL technique using ECL plus Western Blotting Detection System (Amersham Biosciences) according to the manufacturer's instructions.

5.4 Results

5.4.1 Expression of ZnT-1 mRNA in the spinal cord of SOD1^{G93A} mice

In order to verify whether spinal cord motor neurones, selectively affected by ALS-like pathology occurring in SOD1^{G93A} mice, express zinc transporter ZnT-1, we performed *in situ* hybridisation to detect the presence of its messenger RNA. The experiment was carried out on tissue sections of spinal cord of non transgenic and SOD1^{G93A} transgenic mice at presymtomatic, symptomatic and final stage of the disease. Probes for sense sequence and tissue samples previously treated with Rnase were used to verify the specificity of labelling.

5.4.1.1 Distribution of ZnT-1 mRNA in mouse brain

Brain tissue was used as positive control since ZnT-1 protein distribution in mouse brain has been already published (Sekler et al., 2002). However, there

are not data regarding mRNA expression in mouse central nervous system. Probe recognising ZnT-1 was obtained by RT-PCR using oligonucleotide primers which were designed based on published sequence of mouse ZnT-1 (Langmade et al., 2000). Product of 496 bp was cloned in PCR 2.1 vector and use to generate a riboprobe template.

Confirming the results already reported by Sekler and collaborators about the ZnT-1 protein localization in mouse brain, autoradiographic films revealed high expression of ZnT-1 mRNA in frontal cerebral cortex, cerebellum and hippocampus (Figure 5.2 A). Previous treatment of the sections with RNase and the use of probes direct against sense sequence totally abolished the radiolabelling, demonstrating the specificity of the antisense probe for ZnT-1 (Figure 5.2 B).

5.4.1.2 ZnT-1 mRNA expression in spinal motor neurones of SOD1^{G93A} mice

Analysis of silver grain distribution, obtained by dipping the radiolabelled slices in photographic emulsion, showed a very low expression of ZnT-1 mRNA in the whole spinal cord of control mice. In particular, large motor neurones exhibited a very faint signal as demonstrated by the comparison with labelling present in hippocampal neurones (Figure 5.3 A). The expression of ZnT-1 mRNA did not considerably vary in the spinal motor neurones of in SOD1^{G93A} at all stages of the disease (Figure 5.3 B).

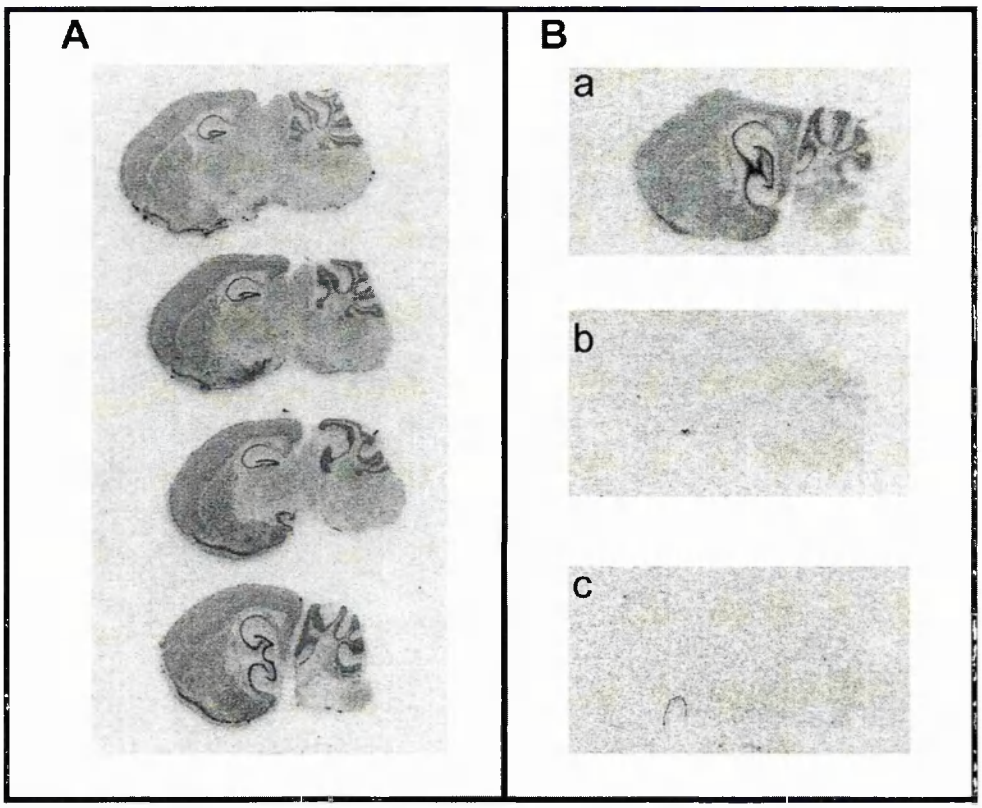

Figure 5.2: ZnT-1 mRNA distribution in mouse brain

(A) In situ hybridisation experiments reveals high expression of ZnT-1 mRNA in frontal cerebral cortex, cerebellum and hippocampus, reflecting the protein distribution previously reported (Sekler et al., 2002). (B) Treatment of the sample with Rnase (b) and the use of probes direct against sense sequence (c) totally abolishes the radiolabelling, demonstrating the specificity of the antisense probe (a) for ZnT-1.

5.4.2 Analysis of ZnT-1 protein distribution in the spinal cord of $SOD1^{G93A}$ mice

In order to evaluate the expression of ZnT-1 protein in the spinal cord of $SOD1^{G93A}$ mice, I performed immunofluorescence experiments using whole antiserum of New Zealand White Rabbits immunized with ZnT-1 peptide, kindly provided by Dr Cousins, University of Florida, USA and Dr Perozzi, University of Rome, Italy (McMahon and Cousins, 1998b). Total IgG fraction was obtained by affinity chromatography from the whole serum and this was used for the experiments. The immunolabelling of spinal cord sections of control mice showed a widespread signal in the whole grey matter of the spinal cord (Figure 5.4 A).

The staining was diffusely present in the ventral horn without specific labelling motor neurones. Dorsal horn was also intensely labeled. Despite several changes of different parameters in the protocol, the widespread nature of the signal remained unaltered and raised doubts about the specificity to ZnT-1 of the total IgG fraction used. In collaboration with the Protein Chemistry and Biochemistry Laboratory at Mario Negri Institute, we synthesized the peptide utilized to immunize the rabbits (McMahon and Cousins, 1998b) and we used it to preadsorb the IgG fraction before the incubation. This treatment did not lead to decrease of the labelling obtained by immunofluorescence in the spinal cord, suggesting the aspecificity of signal (Figure 5.4 B). Further confirmation was obtained by Western blot analysis of protein extract of mouse brain. Immunoblotting carried out with the same IgG fraction revealed bands at

A
Hippocampal neurones
control
Spinal cord motor neurones
control
B
Lumbar spinal cord
SOD1G93A 8 weeks
SOD1G93A 14 weeks
SOD1G93A 19 weeks

Figure 5.3

Figure 5.3: ZnT-1 mRNA levels in the motor neurones of SOD1^{G93A} mice

(A) Analysis of silver grain distribution reveals a very low expression of ZnT-1 mRNA in the whole spinal cord of control mice and in particular in large motor neurons (arrows), as demonstrated by the comparison with labelling present in hyppocampal neurones. (B) The levels of ZnT-1 mRNA are not considerably changed in the spinal motor neurones of in SOD1^{G93A} at all stages of the disease considered. Scale bar: 25 μm.

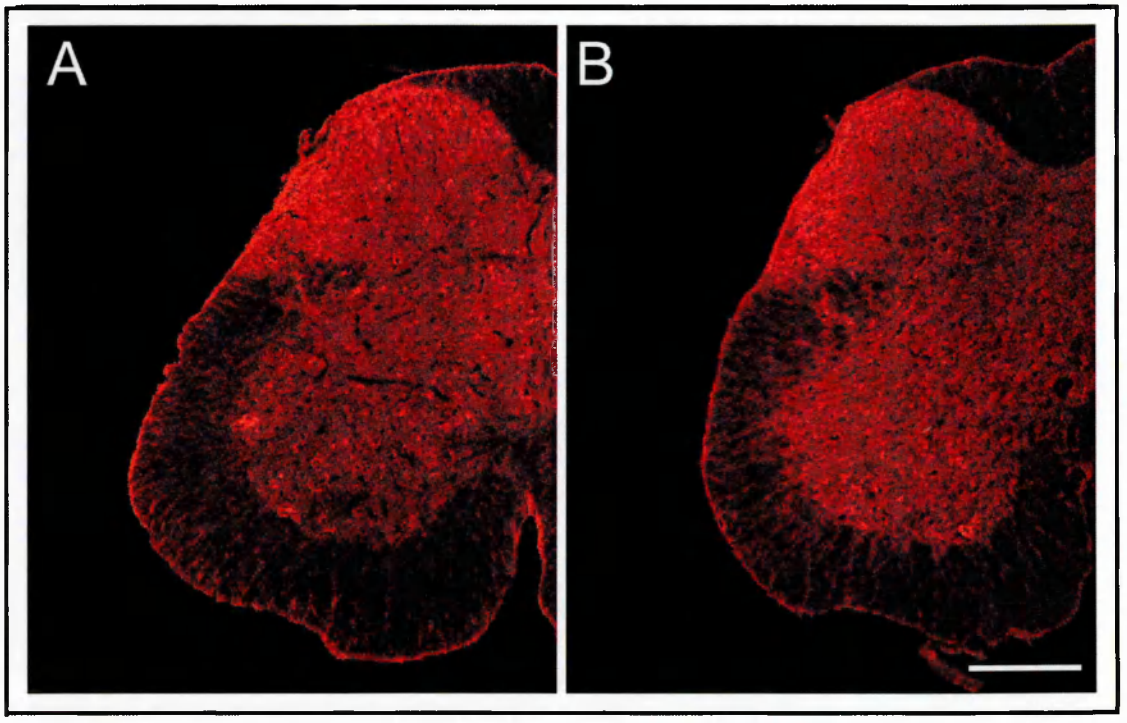

Figure 5.4: ZnT-1 immunoreactivity in the spinal cord of SOD1^{G93A} mice

(A) Immunolabelling for ZnT-1 shows a widespread signal in the whole grey matter of the spinal cord. Both ventral and dorsal horns are diffusely stained, without specific labelling observed in the motor neurones. However, the nature of the signal raised doubts about the specificity to ZnT-1 of the total IgG fraction used. (B) Preadsorbation of the IgG fraction with the peptide utilized to immunize the rabbits (McMahon and Cousins, 1998b) does not abolish the signal suggesting the aspecificity of staining observed. Scale bar: 200 μm.

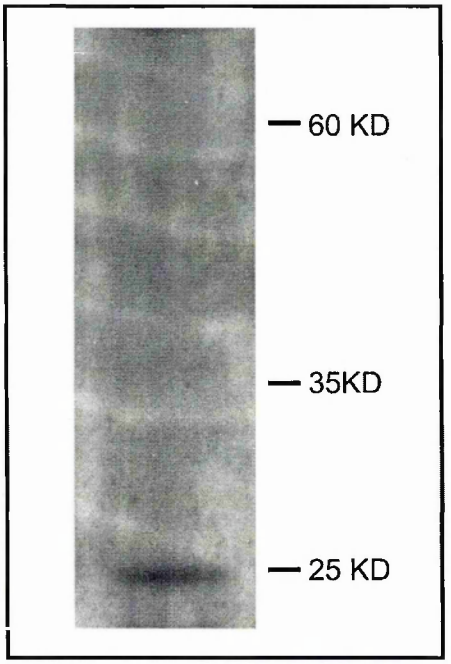

Figure 5.5: Western blot analysis of ZnT-1 in mouse brain

Immunoblotting for ZnT-1 of C57BL/6 mouse brain homogenate reveals a band at about 25 KD, a molecular weight much lower than the one (60KD) previously reported by Sekler et al (Sekler et al., 2002). No bands are observed at this molecular weight. This confirms the low specificity of the total IgG fraction used for these experiments.

molecular weight (25 KD) different from those expected (60 KD) (Sekler et al., 2002) (Figure 5.5).

Thus, distribution and eventual changes in the expression of ZnT-1 protein in the spinal motor neurones of control and $SOD1^{G93A}$ mice could not been elucidated in this study.

5.5 Discussion

This part of the project was designed to investigate the possible role of zinc ions in the neuropathology of ALS. It has been demonstrated that zinc can enter into the neurones through Ca^{2+}-permeable AMPA receptors and that high concentration of cytoplasmic zinc can severely affect mitochondria with consequent ROS production and neuronal injury (Sensi et al., 1999b; Sensi et al., 1999a, 2000; Sensi and Jeng, 2004). Motor neurone cell bodies and dendrites receive numerous glutamatergic nerve terminals containing large vesicles rich in zinc ions (Jo et al., 2000; Wang et al., 2001). Therefore, dysfunction of AMPA receptors due to altered subunit composition and/or their overactivation because of increased glutamate firing on motor neurones might result in abnormal zinc influx into these cells, which in turn could determine mitochondrial damage and motor neurone death. There is no direct demonstration that zinc contributes to motor neurone pathology, however there is indirect evidence: expression of metallothioneins and S100A6, two families of binding protein involved in cytoplasmatic zinc buffering, have been found to be overexpressed in spinal motor neurones of transgenic $SOD1^{G93A}$ mice (Gong

and Elliott, 2000; Hoyaux et al., 2000; Nagano et al., 2001). This could indicate that zinc homeostasis in motor neurones of ALS mice is altered enough to induce overproduction of zinc binding proteins.

For the part of the study presented here, the expression of ZnT-1 was considered to be a possible marker of zinc-mediated injury to the neurones. This transporter acts as zinc exporter, contributing to keep intracellular concentration of zinc below toxic levels. Tsuda and collaborators reported increased level of ZnT-1 mRNA in CA1 pyramidal neurones of gerbil hippocampus after transient ischemia. These neurones accumulated zinc after the ischemic event and died 7 days later (Tsuda et al., 1997). In the same study, the authors also showed that cultured hippocampal neurones exposed to zinc, overexpressed ZnT-1 mRNA. This work was the first evidence concerning the possible role played by ZnT-1 in defending neurones from zinc accumulation following a glutamatergic insult. In fact, the increased expression of ZnT-1 may represent the cellular attempt to defend itself against high toxic level of intracellular zinc by extruding Zn^{2+} through this transporter. Supporting this hypothesis, it has been demonstrated that PC12 cell death induced by exposure to $ZnCl_2$ was attenuated by overexpression of rat ZnT-1, associated with increased zinc efflux (Kim et al., 2000). Thus, overexpression of ZnT-1 in motor neurones of ALS models could represent the demonstration of zinc toxic accumulation in the cytoplasm and, indirectly, of overactivation of calcium-permeable AMPA receptors.

To date, ZnT-1 expression in the central nervous system has been very little investigated and the extent to which spinal motor neurones express ZnT-1

is not known. Secker, Nitzan and collaborators showed ZnT-1 protein expression in brain areas examined by Western blotting and immunohistochemistry techniques (Nitzan et al., 2002; Sekler et al., 2002) but do not report whether or not motor neurones express high levels of this protein. In this study, immunohistochemistry was used using a total IgG fraction against ZnT-1 obtained from whole antiserum raised by Dr Cousins (McMahon and Cousins, 1998b). However, careful analysis suggested that the distribution pattern observed with this antibody in the spinal cord of mice was not specific. In fact, preadsorption of antibody with peptide used to produce it could not abolish the immunolabelling. Moreover, immunoblotting analysis showed bands at unexpected molecular weight. Therefore, further work is required to determine the expression of ZnT1 protein in motor neurones and whether or not the levels of protein are altered during motor neurone disease pathology.

In order to determine the extent of ZnT-1 expression in spinal cord, *in situ* hybridisation experiments were carried out, which revealed very low expression of ZnT-1 mRNA in the spinal cord and in particular in the motor neurones of control mice. The near absence of ZnT-1 mRNA in mouse motor neurones suggests that motor neurones may be very sensitive to potential toxic influx of zinc, in respect to other neurones, since they may not be able to export it. Thus, the almost absent ZnT-1 mRNA expression could represent a selective risk factor for these cell population, rendering them more prone to be injured by glutamate-zinc injury mediated by AMPA receptor dysfunction.

On the other hand, on the basis of work carried out in hippocampus by Tsuda and coworkers (Tsuda et al., 1997), we may have expected an increase

of ZnT-1 mRNA in motor neurones of symptomatic $SOD1^{G93A}$ mice compared to controls, due to zinc influx-mediated enhancing of ZnT-1 transcription. This was not seen. The lack of change in ZnT-1 mRNA levels in motor neurones of transgenic mice may be seen as confirmation of the inability of these cells to conteract the excessive zinc entry. Furthermore, it is also plausible that, in chronic disease such as ALS, increased intracellular concentration of zinc in motor neurones, derived from abnormal functioning of AMPA receptors and low basal expression of zinc extruders, does not reach threshold values sufficient to induce ZnT-1 transcription, even though they result in toxicity for the cells. Therefore, a role of zinc ion in ALS pathology could not be excluded. Direct evidence is required to determine whether or not zinc is involved in motor neurone death. In our laboratory, work is in progress to investigate free zinc concentration in the motor neurones of $SOD1^{G93A}$ mice using fluorescent probes specific to zinc ions.

In conclusion, ZnT-1 does not seem to play an active role in ALS-like pathology occurring in $SOD1^{G93A}$ mice but its low expression might exacerbate vulnerability of motor neurones to altered glutamate stimulation mediated by AMPA receptors.

CHAPTER 6

Study of the expression and function of giutamate transporters in the spinai cord of $SOD1^{G93A}$ transgenic mice and in cultured astrocytes expressing the same mutant

6.1 Introduction

6.1.1 Glutamate transport

An aberrant stimulation of glutamate AMPA receptors and consequent activation of death processes in motor neurones may be triggered by altered functionality of these receptors but also by increased glutamate concentration in the synaptic cleft. Motor neurones receive many glutamatergic inputs from descending fibres and from local interneurones and therefore require efficient removal of glutamate from synapses. Thus, disruption of synaptic glutamate "cleaning" machinery may result in abnormal firing on motor neurones and excitotoxic events.

The clearance of glutamate from extracellular environment is managed by transporter-mediated uptake. Glutamate transporters are expressed by many cell types in central nervous system, including oligodendrocytes, microglia, astrocytes and neurones (Rothstein et al., 1994). It can be sodium-independent and chloride-dependent but this uptake system represents only a small portion (5%) of the total glutamate removal. Five types of high-affinity Na^+-dependent glutamate transporters, designated EAAT1 (known as GLAST in rodents), EAAT2 (named GLT1 in rodents), EAAT3 (EAAC1 in rodents), EAAT4 and EAAT5, have been cloned since 1992 (Kanai and Hediger, 1992; Pines et al., 1992; Storck et al., 1992; Arriza et al., 1997). GLT-1 and GLAST are predominantly localized on astrocytes. GLT-1 is the most abundant glutamate transporter in the forebrain, with GLAST particularly expressed in the

cerebellum. EAAC1 and EAAT4 are considered neuronal transporters, predominantly present on cell bodies and dendrites, with EAAT4 exclusively expressed in cerebellar Purkinje cells. However, no one of these two transporters has been so far detected within the synaptic cleft. EAAT5 has been found to be only expressed in retinal cells.

The majority of glutamate uptake is into astrocytes and is mediated by GLT-1 and GLAST, which are therefore considered the most important in removing glutamate from the synaptic cleft during normal neurotransmission (Rothstein et al., 1996; Danbolt, 2001). GLT-1 and GLAST have 65% of similarity in their amino acid sequences. The secondary structure has not been entirely clarified yet. The existence of either ten or eight transmembrane domains has been proposed. However, it is well established that a pore-loop structure is responsible for glutamate translocation. Two N-glycosylation sites have been discovered on extracellular domains. Uptake of glutamate occurs against concentration gradient (approximately 2 μM of extracellular glutamate against 10 mM in the cytosol), coupling inward cotransport of 3 Na^+ and 1 H^+ and outward counter-transport of 1 K^+. GLT-1 and GLAST seem to have similar affinity for glutamate even though the data about their respective K_m are controversial (Danbolt, 2001), probably because of studies performed on different *in vitro* systems. Energy is required via the action of Na^+-K^+ ATPase to maintain the Na^+ gradient required for glutamate uptake and it has been estimated that more than one ATP molecule is utilized by transporters for each glutamate molecule transported, determining a very high consumption of energy (Anderson and Swanson, 2000). Glutamate uptake may be regulated by both

transporter expression on the cell surface and alteration of their activity. GLT-1 and GLAST have consensus sites for intracellular phosphorylation carried out by protein kinase C (PKC) and cAMP-dependent protein kinase (PKA). Soluble factors released by neurones play a pivotal role in inducing GLT-1 expression in cultured astrocytes, whereas astrocyte-neurone contact seems to be determinant in glial GLAST expression (Gegelashvili et al., 1997). The activity of transporters may be regulated by post-translational modification such as phosphorylation, interaction with zinc and arachidonic acid, membrane translocation, sulfhydryl-based redox regulation and multimerization (Gegelashvili and Schousboe, 1997; Anderson and Swanson, 2000; Danbolt, 2001).

6.1.2 Glutamate transporters and ALS

An alteration of the glutamate uptake capability in astrocytes has been suggested to be the possible cause of excitotoxic motor neurone death in ALS. Any decrease of glutamate uptake by astrocytes can lead to an increase of synaptic glutamate concentration, to overstimulation of glutamate receptors and consequently to excitotoxic insults to motor neurones. In ALS patients it has been shown that there is a marked decrease in the glutamate uptake in synaptosomes from spinal cord and motor cortex (Rothstein et al., 1992) and a massive loss of EAAT2 immunoreactivity in the same areas of the nervous system affected pathologically (Rothstein et al., 1995). Western blot analysis of the spinal cord total proteins of FALS mice carrying $SOD1^{G85R}$ mutant has also

shown a decline of GLT-1 expression (Bruijn et al., 1997b). Since GLT-1 decrease is only evident at the final stage of the disease, it is possible that the downregulation of GLT-1 transporter protein is not a primary cause of ALS but a consequence of motor neurone death. However, a decrease of GLT-1 protein expression before disease onset, when motor neurones are still present, has been found in a transgenic rat model of ALS carrying the $SOD1^{G93A}$ mutation (Howland et al., 2002). Moreover, alterations in the functioning of GLT-1 may also occur even without a clear decrease of the protein levels. A decrease of glutamate uptake activity has been found in synaptosomes from spinal cord of transgenic mice expressing the $SOD1^{G93A}$ mutation only at the end stage of the disease (Canton et al., 1998) but since experiments carried out on synaptosomes may reflect neuronal uptake, the role of glial transporters needs more investigation.

The effect of SOD1 mutations on glutamate transporters may be mediated via oxidative processes. It has been reported that hydrogen peroxide (H_2O_2), reactive oxygen species (ROS) and peroxynitrite (ONOO-) can inhibit glutamate uptake through their oxidant action on cysteine sulphidryl groups of all glutamate transporters (Volterra et al., 1994a; Volterra et al., 1994b; Trotti et al., 1996). Trotti and collaborators have demonstrated that GLT-1-mediated glutamate uptake can be selectively affected by coexpression of SOD1 mutants in oocytes, upon administration of H_2O_2. This effect is thought to involve reactive oxygen species such as hydroxyl radical, generated by mutated SOD1 (A4V or I113T) from hydrogen peroxide (Trotti et al., 1999). However, the role of

oxidative stress as primary event in the pathogenesis of ALS still remains controversial as discussed in the above section 1.8.1.

Thus, whether the expression of mutated human SOD1 can directly alter the mRNA or protein levels of glial glutamate transporters and inhibit glutamate uptake still needs to be investigated properly.

6.2 Hypothesis and aim

The hypothesis evaluated in this thesis section is that the expression of $SOD1^{G93A}$ mutants may reduce the expression and/or the activity of the most important glial glutamate transporter GLT-1, in a way that is consistent with excitotoxic damage to motor neurones.

Thus, in this part of the study, I investigated the expression of glutamate transporter GLT-1 in the spinal cord of $SOD1^{G93A}$ mice and the effect of $SOD1^{G93A}$ mutant on the expression and activity of GLT-1 in isolated cultured astrocytes.

6.3 Methods

6.3.1 Immunohistochemical analysis for GLT-1 in $SOD1^{G93A}$ mice

Immunohistochemical analysis was carried out as described in section 2.5. Frozen spinal cords of non transgenic and $SOD1^{G93A}$ mice at 8, 14 and 19 weeks of age were used

The primary antibodies used were: antibody against GLT-1 (guinea pig polyclonal, 1:5000, Chemicon International) or glial fibrillary acidic protein (GFAP, 1:250 mouse monoclonal, Roche). The optical density of GLT-1 immunostaining in the ventral and dorsal horn of lumbar spinal cord sections was measured relative to the medial dorsal white matter background of individual sections using an image analyser Imaging System KS300 (Zeiss-Kontron). Optical density was measured within a linear range as determined by increasing dilution of the primary antibody. Ventral horn included the laminae VII, VIII and IX, and dorsal horn included the laminae I,II and III of the grey matter at the L2-L4 level of spinal cord. The optical densities of two sections were quantified for each animal and the mean value of these determinations was used as individual data for statistical analysis by One-Way ANOVA followed by Tukey's test (GraphPad Prism 2.0a, GraphPad Software Inc.).

6.3.2 *In situ* hybridisation for GLT-1 mRNA in SOD1^{G93A} mice

In situ hybridisation was performed as described in section2.4. Spinal cord sections of SOD1^{G93A} mice at different stages of disease progression (8,14 and 19 weeks) and non transgenic mice used as controls were used. A rat GLT-1 cDNA fragment was prepared by PCR using standard methods (Molloy et al., 1998). A 327 bp fragment corresponding to bases 1310-1636 of the rat sequence (Pines et al., 1992) was amplified using specific primers (5'-3'): AGC CGT GGC AGC CATC TTC ATA GC (forward) and ATG TCT TCG TGC ATT CGG TGT TGG G (reverse). Then it was cloned into PCR2.1 (Invitrogen).

Riboprobe template was prepared by amplification of the plasmid (2 ng) in a volume of 500 µl with the following primers (5'-3'): ACC GAG CAA TTA A CC CTC ACT AAA GGG CCG CCA GTG TGC TGG AAT TCG (forward) and CGT TGT AAA ACG ACG GCC (reverse), that flanked the insert, and incorporated a T3 and T7 site into the template.

Antisense and sense RNA probes were synthesized by in vitro transcription from 1 µg of linear DNA templates using, respectively, T7 or T3 RNA polymerase enzymes (Promega) in a reaction mixture containing 1X transcription buffer, DTT 10 µM, RNase inhibitor 30 U (Roche), non labelled NTP 0.5 mM and UTP 10 µM (Promega) and ^{35}S-UTP 50 mCi (Amersham Bioscences).

6.3.3 Cell transfection of primary astrocytes with human SOD1 gene

Wild type human SOD1 ($hSOD1^{wt}$) or human SOD1 carrying G93A mutation ($hSOD1^{G93A}$) cDNAs were obtained by RT-PCR from total RNA of transgenic mice expressing $hSOD1^{G93A}$ or $hSOD1^{wt}$ using the following primers (5'-3'): GCC GGA TCC TGC AGT CCT CGG AAC CAG GA (forward) and AAG GAA AGA AGC GGC CGC AGG ATA ACA GAT GAG TTA AGG G (reverse), which introduce a BamHI and a NotI restriction site, respectively. Full-length cDNAs were cloned into the BamHI and NotI sites of the mammalian expression vector pcDNA3 (Invitrogen). The sequence of the resultant clones was confirmed by DNA sequencing (Molecular Biology Unit, King's College London). Primary cortical astrocyte cultures were transfected after 15-16 DIV using

LipofectAMINE 2000 Reagent (Invitrogen), following the manufacturer's protocol. The transfection was performed in a serum-free medium and without antibiotics for 6 hours. Then the medium with lipid-DNA complex were replaced with normal medium containing 10% FBS and incubated at 37°C in a humidified atmosphere of 95% air and 5% CO_2 for 4 days before the experiments. Cultured astrocytes treated with lipofectamine only or transfected with the pcDNA3 vector only were used as negative controls. Transfection efficiency was tested by using the plasmid pWAY21, a mammalian vector containing a Green Fluorescent Protein (GFP) gene, kind gift of Dr Hughes (Lo et al., 1998).

6.3.4 Astrocyte viability and MTT assay

Astrocyte viability was investigated using the Trypan Blue dye exclusion assay. Four days after transfection, cells were washed twice with physiological buffer (140 mM NaCl, 5 mM KCl, 1 mM $CaCl_2$, 1.2 mM $NaHPO_4$, 5 mM Glucose and 20 mM Hepes, pH 7.4) and then stained with 200 μl of 0.4% Trypan Blue (Sigma) for 1 minute, washed twice with PBS and then examined by phase contrast microscope Nikon Eclipse TS100 (Nikon U.K., Surrey, UK). The ability of mitochondrial succinate dehydrogenase to convert 3-(4,5-dimethylthiazol-2-yl)-2,5-diphenyl tetrazolium bromide (MTT) (Sigma) to the blue insoluble formazan salt was investigated. Four days after transfection, astrocytes in culture were washed twice with physiological buffer and incubated with MTT (0.5 mg/ml) dissolved in the same buffer for 1 h at 37°C. The medium was removed and the cells washed twice with PBS and the formazan produced by

the cells was solubilized in 200 µl of dimethyl sulfoxide. Absorbance was measured at 505 nm using an automatic microplate reader Power Wave X340 (Bio-Tek Instruments Inc., Winooski, Vermont, USA).

6.3.5 Western blot analysis for cultured astrocytes

Total cell proteins were extracted using a lysis buffer containing 50 mM Tris/HCl, pH 7.5, 150 mM NaCl, 1% SDS and 100 mM DTT, and diluted in loading buffer (100 mM Tris/HCl, pH 7.5, 15% β-mercaptoethanol, 4% SDS, 15% glycerol, 5 mM EGTA, 5 mM EDTA, 0,2% bromophenol blu) without boiling (Trotti et al., 1998). Equal quantities of total protein (40–80 µg) were loaded into each well, and proteins were separated by electrophoresis on a 7.5% or 12% denaturing polyacrylamide-SDS gel. Following electroblotting, the membranes were blocked in TBS (20 mM Tris/HCl, 150 mM NaCl) containing 5% skimmed milk powder for 1 hour. Membranes were then incubated with primary antibodies diluted in TBS supplemented with 0.05% Tween-20 overnight. Antisera rose in rabbits against GLAST (Anti-A522, rabbit 68488, 0.1 µg/ml) and GLT-1 (Anti-B12, rabbit 26970, 0.06 µg/ml) were used, both kind gifts of Dr Danbolt, Oslo, Norway. For SOD1 a sheep antiserum that recognises the human and murine forms on Western blots (Anti-SOD1, 1:2000, Upstate, Lake Placid, NY, USA) was used. As a control, rabbit-anti Glial Fibrillary Acidic Protein antibody (Anti-GFAP, 1:2000, DAKO, Ely, Cambridgeshire, UK) was used. The membranes were rinsed three times in TBS supplemented with 0.05% Tween-20 and secondary antibodies were then applied (peroxidase-

conjugated goat anti-rabbit IgG, 1:5000, Jackson ImmunoResearch, or rabbit anti-sheep IgG, 1:5000, Chemicon International) for 1 hour. After three washes the protein bands were detected using the ECL-Plus Western Blotting Detection System (Amersham Biosciences), and the membranes applied to Hyperfilms (Amersham Biosciences). Films were scanned and band densities obtained using Bio Image Intelligent Quantifier software (Ann Arbor). Statistical analysis was performed using One-Way ANOVA followed by Bonferroni's post-hoc test (Graph Pad Prism version 3.02, GraphPad Software Inc.)

6.3.6 RT-PCR for cultured astrocytes

Total RNA was extracted using RNABee reagent (Biogenesis) and reverse transcribed using M-MLV reverse transcriptase in the presence of 12.5 μg/ml oligo-dT, 1 mM dNTP, 5 mM $MgCl_2$ and RNasin in 1X RT buffer (all from Promega). Oligonucleotide primers were designed to amplify specific regions of the genes encoding GLAST (653 bp, corresponding to bases 1162-815), GLT-1 (326 bp, corresponding to bases 1310-1636) and β-actin (250 bp, corresponding to bases 1343-1652). The following primers were used (5'-3'): *GLAST*, TCC TCA TTC ATG CCG TCA TCG TCC (forward) and TCT TGG TTT CGC TGT CTG GCA CG (reverse); *GLT-1*, AGC CGT GGC AGC CAT CTT CAT AGC (forward) and ATG TCT TCG TGC ATT CGG TGT TGG G (reverse); *β-actin*, ATC GTG GGC CGC CCT AGG CAC (forward) and TGG CCT TAG GGT TCA GAG GGG C (reverse). Semi-quantitative RT-PCR (Yip et al., 2001) was performed in the presence of 1.5 mM $MgCl_2$, 50 μM dNTP, 0.1 μM sense

and antisense primers, 1.25 U *Taq* DNA polymerase and 2.5 μl of RT product (cDNA), in 1X PCR buffer (all from Promega). In order to verify that amplification of each gene was within the linear range, GLAST and GLT-1 were amplified for 21, 24, 27, 30 cycles and β-actin for 19, 22, 25 cycles. The semi-quantitative analysis was done using 27 cycles for glutamate transporters and 22 cycles for actin (95°C for 30 seconds, 55°C for 45 seconds and 72°C for 1 minute), followed by 10 minutes of final extension at 72°C. PCR products were subjected to agarose gel electrophoresis and visualised by UV illumination in the presence of ethidium bromide. Band intensity was evaluated using UVIsoft Image Acquisition and Analysis software (UVItec, Cambridge, UK). Statistical analysis was performed using One-Way ANOVA followed by Bonferroni's post-hoc test (Graph Pad Prism version 3.02, GraphPad Software Inc.).

6.3.7 ^{3}H-D-aspartate and ^{3}H-GABA uptake

Uptake experiments were performed in physiological buffer (140 mM NaCl, 5 mM KCl, 1 mM $CaCl_2$, 1.2 mM $NaHPO_4$, 5 mM Glucose and 20 mM Hepes, pH 7.4) on 15-16 DIV cultured astrocytes or 4 days after transfection. After washing twice with buffer, the experiment was started by adding buffer with 50 nM ^{3}H-D-Aspartate or 25 nM ^{3}H-GABA (Amersham Biosciences) to the wells. The cells were incubated for 10 minutes at 37°C and the uptake was terminated by two washes with ice cold PBS, followed by immediate lysis of the cells with ice cold 0.1 M NaOH. Radioactivity was determined by liquid scintillation counting. When used, the glutamate uptake inhibitors L-*trans*-2,4-pyrrolidine

dicarboxylate (2,4-PDC) (Tocris, Bristol, UK), dihydrokainic acid (DHK) (Tocris,) and L-serine O-sulfate (L-SOS) (Sigma) were added 5 minutes before and were present during the uptake experiment. Statistical analysis was performed using One-Way ANOVA followed by Bonferroni's post-hoc test (Graph Pad Prism version 3.02, GraphPad Software Inc.).

6.3.8 Immunocytochemical analysis for cultured astrocytes

For immunocytochemistry studies, astrocytes (4 days after transfection) were fixed in PBS containing 4% paraformaldehyde for 1 hour at room temperature. Astrocytes were then permeabilized with 0.2% Triton X-100 made up in PBS containing 1% normal goat serum (blocking solution) for 1 hour and then incubated, with constant agitation, overnight with primary antibody (sheep anti-SOD1, 1:200, Upstate) or for 2 hours with mouse anti-oligodendrocyte Marker 04, (1:200, Chemicon International) in PBS, 0.2% Triton X-100, 1% rabbit serum. After three 10 minutes washes in PBS, astrocytes were incubated with rabbit anti-sheep IgG, (1:500, Chemicon International) or anti-mouse IgG, (1:200, Vector Laboratories) in PBS, 0.2% Triton X-100, 1% goat serum for 1 hour and washed three times for 10 minutes with PBS. The signal was revealed by reaction with 3'-3-diaminobenzidine (DAB peroxidase substrate kit, Vector Laboratories) and analysed using light microscope Nikon Eclipse TS100 (Nikon).

For double-staining immunofluorescence studies, astrocytes were cultured on glass coverslips that had been coated overnight with 1.5µg/ml poly L-

ornithine and then with 2μg/ml laminin for 2hours. Four days after transfection astrocytes were fixed in PBS containing 4% paraformaldehyde for 1hour at room temperature. Astrocytes were then permeabilized with 0.2% Triton X-100 made up in PBS containing 1% normal donkey serum (blocking solution) for 1 hour and then incubated with the first primary antibody sheep anti-SOD1 (1:200, Upstate) in PBS, 0.2% Triton X-100, 1% donkey serum, overnight with constant agitation. After 3 x 10 minutes washes in PBS, astrocytes were incubated with rhodamine-conjugated donkey anti-sheep IgG, (1:100 dilution of stock Jackson Immuno Research) for 2 hours and washed 4 x 10 minutes with PBS. The procedure was repeated using the second primary antibody rabbit anti-GLT-1 (Anti B12, rabbit 26970, 1.5 μg/ml) or anti-GLAST (Anti-A522, rabbit 68488, 2.5 μg /ml). The GLAST and GLT-1 antibodies were kind gifts from Dr Danbolt, Oslo, Norway. Fluorescein-conjugated donkey anti-rabbit IgG secondary antibody at a dilution of (1:100, Jackson ImmunoResearch) was used. The fluorescence was visualized using the Zeiss AxioPlan 2 optical microscope (Carl Zeiss MicroImaging, Inc., Thornwood, NY, USA). Statistical analysis was performed using One-Way ANOVA followed by Bonferroni's post-hoc test (Graph Pad Prism version 3.02, GraphPad Software Inc.)

6.3.9 DCDHF-DA assay for cultured astrocytes

DCDHF-DA assay was performed as previously described (Crossthwaite et al., 2002). Four days after transfection, cultured astrocytes were washed twice with physiological buffer (140 mM NaCl, 5 mM KCl, 1 mM $CaCl_2$, 1.2 mM

$NaHPO_4$, 5 mM Glucose and 20 mM Hepes, pH 7.4). 2',7'-dichlorodihydrofluorescin diacetate (100 μM DCDHF-DA) (Molecular Probes, Eugene, OR, USA) in physiological buffer was placed on the astrocytes for 30 minutes in 5% CO_2/95% air at 37°C. DCDHF-DA is hydrolysed inside the cells to form 2',7'-dichlorodihydrofluorescin which emits fluorescence when it is oxidized to 2',7'-dichlorofluorescein (DCF). Thus the fluorescence emitted by DCF directly reflects the overall oxidative status of a cell (Wang and Joseph, 1999). After the incubation, astrocyte cultures were washed three times with buffer. The relative fluorescence was monitored for 60 minutes using a SPECTRAmax® Gemini microplate spectrofluorometer (Molecular Devices, Wokingham, UK). The emission was recorded at 530 nm after exciting at 500 nm. Each well was scanned in the instrument's well scan mode and the accumulated data from 21 independent points per-well were then transformed to an average signal, expressed in relative light units. All data were calculated and normalized with respect to the increase of fluorescence of untransfected controls. Statistical analysis was performed using One-Way ANOVA followed by Bonferroni`s post-hoc test (Graph Pad Prism version 3.02, GraphPad Software Inc.).

6.3.10 Drug treatments for cultured astrocytes

When used, the glutathione peroxidase inhibitor L-S,R-buthionine sulfoximine (BSO) (Sigma) was added to the culture media at a final concentration of 500 μM 48 hours before the experiments. The catalase

inhibitor, 3-amino-1,2,4-triazole (ATZ) (Sigma) was used at a concentration of 1 mM and added to the culture medium 48 hours before the experiments. The antioxidant compound, 6-hydroxy-2,5,7,8-tetramethylchroman-2-carboxylic acid (Trolox) (Fluka, Poole, UK) was used at a concentration of 200 μM and added to the culture medium 48 hours or 96 hours before the experiments. Statistical analysis was performed using One-Way ANOVA followed by Bonferroni's post-hoc test (Graph Pad Prism version 3.02, GraphPad Software Inc.).

6.4 Results

6.4.1 Study of GLT-1 expression in the spinal cord of $SOD1^{G93A}$ mice

In the first part of this study, we examined the expression of the main astroglial glutamate transporter GLT-1 in the spinal cord of $SOD1^{G93A}$ mice.

6.4.1.1 Immunohistochemistry for GLT-1

In lumbar spinal cord of control mice, the GLT-1 immunoreactivity appeared widespread throughout the grey matter with the highest immunolabelling observed in the substantia gelatinosa of the dorsal horn. The white matter showed a filamentous pattern of strong immunostaining in the ventral and lateral regions of the spinal cord whereas a low signal appears in the dorsomedial region. Compared with non transgenic mice, a marked, decrease in the GLT-1 immunostaining in the ventral horn of the spinal cord

was evident in the SOD1^{G93A} mice at symptomatic and final phases of the disease, when motor impairments were present. However, there was no reduction in GLT-1 in presymptomatic animals at 8 weeks of age compared with age-matched non transgenic mice. No changes were revealed in the dorsal horn of SOD1^{G93A} mice at any of the ages tested (Figure 6.1). Immunostaining for GFAP, a selective marker of astroglial cell, revealed an increased labelling of ventral spinal cord, which gradually augmented during the course of the disease, reflecting the reactive astrocytosis occurring in these mice (Figure 6.2).

6.4.1.2 In situ hybridisation for GLT-1

Analysis of GLT-1 mRNA expression in the spinal cord of SOD1^{G93A} mice was performed by *in situ* hybridisation. The riboprobe for GLT-1 revealed widespread distribution of its mRNA throughout the grey matter of the spinal cord, consistent with the expression of this mRNA in astrocytes. Quantitative analysis of autoradiographic film showed no changes in the levels of GLT-1 mRNA in either the ventral or dorsal regions of the spinal cord of SOD1^{G93A} mice compared with non transgenic controls (Figure 6.3).

Figure 6.1: Immunohistochemical analysis of GLT-1 expression in the spinal cord of SOD1^{G93A} mice

GLT-1 immunoreactivity in sections of the lumbar spinal cord of non transgenic (control) and SOD1^{G93A} mice. In non transgenic mice, GLT-1 immunostaining is mainly distributed throughout the grey matter with the highest signal shown at the level of the substantia gelatinosa of dorsal horn. A gradual decrease of GLT-1 immunostaining in the ventral and intermediate region of the grey matter is evident in SOD1^{G93A} mice at 14 and 19 weeks of age, whereas the dorsal horn maintains high immunostaining at all ages compared with non transgenic controls. Scale bar = 250 µm.

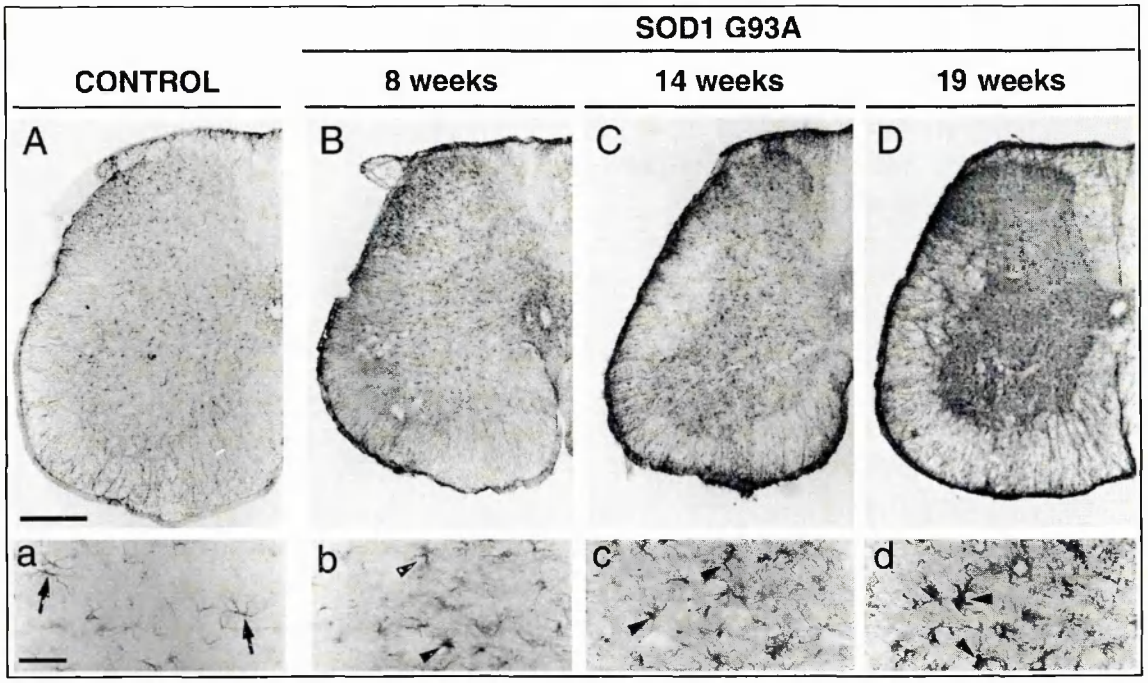

Figure 6.2: GFAP immunoreactivity in the spinal cord of SOD1^{G93A} mice

(A-D) In non transgenic mice (control), GFAP immunostaining is scattered distributed in the grey matter with a filamentous pattern in the white matter. A gradual increase of the GFAP immunostaining in the whole section of the spinal cord appears in SOD1^{G93A} mice during the progression of the desease, with a prominent increase in the grey matter of 14 and 19 week-old mice. (a-b) High magnification of the astrocytes from the ventral horn region shows in control mice a characteristic stellar shape with a tiny cell body surrounded by branched thin processes (arrows), whereas in SOD1^{G93A} mice the astrocytes appeared more intensely stained with hypertrophic cell bodies and processes, particularly in 19 week old mice (arrowheads). Scale bar = (A-D) 250 µm, (a-d) 50 µm.

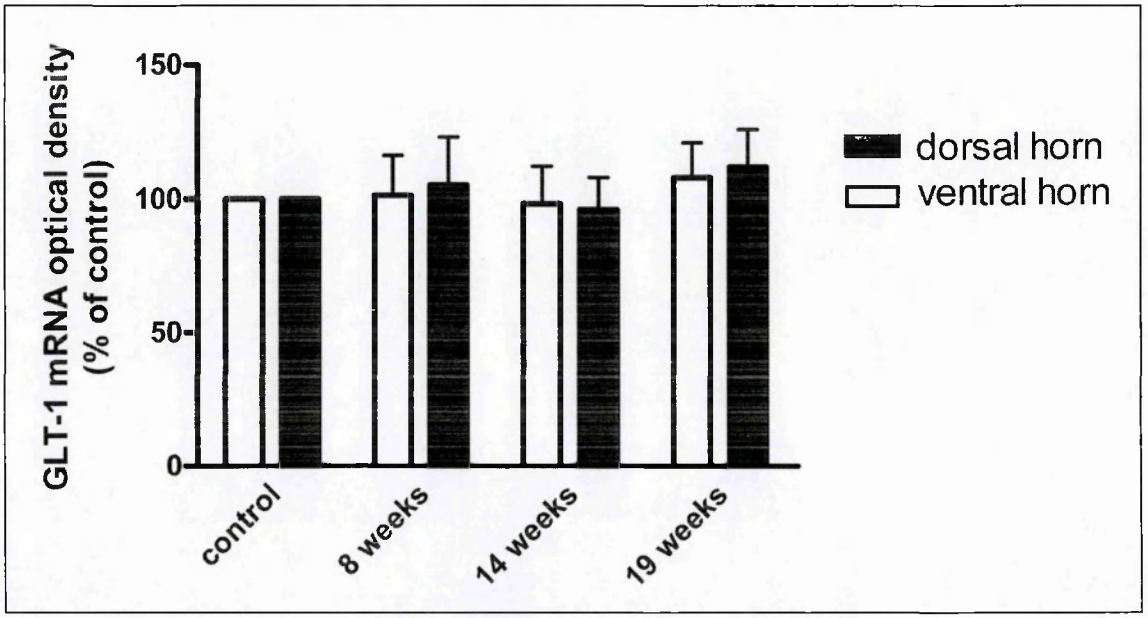

Figure 6.3: GLT-1 mRNA expression in the spinal cord of SOD1^{G93A} mice

Quantitative analysis of autoradiographic opical density revealed no significant variation of GLT-1 mRNA levels in dorsal (laminae I, II, III and IV) and ventral (laminae VII, VIII, and IX) horn of SOD1^{G93A} mouse spinal cord in respect to non transgenic mice (control) at all the ages considered (two sections from each animal). Data are expressed as percentage relative to non transgenic controls. Each column is the mean ± S.E.M. (n = 5 to 6), data analysed by Two-Way ANOVA followed by Tukey's test.

6.4.2 Study of GLT-1 expression and activity in primary cultured astrocytes expressing SOD1^{G93A} mutant. Involvement of oxidative processes

In order to better understand the effect of mutant SOD1 on the expression and activity of GLT-1, we used isolated astrocytes in culture, transfected with human SOD1 carrying G93A mutation to evaluate the levels of GLT-1 and its functionality.

6.4.2.1 Cortical astrocyte cultures express glutamate transporter proteins and mRNAs and support high-affinity ^{3}H-D-aspartate uptake

Primary cortical astrocytes were grown in the presence of cortical neurones for 12-13 DIV as astrocyte-neurone co-cultures. Then, neuronal cells were removed by washing with PBS/glucose solution after 10 and 13 DIV and pure confluent astrocyte cultures were used at 15-16 DIV for the experiments. No oligodendrocytes were detected by immunocytochemistry (results not shown), and no neurones were found upon visual analysis using phase microscopy.

As previously reported (Gegelashvili et al., 1997; Swanson et al., 1997), RT-PCR showed that growing astrocytes in the presence of neuronal cells leads to increased levels of mRNAs encoding the glial glutamate transporters GLT-1 and GLAST compared to astrocytes grown without neurones (Figure 6.4 A). Quantification of PCR bands (Figure 6.4 B) revealed that the expression was

increased threefold for both the transporters and that relative proportion of GLAST and GLT-1 mRNAs was maintained.

Uptake of the glutamate transporter substrate ^{3}H-D-aspartate into cultured astrocytes increases linearly until 15 minutes (results not shown). As a result, all the uptake experiments were carried out for 10 minutes. As shown in Figure 6.4 C, high concentration of the glutamate uptake inhibitors L-*trans*-2,4-pyrrolidine dicarboxylate (2,4-PDC), dihydrokainic acid (DHK) and L-serine O-sulfate (L-SOS) (Bridges et al., 1999) block the majority of ^{3}H-D-Aspartate uptake, demonstrating that uptake was mainly via high affinity glutamate transporters. Subtype-selective concentrations (Bridges et al., 1999) of DHK (0.2 mM), to selectively block GLT-1, and L-SOS (0.2 mM) to mainly block GLAST, each reduce ^{3}H-D-aspartate uptake by about 50%, indicating a similar contribution of the two glial glutamate transporters to ^{3}H-D-aspartate uptake in these astrocyte cultures.

6.4.2.2 Primary astrocyte cultures support high levels of hSOD1^{G93A} or hSOD1^{wt} protein expression after transfection

Transfection was performed on confluent cultured astrocytes with human SOD1 carrying the FALS-linked G93A mutation (hSOD1^{G93A}) or wild type human SOD1 (hSOD1^{wt}), both cloned in the expression vector pcDNA3. Immunocytochemistry revealed large numbers of astrocytes expressing high levels of SOD1 in transfected cultures compared to untransfected cultures (Figure 6.5 A-B). The transfected cells, intensely stained for SOD1, had the

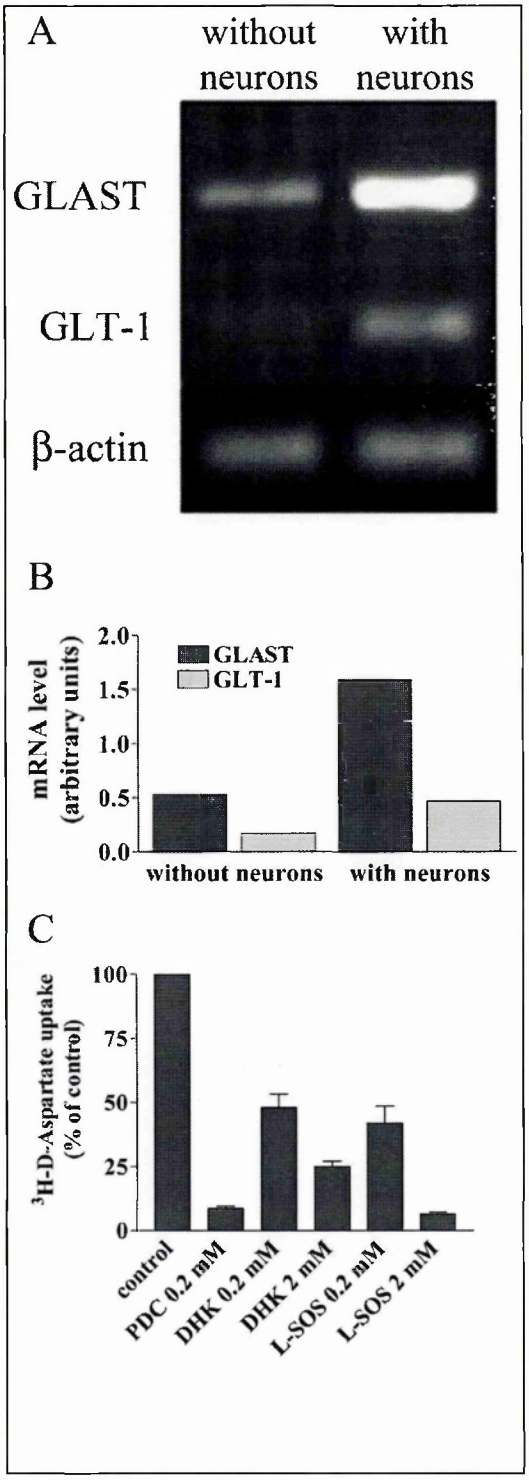
A
without neurons
with neurons
GLAST
GLT-1
β-actin
B
mRNA level (arbitrary units)
2.0
1.5
1.0
0.5
0.0
GLAST
GLT-1
without neurons
with neurons
C
³H-D-Aspartate uptake (% of control)
100
75
50
25
0
control
PDC 0.2 mM
DHK 0.2 mM
DHK 2 mM
L-SOS 0.2 mM
L-SOS 2 mM

Figure 6.4

Figure 6.4: RT-PCR analysis of glial glutamate transporters GLAST and GLT-1 mRNAs in cultured astrocytes

Total RNA extracted from cultured astrocytes grown as pure culture or as co-culture with cortical neurons were used. RT-PCR for β-actin was carried out as control. (A) Bands of the predicted size of 653 bp for GLAST, 326 bp for GLT-1 and 250 bp for β-actin were identified. (B) The expression of both GLAST and GLT-1 mRNAs was increased about threefold in the presence of neurons. Values reported in graph are the ratio of band intensity of glutamate transporters and β-actin from the same samples (n = 3). (C) Effect of glutamate uptake inhibitors on ^{3}H-D-aspartate uptake in cultured astrocytes. 2,4-PDC (0.2 mM), DHK (2 mM) and L-SOS (2 mM) blocked the majority of ^{3}H-D-aspartate uptake. Subtype selective concentrations of 0.2 mM DHK to block GLT-1 or 0.2 mM L-SOS to block GLAST reduced ^{3}H-D-aspartate uptake by 52% and 58% respectively (n = 3).

morphology of astrocytes (Figure 6.5 C). Analyses of GFP expression in cultures transfected with pWAY21 showed that transfection efficiencies were 50% on average, but were somewhat variable (Figure 6.5 D). An antibody that recognizes both human and murine SOD1 as bands of different sizes on Western blots was used to further analyse $hSOD1^{G93A}$ or $hSOD1^{wt}$ expression in transfected astrocytes. Transfected astrocyte cultures express high levels of human SOD1 (Figure 6.5 E) and the amount of total human SOD1 protein increases in a time dependent manner, reaching a slightly higher band intensity compared to murine SOD1 four days after transfection (Fig. 6.5 F). Although the anti-SOD1 antibody recognises murine SOD1 strongly on Western blots, under the conditions used here, it revealed very little labelling of untransfected astrocytes, suggesting that the antisera does not bind well to the epitopes of murine SOD1 that are exposed in this procedure (see Fig. 6.5 A).

6.4.2.3 Expression of $hSOD1^{G93A}$ or $hSOD1^{wt}$ in astrocytes downregulates GLT-1 protein expression without altering GLAST levels

Western blotting analysis was used to assess the regulation of protein levels of glial glutamate transporters after expression of $hSOD1^{G93A}$ or $hSOD1^{wt}$. Using a buffer containing 1% SDS and 100 mM DTT to prevent transporters from oxidation during the protein extraction (Danbolt, 2001), the bulk of the GLT-1 and GLAST proteins appeared as a monomeric band at the apparent molecular weights of 66 and 67 KDa respectively, as expected. A marked decrease of the expression of GLT-1 protein was found in cultured astrocytes expressing

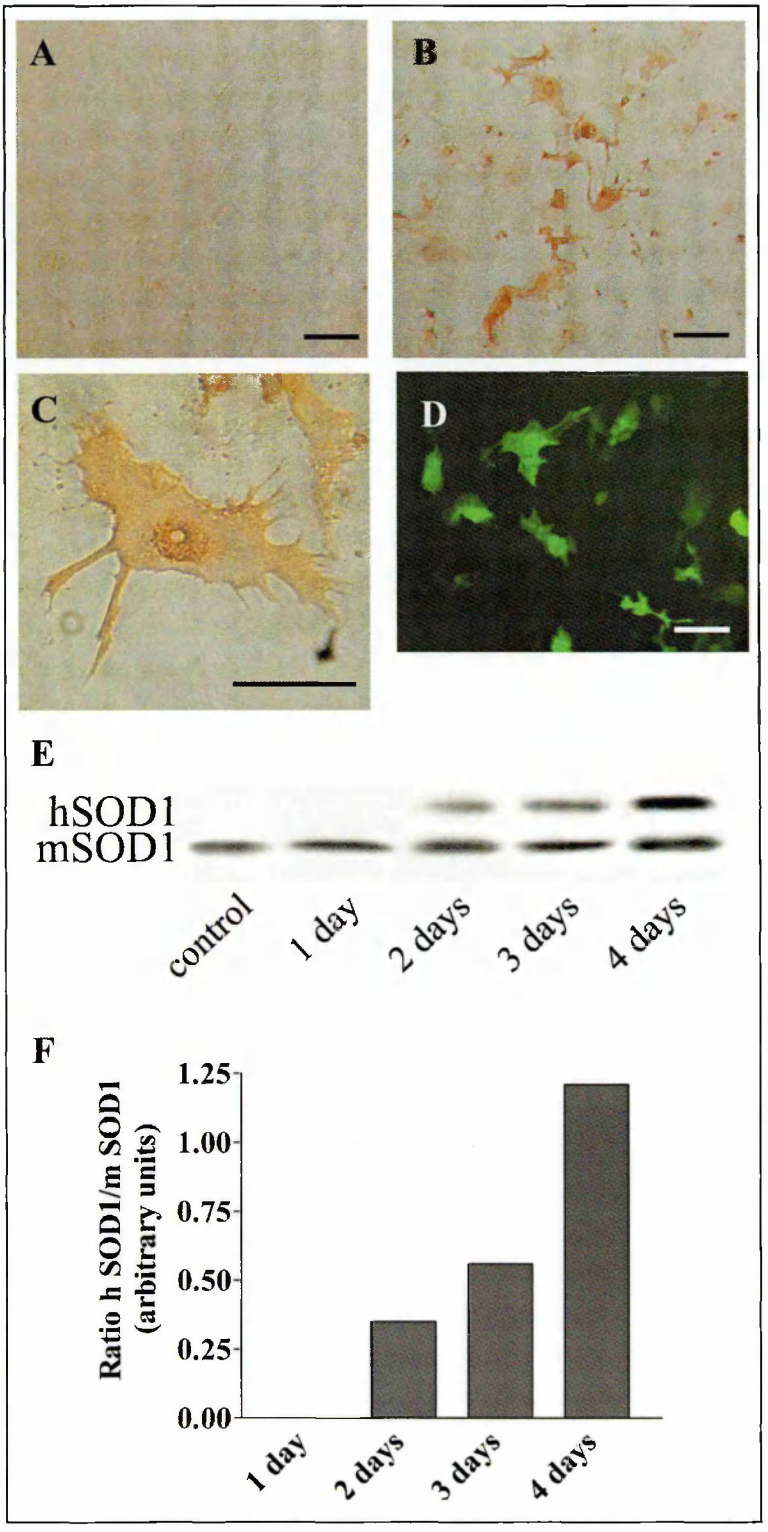
A
B
C
D
E
hSOD1
mSOD1
control
1 day
2 days
3 days
4 days
F
Ratio h SOD1/m SOD1
(arbitrary units)
1.25
1.00
0.75
0.50
0.25
0.00
1 day
2 days
3 days
4 days

Figure 6.5

Figure 6.5: Immunoreactivity for SOD1 in transfected astrocyte

Immunocytochemistry for SOD1 performed on untransfected astrocytes (A) or astrocytes transfected with hSOD1 (B, C). An antibody which recognises both human and murine SOD1 was used. Because of the high level of human protein, transfected cells were distinguishable being much more intensely stained. No differences were found between $hSOD1^{G93A}$ or $hSOD1^{wt}$ transfected astrocytes staining. (D) Evaluation of transfection efficiency by Green Fluorescent Protein (GFP) expression detection. (E) Western blot analysis for SOD1 showed that total human SOD1 expression in transfected cultured astrocytes increased in a time dependent manner reaching a slightly higher levels than total endogenous murine SOD1 four days after transfection. No differences were found between $hSOD1^{G93A}$ or $hSOD1^{wt}$ transfected astrocytes. The same antibody, which recognises both human and murine SOD1 was used. (F) Data shows the ratio between levels of human and murine SOD1 protein. $hSOD1^{G93A}$ and $hSOD1^{wt}$ showed similar levels of expression (not shown). Scale bars (A, B, D) = 50 μm; (C) = 10 μm.

hSOD1^{G93A} (Figure 6.6 A, $p<0.001$) compared to untransfected controls. Astrocytes transfected with hSOD1^{wt} also showed a similar downregulation of GLT-1 expression ($p<0.01$) although the decrease was slightly less than the reduction seen in astrocytes transfected with the mutant hSOD1 (Figure 6.6 A). The effect of the expression of both the forms of hSOD1 was specific for GLT-1 since no changes were revealed in the expression of the other glial glutamate transporter analysed, GLAST (Figure 6.6 B). As an internal control, data were expressed relative to the intensity of the GFAP band obtained from the same blots (Figure 6.6 C, D).

In order to check that the GLT-1 downregulation was not due to the transfection procedure, we performed Western blot experiments on astrocytes either transfected with the pcDNA3 vector only or treated with the transfection reagent only. There was no reduction of GLT-1 protein level under either of these conditions (pcDNA3 results not shown).

It has been demonstrated that glutamate transporters form multimeric complexes under conditions of oxidative stress (Haugeto et al., 1996; Trotti et al., 1998). Since expression of mutated SOD1 has been suggested to induce oxidative damage (Yim et al., 1996; Beal et al., 1997; Ferrante et al., 1997b; Yim et al., 1997), we investigated whether the decrease of monomeric GLT-1 in astrocytes expressing either hSOD1^{G93A} or hSOD1^{wt} was associated with increased formation of high molecular complexes. Figure 6.7 shows a whole blot probed with anti-GLT-1 antibody. In addition to intense 66 KDa monomeric bands, there are lighter bands at the apparent molecular weight of 180 KDa, representing a trimeric complex (Trotti et al., 1998). No bands corresponding to

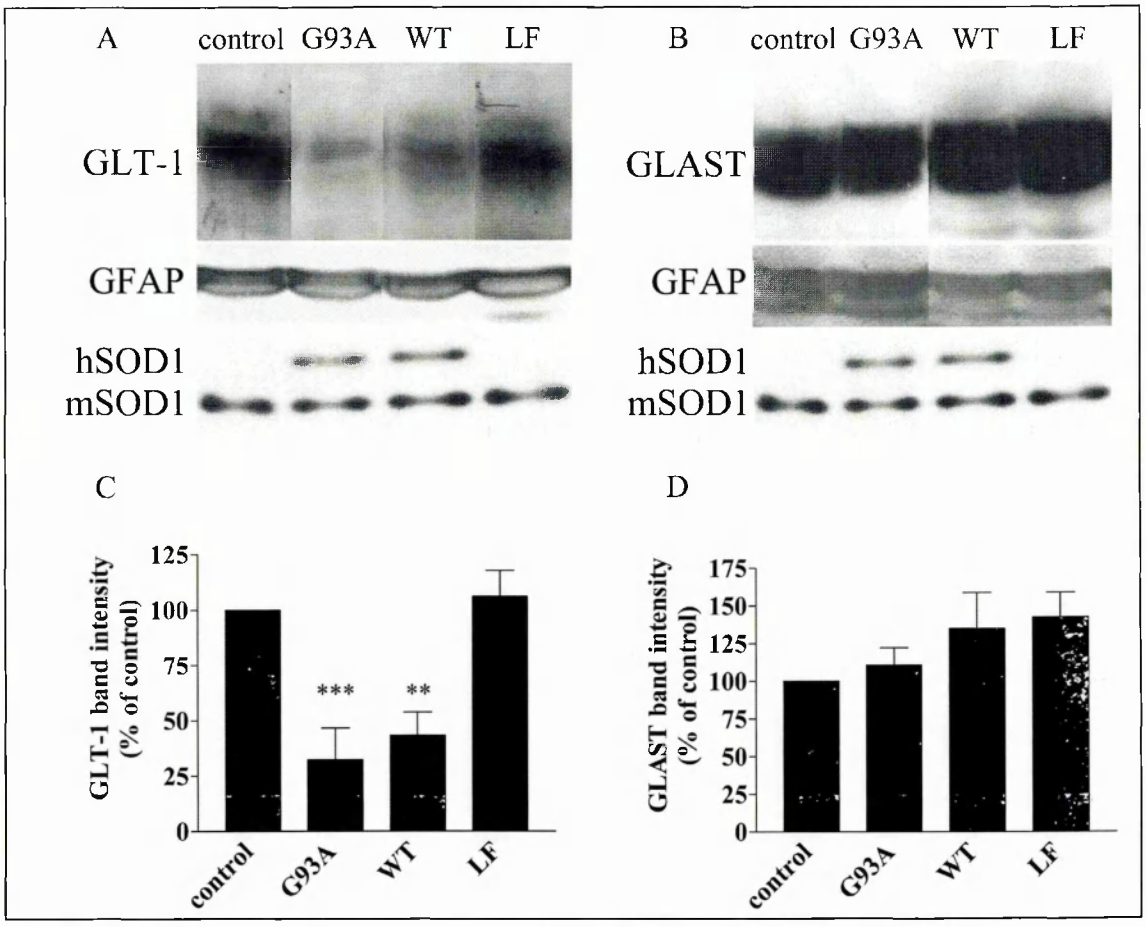
A
control G93A WT LF
GLT-1
GFAP
hSOD1
mSOD1
B
control G93A WT LF
GLAST
GFAP
hSOD1
mSOD1
C
GLT-1 band intensity (% of control)
125
100
75
50
25
0
***
**
control
G93A
WT
LF
D
GLAST band intensity (% of control)
175
150
125
100
75
50
25
0
control
G93A
WT
LF

Figure 6.6

Figure 6.6: Western blot analysis for GLT-1 and GLAST glial glutamate transporters in transfected astrocytes

*(A) Expression of either hSOD1^{G93A} or hSOD1^{wt} caused a decrease of GLT-1 levels in cultured astrocytes compared to untransfected controls with the decrease observed in astrocytes expressing wild type hSOD1 less intense than the reduction seen in astrocytes transfected with the mutant form. (B) No changes in GLAST expression were detected in transfected astrocytes. Transfection with the vector only (data not shown) or treated with the transfection reagent only (LF) did not cause any reduction of GLT-1 protein level. (C, D) Results show GLT-1 protein levels (C) or GLAST protein levels (D) divided by the band intensity of GFAP from the same blots and expressed as percentage relative to untransfected controls. Each column shows the mean ± S.E.M. (n = 6). *** = $p < 0.001$, ** = $p < 0.01$ compared to untransfected control (One-Way ANOVA with Bonferroni's multiple comparison test).*

a dimeric complex were found. Quantification of the band intensities (data not shown) revealed no significant differences in the levels of trimeric bands in astrocytes transfected with $hSOD1^{G93A}$ or $hSOD1^{wt}$ compared to untransfected or lipofectamine treated control cultures. In addition to the band representing the trimeric complex a band of a higher molecular weight (>250 KDa) was observed but the identity of this band is not known.

6.4.2.4 Double labelling of astrocytes reveals low GLT-1 protein levels in cells expressing high SOD1 levels

Cells were stained for SOD1 and GLT-1 or GLAST (Figure 6.8). The cells expressing high levels of SOD1 protein are assumed to represent transfected cells. These highly stained cells occur in a similar proportion to the GFP positive cells as noted above (Figure 6.7 D). Visual analysis of these cultures strongly suggested that cells expressing high levels of $hSOD1^{G93A}$ or $hSOD1^{wt}$ were relatively devoid of GLT-1 immunoreactivity compared to surrounding cells with low levels of SOD1 immunoreactivity (Figure 6.8 A-C). However the levels of GLAST protein in cells with high levels of SOD1 immunoreactivity were similar to, or in some cases higher than, the GLAST levels in untransfected cells (Figure 6.8 D-F). These results therefore confirm the findings from Western blots, that expression of $hSOD1^{G93A}$ or $hSOD1^{wt}$ selectively causes downregulation of GLT-1 but not GLAST protein expression in astrocytes. Furthermore, the SOD1-mediated downregulation of GLT-1 appears to be mediated intracellularly since untransfected cells had normal levels of this

protein compared to transfected cells. In no cases there were visible intracellular inclusions containing SOD1 immunoreactivity.

6.4.2.5 *Expression of hSOD1^{G93A} or hSOD1^{wt} protein in astrocytes does not alter GLT-1 or GLAST mRNA levels*

To determine whether the reduction in GLT-1 protein was mediated by changes in steady-state levels of mRNA, we used semi-quantitative RT-PCR to analyse whether expression of hSOD1^{G93A} or hSOD1^{wt} could alter the levels of GLT-1and GLAST mRNAs. As shown in Figure 6.9 A, there were no changes in GLT-1 or GLAST mRNA levels in cultured astrocytes analysed four days after transfection, in comparison to untransfected controls. The data were expressed relative to the amount of β-actin mRNA from the same samples (Figure 6.9 B).

6.4.2.6 *Expression of hSOD1^{G93A} or hSOD1^{wt} in astrocytes downregulates ^{3}H-D-aspartate uptake*

We wished to test whether the decrease of monomeric form of GLT-1 is associated with downregulation of ^{3}H-D-aspartate uptake in cultured astrocytes expressing hSOD1^{G93A} or hSOD1^{wt}. Transfection with either hSOD1^{G93A} or hSOD1^{wt} caused a small (15%) but significant reduction of ^{3}H-D-aspartate uptake activity compared to untransfected controls (Figure 6.10 A). In order to verify whether using a cationic lipid to transfect astrocytes could affect ^{3}H-D-aspartate uptake by altering membrane properties, we also performed

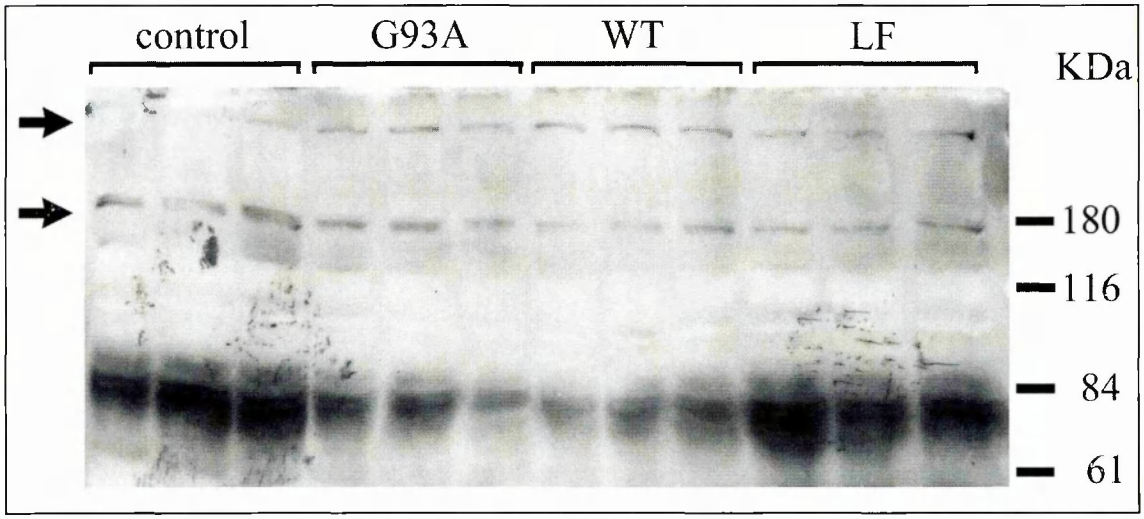

Figure 6.7: Western blot analysis for GLT-1 in transfected astrocytes

Using a buffer containing SDS 1% and 100 mM DTT, without boiling, to prevent oxidation during the sample preparation, the bulk of the GLT-1 proteins appeared as a monomeric GLT-1 (66 KDa) and loss of this monomer is evident in astrocytes expressing $hSOD1^{G93A}$ or $hSOD1^{wt}$ compared to control and reagent only treated astrocytes (LF). Bands at the apparent molecular weight of 180 KDa, representing a GLT-1 trimeric complex, and bands at a much higher molecular weight (>250 KDa) were also present (arrows), but were not altered in astrocytes expressing $hSOD1^{G93A}$ or $hSOD1^{wt}$ compared to controls (n = 6).

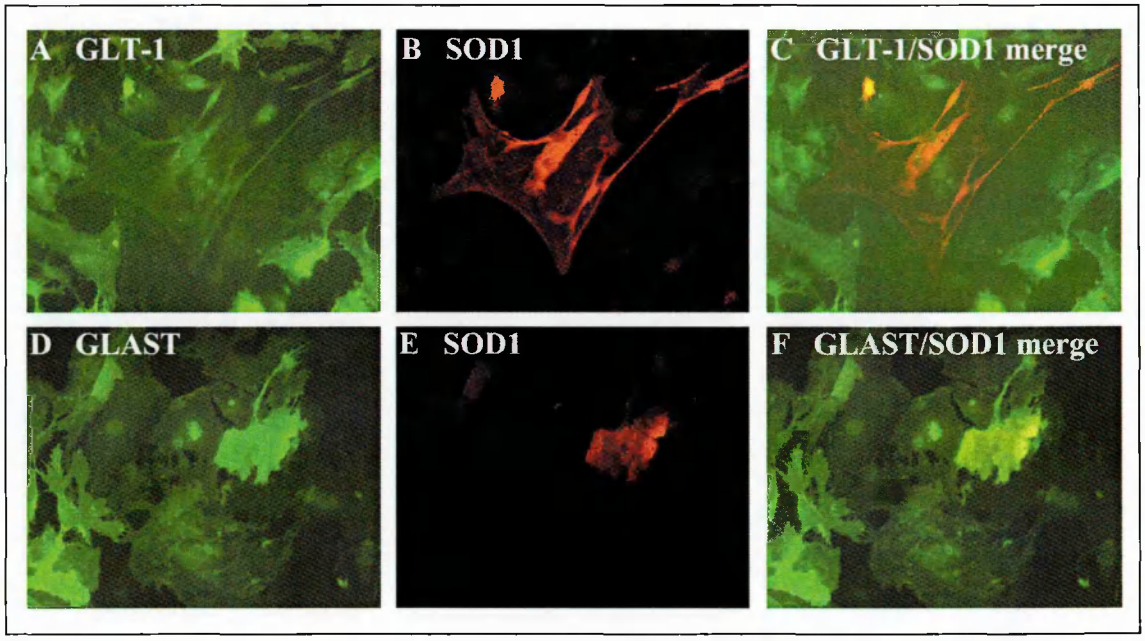

Figure 6.8: Double staining immunofluorescence for SOD1 and for GLT-1 or GLAST in astrocytes transfected with hSOD1^{G93A} or hSOD1^{wt}

(A-C) Visual analysis showed that cells expressing high levels of SOD1 (red staining) were relatively devoid of GLT-1 (green staining) immunoreactivity compared to surrounding cells with low levels of SOD1 immunoreactivity. (D-F) The levels of GLAST (green staining) protein in cells with high levels of SOD1 (red staining) immunoreactivity were similar, or higher in same cases, to the GLAST levels in untransfected cells. hSOD1^{G93A} and hSOD1^{wt} showed similar results. In no cases intracellular inclusions containing SOD1 or GLT-1 immunoreactivity were observed.

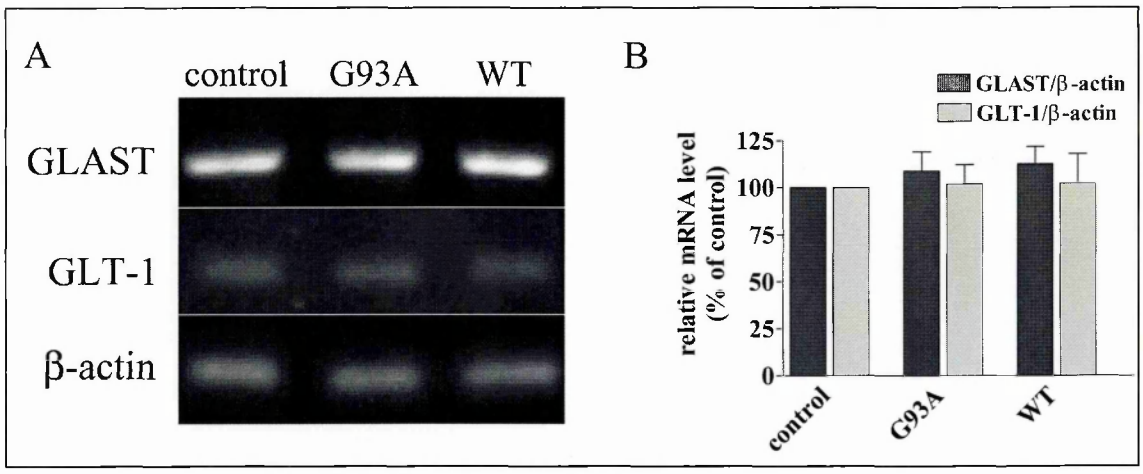

Figure 6.9: Semi-quantitative RT-PCR analysis for glial glutamate transporters GLAST and GLT-1 in transfected astrocytes

Total RNA used for experiments was extracted from untransfected astrocytes as control or from astrocytes transfected with $hSOD1^{G93A}$ or $hSOD1^{wt}$. RT-PCR for β-actin was performed as an internal control. (A) Bands of the predicted size of 653 bp for GLAST, 326 bp for GLT-1 and 250 bp for β-actin were identified. (B) The expression of GLAST mRNA and GLT-1 mRNA were not significantly changed in transfected astrocytes. Graph shows the ratio of transporter band intensity to β-actin band intensity from the same samples expressed as a percentage relative to untransfected control. Each column is the mean ± S.E.M. (n = 6), data analysed by One-Way ANOVA.

experiments on astrocytes treated with transfection reagent only. The reagent caused no significant effect on the uptake (Figure 6.10 A).

In order to determine whether the loss of ^{3}H-D-aspartate uptake was due to a downregulation of GLT-1, we examined the pharmacological characteristics of the uptake activity remaining after transfection of astrocytes with hSOD1^{G93A}. In astrocyte cultures transfected with hSOD1^{G93A}, the GLAST blocker L-SOS (0.2 mM) caused a highly significant inhibition of ^{3}H-D-aspartate uptake (54.6 ± 1.7 %, n = 8), whereas L-SOS (0.2 mM) caused only a 34.6 ± 2.7 % (n =8) inhibition of ^{3}H-D-aspartate uptake in control cultures. Since the ^{3}H-D-aspartate uptake inhibition caused by this GLAST blocker is increased in cultures transfected with hSOD1^{G93A} in comparison to control (untransfected) cultures, this confirms that GLAST, but not GLT-1 predominates after transfection with hSOD1^{G93A}.

Furthermore, inhibition of transport processes was selective for glutamate transporters, which take up ^{3}H-D-aspartate. The uptake of ^{3}H-GABA was not significantly affected by the expression of hSOD1^{G93A} or hSOD1^{wt} in astrocytes (Figure 6.10 B).

6.4.2.7 Expression of hSOD1^{G93A} or hSOD1^{wt} in astrocytes does not cause astrocyte cell death, but reduces MTT conversion

Alterations in GLT-1 levels and glutamate transport activity could potentially result from cell death or damage. We therefore investigated whether expression of hSOD1^{G93A} or hSOD1^{wt} could alter the viability of cultured

astrocytes. Transfection with hSOD1^{G93A} or hSOD1^{wt} does not produce any significant cell death in astrocyte cultures as indicated by trypan blue dye exclusion assay to test cell membrane permeability (data not shown). However, MTT assay showed that hSOD1^{G93A} expression causes a small but significant ($p<0.01$) decrease of MTT conversion compared to control untransfected astrocytes (Figure 6.11). Interestingly, hSOD1^{wt} expression also reduced significantly MTT conversion even if its effect tended to be smaller ($p<0.05$). The transfection reagent alone did not show any effect on cell viability or MTT turnover.

6.4.2.8 The effect of hSOD1^{G93A} or hSOD1^{wt} on GLT-1 protein levels, ^{3}H-D-aspartate uptake or MTT conversion does not involve oxidative processes

In order to investigate whether the effects of hSOD1^{G93A} or hSOD1^{wt} on decrease of GLT-1 protein levels, ^{3}H-D-aspartate uptake and MTT conversion were associated with increased oxidative stress in astrocytes, we measured intracellular reactive oxygen species production using the oxidation sensitive dye 2',7'-dichlorodihydrofluorescin diacetate (DCDHF-DA). After 30 minutes of incubation with DCF-DA 100 μM, the fluorescence emission was recorded for 1 hour. Expression of hSOD1^{G93A} or hSOD1^{wt} in astrocytes does not lead to detectable increase of intracellular reactive oxygen species (Figure 6.12). As a positive control, astrocytes were depleted of endogenous antioxidant stores by

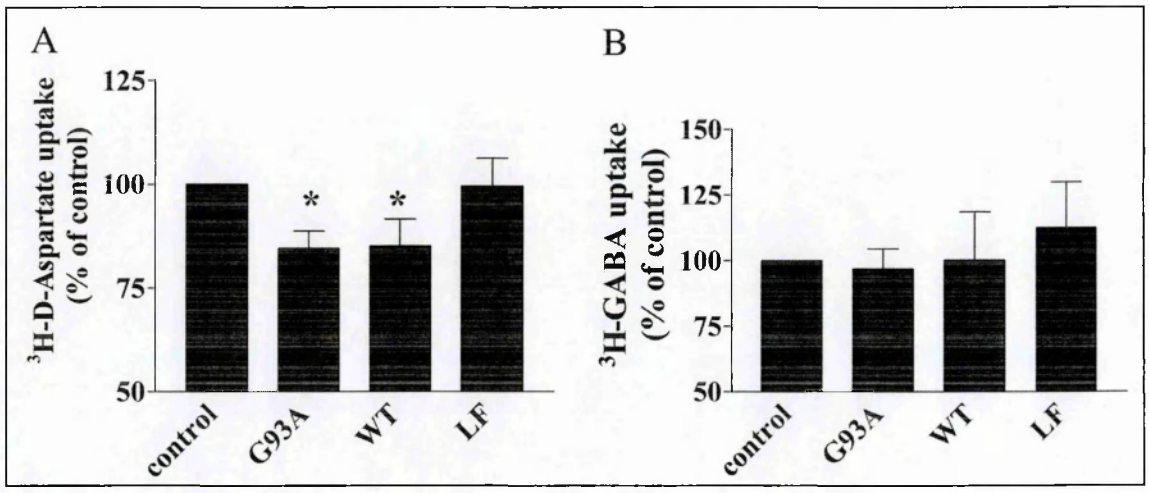

Figure 6.10: ^{3}H-D-aspartate uptake in transfected astrocytes

*(A) Overexpression of hSOD1^{G93A} or hSOD1^{wt} caused a significant decrease of ^{3}H-D-aspartate in cultured astrocytes compared to untransfected control. Treatment with transfection reagent only (LF) did not alter ^{3}H-D-aspartate uptake. (B) No significant change was observed on ^{3}H-GABA uptake in transfected astrocytes expressing hSOD1^{G93A} or hSOD1^{wt}. Values reported in graph represent uptake expressed as percentage relative to untransfected control. Data shows the mean ± S.E.M. (n =12 for D-aspartate uptake, n = 5 for GABA uptake). *= p<0.05, compared to control (One-Way ANOVA with Bonferroni's multiple comparison test).*

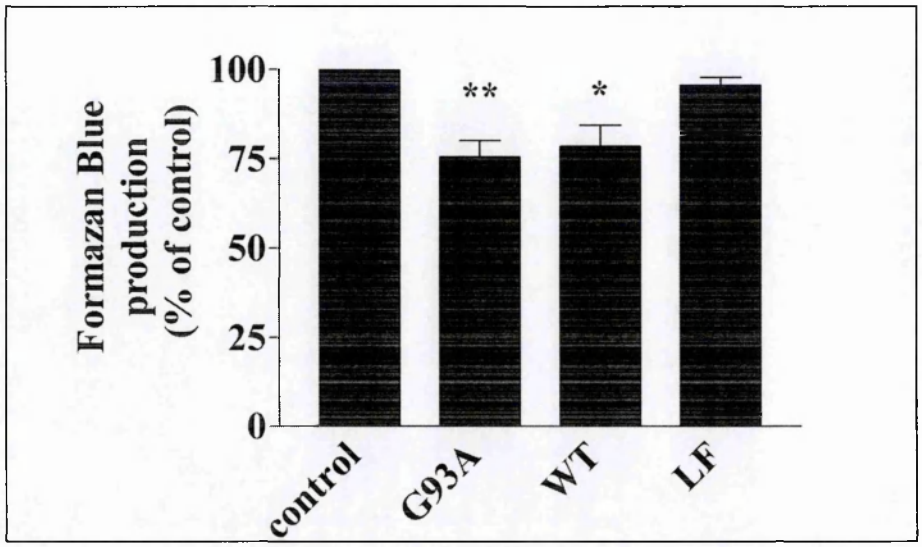

Figure 6.11: MTT assay in transfected astrocytes

*Four days after transfection, cells expressing hSOD1^{G93A} showed a small but significant decrease of complex II activity compared to control untransfected astrocytes or astrocytes treated with transfection reagent only (LF). hSOD1^{wt} expression also reduced significantly MTT conversion even if its effect tended to be milder. No effect of transfection reagent was observed. Data were expressed as the percentage of formazan blue production relative to untransfected control, indicated as 100%. Each column is the mean ± S.E.M. , n = 6 (**= p<0.01, *= p<0.05, compared to untransfected control, One-Way ANOVA with Bonferroni's multiple comparison test).*

treatment for 48 hours with the catalase inhibitor ATZ (1 mM) and the glutathione peroxidase inhibitor BSO (500 μM).

We carried out additional experiments to determine whether the effect of $hSOD1^{G93A}$ or $hSOD1^{wt}$ expression on GLT-1 protein levels or glutamate transporter activity was reversed by treatment with the antioxidant Trolox or enhanced by ATZ and BSO treatment. Downregulation of GLT-1 protein levels caused by $hSOD1^{G93A}$ or $hSOD1^{wt}$ expression in astrocytes was not affected by treatment with Trolox 200 μM for 96 hours before the experiment (Figure 6.13). Treatment with Trolox 200 μM for 48 hours or with ATZ 1 mM and BSO 500 μM for 48 hours did not change the inhibitory effect of $hSOD1^{G93A}$ or $hSOD1^{wt}$ on ^{3}H-D-aspartate uptake in astrocytes (results not shown). The $hSOD1^{G93A}$ or $hSOD1^{wt}$ induced decrease of MTT reduction was not attenuated by treatment with Trolox 200 μM for 48 hors before the experiment or enhanced by treatment with ATZ 1 mM and BSO 500 μM for 48 hours before the experiment (results not shown).

6.5 Discussion

In this part of the project we wished to investigate the role of GLT-1, the most important glial transporter involved in the glutamate uptake, in the pathology of ALS. In fact, alteration of glutamate transport may result in increased concentration of glutamate in the synaptic cleft leading to overstimulation of glutamate receptors on motor neurones and consequently to neuronal damage. Several evidences have indicated the diminished GLT-1

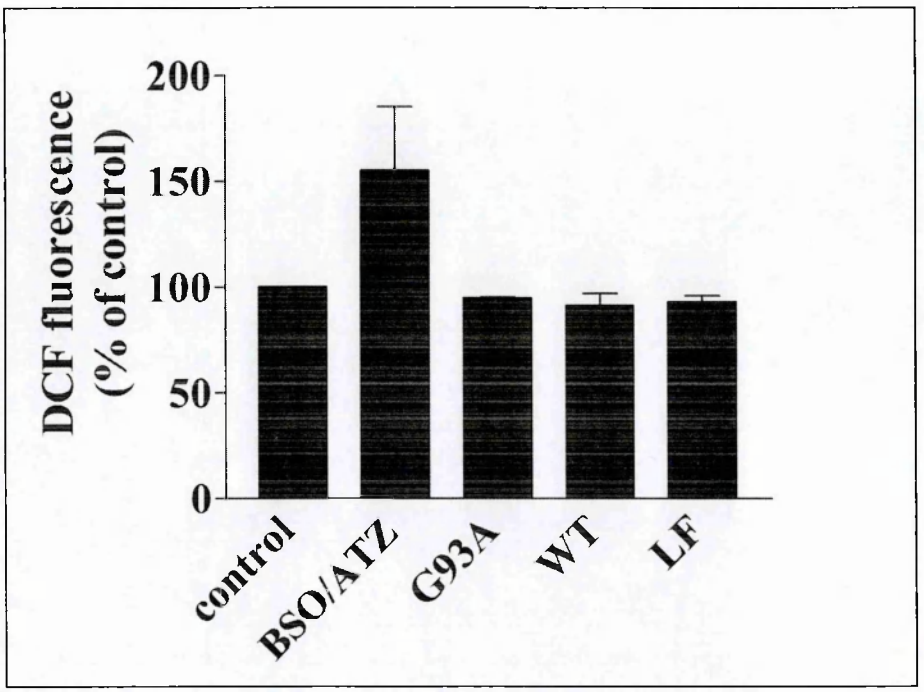

Figure 6.12: DCDHF-DA assay in transfected astrocytes

DCDHF-DA assay was performed in order to determine whether expression of $hSOD1^{G93A}$ or $hSOD1^{wt}$ can induce reactive oxygen species production in transfected astrocytes. After incubation with DCDHF-DA, fluorescence emission was measured for 60 minutes. Data are the relative fluorescence level at 60 minutes expressed as percentage of the values obtained from untransfected controls. Astrocytes treated 48 hour with BSO (500 μM) and ATZ (1 mM) were used as positive control. Each column is the mean ± S.E.M. (n = 3). Data analysed by One-Way ANOVA.

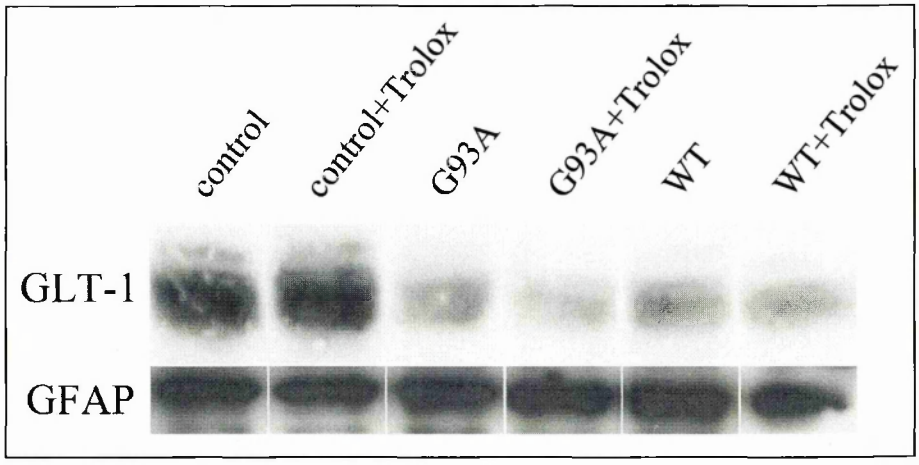

Figure 6.13: Western blot analysis for GLT-1 in transfected astrocytes after treatment with Trolox

The blot shows that the expression of either hSOD1^{G93A} or hSOD1^{wt} caused a decrease of GLT-1 compared to untransfected control. Blots were stripped and reprobed for GFAP to demonstrate equal loading of lanes (lower panel). 96-hour treatment with the antioxidant compound Trolox (200 μM) does not reverse GLT-1 downregulation caused by hSOD1^{G93A} or hSOD1^{wt} (n = 3).

expression as potential phenomenon occurring in the affected areas of central nervous system of ALS patients and animal models of the disease (Rothstein et al., 1995; Bruijn et al., 1997b; Howland et al., 2002). However, the role played by this transporter in the pathogenesis of motor neurone diseases remains rather unclear.

In the first section of this study, we analyzed the expression of GLT-1 in the spinal cord of $SOD1^{G93A}$ mouse model of ALS. Our results revealed that levels of the GLT-1 protein but not of its mRNA, are significantly decreased in the spinal cord of $SOD1^{G93A}$ mice at the advanced but not at the presymptomatic stage of the disease. These findings are in line with a previous study performed on transgenic mice expressing the same SOD1 mutant, which showed that synaptosomal glutamate uptake was significantly decreased only at 21 weeks of age corresponding to final phase of the pathology (Canton et al., 1998). At 8 weeks of age, these transgenic mice do not show motor neurone loss or clinical symptoms although morphological alterations of motor neurones, such as vacuolization of cytoplasm and swelling of mitochondria, are present (Migheli et al., 1999; Bendotti et al., 2001a). Therefore, the present results suggest that the early stage of motor neurone damage in $SOD1^{G93A}$ mice is not associated with changes in GLT-1 protein levels.

Our study demonstrates that the decrease of GLT-1 specifically occurs in the regions affected by the pathology since no significant changes in immunoreactivity were observed in the dorsal horn of the spinal cord where there is no neuronal degeneration. These data are in line with those obtained from post mortem tissues of patients with sporadic and familial ALS showing a

selective decrease of GLT-1 in spinal cord and motor cortex but not in unaffected brain regions (Rothstein et al., 1995). More recently, Fray and collaborators, using quantitative immunohistochemistry for EAAT2, have shown a decreased expression in all regions of the lumbar spinal cords from motor neurone disease patients, but the highest reduction was observed in the ventral horn and intermediate grey matter, the most affected areas (Fray et al., 1998). As shown in ALS patients (Bristol and Rothstein, 1996), we have found no changes in the levels of mRNA of GLT-1 in the lumbar spinal cord of $SOD1^{G93A}$ mice at any stage of the disease. Thus, these results suggest that the decrease of GLT-1 is due to a post-transcriptional regulation of this protein.

It has been demonstrated that glutamate transporters, and in particular GLT-1, are vulnerable to the oxidation resulting in an impaired glutamate uptake function (Volterra et al., 1994a; Trotti et al., 1998; Danbolt, 2001). In particular, it has been shown that the mutant SOD1 protein inactivates the GLT-1 in oocytes upon administration of H_2O_2 (Trotti et al., 1999). Thus, although our study demonstrates that the level of GLT-1 is unchanged in the lumbar spinal cord of young transgenic mice, we cannot exclude that the activity of this transporter is already compromised at this age. This may play a role in the initial process of motor neurone death by inducing an increase of extracellular glutamate concentration.

The changes in GLT-1 seem to be specifically associated with the pathology. In fact, Western blotting analysis on the total protein extract of spinal cord of $SOD1^{G93A}$ mice, performed in collaboration with the Biochemical Neuropharmacology Group at the Wolfson Centre for Age Related Diseases,

King's College, London, showed decresed expression of GLT-1 at the final stage of the disease, but unchanged levels of the another glial transporter, GLAST, during the progression of the disease (Bendotti et al., 2001b). This suggests a differential regulation of these two glial glutamate transporters under these pathological conditions. Since it has been reported that the expression of GLT-1 in astrocytes is under neuronal regulation (Gegelashvili et al., 1997; Swanson et al., 1997), it is plausible that the late decrease of GLT-1 observed in the transgenic FALS mice, as well as in the post mortem tissue of patients with ALS, can result from a loss of neuronal factors regulating the expression of this glial glutamate transporter in the affected regions, derived from motor neurone loss. The fact that GLAST was not changed suggests that these two glial transporters in the spinal cord may be regulated differently by neuronal factors. In order to further investigate a) whether the effects on GLT-1 expression observed in transgenic mice are a direct consequence of mutated SOD1 expression or the effect of surrounding neuronal alterations and b) the possible effect of SOD1 mutant on the activity of the transporter, we used primary astrocytes transiently transfected with human wild type ($hSOD1^{wt}$) and G93A mutant ($hSOD1^{G93A}$) superoxide dismutase.

The main result emerging from this part of the study is the clear decrease of GLT-1 protein expression also in cultured astrocytes in the presence of high levels of $hSOD1^{G93A}$, without changes of mRNA expression, confirming the results obtained in $SOD1^{G93A}$ mice. Also in this experimental paradigm, the expression of $hSOD1^{G93A}$ selectively affected GLT-1 since no significant changes were observed in GLAST protein expression. Reflecting the decline of

GLT-1 protein level, ^{3}H-D-aspartate uptake was also decreased, and the uptake component remaining had a greater proportion of GLAST activity than found in control cultures. Alteration of the glutamate uptake system was accompanied by decreased MTT conversion, without any sign of cell death. Furthermore, our results strongly suggest that these effects do not involve oxidative processes. Interestingly, the effect showed by hSOD1^{G93A} expression in cultured astrocytes was in part also observed after transfection with the wild type form of human SOD1.

The key finding of this part of the study is that hSOD1^{G93A} or hSOD1^{wt} both cause downregulation of GLT-1 protein levels. This decrease was reflected as a functional loss of GLT-1 as the proportion of uptake activity due to GLAST activity (L-SOS sensitive component) was increased in cultures transfected with hSOD1^{G93A}. Using Western blotting, a decreased expression of GLT-1 monomeric protein was observed in astrocytes four days after transfection with hSOD1^{G93A} or hSOD1^{wt}, and these observations were supported by immunocytochemical studies. Although the effect produced by hSOD1^{G93A} was greater, astrocytes expressing hSOD1^{wt} also showed a reduction of GLT-1 expression. Since previous papers only focused on GLT-1 downregulation due to overexpression of mutant hSOD1 in transgenic animal models (Bruijn et al., 1997b; Howland et al., 2002), this results are the first evidence suggesting that hSOD1^{wt} can be as effective as hSOD1^{G93A} in mediating the downregulation of GLT-1. Despite the lack of severe motor pathology in mice overexpressing hSOD1^{wt}, it has been demonstrated that it can produce several potentially neurodegenerative alterations consisting of mitochondria swelling, axonal

degeneration and mild motor dysfunction in old mice (Dal Canto and Gurney, 1995; Jaarsma et al., 2000). Although gain-of-function mutations in SOD1 are necessary to induce clinical signs of motor neurone disease in ALS mice, the overexpression of human wild type protein can have some harmful properties, shared with $SOD1^{G93A}$, which are not enough to produce massive motor neurone death in mouse models but that become evident when expressed in a particular cell culture model like the one used here. However, the fact that $hSOD1^{G93A}$ showed a slightly stronger effect suggests that the properties of SOD1 that produce downregulation of GLT-1 are enhanced in the mutant form of the enzyme.

Our results and evidence already reported (Bruijn et al., 1997b) show that GLT-1 protein expression declines only at the end stage of pathology in two different lines of FALS mice, carrying G93A or G85R mutations on SOD1 gene. As discussed above, the transgenic studies suggest that GLT-1 downregulation could be due to the death of motor neurones occurring at the final stage of disease. Neuronal factors are known to be crucial in regulating glutamate carrier expression and activity in astrocytes (Gegelashvili et al., 1997). These results *in vitro* therefore differ from the transgenic models sine they show a very rapid effect of hSOD1 in downregulating GLT-1 in mouse astrocytes, whereas the downregulation of GLT-1 in transgenic mice is slow. There is a similar overexpression of exogenous SOD1 in both mice and transfected cultured astrocytes; therefore the apparent difference in the timing of GLT-1 downregulation may result from the lack of neurones in astrocyte cultures. We suggest that, in transgenic mice, despite the negative effect of mutated hSOD1

on GLT-1 expression, GLT-1 levels could be maintained by the surrounding motor neurones. In this study, we grew astrocytes initially as co-culture but cultures of astrocytes without neurones were used for transfection, excluding any possible neuronal compensative regulation of hSOD1 effects on GLT-1.

Downregulation of GLT-1 expression after transfection with $hSOD1^{G93A}$ or $hSOD1^{wt}$ was accompanied by small but significant decrease of ^{3}H-D-aspartate uptake. The effects of hSOD1 appear to be selective for glutamate uptake since no decrease of GABA uptake was observed. Despite a large downregulation of GLT-1, the decrease of uptake was relatively small (15%). This can be explained by the fact that the contribution of GLT-1 to the glutamate uptake in our cultures was about 50% of the total and that GLT-1 protein was selectively lost. To test this hypothesis, we performed ^{3}H-D-aspartate uptake experiments on transfected astrocytes in the presence of L-SOS to mainly block GLAST. In this set of experiments, the inhibitory effect of L-SOS on ^{3}H-D-aspartate uptake in untransfected cells was about 35%, but the inhibitor effect of L-SOS in cells transfected with hSOD1G93A was about 55%, indicating a predominant contribution of GLAST (and decreased contribution of GLT-1) after transfection. Studies performed on synaptosomes showed decreased glutamate uptake in ALS patients (Rothstein et al., 1992) and in $SOD1^{G93A}$ mice only at the final stage of the pathology (Canton et al., 1998). In both the cases, decline of V_{max} without changes in K_m was found. These data are consistent with downregulation of GLT-1 protein levels observed in human patients (Rothstein et al., 1995) and in the same transgenic mice strand as reported in our experiments. In human studies typical losses of 40-70% glutamate uptake

activity are observed (Rothstein et al., 1992), but in our study we only find decreases of about 15% in D-aspartate uptake activity (reflecting a loss of about 60% of GLT-1 protein levels). There are a number of major differences between these study systems. In the human studies, the glutamate uptake measured on synaptosomal preparation most likely reflects neuronal uptake, whereas this study reflects astroglial glutamate uptake only. Moreover, the changes reflect the severe pathology (including loss of nerve terminals and gliosis) occurring at the final stage of the disease, whereas the current results focuses on early changes after SOD1 expression.

As mentioned above, it can be hypothesized that glutamate uptake impairment can derive from action of oxidant species on the glutamate transporters that leads to their decreased activity. Trotti and colleagues have demonstrated that GLT-1 function can be selectively affected by co-expression of SOD1 mutants in oocytes, in the presence of oxidative insults (Trotti et al., 1999). As we could not detect ROS production in transfected astrocytes and antioxidant treatment or depletion of endogenous antioxidant system did not change the decrease of ^{3}H-D-aspartate uptake, we suggest that alteration on uptake system in astrocytes expressing hSOD1 is consequent to downregulation of GLT-1 protein expression rather than alteration in the level of GLT-1 activity. One possibility is that hSOD1 expression alters the degradation of GLT-1. The fact that no changes in GLT-1 mRNA levels were also found *in vitro* studies give further support to the hypothesis that the downregulation of the protein is due to post-transcriptional modifications. The effect of hSOD1^{G93A} or hSOD1^{wt} appears to be selective for GLT-1 also in cultured astrocytes since

we observed no downregulation of GLAST protein in these cultures, confirming the results obtained in $SOD1^{G93A}$ mice.

The downregulation of GLT-1 protein by $SOD1^{G93A}$ or $hSOD1^{wt}$ is most likely due firstly to overexpression of the exogenous proteins in astrocytes to produce effects via a variety of potential mechanisms. Formation of intracellular SOD1 aggregates has been proposed as a cause of ALS pathology (Cleveland and Rothstein, 2001). Cytoplasmic inclusions have been reported in motor neurones and astrocytes of ALS mice (Bruijn et al., 1997b) but GLT-1 immunoreactivity was not revealed within the inclusions (Watanabe et al., 2001). However, we could not observe intracellular inclusions containing SOD1 or GLT-1 by immunocytochemistry in transfected astrocytes, suggesting that this is not the mechanism that links hSOD1 expression to GLT-1 downregulation in these cultures. It could be assumed the most likely mechanism underlying hSOD1 downregulation of GLT-1 to be oxidative. It has been suggested that mutant forms of SOD1 can generate ROS through increased peroxidase activity (Yim et al., 1997) and that $hSOD1^{wt}$ transgenic mice show increased oxidative stress in cultured neurones, in muscle and brain tissue (Yim et al., 1996; Bar-Peled et al., 1999). Oxidative conditions may induce the formation of non functional GLT-1 homomultimers, reducing the availability of monomer required for the formation of active oligomeric structure, as revealed by immunoblotting (Haugeto et al., 1996). As well as in $SOD1^{G93A}$ mice (Bendotti et al., 2001b), in our *in vitro* system, Western blot analysis showed high molecular weight bands, corresponding to trimeric GLT-1. In order to prevent transporters from oxidation during the sample preparation (Danbolt,

2001), buffer containing SDS and DTT was used to extract proteins, and the samples were not heated. Thus, the high molecular weight bands observed in transfected astrocytes should derive from oxidative processes that occurred in living cells. An increase in trimeric or other high molecular weight complexes of GLT-1 could potentially explain the decrease of monomeric GLT-1 but no significant changes in the high molecular weight complexes were observed.

More direct exclusion of oxidative processes in regulating GLT-1 levels and function in this system came from experiments performed with DCDHF-DA as marker of intracellular ROS production, which revealed no detectable signs of oxidative stress in astrocyte cultures expressing either $hSOD1^{G93A}$ or $hSOD1^{wt}$. Furthermore the reduction in GLT-1 levels caused by expression of $hSOD1^{G93A}$ or $hSOD1^{wt}$ was not ameliorated by Trolox treatment. This lack of involvement of oxidative stress is somewhat consistent with a recent study that reported that enhancing oxidative stress had no effects on glutamate transporter expression in cultured astrocytes (Miralles et al., 2001). Also indirectly supporting this concept are previous observations showing that astrocyte viability after exposure to oxidative injury was not potentiated by $SOD1^{wt}$ or $SOD1^{G93A}$ overexpression (Chen et al., 2001;Williams et al., 2001). In contrast, NSC-34 motor neuron-like cells showed significant increase of ROS production after infection with adenovirus containing $hSOD1^{G93A}$ but not with $hSOD1^{wt}$ (Liu et al., 2002). Taken together, all these results suggest that $hSOD1^{G93A}$ may induce oxidative damage in a cellular-specific way and astrocytes are resistant to its harmful oxidant properties.

Interestingly, Vanoni and colleagues have recently reported that expression of $SOD1^{G93A}$ downregulates GLT-1 protein levels, without the involvement of oxidative processes, also in MDCK cells. Moreover, they have demonstrated that decrease of GLT-1 expression is consequence of increased internalisation and degradation of the transporter, mediated by cytosolic protein domain (Vanoni et al., 2004).

Our results also showed a decrease of MTT turnover associated with the expression of $hSOD1^{G93A}$ or $hSOD1^{wt}$. This alteration could reflect decreases in mitochondrial succinate dehydrogenase activity, and may directly relate to the pathological effects of hSOD1 expression, although this possibility was not tested in the present study. Accumulation of both the hSOD1 forms in swollen mitochondria of different lines of ALS mice has been reported (Higgins et al., 2002) and it has been reported that $hSOD1^{G93A}$ induces alterations of mitochondrial functions in transgenic mice and in NSC-34 motor neuron-like cells (Liu et al., 2002; Mattiazzi et al., 2002). In the same cell line, complex II activity was slightly decreased also by $hSOD1^{wt}$ (Menzies et al., 2002). The SOD1 induced decrease in MTT conversion in cultured astrocytes was not changed by antioxidants or depletion of endogenous antioxidant system, indicating the lack of involvement of oxidative processes. It is possible that this effect is mediated by direct interaction of SOD1 with mitochondria (Liu et al., 2004; Pasinelli et al., 2004). Further work is necessary to determine whether decreased mitochondrial metabolic activity is directly linked to decreases in GLT-1 levels.

CHAPTER 7

Role of p38MAPK in the pathogenesis of ALS and its possible involvement in excitotoxic processes

7.1 Introduction

7.1.1 p38MAPK, neuronal death and excitotoxicity

Excess of glutamate firing on neuronal cells, due to deficit in synaptic glutamate clearance or altered function of glutamate receptors, leads to cell death through Ca^{2+} cell overloading. This causes generation of free radicals and activation of a variety of calcium-dependent enzymes such as lipases, phospholipases, endonucleases, protein kinase C, nitric oxide synthase and many others, which in turn lead to neurone degeneration (Arundine and Tymianski, 2003). However, it is now well established that aberrant stimulation of glutamate receptors may induce neuronal death also through the activation of intracellular death cascades. One of these pathways involves the Mitogen Activated Protein Kinases (MAPKs).

MAPKs are a family of serine/threonine protein kinases that control several cellular functions in responses to proliferative or harmful stimuli. Members of the MAPK family include extracellular signal-regulated kinases (ERKs), c-Jun-N-terminal kinase or stress activated protein kinase (JNK/SAPK) and the p38 MAP kinase (p38MAPK). Particularly, p38MAPK is implicated in several functions relevant to ALS such as phosphorylation of cytoskeletal proteins, biosynthesis of inflammatory cytokines and production of nitric oxide (Mielke and Herdegen, 2000; Ono and Han, 2000).

Activation of p38MAPK has been recently associated with neuronal degeneration in several neurological pathologies such as Alzheimer's disease

and stroke (Takagi et al., 2000; Zhu et al., 2000; Barone et al., 2001b; Legos et al., 2001; Savage et al., 2002). Moreover, it has been shown that p38MAPK inhibitors can rescue primary cultured neurones from apoptosis induced by neurotrophic factor deprivation (Horstmann et al., 1998) and promote survival of transplanted dopamine neurones in Parkinsonian rats (Zawada et al., 2001).

A large body of evidence demonstrate that p38MAPK pathway is also implicated in neuronal death induced by excitotoxic insults. The neuronal damage occurring within the first minutes/hour after ischemia is essentially due to excitotoxic events and activation of p38MAPK has been documented in this phase (Takagi et al., 2000). Administration of p38MAPK inhibitors showed neuroprotective effects and reduction of infarct size in rats (Legos et al., 2001), suggesting the involvement of p38MAPK pathway in glutamate mediated neuronal damage. Intracortical injection of the glutamate analogue quinolinic acid in rats causes increased p38MAPK immunoreactivity in neurones and astrocytes surrounding the injection site, which precedes cell death (Ferrer et al., 2001). Support to this hypothesis also comes from *in vitro* studies. It has been shown that inhibition of p38MAPK confers protection to cultured neurones against excitotoxic exposure in different experimental paradigms (Kawasaki et al., 1997; Giardina and Beart, 2002; Legos et al., 2002; Chen et al., 2003).

Involvement of p38MAPK pathway in glutamate system regulation and activation is also suggested by recent works indicating the role played by this kinase in the control of glutamate receptor trafficking. Studies on long-term potentiation (LTP) and long-term depression (LTD) have revealed how AMPA receptor activity may be regulated through adding and removing different AMPA

subunits at synaptic level (Huang et al., 2004). In particular, activation of Rap, a member of the Ras superfamily of small GTPases, results involved in removal of AMPA subunits with short cytoplasmic tails, such as GluR2 and GluR3, from the synapses, being this phenomenon mediated by p38MAPK (Zhu et al., 2002a). Recently, it has been reported that inhibition of p38MAPK cascade can reverse the decrease of GluR2 mRNA observed in cortical neurones of neonatal rats after treatment with glutamate (Rivera-Cervantes et al., 2004).

7.1.2 p38MAPK and ALS

To date, the bulk of evidence about the implication of p38MAPK in ALS is based on studies on the effect of minocycline, a semi-synthetic tetracycline, which, among other effects, seems to inhibit p38MAPK pathway and to be protective to neurones. In fact, *in vitro* experiments performed on mixed spinal cord cultures have demonstrated that minocycline is neuroprotective against excitotoxicity by blocking microglia activation *via* p38MAPK inhibition (Tikka et al., 2001; Tikka et al., 2002). Moreover, it has been shown that the inhibitory effect of minocycline on p38MAPK cascade protects cerebellar granule neurones against NO induced cell death (Lin et al., 2001). Three independent studies carried out on two different lines of ALS mice showed beneficial effects of chronic treatment with minocycline on symptom onset, longevity and neuronal degeneration in these animals (Kriz et al., 2002; Van Den Bosch et al., 2002a; Zhu et al., 2002b). Furthermore, Raoul and collaborators have recently showed that FAS-induced death of motor neurones in culture requires activation

of the p38MAPK cascade and that this death signalling is exacerbated in motor neurones expressing $SOD1^{G93A}$ (Raoul et al., 2002).

7.2 Hypothesis and aim

The hypothesis tested in this section of the thesis is that p38MAPK is activated in motor neurones and contributes to ALS pathology. In particular, it is possible that activation of this pathway and its consequent harmful effect to the motor neurones may directly result from excitotoxic injury to these cells or other toxic stimuli. The aim of this part of the study is to evaluate the activation of p38MAPK pathway in the spinal cord of $SOD1^{G93A}$ mice and whether the inhibition of this pathway can ameliorate or arrest the course of the pathology.

7.3 Methods

7.3.1 Western blot analysis of p38MAPK

Spinal cords of $SOD1^{G93A}$ mice at 8 and 19 weeks of age and non transgenic mice used as control (3-5 mice each group) were homogenized in ice cold lysis buffer (20 mM Tris/HCl, pH 7.5, 10 mM EGTA, 500 mM β-glycerophosphate, 10 mM magnesium chloride, 2 mM DTT, 1 mM Na_3VO_4, 50 mM NaF, 1mM PMSF, 1% Triton X-100, 10 mg/ml leupeptin, 10 mg/ml aprotinin) using a teflon-on-glass homogenizer and centrifuged at 13000 rpm for 30 minutes at 4°C. Protein concentrations from supernatant were determined

using a BCA Protein Assay Reagent Kit (Pierce). Lysates (50 µg) from human monocytes treated for 3 minutes with N-Formylmethionine-Leucyl-Phenyl-alanine (f-MLP) 10^{-7} M were loaded as positive controls. Samples were then boiled for 3 minutes in loading buffer (100 mM Tris/HCl, pH 7.5, 15% β-mercaptoethanol, 4% SDS, 15% glycerol, 5 mM EGTA, 5 mM EDTA, 0,2% bromophenol blu) and 100 to 150 µg proteins/lane were run on 10% polyacrylamide-SDS gel and transferred to nitrocellulose membrane (Protran, Scheicher and Schuell). Membrane was incubated in blocking buffer, TBST with 5% skimmed milk, for 2 hours at room temperature, followed by incubation overnight at 4°C with primary antibodies: rabbit anti-p38MAPK or rabbit anti-Phospho p38MAPK (P-p38MAPK) (both 1:1000, Calbiochem), in TBST with 5% bovineserum albumin, goat anti-AKT1 (1:2000, Santa Cruz Biotechnology, Santa Cruz, CA, USA) or with mouse anti-actin (1:2000, Chemicon International) in a buffer TBST with 5% skimmed milk. The blots were then washed in TBST and incubated with secondary antibodies: anti-rabbit, anti-goat or anti-mouse IgG conjugated to horseradish peroxidase (1:2000, Sigma) in TBST with 5% skimmed dry milk, for 1 hour at room temperature. Blots were developed by ECL technique using ECL Western Blotting Detection System (Amersham Biosciences) according to the manufacturer's instructions. Densitometric analysis of autoradiographic bands was done using a computer assisted image analysis system (AIS 3.0, Imaging Research Inc.).

7.3.2 RNA extraction and semiquantitative RT-PCR for p38MAPK

Total RNA was extracted from frozen spinal cord samples of non transgenic mice (controls) and $SOD1^{G93A}$ mice at 10 and 19 weeks of age using the acid guanidium-phenol-chloroform method as previously decribed (Bendotti et al., 2000). Two µg of total RNA was used for cDNA synthesis by MuLV reverse trascriptase (final concentration 2.5 U/µl), in the presence of oligo d(T) 2.5 µM, dNTP mix 1 mM each component, Rnase inhibitor 1 U/µl, $MgCl_2$ 5 mM in PCR Buffer II 1X (Gene Amp RNA PCR Kit, Perkin Elmer, CA, USA). The incubation was carried out for 30 minutes at 42°C, followed by 5 minutes at 99°C and 5 minutes in ice. An aliquot (10 µl) of each cDNA synthetized in RT reaction was used for PCR amplification of cDNA encoding for p38MAPK and α-actin, in presence of AmpliTaq DNA Polymerase (final concentration 2.5 U/100µl), $MgCl_2$ (final concentration 2 mM), PCR Buffer II 1X (Gene Amp RNA PCR Kit, Perkin Elmer, CA, USA) and sense and antisense primers (final concentration 0.15 µM each). The sequences of primers for α-actin were (5'-3'): CACA CTG TGC CCA TCT ACG A (forward) and CAC AGG ATT CCA TAC CCA AG (reverse). The sequences of primers for p38MAPK were (5'-3'): CCG GAT CCT GGA AGA TGT CGC AGG AGAG (forward) and CCG GAT CCC CAG GTG CTC AGG ACA CCAT (reverse). In order to verify that amplification of each gene was within the linear range, p38MAPK was amplified for 25, 28, 31, 34 cycles and α-actin for 16, 19, 22, 25 cycles. Quantitative analysis was made comparing the band of product of 28 cycles for p38MAPK and of 19 cycles for α-actin. Denaturation was reached at 94°C for 1 minute, annealing at

58°C for 1 minute and extension at 72°C for 1 minute. Each sample was run on 1% agarose gel and the optical density of bands was quantified by Image Quant analyzer (Molecular Dynamics, Sunnyvale, CA, USA).

7.3.3 Chronic treatment of SOD1^{G93A} mice with SB 239063

Non transgenic and SOD1^{G93A} mice (10 each group, 3 per cage) received the drug mixed in a defined diet formulation provided by Glaxo Smith Kline (Brentford, Middlesex, UK). The amount of drug in the diet was calculated in such way to reach the dose of 10 mg/Kg mouse body weight per day. The mice had free access to the drug mixed diet from the manger, starting from the seventh week of age through the entire experiment. The same diet formulation without the drug was used as control. The food intake for each cage was measured every week when the diet in the manger was refilled.

7.3.4 Motor behavioral and neurological tests during chronic treatment with ZK 187638

Quantitative assessment of the motor behavioral deficit, carried out by measuring the stride length and rotarod performance, and the evaluation of survival were performed as described in section 4.3.3.

7.4 Results

7.4.1 Study of the expression of p38MAPK protein in the spinal cord of $SOD1^{G93A}$ mice

In order to explore the hypothesis, we investigated the levels of p38MAPK and its phosphorylated (activated) form (P-p38MAPK) in spinal cord extracts from non transgenic (control) and $SOD1^{G93A}$ mice using Western blot technique. Immunobloting analysis revealed a single specific band of about 40 KDa corresponding to the band obtained from human monocytes stimulated with fMLP, used as positive control for activated p38MAPK (Figure 7.1 A).

In $SOD1^{G93A}$ mice at 8 and 19 weeks of age corresponding to presymptomatic and late stage of the disease, the levels of total p38MAPK in the spinal cord were, respectively, 1.5 and 2.2 fold those found in the non transgenic mice (Figure 7.1 B). By contrast, immunoblot analysis of the phosphorylated p38MAPK showed a specific moderately intense band in spinal cord extracts from 19 weeks old $SOD1^{G93A}$ mice. No signal was found in the spinal cord extracts from controls while in tissue from 8 weeks old $SOD1^{G93A}$ mice we observed a very faint specific band, which was under the threshold for quantitative detection. No differences were observed in the level of another intracellular kinase involved in cell signalling cascade, Akt, which is also activated by stimuli such as cytokines, stress, etc. (Figure 7.21 A).

7.4.2 Study of the expression of p38MAPK mRNA in the spinal cord of $SOD1^{G93A}$ mice

We then examined the expression of p38MAPK mRNA by semiquantitative RT-PCR analysis. The increase of p38MAPK protein was not associated with changes in the levels of mRNA (Figure 7.2), suggesting that this protein is under post-translational regulation in the $SOD1^{G93A}$ mice.

7.4.3 Effect of p38MAPK activation inhibitor on symptoms and survival of $SOD1^{G93A}$ mice

In order to verify whether the inhibition of p38MAPK activation may determine the improvement of symptoms and extension of life span in $SOD1^{G93A}$ mice, in this part of the study we examined the effect of treatment with SB 239063, a second generation p38MAPK inhibitor, on the motor dysfunction and survival of these mice.

The drug was mixed in a defined diet formulation which was given to $SOD1^{G93A}$ and non transgenic mice every day, starting from the seventh week of age until the death of $SOD1^{G93A}$ mice, reaching approximately the dose of 10 mg/Kg day. The same diet formulation without the drug was used as control (vehicle). Motor dysfunction was tested by measuring the stride length and by evaluating the performance on rotarod of the mice. Body weight of non transgenic mice progressively increase from the seventh week of age until the end of experiment. However the rise was slightly, but significantly, lower in mice

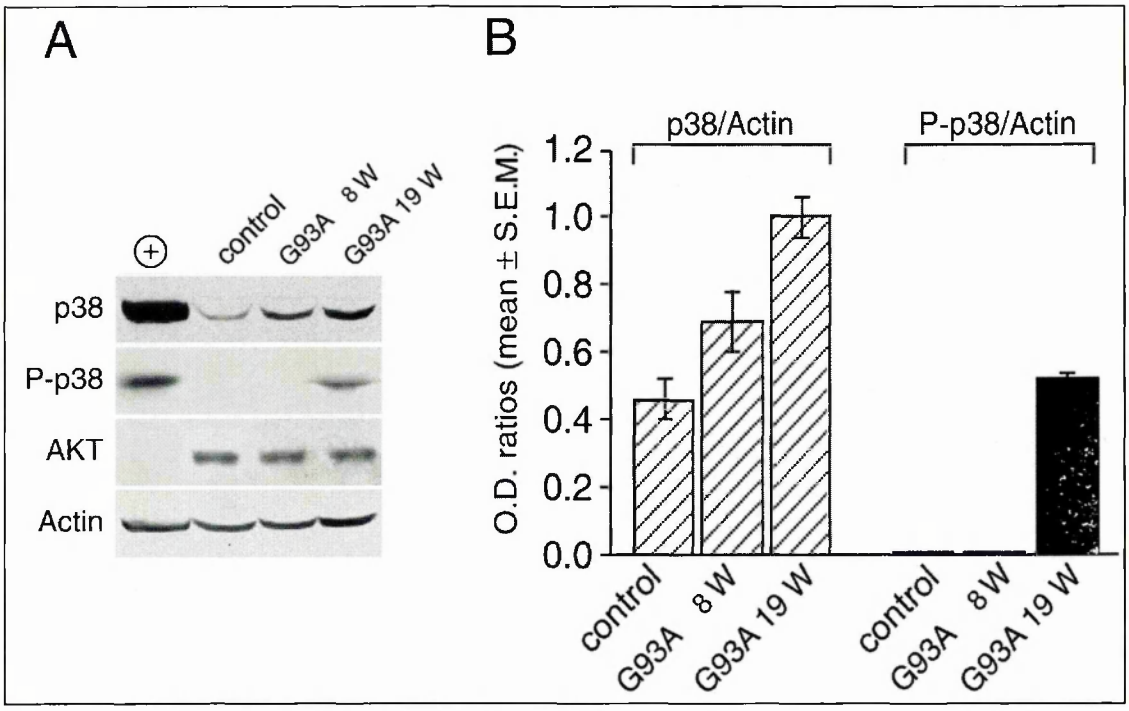

Figure 7.1: Expression of p38MAPK protein in the spinal cord of SOD1^{G93A} mice

(A) Representative immunoblots for total p38MAPK, its phosphorylated form (P-p38MAPK), Akt and actin. The analysis was performed on transgenic mice at early (8 weeks) and late (19 weeks) stage of the disease in comparison to non transgenic mice (control). First lane (+) represent the positive control for P-p38MAPK (human monocytes treated with f-MLP, 50µg proteins). Other lanes are spinal cord homogenates (120 µg protein per lane). (B) Quantitative analysis of the immunoblots for p38MAPK and P-p38MAPK levels. The optical density was evaluated for each autoradiographic band and the values corresponding to the ratio between p38MAPK or P-p38MAPK and actin. Each column is the mean ± S.E.M. (n = 3-5).

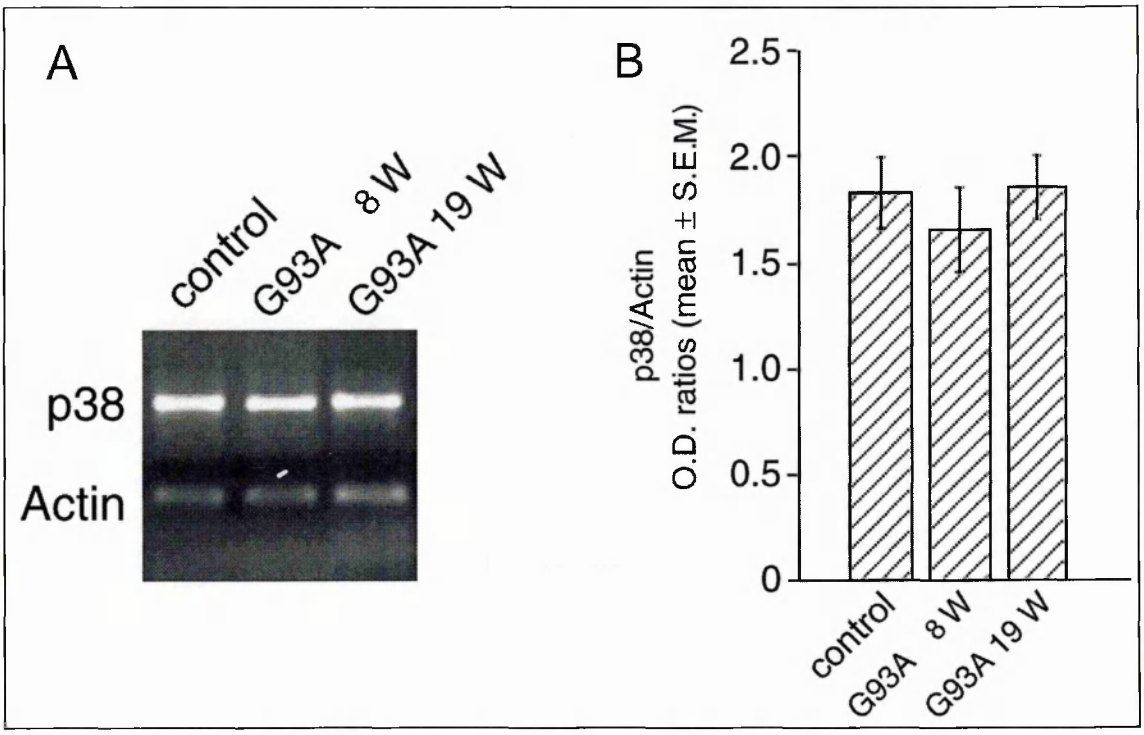

Figure 7.2: Levels of p38MAPK mRNA in the spinal cord of SOD1^{G93A} mice

(A) Representative RT-PCR analysis of p38MAPK and β-actin mRNA from spinal cord of SOD1^{G93A} mice at 8 and 19 weeks of age and controls. (B) Histograms of the quantitative analysis of p38MAPK mRNA relative to β-actin mRNA show no significant differences among groups. Each column is the mean ± S.E.M. (n = 3).

receiving the drug compared to mice fed with normal diet. Body weight of $SOD1^{G93A}$ mice also progressively increased but at a slower rate in respect to non transgenic mice. The maximal body weight in these mice was reached at about 15 weeks of age and then it progressively declined. $SOD1^{G93A}$ receiving the drug showed a significant lower body weight during the entire experiment (Figure 7.3). Surprisingly, while a constant food intake was observed in non transgenic mice that received either normal or drug mixed diet, the $SOD1^{G93A}$ receiving the drug ate about 10-13% more in respect to all other groups.

In non transgenic mice the stride length reached the maximal value around 12 weeks of age, which was maintained stable for the entire time of observation. No remarkable differences were observed between SB 239063 and vehicle groups. Transgenic mice receiving normal diet showed a decline in their stride length after 16 weeks of age whereas, in the group treated with the drug, the onset of gait impairment started at the week 12, maintaining a significant lower stride length in respect to vehicle group (Figure 7.4).

$SOD1^{G93A}$ mice starting at 14 weeks of age showed a progressive decline in their capability to stay on rotating bar. No differences were found between the group receiving the SB 239063 and vehicle group in both transgenic and non transgenic mice (Figure 7.5). No difference was found in the comparison of survival curves of transgenic $SOD1^{G93A}$ mice treated with SB 239063 with those treated with vehicle (Figure 7.6).

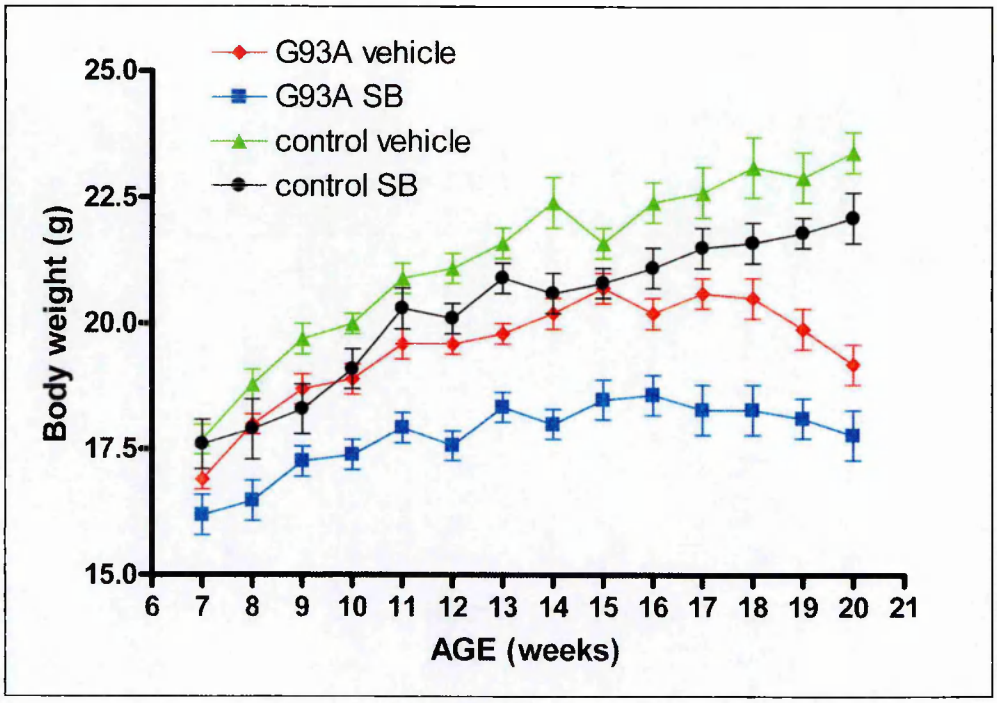

Figure 7.3: Effect of SB 239063 on body weight of SOD1^{G93A} and non transgenic mice

Data from SOD1^{G93A} mice treated with vehicle (red diamonds, n=10) or SB 239063 (blue squares, n=10) and non transgenic mice (control) treated with vehicle (green triangles, n=10) or SB 239063 (black circles, n=10) are presented as mean ± S.E.M. Data were analyzed by ANOVA for repeated measures followed by post-hoc Dunnett's test between treatments. Group non transgenic: F (treatment) 7.3 (df1) p=0.01. Group SOD1^{G93A} : F (treatment) 17.0 (df1) p<0.001

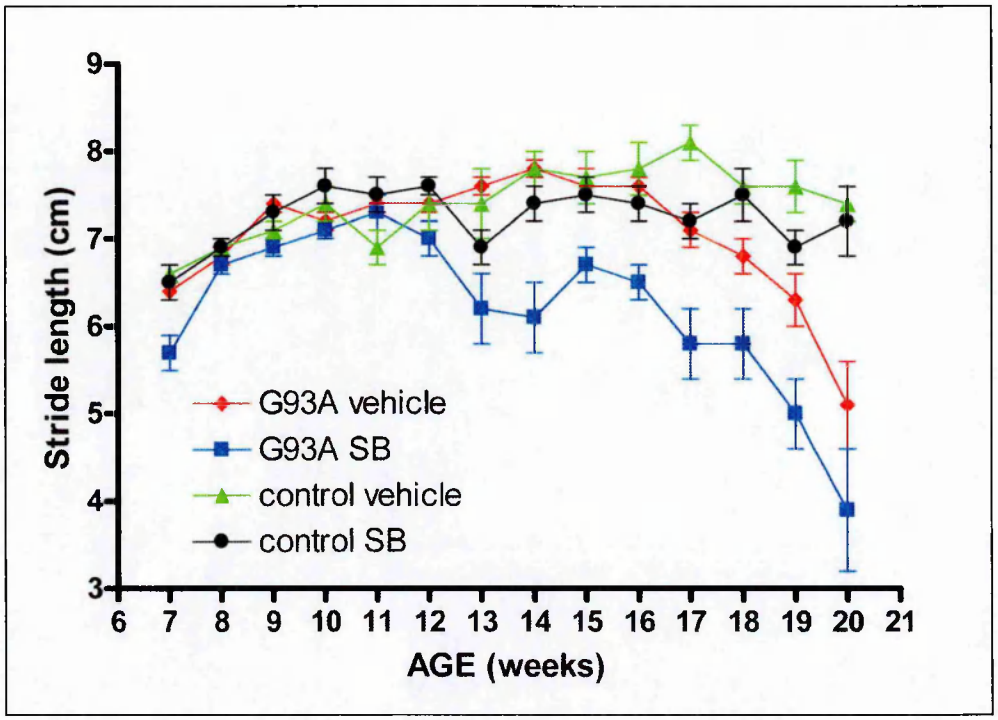

Figure 7.4: Effect of SB 239063 on stride length of SOD1^{G93A} and non transgenic mice

Data from SOD1^{G93A} mice treated with vehicle (red diamonds, n=10) or SB 239063 (blue squares, n=10) and non transgenic mice (control) treated with vehicle (green triangles, n=10) or SB 239063 (black circles, n=10) are presented as mean ± S.E.M. Data were analyzed by ANOVA for repeated measures followed by post-hoc Dunnett's test between treatments. Group non transgenic: F (treatment) 0.9 (df1) NS. Group SOD1^{G93A} : F (treatment) 25.9 (df1) p<0.001.

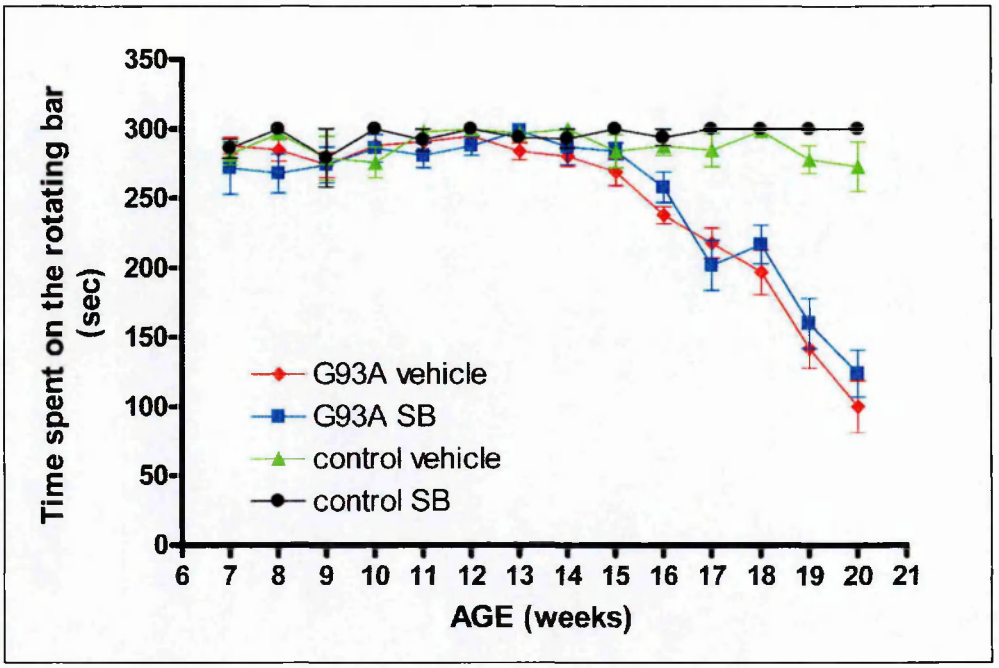

Figure 7.5: Effect of SB 239063 on rotarod performance of SOD1^{G93A} and non transgenic mice

Data from SOD1^{G93A} mice treated with vehicle (red diamonds, n=10) or SB 239063 (blue squares, n=10) and non transgenic mice (control) treated with vehicle (green triangles, n=10) or SB 239063 (black circles, n=10) are presented as mean ± S.E.M. Data were analyzed by ANOVA for repeated measures followed by post-hoc Dunnett's test between treatments. Group non transgenic: F (treatment) 0,7 (df1) NS. Group SOD1G93A : F (treatment) 0,7 (df1) NS.

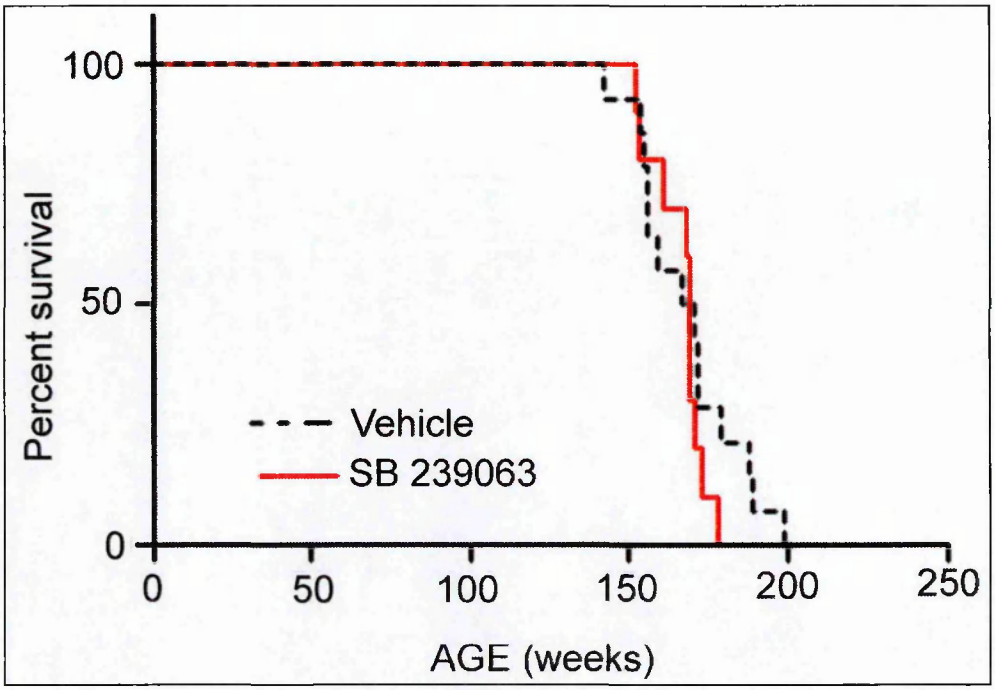

Figure 7.6: Effect of SB 239063 on survival of SOD1^{G93A}

Administration of SB 23906370 did not extende the mean survival of SOD1^{G93A} animals in respect to vehicle treated mice. Data on survival were analysed by the log rank test (n=10 for each group). No significant differences were found.

7.5 Discussion

The involvement of p38MAPK pathway in ALS pathology has been suggested by studies indicating that treatment with minocycline, a semi-synthetic tetracycline with p38MAPK inhibitor properties, improves symptomatology and extend life expectancy of $SOD1^{G93A}$ and $SOD1^{G37R}$ mice (Kriz et al., 2002; Van Den Bosch et al., 2002a; Zhu et al., 2002b). More recently, activation of p38MAPK has been indicated as key factor implicated in selective death process mediated by FAS and occurring in cultured motor neurones (Raoul et al., 2002). The results obtained in this part of the study demonstrated a prominent increase of p38MAPK protein expression and its activated form in the spinal cord of ALS mice carrying $SOD1^{G93A}$ mutant. This was not associated with augmentation of mRNA transcription. Immunohistochemical studies carried out in our laboratory have also demonstarted that spinal motor neurones of transgenic mice selectively show higher levels of phosphorylated p38MAPK already evident at 8 weeks of age, when clinical symptoms are not obvious, which persist till the final stage of the pathology (Figures 7.7). Moreover, double immunostaining for glial fibrillary acidic protein (GFAP), a selective marker for astrocytes (Figure 7.9), or CD11b, a surface molecule that identifies microglial cells (Figure 7.10), and P-p38MAPK revealed a progressive activation of p38MAPK in reactive glial cells during the progression of the disease. This probably explains why Western blot analysis could only reveal the presence of activated p38MAPK at 19 week of age (end phase) but not at presymptomatic stage of the disease. In fact, it can

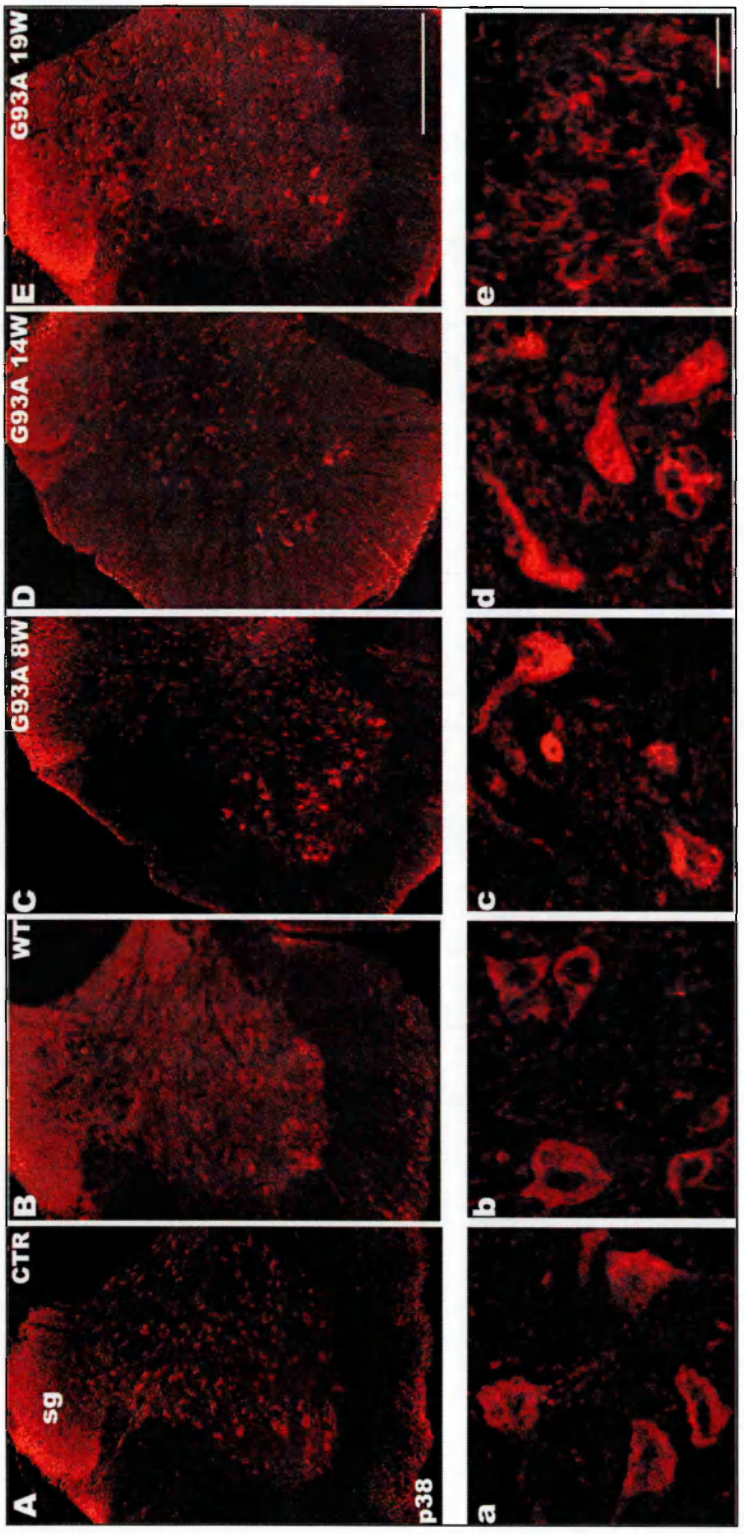

Figure 7.7

Figure 7.7: Immunolocalization of P-p38MAPK in the lumbar spinal cord SOD1^{G93A} mice

SOD1^{G93A} mice (G93A) were analysed at early (8weeks), intermediate (14 weeks) and late (19 weeks) stage of the disease in comparison SOD1^{wt} (WT) and non transgenic mice used as control (CTR). (A-E) In control and SOD1^{wt} mice the labelling is present at a moderate level in the grey matter and it is particularly intense in the substantia gelatinosa (sg) of the dorsal horn. In SOD1^{G93A} mice a remarkable increase of immunoreactivity is observed in the motor neurones at all ages examined as shown at higher magnification (a-e). No remarkable changes are observed in other regions except for an increase of immunofluorescence in the whole grey matter of SOD1^{G93A} mice at 19 weeks of age. Scale bars: (A-E)= 200 µm; (a-e)= 30 µm.

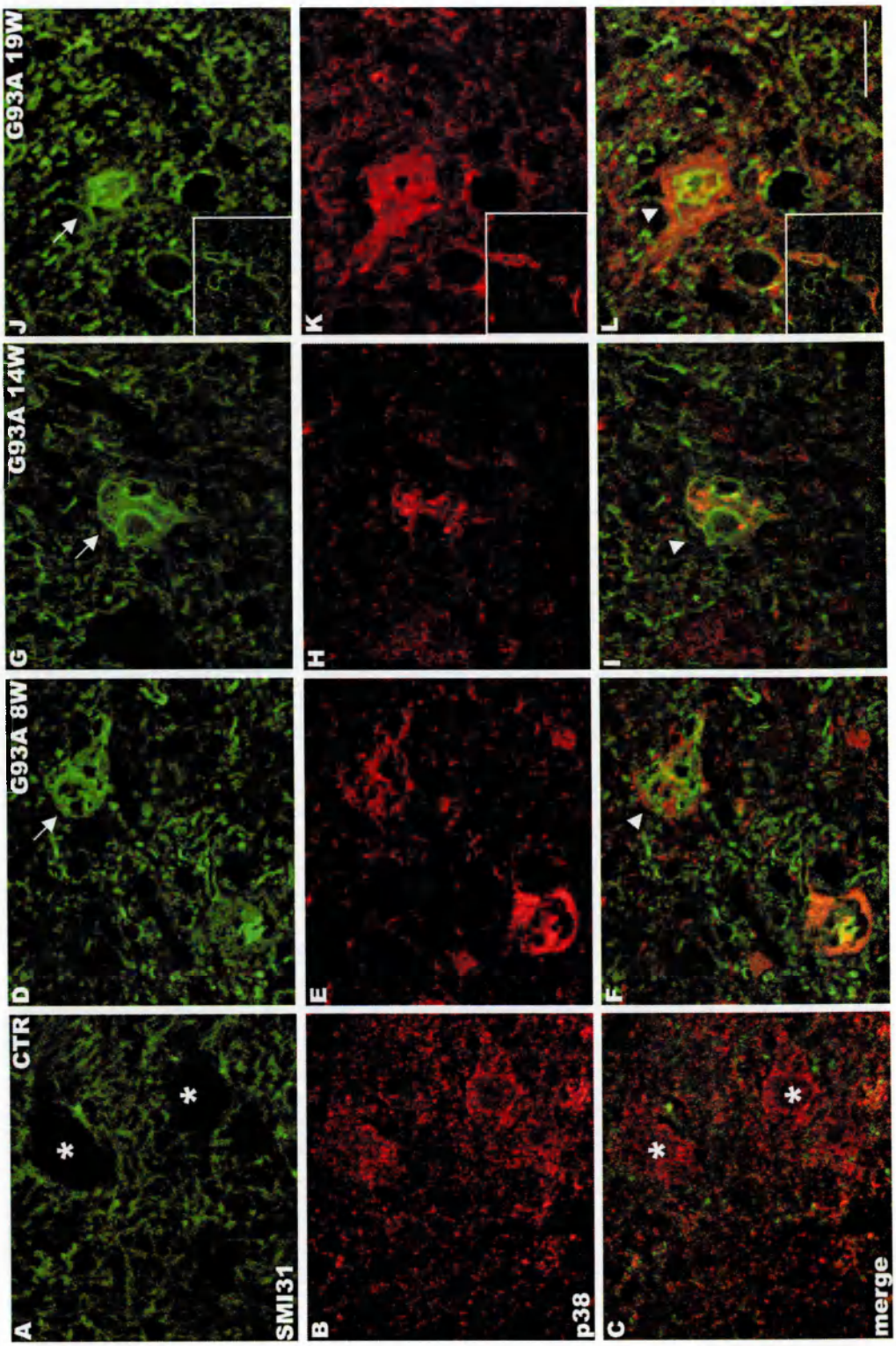

Figure 7.8

Figure 7.8: Colocalization of P-p38MAPK and SMI31 in the lumbar spinal cord SOD1^{G93A} mice

High magnification of laser scanning confocal micrographs of P-p38MAPK and SMI31 immunofluorescence in the ventral horn spinal cord of SOD1^{G93A} mice at different stages of the disease. In non transgenic controls (CTR, A-C) there is a lack of immunostaining for SMI31 in the cell bodies of motor neurones (asterisks in A) and the diffuse immunoreactivity in the neuropil. No colocalisation is observed with P-p38MAPK (asterisks in C). In SOD1^{G93A} mice, at all ages examined, there is an intense immunofluorescence of SMI31 in the vacuolized motor neuronecell bodies (arrows) and the colocalisation of the two antibodies in these cells (arrowheads). In the inserts of panels J,K,L, it is shown at high magnification a vacuolized neurite with almost complete overlapping of SMI31 and P-p38MAPK immunoreactivity. Scale bar : 20 µm.

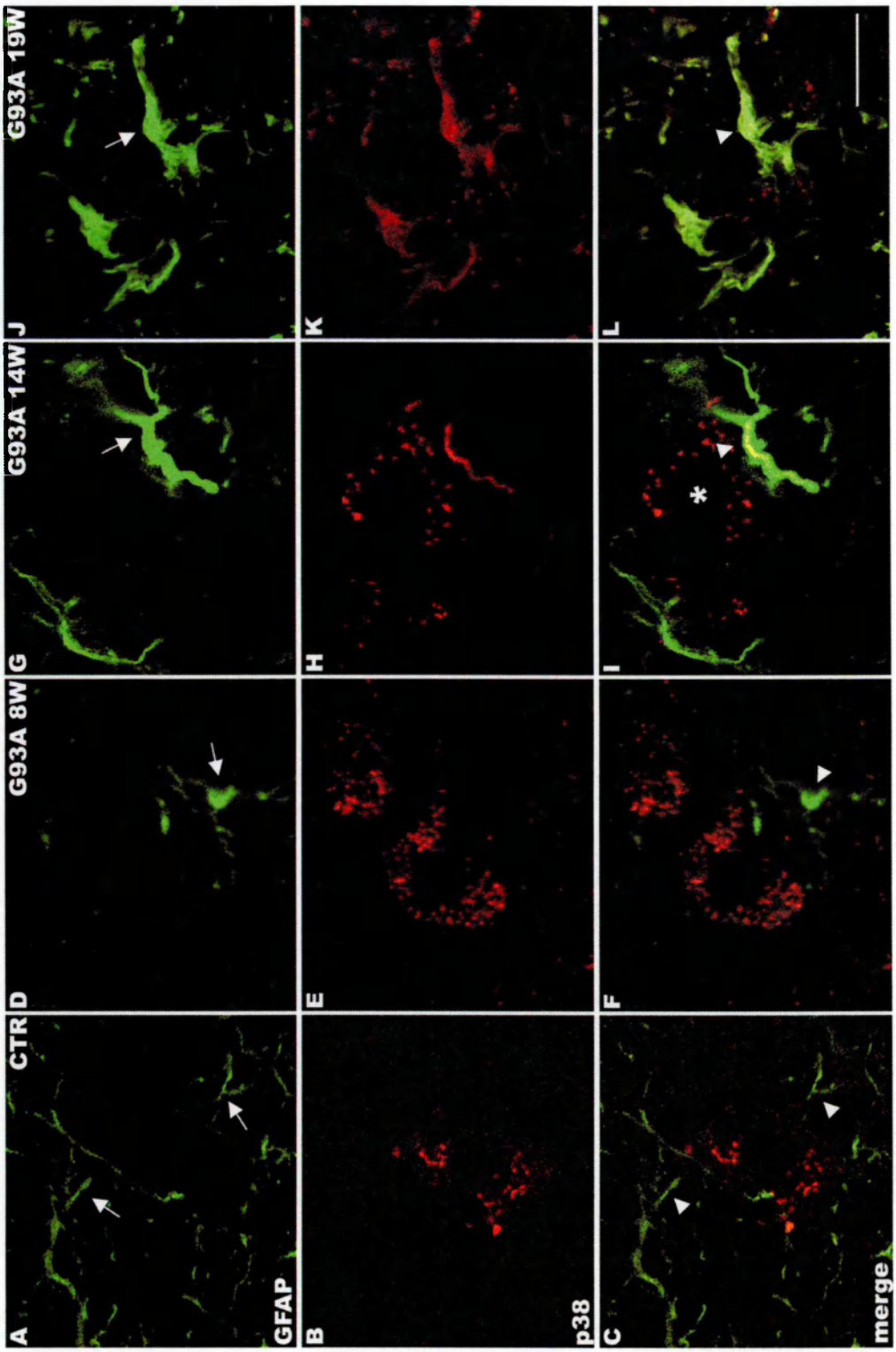

Figure 7.9

Figure 7.9: Colocalization of P-p38MAPK and GFAP in the lumbar spinal cord SOD1G93A mice

High magnification of laser scanning confocal micrographs of P-p38MAPK and GFAP immunofluorescence in the ventral horn spinal cord of $SOD1^{G93A}$ mice at different stages of the disease. In control (CTR), GFAP immunoreactivity is in the thiny processes of astrocytes (arrows in A) and there is no overlapping with P-p38MAPK immunostaining (arrowheads in C). In $SOD1^{G93A}$ mice, GFAP immunoreactive astrocytes show a remarkable hypertrophy which increases with the age (arrows in D,G and J). Panels I and L show a progressive increase of overlapping P-p38MAPK and GFAP immunoreactivities in hypertrophic astrocytes (arrowheads) whereas such colocalization does not appear in hypertrophic astrocytes of $SOD1^{G93A}$ 8 weeks old mice (arrowhead in F). Scale bar: 20 µm.

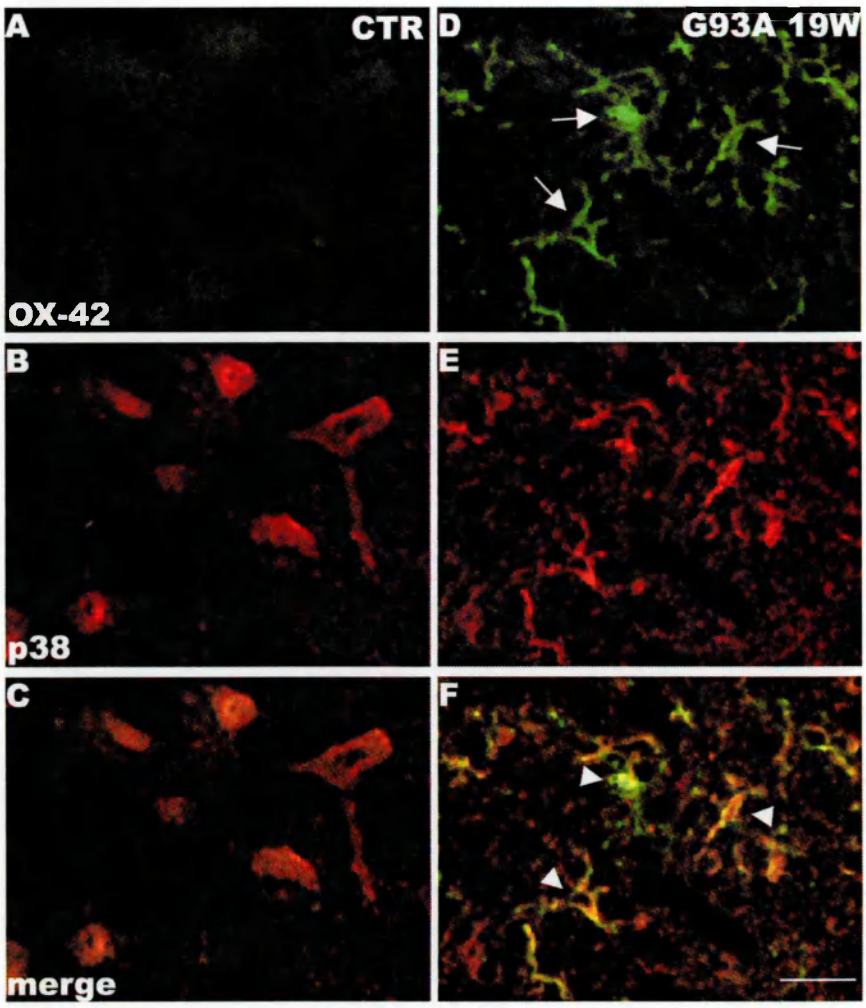

Figure 7.10: Colocalization of P-p38MAPK and OX42 in the lumbar spinal cord SOD1^{G93A} mice

High magnification of laser scanning confocal micrographs of P-p38MAPK and Cd11b (OX42) immunofluorescence in the ventral horn spinal cord of 19 weeks old SOD1^{G93A} mice. Panel A shows the low CD11b staining for microglia in control mice. Panel D shows activated microglial cells with multiple hypertrophic processes (arrows) in which there is an almost complete overlapping with P-p38MAPK immunofluorescence (arrowheads). Scale bar: 30 µm.

be assumed that the detection threshold of the antibody used for immunoblotting of the whole protein extract of spinal cord does not permit to see the increased level of P-p38MAPK when selectively present only in the motor neurones. At the final stage of the disease, marked astrocytosis and microgliosis cause a general prominent increase of activated p38MAPK levels and this allowed to reveal the band in the whole spinal cord homogenate. Western blotting also showed progressive accumulation of total p38MAPK, even without increase of mRNA levels. Thus, it is plausible that pathological processes occurring in motor neurones of ALS mice cause the recruitment of higher levels of p38MAPK protein obtained by slowing its turnover and consequently retarding protein degradation. As a result, the level of phosphorylated and active form of the kinase also results increased. These changes were specific for p38MAPK pathway since no differences were observed in the expression of total Akt, another intracellular kinase involved in the signaling following stress stimuli on the cells.

Our data are in line with those recently published by another group. Using multi-immunoblotting technique, they performed a wide range screening of numerous protein kinases expressed in symptomatic $SOD1^{G93A}$ mice finding, among others, 51% elevation of total p38MAPK and more than ten fold increased level of its phosphorylated form, when compared to normal mice (Hu et al., 2003). Reinforcing these findings, in our laboratory, we have recently demonstrated intense immunoreactivity for activated p38MAPK in degenerating motor neurones and reactive astrocytes of ALS patients (Bendotti et al., 2004).

This result gives further and important support to the possible involvement of p38MAPK in ALS.

On the basis of numerous studies that demonstrated the link existing between activation of p38MAPK pathway and neuronal degeneration mediated by glutamate in different experimental models (Kawasaki et al., 1997; Ferrer et al., 2001; Legos et al., 2001; Giardina and Beart, 2002; Chen et al., 2003), it is reasonable to assume that excitotoxic processes and activation of p38MAPK may be also correlated in ALS pathology. In our studies, both decreased expression of AMPA receptor subunit GluR2 and increased level of phosphorylated p38MAPK have been found in spinal motor neurones of $SOD1^{G93A}$ mice at early stage of the disease, when the symptoms are not already manifest. This suggest that these two phenomena may be related and represent initial events in the outbreak of the symptomatology. However, whether dysfunction of glutamatergic neurotransmission can trigger p38MAPK cascade activity or be, in its turn, the consequence of the direct or indirect action of this kinase is not yet clear.

Increased P-p38MAPK immunoreactivity has been revealed in dying cortical neurones of rats occurring after toxic intracortical injection of the glutamate analogue quinolinic acid (Ferrer et al., 2001). Kawasaky and colleagues found that glutamate-induced death of cultured cerebellar granule cells was associated with activation of p38MAPK pathway and that SB 203580, a specific inhibitor for p38MAPK, inhibited this process. Furthermore, activation of p38MAPK resulted mediated by calcium influx (Kawasaki et al., 1997). Another p38MAPK inhibitor, SB 239063, provided neuroprotection against cell

death *in vitro* induced by moderate excitotoxic exposure (Legos et al., 2002). Taken together, these finding suggest that abnormal calcium influx through glutamate AMPA receptors, due to decreased expression of GluR2, may induce p38MAPK pathway activation, which, in turn, triggers death pathways in motor neurones in ALS. Although studies *in vitro* associate activation of p38MAPK in neurones with apoptotic processes (Kawasaki et al., 1997; Kummer et al., 1997), our previous results showed that morphological changes occurring in motor neurones of $SOD1^{G93A}$ mice were never associated with ultrastructural apoptotic features of the nuclei nor with nuclear DNA fragmentation and cytoplasmic leakage, as demonstrated by *in situ* end-labelling (ISEL) technique, even at the later stages of the disease (Migheli et al., 1999; Bendotti et al., 2001a). Therefore, these *in vivo* results indicate that an increase of phopsphorylated p38MAPK may precede motor neurone death not associated with apoptotic mechanisms. This is in line with the observations reported by Ferrer et al. showing rapid overexpression of activated p38MAPK in the rat cortex injured by intracerebral injection of quinolinic acid, which is consistent with excitotoxic necrosis (Ferrer et al., 2001).

On the other hand, the concomitant decrease of GluR2 protein levels and increase of phosphotylated p38MAPK in the motor neurones of transgenic mice, also gives rise to the hypothesis that other precocious and deleterious factors may trigger the activation p38MAPK pathway, which in turn may negatively influence the glutamatergic neurotransmission, for instance affecting AMPA subunit expression. Zhu and collaborators have demonstrated that AMPA receptor subunits are constantly added to and removed from synapses during

normal activity of neurones. Particularly, removal of GluR2 requires the involvement of Rap, a small GTPases belonging to Ras superfamily, and the activation of p38MAPK (Zhu et al., 2002a). In addition, it has been showed that p38MAPK activation mediates the decrease of GluR2 occurring in neonatal cortical neurones of rats after treatment with glutamate (Rivera-Cervantes et al., 2004). According with these observations, it might be hypothesized that activation of p38MAPK, due to pre-existent harmful stimuli, can cause AMPA receptor disorganization because of augmented internalisation and degradation of GluR2 subunit in motor neurones of ALS mice. Consequently, increase of number of calcium-permeable AMPA receptor would determine excitotoxic firing on motor neurones, contributing to their degeneration.

This theory presumes that earlier pathogenic events lead to p38MAPK recruitment. It is well established that p38MAPK is effectively activated by proinflammatory cytokines such as IL-1 and tumor necrosis factor alpha (TNFα)(Lee et al., 2000). Up regulation of proinflammatory factors, such as the presence of activated microglia, IgG and its receptor for Fc portion (FcgammaRI), ICAM-1 and T lymphocytes in the spinal cord of transgenic $SOD1^{G93A}$ mice at the presymptomatic stages of the disease, strongly suggests that immune-inflammatory factors may be actively involved in the disease process occurring in ALS (Alexianu et al., 2001). Examining a wide range of mRNAs expression by microarray techniques, Yoshihara and collaborators reported that TNFα is one of the earliest factors to be induced in the spinal cord of $SOD1^{G93A}$ mice (Yoshihara et al., 2002). Therefore, an increased TNFα production might contribute to the early and persistent activation of p38MAPK in

motor neurones. During the progression of the disease, activated p38MAPK accumulates not only in degenerating motor neurones but also in hypertrophic astrocytes as demonstrated by colocalization with GFAP. TNFα and/or IL-1 were also reported to strongly activate p38MAPK in mouse astrocytes *in vitro* (Lee et al., 2000). It has been demonstrated that p38MAPK pathway is specifically involved in the activation of inducible nitric oxide synthase (iNOS) expression in mouse astrocytes, resulting in sustained release of large amounts of nitric oxide (NO) (Da Silva et al., 1997). It has been shown that peroxynitrite, which is formed from the reaction between superoxide anions and NO, potently inhibits glutamate uptake (Trotti et al., 1996). Thus, it is possible that p38MAPK activation in astrocytes can affect glutamate system indirectly reducing activity of glial glutamate transporters. Activation of p38MAPK in microglia can also be induced by excess of glutamate and this mechanism has been proposed to play a role in the excitotoxic neuronal death in mixed spinal cord cultures. Tikka *et al.* reported that neuroprotective effect of minocycline against excitotoxicity in spinal cord cultures is due to the inhibition of proliferation and activation of microglia and to inhibition of p38MAPK pathway (Tikka et al., 2001). All these results suggest the existence of a close relation between p38MAPK pathway and glutamate neurotransmission that, in pathological conditions, can generate an autosubstained feedback, which results deleterious to motor neurones.

A possible mechanism related to p38MAPK neurotoxicity involves its interaction with cytoskeleton structure. It has been reported that phosphorylated neurofilaments accumulate in the cell bodies and proximal axons of motor neurones in both sporadic and familial ALS (Hirano et al., 1984a; Hirano et al.,

1984b). Studies performed on mouse models of ALS have shown that neurofilament content and organization strongly influence motor neurone disease induced by mutant SOD1 (Couillard-Despres et al., 1998; Williamson et al., 1998; Couillard-Despres et al., 2000; Kong and Xu, 2000). Among its several biological functions, p38MAPK is involved in phosphorylation of cytoskeletal proteins (Mielke and Herdegen, 2000; Ono and Han, 2000). More recently, Ackerley and its group demonstrated the ability of active p38MAPK in phosphorylating middle and heavy chains of neurofilaments on their side-arm domains *in vitro* (Ackerley et al., 2004). Our results showed that P-p38MAPK colocalized with phosphorylated neurofilaments, labelled with SMI31 antibody that reacts with the phosphorylated epitope of neurofilament H and neurofilament M, in motor neurones of $SOD1^{G93A}$ mice (Figure 7.8). We have also shown that in motor neurones of ALS patients, intracellular aggregates containing ubiquitin and neurofilaments are strongly immunostained for activated p38MAPK (Bendotti et al., 2004). Therefore, activation of p38MAPK pathway, due to pathological circumstances, can determine phosphorylation and consequent disorganization of cytoskeleton architecture, which, in turn, may result in cell death.

Despite the early activation of p38MAPK pathway in the motor neurones of $SOD1^{G93A}$ mice and its probable role in the pathogenesis of ALS, treatment of these mice with p38MAPK inhibitor did not produce any benefit in the course of the disease. In fact, chronic administration of SB 239063 did ameliorate neither the progressive motor impairment nor the survival of transgenic $SOD1^{G93A}$ mice. The lack of neuroprotective effect of SB 239063 is in disagreement with the

recent study showing a dose response protective effect of this drug in two rat stroke models after oral administration (Barone et al., 2001b). The doses showing the protective effect in this study (5-30 mg/Kg) are comparable to those received by our mice in the diet (10 mg/Kg). However the concentrations of drug reached in the nervous system might be dissimilar in the two studies, considering the different neurodegenarative model used. The stroke model implicates a disruption of the blood brain barrier at the site of lesion whereas it has not been proved in chronic degenerative pathologies like motor neurone disease. Moreover, the modality of administration (two bolus per day in respect to a diluted intake by diet) was also different. Therefore, it is plausible that this kind of administration in mice does not allow to reach effective concentration in the spinal cord. Thus, the negative result obtained does not give definite clues about the effectiveness of p38MAPK inhibitors in the treatment of ALS and cannot be excluded that the activation of this enzyme plays a role in the mechanism of motor neurone degeneration in this pathology. In our laboratory we are planning further studies using a different administration that permits to obtain good bioavailability in the central nervous system.

CHAPTER 8

GENERAL DISCUSSION

Amyotrophic lateral sclerosis is the most common disease affecting the motor system. Despite the profuse effort produced in many years of clinical and basic research, this pathology still remains orphan of an effective therapy. In fact, the pathogenetic mechanisms underlying the development of ALS have not yet been clarified. The discovery of mutations in the SOD1 gene carried by a subset of patients affected by familial ALS has represented an important clue about the processes occurring in ALS and has allowed the creations of useful *in vitro* and *in vivo* models of the disease. Transgenic mice expressing some of the SOD1 mutants discovered in ALS patients display symptoms and neuropathological features that closely resemble the human disorder, representing a reliable model of study. Clinical symptoms and neuropathological characteristics showed by patients affected by familial ALS are very similar to those occurring in sporadic case of the disease. This suggests that the same final event represented by selective motor neurone death can be triggered by different events, which affect, however, the same intracellular pathways. Thus, the comprehension of the death processes that lead to the pathology in FALS mice will also be useful to the treatment of sporadic form of ALS. However, ten years after the landmark breakthrough, how mutated SOD1 can trigger the selective motor neurone death still remains unknown.

Studies carried out on post mortem human tissues and mouse models of ALS have revealed the involvement of a large number of different intracellular pathways and alteration of several biochemical systems in motor neurones and surrounding glial cells. Even so, the general picture of the disease and of its pathogenesis still results uncertain, since almost every alteration found can be

consequence or cause of the others. In this regard, a great support comes from the study of the animal models that can give information about which event can trigger or contribute to the motor neurone degeneration. In this study, I have used the $SOD1^{G93A}$ transgenic mice to investigate the role of excitotoxicity and intracellular related pathways in ALS and evaluate the time course of the changes observed during the progression of the disease, in the attempt to establish whether they can be pathogenetic or represent an epiphenomenon (Figure 8.1).

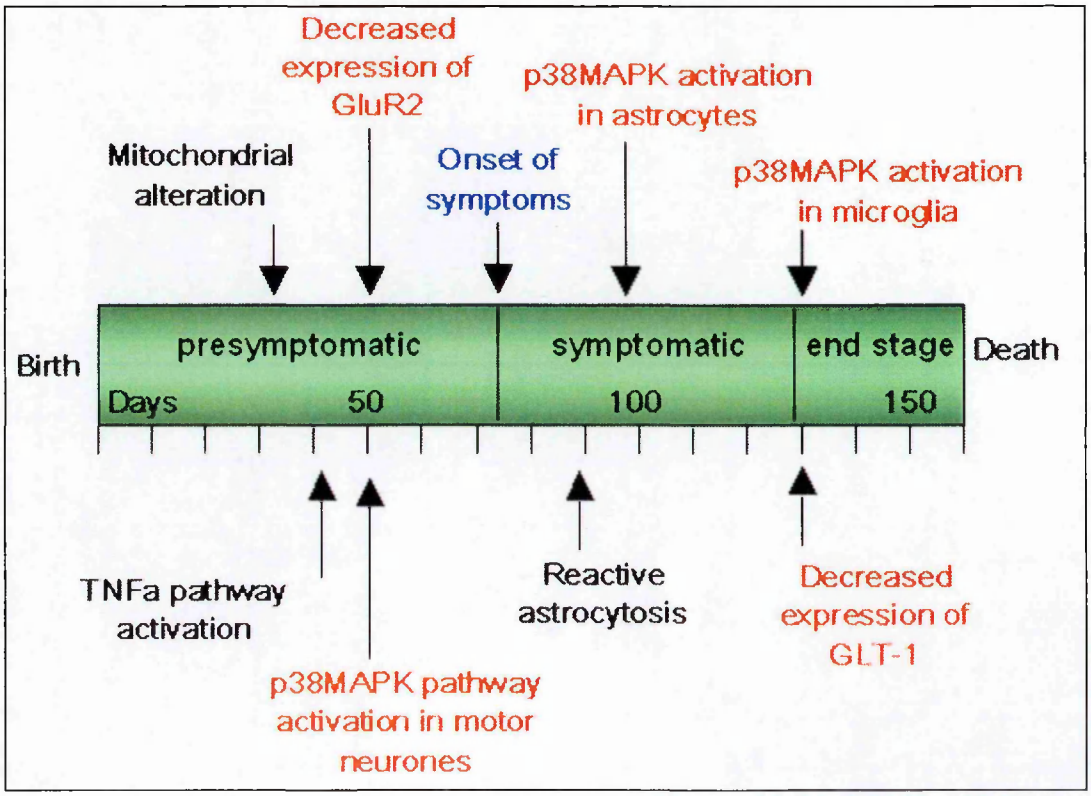

Figure 8.1: Time course of the neurophatological alterations concerning glutamatatergic system that occurs in $SOD1^{G93A}$ mice

In red, the changes observed in this study

As reported in the scheme of Figure 8.1, the first changes observed in the motor neurones of $SOD1^{G93A}$ mice, before they display motor dysfunctions, are the downregulation of AMPA receptor subunit GluR2 (see chapter 3) and the activation of p38MAPK (see chapter 7), suggesting that these alterations can represent trigger events of motor neurone degeneration in $SOD1^{G93A}$ mice. Whether these phenomena are linked or if they represent simultaneous unrelated mechanisms in the motor neurone death process needs to be demonstrated. However, several evidences indicates interplay between AMPA-mediated excitotoxicity and the activation of intracellular signalling, including p38MAPK pathway. Decreased levels of GluR2 generate AMPA receptors highly permeable to divalent ions and to calcium in particular, leading to excitotoxic processes. As demonstrate by previous reports, abnormal Ca^{2+} influx through AMPA receptors in neurones can determine activation of p38MAPK pathway, which, in turn, may contribute to activation of death processes. On the other hand, the action of phosphorylated p38MAPK has also been correlated to internalisation of GLUR2 AMPA subunit, thus suggesting that exceptional activation of p38MAPK can be causative of the decreased GluR2 subunit expression on the cell surface. Over activation of p38MAPK in motor neurones can be consequence of several stimuli. This MAP kinase is activated by the action of TNFα and it has been demonstrated that TNFα is activated in ALS mice at the presymptomatic stage. Preliminary results obtained in our laboratory show that TNFα receptors are over expressed in the motor neurones of presymptomatic $SOD1^{G93A}$ mice. Therefore, a precocious activation of TNF pathway might result in activation of p38MAPK in motor neurones, which in turn

may lead to decreased expression of GluR2 subunit in these cells. Although suggestive, this hypothesis needs to be demonstrated.

Increased number of GluR2-lacking AMPA receptors causes the excessive influx of calcium in the motor neurones. However, this kind of receptors is also highly permeable to Zn^{2+}. Zinc-mediated excitotoxicity requires much lower intracellular concentrations of zinc than calcium and cause a prominent mitochondrial dysfunction in neurones. One of the earliest neuropathological feature observed in the motor neurones of $SOD1^{G93A}$ mice is represented by mitochondrial swelling. Since motor neurones are in contact with numerous glutamatergic terminals rich in zinc, excessive influx of this ion through GluR2-lacking AMPA receptors could be a possible cause of motor neurone death in ALS. An excess of intracellular zinc is usually counteracted by the activation of a zinc transporter, ZnT-1, that favour the expulsion of the ion from the cytoplasm. Here, we have found a very low expression of ZnT-1 in spinal motor neurones of $SOD1^{G93A}$ mice as well as in non transgenic mice (see chapter 5). As this transporter plays a neuroprotective role, our results suggest that the almost absent expression of ZnT-1 can represent a risk factor that predisposes motor neurones to AMPA-mediated toxicity. However, the evaluation of free zinc accumulation in degenerating motor neurones needs to be demonstrated.

With the progression of the disease, a massive activation of glial cells, both astrocytes and microglia, occur in the ventral horn of lumbar spinal cord of $SOD1^{G93A}$ mice. Our results show that p38MAPK is remarkably activated also in these cells during the progression of the pathology (see chapter 7). Activation of p38MAPK in glial cells of ALS mice could derive from several factors such as

excitotoxic stimulation, interaction with inflammatory cytokines or undiscovered neuronal factors released by affected motor neurones. On the other hand, it has been demonstrated that activation of p38MAPK in astrocytes and microglia is implicated, in its turn, in the production of inflammatory mediators such as TNFα and IL-1β, originating a positive feedback which can result detrimental to motor neurones. Activation p38MAPK pathway has also been associated to the activation of inducible nitric-oxide synthase (iNOS) transcription in astrocytes that result in sustained release of large amounts of nitric oxide (NO). NO can generate harmful oxidant species that can affect glutamate transporters and their uptake capability. Thus, p38MAPK activation in astrocytes could indirectly lead to excitotoxicity on motor neurones.

Although the prominent astrocytosis occurring in the spinal cord of $SOD1^{G93A}$ mice during the development of the pathology, we showed that the expression of the main glial glutamate transporter GLT-1 is selectively decreased in lumbar spinal cord of $SOD1^{G93A}$ mice at the advanced state of the disease, without significant changes in its mRNA levels. Since expression of glutamate transporters is strictly regulated by neuronal factors, these results suggest that the downregulation of GLT-1 levels can represent an epiphenomenon deriving from the motor neurone loss occurring at the end stage of the pathology rather than a trigger factor involved in the motor neurone degeneration.

To better understand the mechanisms underlying the decreased expression of GLT-1 in $SOD1^{G93A}$ mice, we transfected cultured astrocytes with human $SOD1^{G93A}$ mutant and we evaluated levels and function of GLT-1 (see

chapter 6). In line with the in vivo studies, the results showed that the levels of a glutamate transporter GLT-1 were downregulated in astrocytes transfected with $SOD1^{G93A}$, without alterations of its mRNA level. This effect was selective to GLT-1, since the protein and mRNA levels of another glutamate transporter, GLAST, were not altered. Reflecting the decrease of GLT-1 protein, ^{3}H-D-aspartate uptake in transfected astrocytes was also reduced. Interestingly, both the effects were not reverted by the use of antioxidants and there was no evidence of increased reactive oxygen species in transfected astrocytes. These data suggest that the decreased GLT-1 expression can be also due to a direct action of mutated SOD1 on the protein levels of the transporter and that the reduced uptake capability is a consequence of the decreased transporter availability rather than oxidative processes. It is noteworthy that the over expression of wild type human SOD1 also produces effects similar to those induced by the mutant form, even if with less intensity. It has been reported that mice overexpressing wild type enzyme showed some neuropathological alteration in motor neurones without developing of the disease. This suggests that, although the gain of a new adverse function by the SOD1 mutants is necessary to induce clinical signs of motor neurone disease in ALS mice, the overexpression of human wild type protein can also have some harmful properties, which are not enough to produce massive motor neurone death in mouse models but that become evident when expressed in a particular cell culture model like the one used in our study.

In conclusion, we have demonstrated that altered composition of glutamate AMPA receptors in motor neurones of $SOD1^{G93A}$, associated to

activation of p38MAPK pathway, represents an early event that probably plays a pivotal role in the trigger of motor neurone death. The vulnerability of these neurones, in respect to glutamate-induced degeneration, is likely exacerbated by the low expression of zinc transporter ZnT-1. Decreased levels of glutamate transporter GLT-1 in astrocytes, caused by the expression mutant SOD1, become evident only at the late stage of the pathology, contributing to excitotoxic insult to motor neurones but probably not representing a causative factor of their death.

The hypothesis regarding the involvement of AMPA glutamate receptors in ALS pathology is reinforced by our results showing the positive effects of the treatment with a new AMPA receptor antagonist, ZK 187638, on symptoms and survival of $SOD1^{G93A}$ mice (see chapter 4). This observation is in line with previous studies reporting similar effects obtained treating different mouse models of motor neurone disease with other AMPA antagonists. However, the compound used in our study offers a better bioavailability associated to an easier administration and shows a good efficacy also when administrated after the appearance of symptoms. Moreover, it works as an allosteric modulator of the glutamate binding site, minimizing the side effects.

The hope is that the results obtained in this study may contribute to the development of future new therapeutic strategies, which can help people affected by this devastating pathology.

CHAPTER 9

REFERENCES

Abalkhail H, Mitchell J, Habgood J, Orrell R, de Belleroche J (2003) A new familial amyotrophic lateral sclerosis locus on chromosome 16q12.1-16q12.2. Am J Hum Genet 73:383-389.

Ackerley S, Grierson AJ, Banner S, Perkinton MS, Brownlees J, Byers HL, Ward M, Thornhill P, Hussain K, Waby JS, Anderton BH, Cooper JD, Dingwall C, Leigh PN, Shaw CE, Miller CC (2004) p38alpha stress-activated protein kinase phosphorylates neurofilaments and is associated with neurofilament pathology in amyotrophic lateral sclerosis. Mol Cell Neurosci 26:354-364.

Adams JL, Badger AM, Kumar S, Lee JC (2001) p38 MAP kinase: molecular target for the inhibition of pro-inflammatory cytokines. Prog Med Chem 38:1-60.

Ahmad-Annuar A, Shah P, Hafezparast M, Hummerich H, Witherden AS, Morrison KE, Shaw PJ, Kirby J, Warner TT, Crosby A, Proukakis C, Wilkinson P, Orrell RW, Bradley L, Martin JE, Fisher EM (2003) No association with common Caucasian genotypes in exons 8, 13 and 14 of the human cytoplasmic dynein heavy chain gene (DNCHC1) and familial motor neuron disorders. Amyotroph Lateral Scler Other Motor Neuron Disord 4:150-157.

Albuquerque C, Lee CJ, Jackson AC, MacDermott AB (1999) Subpopulations of GABAergic and non-GABAergic rat dorsal horn neurons express Ca2+-permeable AMPA receptors. Eur J Neurosci 11:2758-2766.

Al-Chalabi A, Andersen PM, Nilsson P, Chioza B, Andersson JL, Russ C, Shaw CE, Powell JF, Leigh PN (1999) Deletions of the heavy neurofilament subunit tail in amyotrophic lateral sclerosis. Hum Mol Genet 8:157-164.

Alexianu ME, Kozovska M, Appel SH (2001) Immune reactivity in a mouse model of familial ALS correlates with disease progression. Neurology 57:1282-1289.

Almer G, Guegan C, Teismann P, Naini A, Rosoklija G, Hays AP, Chen C, Przedborski S (2001) Increased expression of the pro-inflammatory enzyme cyclooxygenase-2 in amyotrophic lateral sclerosis. Ann Neurol 49:176-185.

Andersen PM, Nilsson P, Ala-Hurula V, Keranen ML, Tarvainen I, Haltia T, Nilsson L, Binzer M, Forsgren L, Marklund SL (1995) Amyotrophic lateral sclerosis associated with homozygosity for an Asp90Ala mutation in CuZn-superoxide dismutase. Nat Genet 10:61-66.

Anderson CM, Swanson RA (2000) Astrocyte glutamate transport: review of properties, regulation, and physiological functions. Glia 32:1-14.

Andrus PK, Fleck TJ, Gurney ME, Hall ED (1998) Protein oxidative damage in a transgenic mouse model of familial amyotrophic lateral sclerosis. J Neurochem 71:2041-2048.

Arriza JL, Eliasof S, Kavanaugh MP, Amara SG (1997) Excitatory amino acid transporter 5, a retinal glutamate transporter coupled to a chloride conductance. Proc Natl Acad Sci U S A 94:4155-4160.

Arundine M, Tymianski M (2003) Molecular mechanisms of calcium-dependent neurodegeneration in excitotoxicity. Cell Calcium 34:325-337.

Assaf SY, Chung SH (1984) Release of endogenous Zn2+ from brain tissue during activity. Nature 308:734-736.

Azari MF, Galle A, Lopes EC, Kurek J, Cheema SS (2001) Leukemia inhibitory factor by systemic administration rescues spinal motor neurons in the SOD1 G93A murine model of familial amyotrophic lateral sclerosis. Brain Res 922:144-147.

Barone FC, Irving EA, Ray AM, Lee JC, Kassis S, Kumar S, Badger AM, Legos JJ, Erhardt JA, Ohlstein EH, Hunter AJ, Harrison DC, Philpott K, Smith BR, Adams JL, Parsons AA (2001a) Inhibition of p38 mitogen-activated protein kinase provides neuroprotection in cerebral focal ischemia. Med Res Rev 21:129-145.

Barone FC, Irving EA, Ray AM, Lee JC, Kassis S, Kumar S, Badger AM, White RF, McVey MJ, Legos JJ, Erhardt JA, Nelson AH, Ohlstein EH, Hunter AJ, Ward K, Smith BR, Adams JL, Parsons AA (2001b) SB 239063, a second-generation p38 mitogen-activated protein kinase inhibitor, reduces brain injury and neurological deficits in cerebral focal ischemia. J Pharmacol Exp Ther 296:312-321.

Bar-Peled O, O'Brien RJ, Morrison JH, Rothstein JD (1999) Cultured motor neurons possess calcium-permeable AMPA/kainate receptors. Neuroreport 10:855-859.

Beal MF, Ferrante RJ, Browne SE, Matthews RT, Kowall NW, Brown RH, Jr. (1997) Increased 3-nitrotyrosine in both sporadic and familial amyotrophic lateral sclerosis. Ann Neurol 42:644-654.

Beckman JS, Carson M, Smith CD, Koppenol WH (1993) ALS, SOD and peroxynitrite. Nature 364:584.

Bendotti C, Carri MT (2004) Lessons from models of SOD1-linked familial ALS. Trends Mol Med 10:393-400.

Bendotti C, Guglielmetti F, Tortarolo M, Samanin R, Hirst WD (2000) Differential expression of S100beta and glial fibrillary acidic protein in the hippocampus after kainic acid-induced lesions and mossy fiber sprouting in adult rat. Exp Neurol 161:317-329.

Bendotti C, Hohmann C, Forloni G, Reeves R, Coyle JT, Oster-Granite ML (1990) Developmental expression of somatostatin in mouse brain. II. In situ hybridization. Brain Res Dev Brain Res 53:26-39.

Bendotti C, Atzori C, Piva R, Tortarolo M, Strong MJ, DeBiasi S, Migheli A (2004) Activated p38MAPK is a novel component of the intracellular inclusions found in human amyotrophic lateral sclerosis and mutant SOD1 transgenic mice. J Neuropathol Exp Neurol 63:113-119.

Bendotti C, Calvaresi N, Chiveri L, Prelle A, Moggio M, Braga M, Silani V, De Biasi S (2001a) Early vacuolization and mitochondrial damage in motor neurons of FALS mice are not associated with apoptosis or with changes in cytochrome oxidase histochemical reactivity. J Neurol Sci 191:25-33.

Bendotti C, Tortarolo M, Suchak SK, Calvaresi N, Carvelli L, Bastone A, Rizzi M, Rattray M, Mennini T (2001b) Transgenic SOD1 G93A mice develop reduced GLT-1 in spinal cord without alterations in cerebrospinal fluid glutamate levels. J Neurochem 79:737-746.

Bleakman D, Ballyk BA, Schoepp DD, Palmer AJ, Bath CP, Sharpe EF, Woolley ML, Bufton HR, Kamboj RK, Tarnawa I, Lodge D (1996) Activity of 2,3-benzodiazepines at native rat and recombinant human glutamate receptors in vitro: stereospecificity and selectivity profiles. Neuropharmacology 35:1689-1702.

Borasio GD, Robberecht W, Leigh PN, Emile J, Guiloff RJ, Jerusalem F, Silani V, Vos PE, Wokke JH, Dobbins T (1998) A placebo-controlled trial of insulin-like growth factor-I in amyotrophic lateral sclerosis. European ALS/IGF-I Study Group. Neurology 51:583-586.

Borthwick GM, Johnson MA, Ince PG, Shaw PJ, Turnbull DM (1999) Mitochondrial enzyme activity in amyotrophic lateral sclerosis: implications for the role of mitochondria in neuronal cell death. Ann Neurol 46:787-790.

Bridges RJ, Kavanaugh MP, Chamberlin AR (1999) A pharmacological review of competitive inhibitors and substrates of high-affinity, sodium-dependent glutamate transport in the central nervous system. Curr Pharm Des 5:363-379.

Bristol LA, Rothstein JD (1996) Glutamate transporter gene expression in amyotrophic lateral sclerosis motor cortex. Ann Neurol 39:676-679.

Bronson RT, Lake BD, Cook S, Taylor S, Davisson MT (1993) Motor neuron degeneration of mice is a model of neuronal ceroid lipofuscinosis (Batten's disease). Ann Neurol 33:381-385.

Browne SE, Bowling AC, Baik MJ, Gurney M, Brown RH, Jr., Beal MF (1998) Metabolic dysfunction in familial, but not sporadic, amyotrophic lateral sclerosis. J Neurochem 71:281-287.

Bruijn LI, Beal MF, Becher MW, Schulz JB, Wong PC, Price DL, Cleveland DW (1997a) Elevated free nitrotyrosine levels, but not protein-bound nitrotyrosine or hydroxyl radicals, throughout amyotrophic lateral sclerosis (ALS)-like disease implicate tyrosine nitration as an aberrant in vivo property of one familial ALS-linked superoxide dismutase 1 mutant. Proc Natl Acad Sci U S A 94:7606-7611.

Bruijn LI, Houseweart MK, Kato S, Anderson KL, Anderson SD, Ohama E, Reaume AG, Scott RW, Cleveland DW (1998) Aggregation and motor neuron toxicity of an ALS-linked SOD1 mutant independent from wild-type SOD1. Science 281:1851-1854.

Bruijn LI, Becher MW, Lee MK, Anderson KL, Jenkins NA, Copeland NG, Sisodia SS, Rothstein JD, Borchelt DR, Price DL, Cleveland DW (1997b) ALS-linked SOD1 mutant G85R mediates damage to astrocytes and promotes rapidly progressive disease with SOD1-containing inclusions. Neuron 18:327-338.

Brunialti AL, Poirier C, Schmalbruch H, Guenet JL (1995) The mouse mutation progressive motor neuronopathy (pmn) maps to chromosome 13. Genomics 29:131-135.

Camu W, Billiard M, Baldy-Moulinier M (1993) Fasting plasma and CSF amino acid levels in amyotrophic lateral sclerosis: a subtype analysis. Acta Neurol Scand 88:51-55.

Canton T, Pratt J, Stutzmann JM, Imperato A, Boireau A (1998) Glutamate uptake is decreased tardively in the spinal cord of FALS mice. Neuroreport 9:775-778.

Canton T, Bohme GA, Boireau A, Bordier F, Mignani S, Jimonet P, Jahn G, Alavijeh M, Stygall J, Roberts S, Brealey C, Vuilhorgne M, Debono MW, Le Guern S, Laville M, Briet D, Roux M, Stutzmann JM, Pratt J (2001) RPR 119990, a novel alpha-amino-3-hydroxy-5-methyl-4-isoxazolepropionic acid antagonist: synthesis, pharmacological properties, and activity in an animal model of amyotrophic lateral sclerosis. J Pharmacol Exp Ther 299:314-322.

Carriedo SG, Yin HZ, Weiss JH (1996) Motor neurons are selectively vulnerable to AMPA/kainate receptor-mediated injury in vitro. J Neurosci 16:4069-4079.

Carriedo SG, Yin HZ, Lamberta R, Weiss JH (1995) In vitro kainate injury to large, SMI-32(+) spinal neurons is Ca2+ dependent. Neuroreport 6:945-948.

Carriedo SG, Sensi SL, Yin HZ, Weiss JH (2000) AMPA exposures induce mitochondrial Ca(2+) overload and ROS generation in spinal motor neurons in vitro. J Neurosci 20:240-250.

Carroll RC, Beattie EC, Xia H, Luscher C, Altschuler Y, Nicoll RA, Malenka RC, von Zastrow M (1999) Dynamin-dependent endocytosis of ionotropic glutamate receptors. Proc Natl Acad Sci U S A 96:14112-14117.

Chance PF, Rabin BA, Ryan SG, Ding Y, Scavina M, Crain B, Griffin JW, Cornblath DR (1998) Linkage of the gene for an autosomal dominant

form of juvenile amyotrophic lateral sclerosis to chromosome 9q34. Am J Hum Genet 62:633-640.

Chen M, Ona VO, Li M, Ferrante RJ, Fink KB, Zhu S, Bian J, Guo L, Farrell LA, Hersch SM, Hobbs W, Vonsattel JP, Cha JH, Friedlander RM (2000) Minocycline inhibits caspase-1 and caspase-3 expression and delays mortality in a transgenic mouse model of Huntington disease. Nat Med 6:797-801.

Chen RW, Qin ZH, Ren M, Kanai H, Chalecka-Franaszek E, Leeds P, Chuang DM (2003) Regulation of c-Jun N-terminal kinase, p38 kinase and AP-1 DNA binding in cultured brain neurons: roles in glutamate excitotoxicity and lithium neuroprotection. J Neurochem 84:566-575.

Chen YZ, Bennett CL, Huynh HM, Blair IP, Puls I, Irobi J, Dierick I, Abel A, Kennerson ML, Rabin BA, Nicholson GA, Auer-Grumbach M, Wagner K, De Jonghe P, Griffin JW, Fischbeck KH, Timmerman V, Cornblath DR, Chance PF (2004) DNA/RNA helicase gene mutations in a form of juvenile amyotrophic lateral sclerosis (ALS4). Am J Hum Genet 74:1128-1135.

Cid C, Alvarez-Cermeno JC, Regidor I, Salinas M, Alcazar A (2003) Low concentrations of glutamate induce apoptosis in cultured neurons: implications for amyotrophic lateral sclerosis. J Neurol Sci 206:91-95.

Cleveland DW, Rothstein JD (2001) From Charcot to Lou Gehrig: deciphering selective motor neuron death in ALS. Nat Rev Neurosci 2:806-819.

Cook SA, Johnson KR, Bronson RT, Davisson MT (1995) Neuromuscular degeneration (nmd): a mutation on mouse chromosome 19 that causes motor neuron degeneration. Mamm Genome 6:187-191.

Corbo M, Hays AP (1992) Peripherin and neurofilament protein coexist in spinal spheroids of motor neuron disease. J Neuropathol Exp Neurol 51:531-537.

Corcia P, Mayeux-Portas V, Khoris J, de Toffol B, Autret A, Muh JP, Camu W, Andres C (2002) Abnormal SMN1 gene copy number is a susceptibility factor for amyotrophic lateral sclerosis. Ann Neurol 51:243-246.

Cote F, Collard JF, Julien JP (1993) Progressive neuronopathy in transgenic mice expressing the human neurofilament heavy gene: a mouse model of amyotrophic lateral sclerosis. Cell 73:35-46.

Couillard-Despres S, Meier J, Julien JP (2000) Extra axonal neurofilaments do not exacerbate disease caused by mutant Cu,Zn superoxide dismutase. Neurobiol Dis 7:462-470.

Couillard-Despres S, Zhu Q, Wong PC, Price DL, Cleveland DW, Julien JP (1998) Protective effect of neurofilament heavy gene overexpression in motor neuron disease induced by mutant superoxide dismutase. Proc Natl Acad Sci U S A 95:9626-9630.

Couratier P, Hugon J, Sindou P, Vallat JM, Dumas M (1993) Cell culture evidence for neuronal degeneration in amyotrophic lateral sclerosis being linked to glutamate AMPA/kainate receptors. Lancet 341:265-268.

Couratier P, Sindou P, Esclaire F, Louvel E, Hugon J (1994) Neuroprotective effects of riluzole in ALS CSF toxicity. Neuroreport 5:1012-1014.

Cox GA, Mahaffey CL, Frankel WN (1998) Identification of the mouse neuromuscular degeneration gene and mapping of a second site suppressor allele. Neuron 21:1327-1337.

Crossthwaite AJ, Hasan S, Williams RJ (2002) Hydrogen peroxide-mediated phosphorylation of ERK1/2, Akt/PKB and JNK in cortical neurones: dependence on Ca(2+) and PI3-kinase. J Neurochem 80:24-35.

Da Silva J, Pierrat B, Mary JL, Lesslauer W (1997) Blockade of p38 mitogen-activated protein kinase pathway inhibits inducible nitric-oxide synthase expression in mouse astrocytes. J Biol Chem 272:28373-28380.

Dal Canto MC, Gurney ME (1995) Neuropathological changes in two lines of mice carrying a transgene for mutant human Cu,Zn SOD, and in mice overexpressing wild type human SOD: a model of familial amyotrophic lateral sclerosis (FALS). Brain Res 676:25-40.

Danbolt NC (2001) Glutamate uptake. Prog Neurobiol 65:1-105.

Das S, Sasaki YF, Rothe T, Premkumar LS, Takasu M, Crandall JE, Dikkes P, Conner DA, Rayudu PV, Cheung W, Chen HS, Lipton SA, Nakanishi N (1998) Increased NMDA current and spine density in mice lacking the NMDA receptor subunit NR3A. Nature 393:377-381.

Desnuelle C, Dib M, Garrel C, Favier A (2001) A double-blind, placebo-controlled randomized clinical trial of alpha-tocopherol (vitamin E) in the treatment of amyotrophic lateral sclerosis. ALS riluzole-tocopherol Study Group. Amyotroph Lateral Scler Other Motor Neuron Disord 2:9-18.

Dingledine R, Borges K, Bowie D, Traynelis SF (1999) The glutamate receptor ion channels. Pharmacol Rev 51:7-61.

Doble A (1996) The pharmacology and mechanism of action of riluzole. Neurology 47:S233-241.

Elliott JL (2001) Cytokine upregulation in a murine model of familial amyotrophic lateral sclerosis. Brain Res Mol Brain Res 95:172-178.

Estevez AG, Crow JP, Sampson JB, Reiter C, Zhuang Y, Richardson GJ, Tarpey MM, Barbeito L, Beckman JS (1999) Induction of nitric oxide-dependent apoptosis in motor neurons by zinc-deficient superoxide dismutase. Science 286:2498-2500.

Ferrante RJ, Shinobu LA, Schulz JB, Matthews RT, Thomas CE, Kowall NW, Gurney ME, Beal MF (1997a) Increased 3-nitrotyrosine and oxidative damage in mice with a human copper/zinc superoxide dismutase mutation. Ann Neurol 42:326-334.

Ferrante RJ, Browne SE, Shinobu LA, Bowling AC, Baik MJ, MacGarvey U, Kowall NW, Brown RH, Jr., Beal MF (1997b) Evidence of increased oxidative damage in both sporadic and familial amyotrophic lateral sclerosis. J Neurochem 69:2064-2074.

Ferrer I, Blanco R, Carmona M (2001) Differential expression of active, phosphorylation-dependent MAP kinases, MAPK/ERK, SAPK/JNK and p38, and specific transcription factor substrates following quinolinic acid excitotoxicity in the rat. Brain Res Mol Brain Res 94:48-58.

Fray AE, Ince PG, Banner SJ, Milton ID, Usher PA, Cookson MR, Shaw PJ (1998) The expression of the glial glutamate transporter protein EAAT2 in motor neuron disease: an immunohistochemical study. Eur J Neurosci 10:2481-2489.

Frederickson CJ (1989) Neurobiology of zinc and zinc-containing neurons. Int Rev Neurobiol 31:145-238.

Frederickson CJ, Hernandez MD, McGinty JF (1989) Translocation of zinc may contribute to seizure-induced death of neurons. Brain Res 480:317-321.

Friedman LK, Pellegrini-Giampietro DE, Sperber EF, Bennett MV, Moshe SL, Zukin RS (1994) Kainate-induced status epilepticus alters glutamate and GABAA receptor gene expression in adult rat hippocampus: an in situ hybridization study. J Neurosci 14:2697-2707.

Furuyama T, Kiyama H, Sato K, Park HT, Maeno H, Takagi H, Tohyama M (1993) Region-specific expression of subunits of ionotropic glutamate receptors (AMPA-type, KA-type and NMDA receptors) in the rat spinal cord with special reference to nociception. Brain Res Mol Brain Res 18:141-151.

Gegelashvili G, Schousboe A (1997) High affinity glutamate transporters: regulation of expression and activity. Mol Pharmacol 52:6-15.

Gegelashvili G, Danbolt NC, Schousboe A (1997) Neuronal soluble factors differentially regulate the expression of the GLT1 and GLAST glutamate transporters in cultured astroglia. J Neurochem 69:2612-2615.

Giardina SF, Beart PM (2002) Kainate receptor-mediated apoptosis in primary cultures of cerebellar granule cells is attenuated by mitogen-activated protein and cyclin-dependent kinase inhibitors. Br J Pharmacol 135:1733-1742.

Gong YH, Elliott JL (2000) Metallothionein expression is altered in a transgenic murine model of familial amyotrophic lateral sclerosis. Exp Neurol 162:27-36.

Gong YH, Parsadanian AS, Andreeva A, Snider WD, Elliott JL (2000) Restricted expression of G86R Cu/Zn superoxide dismutase in astrocytes results in astrocytosis but does not cause motoneuron degeneration. J Neurosci 20:660-665.

Greig A, Donevan SD, Mujtaba TJ, Parks TN, Rao MS (2000) Characterization of the AMPA-activated receptors present on motoneurons. J Neurochem 74:179-191.

Groeneveld GJ, de Leeuw van Weenen J, van Muiswinkel FL, Veldman H, Veldink JH, Wokke JH, Bar PR, van den Berg LH (2003) Zinc amplifies mSOD1-mediated toxicity in a transgenic mouse model of amyotrophic lateral sclerosis. Neurosci Lett 352:175-178.

Grossman SD, Wolfe BB, Yasuda RP, Wrathall JR (1999) Alterations in AMPA receptor subunit expression after experimental spinal cord contusion injury. J Neurosci 19:5711-5720.

Gurney ME, Cutting FB, Zhai P, Doble A, Taylor CP, Andrus PK, Hall ED (1996) Benefit of vitamin E, riluzole, and gabapentin in a transgenic model of familial amyotrophic lateral sclerosis. Ann Neurol 39:147-157.

Gurney ME, Pu H, Chiu AY, Dal Canto MC, Polchow CY, Alexander DD, Caliendo J, Hentati A, Kwon YW, Deng HX, et al. (1994) Motor neuron degeneration in mice that express a human Cu,Zn superoxide dismutase mutation. Science 264:1772-1775.

Hall ED, Oostveen JA, Gurney ME (1998) Relationship of microglial and astrocytic activation to disease onset and progression in a transgenic model of familial ALS. Glia 23:249-256.

Hammer RP, Jr., Tomiyasu U, Scheibel AB (1979) Degeneration of the human Betz cell due to amyotrophic lateral sclerosis. Exp Neurol 63:336-346.

Haugeto O, Ullensvang K, Levy LM, Chaudhry FA, Honore T, Nielsen M, Lehre KP, Danbolt NC (1996) Brain glutamate transporter proteins form homomultimers. J Biol Chem 271:27715-27722.

Heath PR, Shaw PJ (2002) Update on the glutamatergic neurotransmitter system and the role of excitotoxicity in amyotrophic lateral sclerosis. Muscle Nerve 26:438-458.

Heath PR, Tomkins J, Ince PG, Shaw PJ (2002) Quantitative assessment of AMPA receptor mRNA in human spinal motor neurons isolated by laser capture microdissection. Neuroreport 13:1753-1757.

Hensley K, Fedynyshyn J, Ferrell S, Floyd RA, Gordon B, Grammas P, Hamdheydari L, Mhatre M, Mou S, Pye QN, Stewart C, West M, West S, Williamson KS (2003) Message and protein-level elevation of tumor necrosis factor alpha (TNF alpha) and TNF alpha-modulating cytokines in spinal cords of the G93A-SOD1 mouse model for amyotrophic lateral sclerosis. Neurobiol Dis 14:74-80.

Hentati A, Ouahchi K, Pericak-Vance MA, Nijhawan D, Ahmad A, Yang Y, Rimmler J, Hung W, Schlotter B, Ahmed A, Ben Hamida M, Hentati F, Siddique T (1998) Linkage of a commoner form of recessive amyotrophic

lateral sclerosis to chromosome 15q15-q22 markers. Neurogenetics 2:55-60.

Higgins CM, Jung C, Ding H, Xu Z (2002) Mutant Cu, Zn superoxide dismutase that causes motoneuron degeneration is present in mitochondria in the CNS. J Neurosci 22:RC215.

Hirano A, Donnenfeld H, Sasaki S, Nakano I (1984a) Fine structural observations of neurofilamentous changes in amyotrophic lateral sclerosis. J Neuropathol Exp Neurol 43:461-470.

Hirano A, Nakano I, Kurland LT, Mulder DW, Holley PW, Saccomanno G (1984b) Fine structural study of neurofibrillary changes in a family with amyotrophic lateral sclerosis. J Neuropathol Exp Neurol 43:471-480.

Hishikawa N, Niwa J, Doyu M, Ito T, Ishigaki S, Hashizume Y, Sobue G (2003) Dorfin localizes to the ubiquitylated inclusions in Parkinson's disease, dementia with Lewy bodies, multiple system atrophy, and amyotrophic lateral sclerosis. Am J Pathol 163:609-619.

Horstmann S, Kahle PJ, Borasio GD (1998) Inhibitors of p38 mitogen-activated protein kinase promote neuronal survival in vitro. J Neurosci Res 52:483-490.

Howland DS, Liu J, She Y, Goad B, Maragakis NJ, Kim B, Erickson J, Kulik J, DeVito L, Psaltis G, DeGennaro LJ, Cleveland DW, Rothstein JD (2002) Focal loss of the glutamate transporter EAAT2 in a transgenic rat model of SOD1 mutant-mediated amyotrophic lateral sclerosis (ALS). Proc Natl Acad Sci U S A 99:1604-1609.

Hoyaux D, Alao J, Fuchs J, Kiss R, Keller B, Heizmann CW, Pochet R, Frermann D (2000) S100A6, a calcium- and zinc-binding protein, is overexpressed in SOD1 mutant mice, a model for amyotrophic lateral sclerosis. Biochim Biophys Acta 1498:264-272.

Hu JH, Chernoff K, Pelech S, Krieger C (2003) Protein kinase and protein phosphatase expression in the central nervous system of G93A mSOD over-expressing mice. J Neurochem 85:422-431.

Huang CC, You JL, Wu MY, Hsu KS (2004) Rap1-induced p38 mitogen-activated protein kinase activation facilitates AMPA receptor trafficking via the GDI.Rab5 complex. Potential role in (S)-3,5-dihydroxyphenylglycene-induced long term depression. J Biol Chem 279:12286-12292.

Huang L, Gitschier J (1997) A novel gene involved in zinc transport is deficient in the lethal milk mouse. Nat Genet 17:292-297.

Ikonomidou C, Qin Qin Y, Labruyere J, Olney JW (1996) Motor neuron degeneration induced by excitotoxin agonists has features in common with those seen in the SOD-1 transgenic mouse model of amyotrophic lateral sclerosis. J Neuropathol Exp Neurol 55:211-224.

Ince P, Stout N, Shaw P, Slade J, Hunziker W, Heizmann CW, Baimbridge KG (1993) Parvalbumin and calbindin D-28k in the human motor system and in motor neuron disease. Neuropathol Appl Neurobiol 19:291-299.

Iwasaki Y, Ikeda K, Shiojima T, Tagaya M, Kinoshita M (1995) Amyotrophic lateral sclerosis cerebrospinal fluid is not toxic to cultured spinal motor neurons. Neurol Res 17:393-395.

Jaarsma D, Haasdijk ED, Grashorn JA, Hawkins R, van Duijn W, Verspaget HW, London J, Holstege JC (2000) Human Cu/Zn superoxide dismutase (SOD1) overexpression in mice causes mitochondrial vacuolization, axonal degeneration, and premature motoneuron death and accelerates motoneuron disease in mice expressing a familial amyotrophic lateral sclerosis mutant SOD1. Neurobiol Dis 7:623-643.

Jackson M, Morrison KE, Al-Chalabi A, Bakker M, Leigh PN (1996) Analysis of chromosome 5q13 genes in amyotrophic lateral sclerosis: homozygous NAIP deletion in a sporadic case. Ann Neurol 39:796-800.

Jo SM, Danscher G, Daa Schroder H, Won MH, Cole TB (2000) Zinc-enriched (ZEN) terminals in mouse spinal cord: immunohistochemistry and autometallography. Brain Res 870:163-169.

Johnston JA, Dalton MJ, Gurney ME, Kopito RR (2000) Formation of high molecular weight complexes of mutant Cu, Zn-superoxide dismutase in a mouse model for familial amyotrophic lateral sclerosis. Proc Natl Acad Sci U S A 97:12571-12576.

Kabashi E, Agar JN, Taylor DM, Minotti S, Durham HD (2004) Focal dysfunction of the proteasome: a pathogenic factor in a mouse model of amyotrophic lateral sclerosis. J Neurochem 89:1325-1335.

Kalra S, Cashman NR, Genge A, Arnold DL (1998) Recovery of N-acetylaspartate in corticomotor neurons of patients with ALS after riluzole therapy. Neuroreport 9:1757-1761.

Kanai Y, Hediger MA (1992) Primary structure and functional characterization of a high-affinity glutamate transporter. Nature 360:467-471.

Kanki R, Nakamizo T, Yamashita H, Kihara T, Sawada H, Uemura K, Kawamata J, Shibasaki H, Akaike A, Shimohama S (2004) Effects of mitochondrial dysfunction on glutamate receptor-mediated neurotoxicity in cultured rat spinal motor neurons. Brain Res 1015:73-81.

Kaupmann K, Simon-Chazottes D, Guenet JL, Jockusch H (1992) Wobbler, a mutation affecting motoneuron survival and gonadal functions in the mouse, maps to proximal chromosome 11. Genomics 13:39-43.

Kawahara Y, Ito K, Sun H, Aizawa H, Kanazawa I, Kwak S (2004) Glutamate receptors: RNA editing and death of motor neurons. Nature 427:801.

Kawahara Y, Kwak S, Sun H, Ito K, Hashida H, Aizawa H, Jeong SY, Kanazawa I (2003) Human spinal motoneurons express low relative abundance of GluR2 mRNA: an implication for excitotoxicity in ALS. J Neurochem 85:680-689.

Kawamata T, Akiyama H, Yamada T, McGeer PL (1992) Immunologic reactions in amyotrophic lateral sclerosis brain and spinal cord tissue. Am J Pathol 140:691-707.

Kawasaki H, Morooka T, Shimohama S, Kimura J, Hirano T, Gotoh Y, Nishida E (1997) Activation and involvement of p38 mitogen-activated protein kinase in glutamate-induced apoptosis in rat cerebellar granule cells. J Biol Chem 272:18518-18521.

Kiernan JA, Hudson AJ (1991) Changes in sizes of cortical and lower motor neurons in amyotrophic lateral sclerosis. Brain 114 (Pt 2):843-853.

Kim AH, Sheline CT, Tian M, Higashi T, McMahon RJ, Cousins RJ, Choi DW (2000) L-type Ca(2+) channel-mediated Zn(2+) toxicity and modulation by ZnT-1 in PC12 cells. Brain Res 886:99-107.

Klivenyi P, Ferrante RJ, Matthews RT, Bogdanov MB, Klein AM, Andreassen OA, Mueller G, Wermer M, Kaddurah-Daouk R, Beal MF (1999) Neuroprotective effects of creatine in a transgenic animal model of amyotrophic lateral sclerosis. Nat Med 5:347-350.

Koh JY, Suh SW, Gwag BJ, He YY, Hsu CY, Choi DW (1996) The role of zinc in selective neuronal death after transient global cerebral ischemia. Science 272:1013-1016.

Kong J, Xu Z (2000) Overexpression of neurofilament subunit NF-L and NF-H extends survival of a mouse model for amyotrophic lateral sclerosis. Neurosci Lett 281:72-74.

Kriz J, Nguyen MD, Julien JP (2002) Minocycline slows disease progression in a mouse model of amyotrophic lateral sclerosis. Neurobiol Dis 10:268-278.

Kruman, II, Pedersen WA, Springer JE, Mattson MP (1999) ALS-linked Cu/Zn-SOD mutation increases vulnerability of motor neurons to excitotoxicity by a mechanism involving increased oxidative stress and perturbed calcium homeostasis. Exp Neurol 160:28-39.

Kummer JL, Rao PK, Heidenreich KA (1997) Apoptosis induced by withdrawal of trophic factors is mediated by p38 mitogen-activated protein kinase. J Biol Chem 272:20490-20494.

Laake JH, Slyngstad TA, Haug FM, Ottersen OP (1995) Glutamine from glial cells is essential for the maintenance of the nerve terminal pool of glutamate: immunogold evidence from hippocampal slice cultures. J Neurochem 65:871-881.

Lai EC, Felice KJ, Festoff BW, Gawel MJ, Gelinas DF, Kratz R, Murphy MF, Natter HM, Norris FH, Rudnicki SA (1997) Effect of recombinant human insulin-like growth factor-I on progression of ALS. A placebo-controlled study. The North America ALS/IGF-I Study Group. Neurology 49:1621-1630.

Langmade SJ, Ravindra R, Daniels PJ, Andrews GK (2000) The transcription factor MTF-1 mediates metal regulation of the mouse ZnT1 gene. J Biol Chem 275:34803-34809.

Laslo P, Lipski J, Nicholson LF, Miles GB, Funk GD (2001) GluR2 AMPA receptor subunit expression in motoneurons at low and high risk for degeneration in amyotrophic lateral sclerosis. Exp Neurol 169:461-471.

Launey T, Ivanov A, Ferrand N, Gueritaud JP (1998) Developing rat brainstem motoneurones in organotypic culture express calcium permeable AMPA-gated receptors. Brain Res 781:148-158.

Lee SH, Simonetta A, Sheng M (2004) Subunit rules governing the sorting of internalized AMPA receptors in hippocampal neurons. Neuron 43:221-236.

Lee YB, Schrader JW, Kim SU (2000) p38 map kinase regulates TNF-alpha production in human astrocytes and microglia by multiple mechanisms. Cytokine 12:874-880.

Legos JJ, Erhardt JA, White RF, Lenhard SC, Chandra S, Parsons AA, Tuma RF, Barone FC (2001) SB 239063, a novel p38 inhibitor, attenuates early neuronal injury following ischemia. Brain Res 892:70-77.

Legos JJ, McLaughlin B, Skaper SD, Strijbos PJ, Parsons AA, Aizenman E, Herin GA, Barone FC, Erhardt JA (2002) The selective p38 inhibitor SB-239063 protects primary neurons from mild to moderate excitotoxic injury. Eur J Pharmacol 447:37-42.

Leigh PN, Dodson A, Swash M, Brion JP, Anderton BH (1989) Cytoskeletal abnormalities in motor neuron disease. An immunocytochemical study. Brain 112 (Pt 2):521-535.

Leigh PN, Anderton BH, Dodson A, Gallo JM, Swash M, Power DM (1988) Ubiquitin deposits in anterior horn cells in motor neurone disease. Neurosci Lett 93:197-203.

Lin CL, Bristol LA, Jin L, Dykes-Hoberg M, Crawford T, Clawson L, Rothstein JD (1998) Aberrant RNA processing in a neurodegenerative disease: the cause for absent EAAT2, a glutamate transporter, in amyotrophic lateral sclerosis. Neuron 20:589-602.

Lin S, Zhang Y, Dodel R, Farlow MR, Paul SM, Du Y (2001) Minocycline blocks nitric oxide-induced neurotoxicity by inhibition p38 MAP kinase in rat cerebellar granule neurons. Neurosci Lett 315:61-64.

Lino MM, Schneider C, Caroni P (2002) Accumulation of SOD1 mutants in postnatal motoneurons does not cause motoneuron pathology or motoneuron disease. J Neurosci 22:4825-4832.

Lissin DV, Carroll RC, Nicoll RA, Malenka RC, von Zastrow M (1999) Rapid, activation-induced redistribution of ionotropic glutamate receptors in cultured hippocampal neurons. J Neurosci 19:1263-1272.

Liu D, Wen J, Liu J, Li L (1999) The roles of free radicals in amyotrophic lateral sclerosis: reactive oxygen species and elevated oxidation of protein, DNA, and membrane phospholipids. Faseb J 13:2318-2328.

Liu J, Lillo C, Jonsson PA, Velde CV, Ward CM, Miller TM, Subramaniam JR, Rothstein JD, Marklund S, Andersen PM, Brannstrom T, Gredal O, Wong PC, Williams DS, Cleveland DW (2004) Toxicity of Familial ALS-Linked SOD1 Mutants from Selective Recruitment to Spinal Mitochondria. Neuron 43:5-17.

Liu R, Althaus JS, Ellerbrock BR, Becker DA, Gurney ME (1998) Enhanced oxygen radical production in a transgenic mouse model of familial amyotrophic lateral sclerosis. Ann Neurol 44:763-770.

Liu R, Li B, Flanagan SW, Oberley LW, Gozal D, Qiu M (2002) Increased mitochondrial antioxidative activity or decreased oxygen free radical propagation prevent mutant SOD1-mediated motor neuron cell death and increase amyotrophic lateral sclerosis-like transgenic mouse survival. J Neurochem 80:488-500.

Lo W, Rodgers W, Hughes T (1998) Making genes green: creating green fluorescent protein (GFP) fusions with blunt-end PCR products. Biotechniques 25:94-96, 98.

Ludolph AC, Spencer PS (1996) Toxic models of upper motor neuron disease. J Neurol Sci 139 Suppl:53-59.

Ludolph AC, Hugon J, Dwivedi MP, Schaumburg HH, Spencer PS (1987) Studies on the aetiology and pathogenesis of motor neuron diseases. 1. Lathyrism: clinical findings in established cases. Brain 110 (Pt 1):149-165.

Luscher C, Nicoll RA, Malenka RC, Muller D (2000) Synaptic plasticity and dynamic modulation of the postsynaptic membrane. Nat Neurosci 3:545-550.

Masseroli M, Bollea A, Bendotti C, Forloni G (1993) In situ hybridization histochemistry quantification: automatic count on single cell in digital image. J Neurosci Methods 47:93-103.

Matsuura T, Ogata A, Demura T, Moriwaka F, Tashiro K, Koyanagi T, Nagashima K (1993) Identification of androgen receptor in the rat spinal motoneurons. Immunohistochemical and immunoblotting analyses with monoclonal antibody. Neurosci Lett 158:5-8.

Mattiazzi M, D'Aurelio M, Gajewski CD, Martushova K, Kiaei M, Beal MF, Manfredi G (2002) Mutated human SOD1 causes dysfunction of oxidative phosphorylation in mitochondria of transgenic mice. J Biol Chem 277:29626-29633.

McGeer EG, McGeer PL (2003) Inflammatory processes in Alzheimer's disease. Prog Neuropsychopharmacol Biol Psychiatry 27:741-749.

McGeer PL, McGeer EG (2004) Inflammation and neurodegeneration in Parkinson's disease. Parkinsonism Relat Disord 10 Suppl 1:S3-7.

McMahon RJ, Cousins RJ (1998a) Mammalian zinc transporters. J Nutr 128:667-670.

McMahon RJ, Cousins RJ (1998b) Regulation of the zinc transporter ZnT-1 by dietary zinc. Proc Natl Acad Sci U S A 95:4841-4846.

Meguro H, Mori H, Araki K, Kushiya E, Kutsuwada T, Yamazaki M, Kumanishi T, Arakawa M, Sakimura K, Mishina M (1992) Functional characterization of a heteromeric NMDA receptor channel expressed from cloned cDNAs. Nature 357:70-74.

Mennini T, Bigini P, Ravizza T, Vezzani A, Calvaresi N, Tortarolo M, Bendotti C (2002) Expression of glutamate receptor subtypes in the spinal cord of control and mnd mice, a model of motor neuron disorder. J Neurosci Res 70:553-560.

Mennini T, Cagnotto A, Carvelli L, Comoletti D, Manzoni C, Muzio V, Rizzi M, Vezzani A (1999) Biochemical and pharmacological evidence of a functional role of AMPA receptors in motor neuron dysfunction in mnd mice. Eur J Neurosci 11:1705-1710.

Menzies FM, Cookson MR, Taylor RW, Turnbull DM, Chrzanowska-Lightowlers ZM, Dong L, Figlewicz DA, Shaw PJ (2002) Mitochondrial dysfunction in a cell culture model of familial amyotrophic lateral sclerosis. Brain 125:1522-1533.

Messer A, Strominger NL, Mazurkiewicz JE (1987) Histopathology of the late-onset motor neuron degeneration (Mnd) mutant in the mouse. J Neurogenet 4:201-213.

Michaelis EK (1998) Molecular biology of glutamate receptors in the central nervous system and their role in excitotoxicity, oxidative stress and aging. Prog Neurobiol 54:369-415.

Mielke K, Herdegen T (2000) JNK and p38 stresskinases--degenerative effectors of signal-transduction-cascades in the nervous system. Prog Neurobiol 61:45-60.

Migheli A, Attanasio A, Schiffer D (1994) Ubiquitin and neurofilament expression in anterior horn cells in amyotrophic lateral sclerosis: possible clues to the pathogenesis. Neuropathol Appl Neurobiol 20:282-289.

Migheli A, Atzori C, Piva R, Tortarolo M, Girelli M, Schiffer D, Bendotti C (1999) Lack of apoptosis in mice with ALS. Nat Med 5:966-967.

Miller RG, Bouchard JP, Duquette P, Eisen A, Gelinas D, Harati Y, Munsat TL, Powe L, Rothstein J, Salzman P, Sufit RL (1996) Clinical trials of riluzole in patients with ALS. ALS/Riluzole Study Group-II. Neurology 47:S86-90; discussion S90-82.

Mitsumoto H, Bradley WG (1982) Murine motor neuron disease (the wobbler mouse): degeneration and regeneration of the lower motor neuron. Brain 105 (Pt 4):811-834.

Mizusawa H, Nakamura H, Wakayama I, Yen SH, Hirano A (1991) Skein-like inclusions in the anterior horn cells in motor neuron disease. J Neurol Sci 105:14-21.

Mizusawa H, Matsumoto S, Yen SH, Hirano A, Rojas-Corona RR, Donnenfeld H (1989) Focal accumulation of phosphorylated neurofilaments within anterior horn cell in familial amyotrophic lateral sclerosis. Acta Neuropathol (Berl) 79:37-43.

Molloy GY, Rattray M, Williams RJ (1998) Genes encoding multiple forms of phospholipase A2 are expressed in rat brain. Neurosci Lett 258:139-142.

Morrison BM, Janssen WG, Gordon JW, Morrison JH (1998) Light and electron microscopic distribution of the AMPA receptor subunit, GluR2, in the spinal cord of control and G86R mutant superoxide dismutase transgenic mice. J Comp Neurol 395:523-534.

Murayama S, Ookawa Y, Mori H, Nakano I, Ihara Y, Kuzuhara S, Tomonaga M (1989) Immunocytochemical and ultrastructural study of Lewy body-like hyaline inclusions in familial amyotrophic lateral sclerosis. Acta Neuropathol (Berl) 78:143-152.

Myers SJ, Peters J, Huang Y, Comer MB, Barthel F, Dingledine R (1998) Transcriptional regulation of the GluR2 gene: neural-specific expression, multiple promoters, and regulatory elements. J Neurosci 18:6723-6739.

Nagano S, Satoh M, Sumi H, Fujimura H, Tohyama C, Yanagihara T, Sakoda S (2001) Reduction of metallothioneins promotes the disease expression of familial amyotrophic lateral sclerosis mice in a dose-dependent manner. Eur J Neurosci 13:1363-1370.

Nakamura S, Kawamoto Y, Nakano S, Ikemoto A, Akiguchi I, Kimura J (1997) Cyclin-dependent kinase 5 in Lewy body-like inclusions in anterior horn cells of a patient with sporadic amyotrophic lateral sclerosis. Neurology 48:267-270.

Nakano I, Hirano A (1987) Atrophic cell processes of large motor neurons in the anterior horn in amyotrophic lateral sclerosis: observation with silver impregnation method. J Neuropathol Exp Neurol 46:40-49.

Nitzan YB, Sekler I, Hershfinkel M, Moran A, Silverman WF (2002) Postnatal regulation of ZnT-1 expression in the mouse brain. Brain Res Dev Brain Res 137:149-157.

Olney JW, Misra CH, de Gubareff T (1975) Cysteine-S-sulfate: brain damaging metabolite in sulfite oxidase deficiency. J Neuropathol Exp Neurol 34:167-177.

Ono K, Han J (2000) The p38 signal transduction pathway: activation and function. Cell Signal 12:1-13.

Oosthuyse B, Moons L, Storkebaum E, Beck H, Nuyens D, Brusselmans K, Van Dorpe J, Hellings P, Gorselink M, Heymans S, Theilmeier G, Dewerchin M, Laudenbach V, Vermylen P, Raat H, Acker T, Vleminckx V, Van Den Bosch L, Cashman N, Fujisawa H, Drost MR, Sciot R, Bruyninckx F, Hicklin DJ, Ince C, Gressens P, Lupu F, Plate KH, Robberecht W, Herbert JM, Collen D, Carmeliet P (2001) Deletion of the hypoxia-response element in the vascular endothelial growth factor promoter causes motor neuron degeneration. Nat Genet 28:131-138.

Palmiter RD, Findley SD (1995) Cloning and functional characterization of a mammalian zinc transporter that confers resistance to zinc. Embo J 14:639-649.

Palmiter RD, Cole TB, Findley SD (1996) ZnT-2, a mammalian protein that confers resistance to zinc by facilitating vesicular sequestration. Embo J 15:1784-1791.

Park E, Liu Y, Fehlings MG (2003) Changes in glial cell white matter AMPA receptor expression after spinal cord injury and relationship to apoptotic cell death. Exp Neurol 182:35-48.

Pasinelli P, Belford ME, Lennon N, Bacskai BJ, Hyman BT, Trotti D, Brown RH, Jr. (2004) Amyotrophic lateral sclerosis-associated SOD1 mutant proteins bind and aggregate with Bcl-2 in spinal cord mitochondria. Neuron 43:19-30.

Paternain AV, Morales M, Lerma J (1995) Selective antagonism of AMPA receptors unmasks kainate receptor-mediated responses in hippocampal neurons. Neuron 14:185-189.

Pedersen WA, Fu W, Keller JN, Markesbery WR, Appel S, Smith RG, Kasarskis E, Mattson MP (1998) Protein modification by the lipid peroxidation product 4-hydroxynonenal in the spinal cords of amyotrophic lateral sclerosis patients. Ann Neurol 44:819-824.

Pellegrini-Giampietro DE, Pulsinelli WA, Zukin RS (1994) NMDA and non-NMDA receptor gene expression following global brain ischemia in rats: effect of NMDA and non-NMDA receptor antagonists. J Neurochem 62:1067-1073.

Pellegrini-Giampietro DE, Gorter JA, Bennett MV, Zukin RS (1997) The GluR2 (GluR-B) hypothesis: Ca(2+)-permeable AMPA receptors in neurological disorders. Trends Neurosci 20:464-470.

Pellegrini-Giampietro DE, Zukin RS, Bennett MV, Cho S, Pulsinelli WA (1992) Switch in glutamate receptor subunit gene expression in CA1 subfield of

hippocampus following global ischemia in rats. Proc Natl Acad Sci U S A 89:10499-10503.

Perry TL, Hansen S, Jones K (1987) Brain glutamate deficiency in amyotrophic lateral sclerosis. Neurology 37:1845-1848.

Perry TL, Krieger C, Hansen S, Eisen A (1990) Amyotrophic lateral sclerosis: amino acid levels in plasma and cerebrospinal fluid. Ann Neurol 28:12-17.

Pines G, Danbolt NC, Bjoras M, Zhang Y, Bendahan A, Eide L, Koepsell H, Storm-Mathisen J, Seeberg E, Kanner BI (1992) Cloning and expression of a rat brain L-glutamate transporter. Nature 360:464-467.

Plaitakis A, Caroscio JT (1987) Abnormal glutamate metabolism in amyotrophic lateral sclerosis. Ann Neurol 22:575-579.

Pollard H, Heron A, Moreau J, Ben-Ari Y, Khrestchatisky M (1993) Alterations of the GluR-B AMPA receptor subunit flip/flop expression in kainate-induced epilepsy and ischemia. Neuroscience 57:545-554.

Poloni M, Facchetti D, Mai R, Micheli A, Agnoletti L, Francolini G, Mora G, Camana C, Mazzini L, Bachetti T (2000) Circulating levels of tumour necrosis factor-alpha and its soluble receptors are increased in the blood of patients with amyotrophic lateral sclerosis. Neurosci Lett 287:211-214.

Pramatarova A, Laganiere J, Roussel J, Brisebois K, Rouleau GA (2001) Neuron-specific expression of mutant superoxide dismutase 1 in transgenic mice does not lead to motor impairment. J Neurosci 21:3369-3374.

Ranta S, Zhang Y, Ross B, Lonka L, Takkunen E, Messer A, Sharp J, Wheeler R, Kusumi K, Mole S, Liu W, Soares MB, Bonaldo MF, Hirvasniemi A, de la Chapelle A, Gilliam TC, Lehesjoki AE (1999) The neuronal ceroid lipofuscinoses in human EPMR and mnd mutant mice are associated with mutations in CLN8. Nat Genet 23:233-236.

Raoul C, Estevez AG, Nishimune H, Cleveland DW, deLapeyriere O, Henderson CE, Haase G, Pettmann B (2002) Motoneuron death triggered by a specific pathway downstream of Fas. potentiation by ALS-linked SOD1 mutations. Neuron 35:1067-1083.

Reaume AG, Elliott JL, Hoffman EK, Kowall NW, Ferrante RJ, Siwek DF, Wilcox HM, Flood DG, Beal MF, Brown RH, Jr., Scott RW, Snider WD (1996) Motor neurons in Cu/Zn superoxide dismutase-deficient mice develop normally but exhibit enhanced cell death after axonal injury. Nat Genet 13:43-47.

Rembach A, Turner BJ, Bruce S, Cheah IK, Scott RL, Lopes EC, Zagami CJ, Beart PM, Cheung NS, Langford SJ, Cheema SS (2004) Antisense peptide nucleic acid targeting GluR3 delays disease onset and progression in the SOD1 G93A mouse model of familial ALS. J Neurosci Res 77:573-582.

Ripps ME, Huntley GW, Hof PR, Morrison JH, Gordon JW (1995a) Transgenic mice expressing an altered murine superoxide dismutase gene provide an animal model of amyotrophic lateral sclerosis.

Ripps ME, Huntley GW, Hof PR, Morrison JH, Gordon JW (1995b) Transgenic mice expressing an altered murine superoxide dismutase gene provide

an animal model of amyotrophic lateral sclerosis. Proc Natl Acad Sci U S A 92:689-693.

Rivera-Cervantes MC, Torres JS, Feria-Velasco A, Armendariz-Borunda J, Beas-Zarate C (2004) NMDA and AMPA receptor expression and cortical neuronal death are associated with p38 in glutamate-induced excitotoxicity in vivo. J Neurosci Res 76:678-687.

Riviere M, Meininger V, Zeisser P, Munsat T (1998) An analysis of extended survival in patients with amyotrophic lateral sclerosis treated with riluzole. Arch Neurol 55:526-528.

Roisen FJ, Bartfeld H, Donnenfeld H, Baxter J (1982) Neuron specific in vitro cytotoxicity of sera from patients with amyotrophic lateral sclerosis. Muscle Nerve 5:48-53.

Rosen DR, Siddique T, Patterson D, Figlewicz DA, Sapp P, Hentati A, Donaldson D, Goto J, O'Regan JP, Deng HX, et al. (1993) Mutations in Cu/Zn superoxide dismutase gene are associated with familial amyotrophic lateral sclerosis. Nature 362:59-62.

Rothstein JD, Martin LJ, Kuncl RW (1992) Decreased glutamate transport by the brain and spinal cord in amyotrophic lateral sclerosis. N Engl J Med 326:1464-1468.

Rothstein JD, Jin L, Dykes-Hoberg M, Kuncl RW (1993) Chronic inhibition of glutamate uptake produces a model of slow neurotoxicity. Proc Natl Acad Sci U S A 90:6591-6595.

Rothstein JD, Van Kammen M, Levey AI, Martin LJ, Kuncl RW (1995) Selective loss of glial glutamate transporter GLT-1 in amyotrophic lateral sclerosis. Ann Neurol 38:73-84.

Rothstein JD, Martin L, Levey AI, Dykes-Hoberg M, Jin L, Wu D, Nash N, Kuncl RW (1994) Localization of neuronal and glial glutamate transporters. Neuron 13:713-725.

Rothstein JD, Tsai G, Kuncl RW, Clawson L, Cornblath DR, Drachman DB, Pestronk A, Stauch BL, Coyle JT (1990) Abnormal excitatory amino acid metabolism in amyotrophic lateral sclerosis. Ann Neurol 28:18-25.

Rothstein JD, Dykes-Hoberg M, Pardo CA, Bristol LA, Jin L, Kuncl RW, Kanai Y, Hediger MA, Wang Y, Schielke JP, Welty DF (1996) Knockout of glutamate transporters reveals a major role for astroglial transport in excitotoxicity and clearance of glutamate. Neuron 16:675-686.

Roy J, Minotti S, Dong L, Figlewicz DA, Durham HD (1998) Glutamate potentiates the toxicity of mutant Cu/Zn-superoxide dismutase in motor neurons by postsynaptic calcium-dependent mechanisms. J Neurosci 18:9673-9684.

Saroff D, Delfs J, Kuznetsov D, Geula C (2000) Selective vulnerability of spinal cord motor neurons to non-NMDA toxicity. Neuroreport 11:1117-1121.

Sasaki S, Maruyama S (1991) Immunocytochemical and ultrastructural studies of hyaline inclusions in sporadic motor neuron disease. Acta Neuropathol (Berl) 82:295-301.

Sasaki S, Maruyama S (1993) Ultrastructural study of Bunina bodies in the anterior horn neurons of patients with amyotrophic lateral sclerosis. Neurosci Lett 154:117-120.

Savage MJ, Lin YG, Ciallella JR, Flood DG, Scott RW (2002) Activation of c-Jun N-terminal kinase and p38 in an Alzheimer's disease model is associated with amyloid deposition. J Neurosci 22:3376-3385.

Schiffer D, Autilio-Gambetti L, Chio A, Gambetti P, Giordana MT, Gullotta F, Migheli A, Vigliani MC (1991) Ubiquitin in motor neuron disease: study at the light and electron microscope. J Neuropathol Exp Neurol 50:463-473.

Schmalbruch H, Jensen HJ, Bjaerg M, Kamieniecka Z, Kurland L (1991) A new mouse mutant with progressive motor neuronopathy. J Neuropathol Exp Neurol 50:192-204.

Schochet SS, Jr., Hardman JM, Ladewig PP, Earle KM (1969) Intraneuronal conglomerates in sporadic motor neuron disease. A light and electron microscopic study. Arch Neurol 20:548-553.

Sekizawa T, Openshaw H, Ohbo K, Sugamura K, Itoyama Y, Niland JC (1998) Cerebrospinal fluid interleukin 6 in amyotrophic lateral sclerosis: immunological parameter and comparison with inflammatory and non-inflammatory central nervous system diseases. J Neurol Sci 154:194-199.

Sekler I, Moran A, Hershfinkel M, Dori A, Margulis A, Birenzweig N, Nitzan Y, Silverman WF (2002) Distribution of the zinc transporter ZnT-1 in comparison with chelatable zinc in the mouse brain. J Comp Neurol 447:201-209.

Sensi SL, Jeng JM (2004) Rethinking the excitotoxic ionic milieu: the emerging role of Zn(2+) in ischemic neuronal injury. Curr Mol Med 4:87-111.

Sensi SL, Yin HZ, Weiss JH (1999a) Glutamate triggers preferential Zn2+ flux through Ca2+ permeable AMPA channels and consequent ROS production. Neuroreport 10:1723-1727.

Sensi SL, Yin HZ, Weiss JH (2000) AMPA/kainate receptor-triggered Zn2+ entry into cortical neurons induces mitochondrial Zn2+ uptake and persistent mitochondrial dysfunction. Eur J Neurosci 12:3813-3818.

Sensi SL, Yin HZ, Carriedo SG, Rao SS, Weiss JH (1999b) Preferential Zn2+ influx through Ca2+-permeable AMPA/kainate channels triggers prolonged mitochondrial superoxide production. Proc Natl Acad Sci U S A 96:2414-2419.

Shaw PJ, Ince PG, Falkous G, Mantle D (1995a) Oxidative damage to protein in sporadic motor neuron disease spinal cord. Ann Neurol 38:691-695.

Shaw PJ, Forrest V, Ince PG, Richardson JP, Wastell HJ (1995b) CSF and plasma amino acid levels in motor neuron disease: elevation of CSF glutamate in a subset of patients. Neurodegeneration 4:209-216.

Shaw PJ, Williams TL, Slade JY, Eggett CJ, Ince PG (1999) Low expression of GluR2 AMPA receptor subunit protein by human motor neurons. Neuroreport 10:261-265.

Siddons MA, Pickering-Brown SM, Mann DM, Owen F, Cooper PN (1996) Debrisoquine hydroxylase gene polymorphism frequencies in patients with amyotrophic lateral sclerosis. Neurosci Lett 208:65-68.

Silani V, Fogh I, Ratti A, Sassone J, Ciammola A, Cova L (2002) Stem cells in the treatment of amyotrophic lateral sclerosis (ALS). Amyotroph Lateral Scler Other Motor Neuron Disord 3:173-181.

Singh RJ, Karoui H, Gunther MR, Beckman JS, Mason RP, Kalyanaraman B (1998) Reexamination of the mechanism of hydroxyl radical adducts formed from the reaction between familial amyotrophic lateral sclerosis-associated Cu,Zn superoxide dismutase mutants and H2O2. Proc Natl Acad Sci U S A 95:6675-6680.

Smart TG, Xie X, Krishek BJ (1994) Modulation of inhibitory and excitatory amino acid receptor ion channels by zinc. Prog Neurobiol 42:393-341.

Sobue G, Hashizume Y, Yasuda T, Mukai E, Kumagai T, Mitsuma T, Trojanowski JQ (1990) Phosphorylated high molecular weight neurofilament protein in lower motor neurons in amyotrophic lateral sclerosis and other neurodegenerative diseases involving ventral horn cells. Acta Neuropathol (Berl) 79:402-408.

Spalloni A, Albo F, Ferrari F, Mercuri N, Bernardi G, Zona C, Longone P (2004) Cu/Zn-superoxide dismutase (GLY93-->ALA) mutation alters AMPA receptor subunit expression and function and potentiates kainate-mediated toxicity in motor neurons in culture. Neurobiol Dis 15:340-350.

Standley S, Baudry M (2000) The role of glycosylation in ionotropic glutamate receptor ligand binding, function, and trafficking. Cell Mol Life Sci 57:1508-1516.

Stieber A, Gonatas JO, Gonatas NK (2000) Aggregation of ubiquitin and a mutant ALS-linked SOD1 protein correlate with disease progression and fragmentation of the Golgi apparatus. J Neurol Sci 173:53-62.

Storck T, Schulte S, Hofmann K, Stoffel W (1992) Structure, expression, and functional analysis of a Na(+)-dependent glutamate/aspartate transporter from rat brain. Proc Natl Acad Sci U S A 89:10955-10959.

Suh SW, Chen JW, Motamedi M, Bell B, Listiak K, Pons NF, Danscher G, Frederickson CJ (2000) Evidence that synaptically-released zinc contributes to neuronal injury after traumatic brain injury. Brain Res 852:268-273.

Swanson RA, Liu J, Miller JW, Rothstein JD, Farrell K, Stein BA, Longuemare MC (1997) Neuronal regulation of glutamate transporter subtype expression in astrocytes. J Neurosci 17:932-940.

Tachibana M, Wenthold RJ, Morioka H, Petralia RS (1994) Light and electron microscopic immunocytochemical localization of AMPA-selective glutamate receptors in the rat spinal cord. J Comp Neurol 344:431-454.

Takagi Y, Nozaki K, Sugino T, Hattori I, Hashimoto N (2000) Phosphorylation of c-Jun NH(2)-terminal kinase and p38 mitogen-activated protein kinase after transient forebrain ischemia in mice. Neurosci Lett 294:117-120.

Takuma H, Kwak S, Yoshizawa T, Kanazawa I (1999) Reduction of GluR2 RNA editing, a molecular change that increases calcium influx through AMPA receptors, selective in the spinal ventral gray of patients with amyotrophic lateral sclerosis. Ann Neurol 46:806-815.

Teitelbaum JS, Zatorre RJ, Carpenter S, Gendron D, Evans AC, Gjedde A, Cashman NR (1990) Neurologic sequelae of domoic acid intoxication due to the ingestion of contaminated mussels. N Engl J Med 322:1781-1787.

Terro F, Yardin C, Esclaire F, Ayer-Lelievre C, Hugon J (1998) Mild kainate toxicity produces selective motoneuron death with marked activation of CA(2+)-permeable AMPA/kainate receptors. Brain Res 809:319-324.

Tikka T, Fiebich BL, Goldsteins G, Keinanen R, Koistinaho J (2001) Minocycline, a tetracycline derivative, is neuroprotective against excitotoxicity by inhibiting activation and proliferation of microglia. J Neurosci 21:2580-2588.

Tikka TM, Vartiainen NE, Goldsteins G, Oja SS, Andersen PM, Marklund SL, Koistinaho J (2002) Minocycline prevents neurotoxicity induced by cerebrospinal fluid from patients with motor neurone disease. Brain 125:722-731.

Tomiyama M, Rodriguez-Puertas R, Cortes R, Pazos A, Palacios JM, Mengod G (2002) Flip and flop splice variants of AMPA receptor subunits in the spinal cord of amyotrophic lateral sclerosis. Synapse 45:245-249.

Toyoshima I, Sugawara M, Kato K, Wada C, Hirota K, Hasegawa K, Kowa H, Sheetz MP, Masamune O (1998) Kinesin and cytoplasmic dynein in spinal spheroids with motor neuron disease. J Neurol Sci 159:38-44.

Trotti D, Danbolt NC, Volterra A (1998) Glutamate transporters are oxidant-vulnerable: a molecular link between oxidative and excitotoxic neurodegeneration? Trends Pharmacol Sci 19:328-334.

Trotti D, Rolfs A, Danbolt NC, Brown RH, Jr., Hediger MA (1999) SOD1 mutants linked to amyotrophic lateral sclerosis selectively inactivate a glial glutamate transporter. Nat Neurosci 2:848.

Trotti D, Rossi D, Gjesdal O, Levy LM, Racagni G, Danbolt NC, Volterra A (1996) Peroxynitrite inhibits glutamate transporter subtypes. J Biol Chem 271:5976-5979.

Tsuda M, Imaizumi K, Katayama T, Kitagawa K, Wanaka A, Tohyama M, Takagi T (1997) Expression of zinc transporter gene, ZnT-1, is induced after transient forebrain ischemia in the gerbil. J Neurosci 17:6678-6684.

Van Damme P, Leyssen M, Callewaert G, Robberecht W, Van Den Bosch L (2003) The AMPA receptor antagonist NBQX prolongs survival in a transgenic mouse model of amyotrophic lateral sclerosis. Neurosci Lett 343:81-84.

Van Den Bosch L, Tilkin P, Lemmens G, Robberecht W (2002a) Minocycline delays disease onset and mortality in a transgenic model of ALS. Neuroreport 13:1067-1070.

Van Den Bosch L, Vandenberghe W, Klaassen H, Van Houtte E, Robberecht W (2000) Ca(2+)-permeable AMPA receptors and selective vulnerability of motor neurons. J Neurol Sci 180:29-34.

Van Den Bosch L, Verhoeven K, De Smedt H, Wuytack F, Missiaen L, Robberecht W (1999) Calcium handling proteins in isolated spinal motoneurons. Life Sci 65:1597-1606.

Van Den Bosch L, Schwaller B, Vleminckx V, Meijers B, Stork S, Ruehlicke T, Van Houtte E, Klaassen H, Celio MR, Missiaen L, Robberecht W,

Berchtold MW (2002b) Protective effect of parvalbumin on excitotoxic motor neuron death. Exp Neurol 174:150-161.

Vandenberghe W, Robberecht W, Brorson JR (2000a) AMPA receptor calcium permeability, GluR2 expression, and selective motoneuron vulnerability. J Neurosci 20:123-132.

Vandenberghe W, Ihle EC, Patneau DK, Robberecht W, Brorson JR (2000b) AMPA receptor current density, not desensitization, predicts selective motoneuron vulnerability. J Neurosci 20:7158-7166.

Vandenberghe W, Bindokas VP, Miller RJ, Robberecht W, Brorson JR (2001) Subcellular localization of calcium-permeable AMPA receptors in spinal motoneurons. Eur J Neurosci 14:305-314.

Vanoni C, Massari S, Losa M, Carrega P, Perego C, Conforti L, Pietrini G (2004) Increased internalisation and degradation of GLT-1 glial glutamate transporter in a cell model for familial amyotrophic lateral sclerosis (ALS). J Cell Sci 117:5417-5426.

Virgo L, Samarasinghe S, de Belleroche J (1996) Analysis of AMPA receptor subunit mRNA expression in control and ALS spinal cord. Neuroreport 7:2507-2511.

Volterra A, Trotti D, Floridi S, Racagni G (1994a) Reactive oxygen species inhibit high-affinity glutamate uptake: molecular mechanism and neuropathological implications. Ann N Y Acad Sci 738:153-162.

Volterra A, Trotti D, Tromba C, Floridi S, Racagni G (1994b) Glutamate uptake inhibition by oxygen free radicals in rat cortical astrocytes. J Neurosci 14:2924-2932.

Wang H, Joseph JA (1999) Quantifying cellular oxidative stress by dichlorofluorescein assay using microplate reader. Free Radic Biol Med 27:612-616.

Wang Z, Li JY, Dahlstrom A, Danscher G (2001) Zinc-enriched GABAergic terminals in mouse spinal cord. Brain Res 921:165-172.

Watanabe M, Dykes-Hoberg M, Culotta VC, Price DL, Wong PC, Rothstein JD (2001) Histological evidence of protein aggregation in mutant SOD1 transgenic mice and in amyotrophic lateral sclerosis neural tissues. Neurobiol Dis 8:933-941.

Weiss JH, Choi DW (1991) Slow non-NMDA receptor mediated neurotoxicity and amyotrophic lateral sclerosis. Adv Neurol 56:311-318.

Wenzel HJ, Cole TB, Born DE, Schwartzkroin PA, Palmiter RD (1997) Ultrastructural localization of zinc transporter-3 (ZnT-3) to synaptic vesicle membranes within mossy fiber boutons in the hippocampus of mouse and monkey. Proc Natl Acad Sci U S A 94:12676-12681.

Wiedau-Pazos M, Goto JJ, Rabizadeh S, Gralla EB, Roe JA, Lee MK, Valentine JS, Bredesen DE (1996) Altered reactivity of superoxide dismutase in familial amyotrophic lateral sclerosis. Science 271:515-518.

Williams TL, Day NC, Ince PG, Kamboj RK, Shaw PJ (1997) Calcium-permeable alpha-amino-3-hydroxy-5-methyl-4-isoxazole propionic acid receptors: a molecular determinant of selective vulnerability in amyotrophic lateral sclerosis. Ann Neurol 42:200-207.

Williamson TL, Cleveland DW (1999) Slowing of axonal transport is a very early event in the toxicity of ALS-linked SOD1 mutants to motor neurons. Nat Neurosci 2:50-56.

Williamson TL, Bruijn LI, Zhu Q, Anderson KL, Anderson SD, Julien JP, Cleveland DW (1998) Absence of neurofilaments reduces the selective vulnerability of motor neurons and slows disease caused by a familial amyotrophic lateral sclerosis-linked superoxide dismutase 1 mutant. Proc Natl Acad Sci U S A 95:9631-9636.

Wong PC, Pardo CA, Borchelt DR, Lee MK, Copeland NG, Jenkins NA, Sisodia SS, Cleveland DW, Price DL (1995) An adverse property of a familial ALS-linked SOD1 mutation causes motor neuron disease characterized by vacuolar degeneration of mitochondria. Neuron 14:1105-1116.

Wu DC, Jackson-Lewis V, Vila M, Tieu K, Teismann P, Vadseth C, Choi DK, Ischiropoulos H, Przedborski S (2002) Blockade of microglial activation is neuroprotective in the 1-methyl-4-phenyl-1,2,3,6-tetrahydropyridine mouse model of Parkinson disease. J Neurosci 22:1763-1771.

Xu Z, Cork LC, Griffin JW, Cleveland DW (1993) Increased expression of neurofilament subunit NF-L produces morphological alterations that resemble the pathology of human motor neuron disease. Cell 73:23-33.

Yang Y, Hentati A, Deng HX, Dabbagh O, Sasaki T, Hirano M, Hung WY, Ouahchi K, Yan J, Azim AC, Cole N, Gascon G, Yagmour A, Ben-Hamida M, Pericak-Vance M, Hentati F, Siddique T (2001) The gene encoding alsin, a protein with three guanine-nucleotide exchange factor

domains, is mutated in a form of recessive amyotrophic lateral sclerosis. Nat Genet 29:160-165.

Yasojima K, Tourtellotte WW, McGeer EG, McGeer PL (2001) Marked increase in cyclooxygenase-2 in ALS spinal cord: implications for therapy. Neurology 57:952-956.

Yim HS, Kang JH, Chock PB, Stadtman ER, Yim MB (1997) A familial amyotrophic lateral sclerosis-associated A4V Cu, Zn-superoxide dismutase mutant has a lower Km for hydrogen peroxide. Correlation between clinical severity and the Km value. J Biol Chem 272:8861-8863.

Yim MB, Kang JH, Yim HS, Kwak HS, Chock PB, Stadtman ER (1996) A gain-of-function of an amyotrophic lateral sclerosis-associated Cu,Zn-superoxide dismutase mutant: An enhancement of free radical formation due to a decrease in Km for hydrogen peroxide. Proc Natl Acad Sci U S A 93:5709-5714.

Yip PK, Meldrum BS, Rattray M (2001) Elevated levels of group-III metabotropic glutamate receptors in the inferior colliculus of genetically epilepsy-prone rats following intracollicular administration of L-serine-O-phosphate. J Neurochem 78:13-23.

Yoshihara T, Ishigaki S, Yamamoto M, Liang Y, Niwa J, Takeuchi H, Doyu M, Sobue G (2002) Differential expression of inflammation- and apoptosis-related genes in spinal cords of a mutant SOD1 transgenic mouse model of familial amyotrophic lateral sclerosis. J Neurochem 80:158-167.

Yrjanheikki J, Keinanen R, Pellikka M, Hokfelt T, Koistinaho J (1998) Tetracyclines inhibit microglial activation and are neuroprotective in global brain ischemia. Proc Natl Acad Sci U S A 95:15769-15774.

Yrjanheikki J, Tikka T, Keinanen R, Goldsteins G, Chan PH, Koistinaho J (1999) A tetracycline derivative, minocycline, reduces inflammation and protects against focal cerebral ischemia with a wide therapeutic window. Proc Natl Acad Sci U S A 96:13496-13500.

Zawada WM, Meintzer MK, Rao P, Marotti J, Wang X, Esplen JE, Clarkson ED, Freed CR, Heidenreich KA (2001) Inhibitors of p38 MAP kinase increase the survival of transplanted dopamine neurons. Brain Res 891:185-196.

Zhou Q, Xiao M, Nicoll RA (2001) Contribution of cytoskeleton to the internalization of AMPA receptors. Proc Natl Acad Sci U S A 98:1261-1266.

Zhu JJ, Qin Y, Zhao M, Van Aelst L, Malinow R (2002a) Ras and Rap control AMPA receptor trafficking during synaptic plasticity. Cell 110:443-455.

Zhu S, Stavrovskaya IG, Drozda M, Kim BY, Ona V, Li M, Sarang S, Liu AS, Hartley DM, Wu du C, Gullans S, Ferrante RJ, Przedborski S, Kristal BS, Friedlander RM (2002b) Minocycline inhibits cytochrome c release and delays progression of amyotrophic lateral sclerosis in mice. Nature 417:74-78.

Zhu X, Rottkamp CA, Boux H, Takeda A, Perry G, Smith MA (2000) Activation of p38 kinase links tau phosphorylation, oxidative stress, and cell cycle-related events in Alzheimer disease. J Neuropathol Exp Neurol 59:880-888.

Zukin RS, Bennett MV (1995) Alternatively spliced isoforms of the NMDARI receptor subunit. Trends Neurosci 18:306-313.